

Unraveling platelet function in inflammation and thrombosis

Citation for published version (APA):

Coenen, D. (2021). *Unraveling platelet function in inflammation and thrombosis: Secretory pathways and vascular interactions*. [Doctoral Thesis, Maastricht University]. Maastricht University. <https://doi.org/10.26481/dis.20210625dc>

Document status and date:

Published: 01/01/2021

DOI:

[10.26481/dis.20210625dc](https://doi.org/10.26481/dis.20210625dc)

Document Version:

Publisher's PDF, also known as Version of record

Please check the document version of this publication:

- A submitted manuscript is the version of the article upon submission and before peer-review. There can be important differences between the submitted version and the official published version of record. People interested in the research are advised to contact the author for the final version of the publication, or visit the DOI to the publisher's website.
- The final author version and the galley proof are versions of the publication after peer review.
- The final published version features the final layout of the paper including the volume, issue and page numbers.

[Link to publication](#)

General rights

Copyright and moral rights for the publications made accessible in the public portal are retained by the authors and/or other copyright owners and it is a condition of accessing publications that users recognise and abide by the legal requirements associated with these rights.

- Users may download and print one copy of any publication from the public portal for the purpose of private study or research.
- You may not further distribute the material or use it for any profit-making activity or commercial gain
- You may freely distribute the URL identifying the publication in the public portal.

If the publication is distributed under the terms of Article 25fa of the Dutch Copyright Act, indicated by the "Taverne" license above, please follow below link for the End User Agreement:

www.umlib.nl/taverne-license

Take down policy

If you believe that this document breaches copyright please contact us at:

repository@maastrichtuniversity.nl

providing details and we will investigate your claim.

Unravelling platelet function in inflammation and thrombosis

Secretory pathways and vascular interactions

Daniëlle Coenen

Unravelling platelet function in inflammation and thrombosis – Secretory pathways and vascular interactions

Thesis: Maastricht University

ISBN: 978-94-6423-271-4

Production: Proefschriftmaken || www.proefschriftmaken.nl

© Daniëlle Coenen, Maastricht 2021

Cover design by Jan Karen Campbell || www.jankaren.com/

*Unraveling platelet function in inflammation and
thrombosis
Secretory pathways and vascular interactions*

Proefschrift

ter verkrijging van de graad van doctor aan de Universiteit Maastricht,
op gezag van de Rector Magnificus, Prof. Dr. Rianne M. Letschert,
volgens het besluit van het College van Decanen,
in het openbaar te verdedigen op

vrijdag 25 juni 2021 om 16.00 uur

door

Daniëlle Marije Coenen
Geboren op 29 juni 1992 te Alphen aan de Rijn

Promotor

Dr. J.M.E.M. Cosemans

Copromotor

Dr. R.R. Koenen

Beoordelingscommissie

Prof. Dr. P.A. da Costa Martins (voorzitter)

Prof. Dr. J.D. van Buul (Universiteit van Amsterdam/Sanquin)

Dr. M.M.P.C. Donners

Prof. Dr. A.W.J. van 't Hof

Prof. Dr. S.W. Whiteheart (University of Kentucky, USA)

The research described in this thesis was supported by a grant of the Dutch Heart Foundation (2015T079)

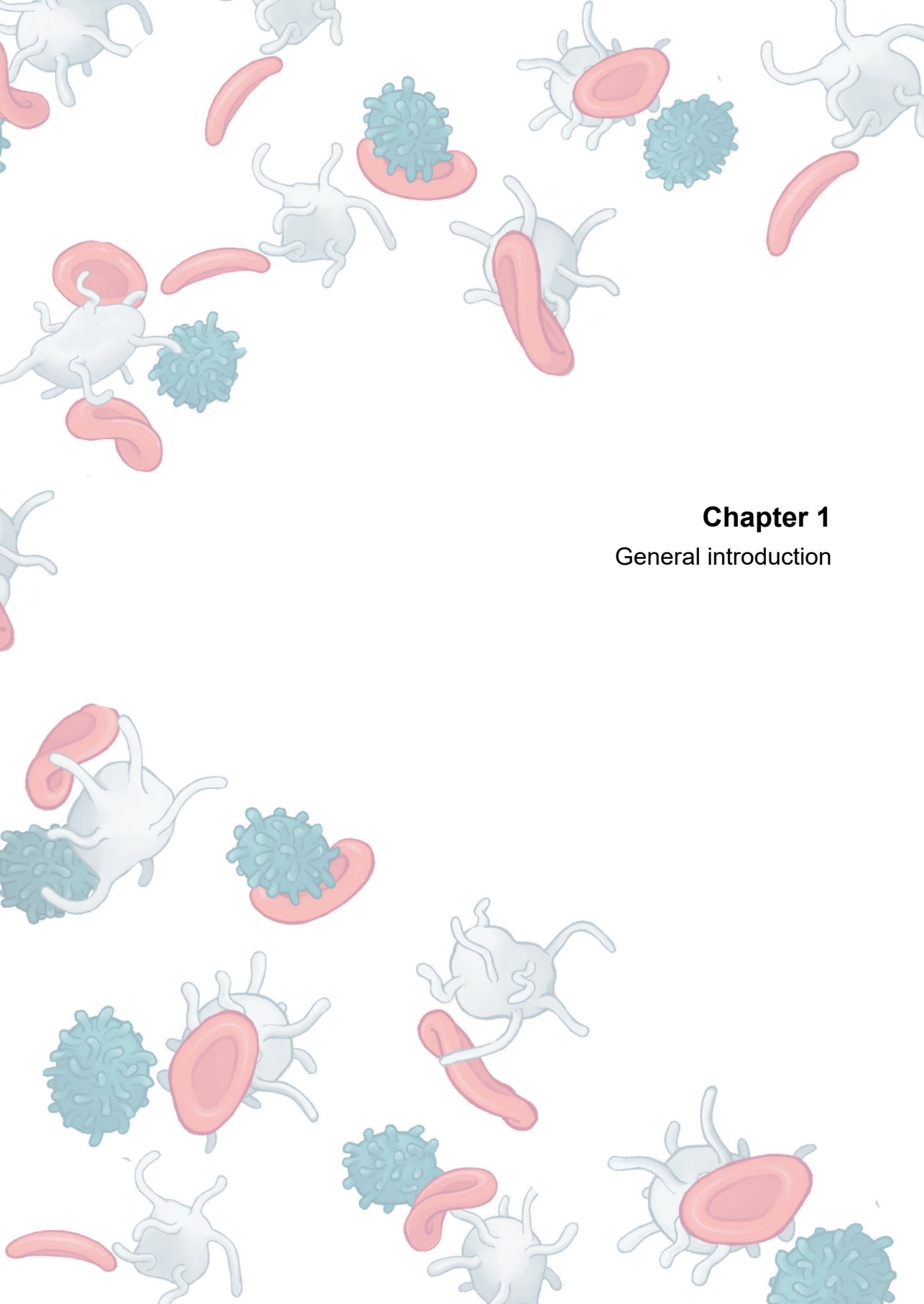
Financial support for publication of this thesis by the Dutch Heart Foundation is gratefully acknowledged

Financial support by Stichting Hart Onderzoek Nederland (www.hartonderzoek.nu) is gratefully acknowledged



Table of contents

Chapter 1	General introduction
Chapter 2	Platelet interaction with activated endothelium – mechanistic insights from microfluidics
Chapter 3	The multifaceted contribution of platelets in the emergence and aftermath of acute cardiovascular events
Chapter 4	Inhibition of phosphodiesterase 3A by cilostazol dampens pro-inflammatory platelet functions
Chapter 5	Combined antiplatelet therapy reduces the pro-inflammatory properties of activated platelets
Chapter 6	Plasma measurements of endothelial-, leukocyte- and platelet (dys)function in HFpEF patients
Chapter 7	SLC44A2 deficient mice have a reduced response in stenosis but not in hypercoagulability driven venous thrombosis
Chapter 8	Finding the “switch” in platelet activation – Prediction of key mediators involved in platelet hyperreactivity using a network biology approach
Chapter 9	General discussion
Chapter 10	Summary
	Samenvatting
	Impact
	Curriculum Vitae
	Publications
	Dankwoord



Chapter 1

General introduction

Platelets are essential in haemostasis and thrombosis but also harbour inflammatory properties

Despite their small size (ø2-4 µm) and the lack of a nucleus, platelets play a substantial role in the blood circulation. Under physiological circumstances, the endothelial lining of the vessel wall possesses mechanisms to dampen platelet activation, amongst others the secretion of prostacyclin (PGI₂) and nitric oxide. Cyclic adenosine monophosphate (cAMP) and cyclic guanosine monophosphate (cGMP) are key second messengers in platelets via which the platelet inhibitory effects of PGI₂ and NO are transduced. cAMP and cGMP levels are tightly regulated by phosphodiesterases (PDEs). Vascular damage and exposure of matrix proteins such as collagen and von Willebrand factor (VWF) activate platelets to fulfil their haemostatic function, *i.e.* prevent bleeding by the formation of a platelet-fibrin plug.^{1,2}

In pathological conditions, excessive platelet activation, for example following atherosclerotic plaque rupture or erosion, can lead to the development of large thrombi and consequent vessel occlusion and/or release of an embolus and multiple clinical presentations, including stroke and ischemic heart disease/myocardial infarction.³ Treatment hereof with antiplatelet drugs (aspirin and P2Y₁₂ antagonists) is mainly focused on the inhibition of platelet activation and subsequent platelet thrombus formation. However, stroke and ischemic heart disease are still a large load for global healthcare, of which more specifics are given in Figure 1. This is partly caused by the inefficiency of the current treatment in preventing the development of recurrent events, making one consider whether different pathways should be targeted. Atherosclerosis, a predominantly inflammation-driven disease, is the main underlying pathology of cardiovascular diseases. The interwovenness of inflammation and thrombosis in these diseases is increasingly being acknowledged. This is supported by the fact that platelet function is not only limited to haemostasis and thrombosis, but also extends to inflammation and immunity.⁴ Pro-inflammatory platelet responses are characterized by direct and indirect interactions with activated endothelium and leukocytes.^{5,6} Secretory factors and the corresponding signalling pathways are central elements in indirect communication between platelets, endothelial cells and leukocytes, as further described below and in Figure 2. In spite of the recognition that platelets possess inflammatory capacity, there is a lack of knowledge how platelets affect inflammation and the relevance thereof in (patho)physiology.

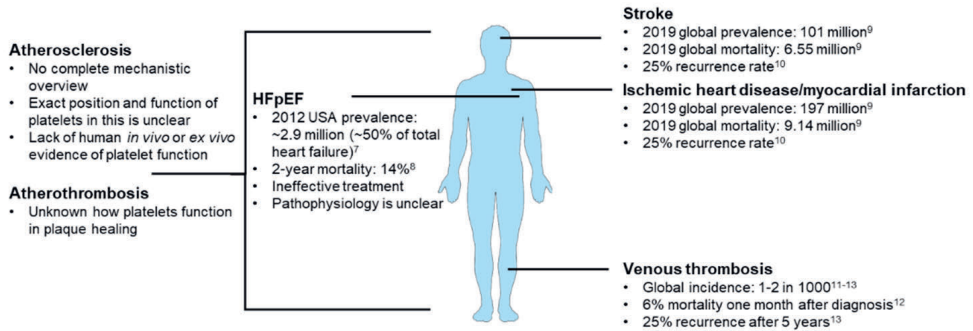


Figure 1. This thesis describes a number of clinical problems with a high global burden and an established or potential underlying mechanistic role for platelets. The data represented are from the references referred to in the figure.

Role for platelet-derived constituents and -vesicles in vascular interactions

Histological analyses revealed that in half to two-third of patients with acute myocardial infarction, coronary thrombi were days to weeks old, suggestive of an irregular period of plaque instability and thrombus growth prior to vessel occlusion.^{14,15} As platelets become activated, they secrete α - and dense-granules.¹⁶ There are >300 soluble proteins released by platelet α -granules, ranging from growth factors, proteases, immune mediators, microbicidal proteins to (anti)coagulant and fibrinolytic proteins.¹⁷ Dense granules release the autocrine and paracrine agent adenosine diphosphate (ADP), among others. ADP release creates a positive feedback mechanism by binding to the respective G protein-coupled receptors P2Y₁ and P2Y₁₂.¹⁸ Signalling downstream of ADP-P2Y₁₂ involves a reduction in the intracellular platelet concentration of the second messenger cAMP. The combined release of these mediators may evoke persistent thrombus activity and propagation of pathological platelet responses.¹⁹ The cargo of platelet α - and dense-granules can be released locally and serve as a bridge between platelets and other vascular cells (20). Important in these interactions are chemokines, specifically chemokine (C-X-C motif) ligand 4 (CXCL4; platelet factor 4, PF4) and chemokine (C-C motif) ligand 5 (CCL5; RANTES).^{5,21-23} Previously, we have shown that platelet-derived matrix metalloproteinases are capable of degrading a collagen matrix at the site of thrombus formation *in vitro*.²⁴ This suggests that platelet-derived constituents may exert prolonged effects on a damaged vessel wall. Yet, additional *in vivo* evidence is required to substantiate this hypothesis. Moreover, more insight is required into the underlying mechanisms of how platelet-derived constituents interact with a healthy, inflamed and damaged vessel wall, see Figure 2.

Technical advances led to an increased interest in platelet extracellular vesicles (EVs) and their potential role in disease.²⁵ Common to an emerging field, the interpretation of EV measurements is currently hampered by a lack of standardization.²⁶ The membrane and content of extracellular vesicles resembles

their parent cell, generating a large variety of EVs and EV subsets, of which the functional relevance is not fully understood. The type of platelet extracellular vesicles, released upon platelet activation,²⁷ depends on the activation stimulus. Platelet extracellular vesicles can also release their content systemically by moving through the circulation or even through the endothelial cell layer or the blood-brain barrier.²⁸ This is indicative for the therapeutic and diagnostic potential of EVs, either in the treatment of injuries and trauma or as a biomarker of a wide variety of diseases.²⁹⁻³³

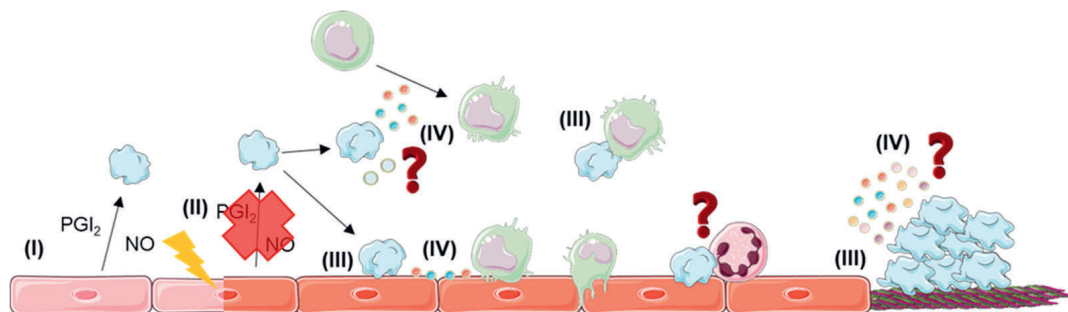


Figure 2. Direct and indirect interactions between platelets, endothelial cells, and leukocytes. (I) Secreted prostacyclin and nitric oxide by endothelial cells dampen platelet activation. (II) Endothelial activation weakens these mechanisms, leading to platelet activation. (III) Platelets can interact directly with the endothelium, leukocytes or extracellular matrix proteins. (IV) Platelet-derived constituents or extracellular vesicles are deposited on the endothelium or released in the circulation. Mechanisms how these constituents and vesicles interact with the vessel wall and leukocytes and what the implications are for the underlying pathophysiology of cardiovascular diseases requires more mechanistic insights.

SLC44A2 as a potential novel genetic determinant of venous thrombosis

Genetics play an important role in the underlying pathophysiology of bleeding and thrombotic disorders, for example in haemophilia, von Willebrand disease, and venous thrombosis (VT).⁽³⁴⁻³⁶⁾ Although multiple genetic and other risk factors have already been discovered, VT still causes a major burden on public health with an incidence of 1-2 per 1000 people and a high recurrence and mortality (Figure 1 and references¹¹⁻¹³). Genome-wide association studies (GWAS) have been used in an attempt to identify genetic risk factors for VT and discovered solute carrier family 44 member 2 (SLC44A2) as a novel candidate gene.³⁷⁻⁴⁰ SLC44A2, or choline transporter-like protein 2, is a transmembrane glycoprotein and a presumed choline transporter.⁴¹ Two transcription variants of SLC44A2 exist which are expressed in many tissues and cells, including platelets.^{41,42} Interestingly, the function of the transcription variant in platelets and neutrophils is not related to choline transport, but still unknown. Recently, SLC44A2 has been suggested as a binding partner of the VWF A1 domain, which binds to platelet GPIIb/IIIa.^{43,44} A mutation in the human neutrophil antigen 3 (HNA3) epitope on SLC44A2 is involved in immune diseases,⁴⁵⁻⁴⁷ and the same variant is associated with venous

thrombosis.^{37,48} The role of neutrophils and platelets and their interactions in venous thrombosis has previously been investigated, however, the results are inconclusive and highly depend on the experimental model used.⁴⁹⁻⁵¹ The role of SLC44A2 herein is still unknown and needs to be explored further.

HFpEF: a disease with a complicated and poorly recognized aetiology

Heart failure is a complex disease with a high prevalence, incidence and mortality (Figure 1 and reference⁵²) and is often preceded by and accompanied with other (metabolic) syndromes, such as hypertension, type 2 diabetes mellitus, and obesity.⁵³ More than half of the patients suffer from the subtype heart failure with preserved ejection fraction (HFpEF), presenting structural and functional cardiac alterations.⁵⁴ Treatment of HFpEF is still inadequate partially due to the underlying pathophysiology which is complex and not completely understood.^{53,55} HFpEF patients usually display a pro-inflammatory state involving leukocyte activation and endothelial dysfunction.^{56,57} Vascular inflammation is a main focus of mechanistic HFpEF research, making it remarkable that the *ex vivo* role of platelets herein has not yet been investigated, despite their known inflammatory functions.

GWAS and network biology: generation and analysis of big data

The high global burden of, amongst others, the diseases displayed in Figure 1 and the lack of effective treatment and/or mechanistic knowledge, requires a different research approach. The invention of high-throughput technologies, such as GWAS and ‘-omics’ techniques, and emergence of digitization has resulted in the generation of large and complex datasets, also referred to as ‘big data’.⁵⁸ In GWAS, the entire genome of a study group with a specific phenotype or disease is studied and compared to a control group to identify single nucleotide polymorphisms (SNPs) associated with the phenotype or disease.^{59,60} The use of GWAS has mainly been implemented in cardiovascular diseases,⁶¹⁻⁶³ but is also being used in investigating cancer and other diseases.⁶⁴

In addition to GWAS, the use of ‘-omics’ technologies in cardiovascular research, including platelet research, is expanding.^{34,65-69} A powerful tool to analyse the large datasets generated by these technologies is network biology. Network biology can be defined in multiple ways.⁷⁰⁻⁷² In contrast to computational modelling and simulations, the application of network and pathway analysis in haemostasis is still limited, although increasing.⁷³⁻⁷⁷ Using open sources such as PlateletWeb, Reactome, Gene Ontology and Cytoscape, one can create a clear and structured visualization of their own datasets.⁷⁸⁻⁸¹ This does not only make big data analysis more approachable, but also allows prediction of new therapeutic targets. Together, this creates a vast opportunity to pursue open research questions.

Aims and outline of this thesis

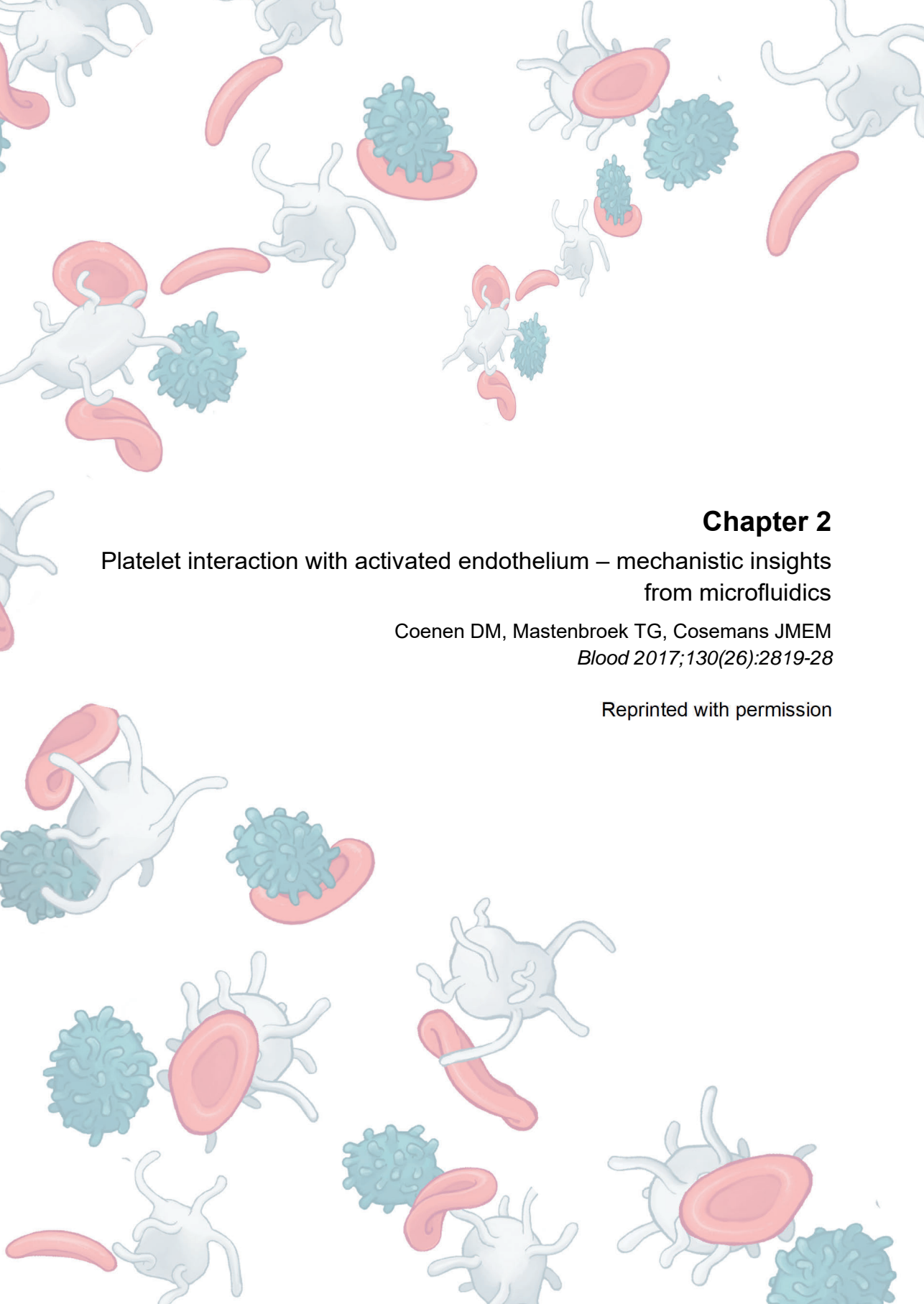
In this thesis, we aimed to provide novel insight into the inflammatory and haemostatic functions of platelets by making use of emerging technologies. Emphasis is placed on the involved signalling pathways and the interaction with endothelial cells and leukocytes. In *Chapter 1*, relevant background information is given regarding the main subjects of this thesis, in combination with a brief introduction about the known role of all factors involving platelet activation in a thrombotic or inflammatory environment. *Chapter 2* provides an in-depth mechanistic overview of the interactions between platelets and the activated endothelium, integrated with essential methodological variables of microfluidic studies. In *Chapter 3*, the role of platelets in atherosclerosis is described, from atherosclerosis initiation and plaque formation, to plaque rupture and atherothrombosis, and eventually plaque healing. *Chapter 4* gives new insights into the effects of platelet phosphodiesterase 3 and -5 inhibition in thrombo-inflammatory conditions. Of particular importance herein are pro-coagulant and pro-inflammatory platelet responses via the secretion of chemokines and extracellular vesicles. The effects of anti-platelet medication on the release of platelet-derived chemokines and on monocyte migration are further discussed in *Chapter 5*. In *Chapter 6*, endothelial-, leukocyte- and platelet (dys)function are determined in patients with HFpEF, a disease in which vascular inflammation plays an important, but yet undefined role. In particular, determination of platelet activation and the stratification for type 2 diabetes mellitus might contribute to a better understanding of HFpEF pathophysiology and the involvement of comorbidities. *Chapter 7* aims to identify the role of a newly identified gene in venous thrombosis. Using different murine thrombosis models, this study aims to shed light on the role of SLC44A2 in venous thrombosis and the involvement of platelets and neutrophils herein. *Chapter 8* highlights the use of network analyses in order to have a comprehensive look into signalling pathways and revealing possible new targets or processes important in platelet activation. In the final *Chapter 9*, the most important findings of this thesis are critically discussed in relation to the literature.

References

1. Kaplan ZS, Jackson SP. The role of platelets in atherothrombosis. *Hematology Am Soc Hematol Educ Program*. 2011;2011:51-61.
2. Versteeg HH, Heemskerk JW, Levi M, et al. New fundamentals in hemostasis. *Physiol Rev*. 2013;93(1):327-58.
3. Libby P, Buring JE, Badimon L, et al. Atherosclerosis. *Nat Rev Dis Primers*. 2019;5(1):56.
4. Weyrich AS, Lindemann S, Zimmerman GA. The evolving role of platelets in inflammation. *J Thromb Haemost*. 2003;1(9):1897-905.
5. Projahn D, Koenen RR. Platelets: key players in vascular inflammation. *J Leukoc Biol*. 2012;92(6):1167-75.
6. van Gils JM, Zwaginga JJ, Hordijk PL. Molecular and functional interactions among monocytes, platelets, and endothelial cells and their relevance for cardiovascular diseases. *J Leukoc Biol*. 2009;85(2):195-204.
7. Dunlay SM, Roger VL, Redfield MM. Epidemiology of heart failure with preserved ejection fraction. *Nat Rev Cardiol*. 2017;14(10):591-602.
8. Lam CSP, Gamble GD, Ling LH, et al. Mortality associated with heart failure with preserved vs. reduced ejection fraction in a prospective international multi-ethnic cohort study. *Eur Heart J*. 2018;39(20):1770-80.
9. Roth GA, Mensah GA, Johnson CO, et al. Global burden of cardiovascular diseases and risk factors, 1990-2019: update from the GBD 2019 study. *J Am Coll Cardiol*. 2020;76(25):2982-3021.
10. Benjamin EJ, Virani SS, Callaway CW, et al. Heart disease and stroke statistics-2018 update: a report from the American heart association. *Circulation*. 2018;137(12):e67-e492.
11. Raskob GE, Angchaisuksiri P, Blanco AN, et al. Thrombosis: a major contributor to global disease burden. *Arterioscler Thromb Vasc Biol*. 2014;34(11):2363-71.
12. NÆSs IA, Christiansen SC, Romundstad P, et al. Incidence and mortality of venous thrombosis: a population-based study. *J Thromb Haemost*. 2007;5(4):692-9.
13. Kyrle PA, Rosendaal FR, Eichinger S. Risk assessment for recurrent venous thrombosis. *Lancet*. 2010;376(9757):2032-9.
14. Kramer MC, van der Wal AC, Koch KT, et al. Presence of older thrombus is an independent predictor of long-term mortality in patients with ST-elevation myocardial infarction treated with thrombus aspiration during primary percutaneous coronary intervention. *Circulation*. 2008;118(18):1810-6.
15. Rittersma SZ, van der Wal AC, Koch KT, et al. Plaque instability frequently occurs days or weeks before occlusive coronary thrombosis: a pathological thrombectomy study in primary percutaneous coronary intervention. *Circulation*. 2005;111(9):1160-5.
16. Jenne CN, Urrutia R, Kubes P. Platelets: bridging hemostasis, inflammation, and immunity. *Int J Lab Hematol*. 2013;35(3):254-61.
17. Coppinger JA, Cagney G, Toomey S, et al. Characterization of the proteins released from activated platelets leads to localization of novel platelet proteins in human atherosclerotic lesions. *Blood*. 2004;103(6):2096-104.
18. Offermanns S. Activation of platelet function through G protein-coupled receptors. *Circ Res*. 2006;99(12):1293-304.
19. Mastenbroek TG, van Geffen JP, Heemskerk JW, et al. Acute and persistent platelet and coagulant activities in atherothrombosis. *J Thromb Haemost*. 2015;13 Suppl 1:S272-80.
20. Randriamboavonjy V, Fleming I. Platelet communication with the vascular wall: role of platelet-derived microparticles and non-coding RNAs. *Clin Sci (Lond)*. 2018;132(17):1875-88.
21. Bakogiannis C, Sachse M, Stamatielopoulou K, et al. Platelet-derived chemokines in inflammation and atherosclerosis. *Cytokine*. 2019;122:154157.
22. Duchene J, von Hundelshausen P. Platelet-derived chemokines in atherosclerosis. *Hamostaseologie*. 2015;35(2):137-41.
23. Karshovska E, Weber C, von Hundelshausen P. Platelet chemokines in health and disease. *Thromb Haemost*. 2013;110(5):894-902.
24. Mastenbroek TG, Feijge MA, Kremers RM, et al. Platelet-associated matrix metalloproteinases regulate thrombus formation and exert local collagenolytic activity. *Arterioscler Thromb Vasc Biol*. 2015;35(12):2554-61.
25. Dickhout A, Koenen RR. Extracellular vesicles as biomarkers in cardiovascular disease: chances and risks. *Front Cardiovasc Med*. 2018;5:113.
26. van der Pol E, Sturk A, van Leeuwen T, et al. Standardization of extracellular vesicle measurements by flow cytometry through vesicle diameter approximation. *J Thromb Haemost*. 2018;16(6):1236-45.

27. Ferreira PM, Bozbas E, Tannetta SD, et al. Mode of induction of platelet-derived extracellular vesicles is a critical determinant of their phenotype and function. *Sci Rep*. 2020;10(1):18061.
28. Puhm F, Boilard E, Machlus KR. Platelet extracellular vesicles: beyond the blood. *Arterioscler Thromb Vasc Biol*. 2021;41(1):87-96.
29. Boulanger CM, Loyer X, Rautou PE, et al. Extracellular vesicles in coronary artery disease. *Nat Rev Cardiol*. 2017;14(5):259-72.
30. Erdbrugger U, Le TH. Extracellular vesicles in renal diseases: more than novel biomarkers? *J Am Soc Nephrol*. 2016;27(1):12-26.
31. Guo SC, Tao SC, Yin WJ, et al. Exosomes derived from platelet-rich plasma promote the re-epithelization of chronic cutaneous wounds via activation of YAP in a diabetic rat model. *Theranostics*. 2017;7(1):81-96.
32. Hayon Y, Dashevsky O, Shai E, et al. Platelet microparticles induce angiogenesis and neurogenesis after cerebral ischemia. *Curr Neurovasc Res*. 2012;9(3):185-92.
33. Melki I, Tessandier N, Zufferey A, et al. Platelet microvesicles in health and disease. *Platelets*. 2017;28(3):214-21.
34. Downes K, Megy K, Duarte D, et al. Diagnostic high-throughput sequencing of 2396 patients with bleeding, thrombotic, and platelet disorders. *Blood*. 2019;134(23):2082-91.
35. Peyvandi F, Jayandharan G, Chandry M, et al. Genetic diagnosis of haemophilia and other inherited bleeding disorders. *Haemophilia*. 2006;12 Suppl 3:82-9.
36. Rosendaal FR, Reitsma PH. Genetics of venous thrombosis. *J Thromb Haemost*. 2009;7 Suppl 1:301-4.
37. Germain M, Chasman DI, de Haan H, et al. Meta-analysis of 65,734 individuals identifies TSPAN15 and SLC44A2 as two susceptibility loci for venous thromboembolism. *Am J Hum Genet*. 2015;96(4):532-42.
38. Germain M, Saut N, Greliche N, et al. Genetics of venous thrombosis: insights from a new genome wide association study. *PLoS One*. 2011;6(9):e25581.
39. Hinds DA, Buil A, Ziemek D, et al. Genome-wide association analysis of self-reported events in 6135 individuals and 252 827 controls identifies 8 loci associated with thrombosis. *Hum Mol Genet*. 2016;25(9):1867-74.
40. Tregouet DA, Heath S, Saut N, et al. Common susceptibility alleles are unlikely to contribute as strongly as the FV and ABO loci to VTE risk: results from a GWAS approach. *Blood*. 2009;113(21):5298-303.
41. Flesch BK, Wesche J, Berthold T, et al. Expression of the CTL2 transcript variants in human peripheral blood cells and human tissues. *Transfusion*. 2013;53(12):3217-23.
42. Kommareddi PK, Nair TS, Thang LV, et al. Isoforms, expression, glycosylation, and tissue distribution of CTL2/SLC44A2. *Protein J*. 2010;29(6):417-26.
43. Bayat B, Tjahjono Y, Berghofer H, et al. Choline Transporter-Like Protein-2: New von Willebrand Factor-Binding Partner Involved in Antibody-Mediated Neutrophil Activation and Transfusion-Related Acute Lung Injury. *Arterioscler Thromb Vasc Biol*. 2015;35(7):1616-22.
44. Ruggeri ZM. Structure of von Willebrand factor and its function in platelet adhesion and thrombus formation. *Best Pract Res Clin Haematol*. 2001;14(2):257-79.
45. Nair TS, Kozma KE, Hoefling NL, et al. Identification and characterization of choline transporter-like protein 2, an inner ear glycoprotein of 68 and 72 kDa that is the target of antibody-induced hearing loss. *J Neurosci*. 2004;24(7):1772-9.
46. Storch EK, Hillyer CD, Shaz BH. Spotlight on pathogenesis of TRALI: HNA-3a (CTL2) antibodies. *Blood*. 2014;124(12):1868-72.
47. Greinacher A, Wesche J, Hammer E, et al. Characterization of the human neutrophil alloantigen-3a. *Nat Med*. 2010;16(1):45-8.
48. Reil A, Wesche J, Greinacher A, et al. Geno- and phenotyping and immunogenicity of HNA-3. *Transfusion*. 2011;51(1):18-24.
49. Heestermans M, Salloum-Asfar S, Streef T, et al. Mouse venous thrombosis upon silencing of anticoagulants depends on tissue factor and platelets, not FXII or neutrophils. *Blood*. 2019;133(19):2090-9.
50. von Bruhl ML, Stark K, Steinhart A, et al. Monocytes, neutrophils, and platelets cooperate to initiate and propagate venous thrombosis in mice in vivo. *J Exp Med*. 2012;209(4):819-35.
51. Wolberg AS, Rosendaal FR, Weitz JI, et al. Venous thrombosis. *Nat Rev Dis Primers*. 2015;1:15006.
52. Nair N. Epidemiology and pathogenesis of heart failure with preserved ejection fraction. *Rev Cardiovasc Med*. 2020;21(4):531-40.
53. Tanai E, Frantz S. Pathophysiology of Heart Failure. *Compr Physiol*. 2015;6(1):187-214.

54. Oren O, Goldberg S. Heart Failure with Preserved Ejection Fraction: Diagnosis and Management. *Am J Med.* 2017;130(5):510-6.
55. Borlaug BA, Paulus WJ. Heart failure with preserved ejection fraction: pathophysiology, diagnosis, and treatment. *Eur Heart J.* 2011;32(6):670-9.
56. Cuijpers I, Simmonds SJ, van Bilsen M, et al. Microvascular and lymphatic dysfunction in HFpEF and its associated comorbidities. *Basic Res Cardiol.* 2020;115(4):39.
57. Simmonds SJ, Cuijpers I, Heymans S, et al. Cellular and Molecular Differences between HFpEF and HFrEF: a step ahead in an improved pathological understanding. *Cells.* 2020;9(1).
58. Fillinger S, de la Garza L, Peltzer A, et al. Challenges of big data integration in the life sciences. *Anal Bioanal Chem.* 2019;411(26):6791-800.
59. Hirschhorn JN, Daly MJ. Genome-wide association studies for common diseases and complex traits. *Nat Rev Genet.* 2005;6(2):95-108.
60. Manolio TA. Genomewide association studies and assessment of the risk of disease. *N Engl J Med.* 2010;363(2):166-76.
61. Ikram MA, Seshadri S, Bis JC, et al. Genomewide association studies of stroke. *N Engl J Med.* 2009;360(17):1718-28.
62. Kathiresan S, Srivastava D. Genetics of human cardiovascular disease. *Cell.* 2012;148(6):1242-57.
63. Small AM, O'Donnell CJ, Damrauer SM. Large-Scale Genomic Biobanks and Cardiovascular Disease. *Curr Cardiol Rep.* 2018;20(4):22.
64. Buniello A, MacArthur JAL, Cerezo M, et al. The NHGRI-EBI GWAS catalog of published genome-wide association studies, targeted arrays and summary statistics 2019. *Nucleic Acids Res.* 2019;47(D1):D1005-D12.
65. Beck F, Geiger J, Gambaryan S, et al. Temporal quantitative phosphoproteomics of ADP stimulation reveals novel central nodes in platelet activation and inhibition. *Blood.* 2017;129(2):e1-e12.
66. Burkhart JM, Vaudel M, Gambaryan S, et al. The first comprehensive and quantitative analysis of human platelet protein composition allows the comparative analysis of structural and functional pathways. *Blood.* 2012;120(15):e73-82.
67. Lau E, Wu JC. Omics, big data, and precision medicine in cardiovascular sciences. *Circ Res.* 2018;122(9):1165-8.
68. Loosse C, Swieringa F, Heemskerk JWM, et al. Platelet proteomics: from discovery to diagnosis. *Expert Rev Proteomics.* 2018;15(6):467-76.
69. Macaulay IC, Carr P, Gusnanto A, et al. Platelet genomics and proteomics in human health and disease. *J Clin Invest.* 2005;115(12):3370-7.
70. Altaf-Ul-Amin M, Afendi FM, Kiboi SK, et al. Systems biology in the context of big data and networks. *Biomed Res Int.* 2014;2014:428570.
71. Cavill R, Jennen D, Kleinjans J, et al. Transcriptomic and metabolomic data integration. *Brief Bioinform.* 2016;17(5):891-901.
72. Kitano H. Systems biology: a brief overview. *Science.* 2002;295(5560):1662-4.
73. Baaten C, Meacham S, de Witt SM, et al. A synthesis approach of mouse studies to identify genes and proteins in arterial thrombosis and bleeding. *Blood.* 2018;132(24):e35-e46.
74. Belyaev AV, Dunster JL, Gibbins JM, et al. Modeling thrombosis in silico: frontiers, challenges, unresolved problems and milestones. *Phys Life Rev.* 2018;26-27:57-95.
75. Chen Y, Corey SJ, Kim OV, et al. Systems biology of platelet-vessel wall interactions. *Adv Exp Med Biol.* 2014;844:85-98.
76. Diamond SL. Systems analysis of thrombus formation. *Circ Res.* 2016;118(9):1348-62.
77. Nagy M, van Geffen JP, Stegner D, et al. Comparative analysis of microfluidics thrombus formation in multiple genetically modified mice: link to thrombosis and hemostasis. *Front Cardiovasc Med.* 2019;6:99.
78. Boyanova D, Nilla S, Birschmann I, et al. PlateletWeb: a systems biologic analysis of signaling networks in human platelets. *Blood.* 2012;119(3):e22-34.
79. Croft D, Mundo AF, Haw R, et al. The Reactome pathway knowledgebase. *Nucleic Acids Res.* 2014;42(Database issue):D472-7.
80. Smoot ME, Ono K, Ruscheinski J, et al. Cytoscape 2.8: new features for data integration and network visualization. *Bioinformatics.* 2011;27(3):431-2.
81. The Gene Ontology Consortium. The Gene Ontology Resource: 20 years and still GOing strong. *Nucleic Acids Res.* 2019;47(D1):D330-D8.



Chapter 2

Platelet interaction with activated endothelium – mechanistic insights from microfluidics

Coenen DM, Mastenbroek TG, Cosemans JMEM
Blood 2017;130(26):2819-28

Reprinted with permission

Abstract

Traditionally, *in vitro* flow chamber experiments and *in vivo* arterial thrombosis studies have been proved to be of vital importance to elucidate the mechanisms of platelet thrombus formation after vessel wall injury. In recent years, it has become clear that platelets also act as modulators of inflammatory processes, such as atherosclerosis. A key element herein is the complex cross talk between platelets, the coagulation system, leukocytes, and the activated endothelium. This review provides insight into the platelet- endothelial interface, based on *in vitro* flow chamber studies and cross referenced with *in vivo* thrombosis studies. The main mechanisms of platelet interaction with the activated endothelium encompass **(1)** platelet rolling via interaction of platelet glycoprotein Ib-IX-V with endothelial-released von Willebrand factor with a supporting role for the P-selectin/P-selectin glycoprotein ligand 1 axis, followed by **(2)** firm platelet adhesion to the endothelium via interaction of platelet $\alpha_{IIb}\beta_3$ with endothelial $\alpha_v\beta_3$ and intercellular adhesion molecule 1, and **(3)** a stimulatory role for thrombin, the thrombospondin-1/CD36 axis and cyclooxygenase 1 in subsequent platelet activation and stable thrombus formation. In addition, the molecular mechanisms underlying the stimulatory effect of platelets on leukocyte transendothelial migration, a key mediator of atheroprogession, are discussed. Throughout the review, emphasis is placed on recommendations for setting up, reporting, interpreting, and comparing endothelial-lined flow chamber studies and suggestions for future studies.

Introduction

Under physiological conditions, platelets, the coagulation system and the endothelium function in favour of each other. Platelets maintain the integrity of the endothelium, while this endothelium releases nitric oxide and prostacyclin and expresses the ectonucleotidase CD39 to keep platelets in a resting state.¹ Additionally, platelets arrest bleeding (haemostasis) after vessel wall injury by forming a thrombus. Our understanding of the reactions leading to thrombus formation after injury of a healthy, non-atherosclerotic artery has been largely based on *in vitro* flow chamber studies with human and mouse blood and *in vivo* mouse studies, with the main processes being platelet activation, thrombin generation, and fibrin clot formation.² In spite of different characteristics of mouse platelets in comparison with human platelets, such as the lack of the protease activated receptor-1 (PAR1) receptor, an approximately twofold higher plasma concentration, and a shorter life span,³ the thrombus forming process of human and mouse platelets over surfaces coated with collagen occurs via similar mechanisms.^{4,5} Moreover, the experimental outcome of these flow chamber experiments correlates well with the outcome of *in vivo* arterial thrombosis models.⁶ Commonly used schemes of haemostasis start with platelet adhesion to von Willebrand factor (VWF), which is facilitated by the high shear rate at the arterial vessel wall. Subsequent activation of platelets is promoted by the release of paracrine mediators, like adenosine

diphosphate (ADP) and thromboxane.² Thrombin, generated at the surface of a subpopulation of pro-coagulant platelets and at disrupted subendothelial membranes, activates platelets and cleaves fibrinogen into fibrin,^{5,7} promoting thrombus growth and stabilization.⁴ Thrombin also activates a negative feedback loop to suppress its own generation by binding to endothelial-expressed thrombomodulin. Thrombomodulin-bound thrombin proteolytically activates the anticoagulant factor protein C, which is also bound to the endothelium via endothelial protein C receptor. Activated protein C inactivates coagulation factors Va and VIIIa leading to dampening of thrombin generation.²

Under inflammatory conditions, the cross talk between platelets, the coagulation system, and the endothelium is no longer favourable but is thought to exacerbate inflammation.^{8,9} Although some players in this cross talk have been identified, the puzzle is far from complete. A key aspect in the cross talk appears to be the stimulatory effect of platelets and platelet-derived microvesicles on leukocyte transendothelial migration, which is a known mediator of atheroprogession. Platelets interact via P-selectin with leukocyte P-selectin glycoprotein ligand 1 (PSGL-1). The platelet-leukocyte interaction is strengthened via interaction of leukocyte $\alpha_M\beta_2$ integrin with platelet receptors glycoprotein Ib (GPIb), junctional adhesion molecule A or junctional adhesion molecule C, or $\alpha_{IIb}\beta_3$ (via fibrinogen).¹⁰⁻¹³ Vice versa, leukocytes can secrete substances, like human neutrophil peptides,¹⁴ that induce platelet activation. An important consequence of these cellular interactions is platelet-, leukocyte-, and endothelial cell (EC)-granular secretion, leading to the release of soluble constituents and to an increased surface expression of membrane receptors, which fuels a complex and vicious pro-inflammatory circle. Interestingly, platelets can also actively deposit granular constituents on the inflamed endothelium, as demonstrated for the chemokines CCL5 (RANTES) and CXCL4 (platelet factor 4). The presence of CXCL4 was found to enhance the CCL5-induced arrest of leukocytes on activated ECs.¹⁵ For a more in-depth description about the role of chemokines in inflammatory and thrombotic processes, the authors refer to recent reviews by van der Vorst et al.,¹⁶ Koenen,¹⁷ and Soehlein et al..¹⁸

A true challenge for the future is not to obtain new pieces of the puzzle, but to integrate the mechanistic evidence and identify the main players in this cross talk in the human system. This review article provides a means to do so with regard to the direct cell-cell interactions between platelets and the endothelium.

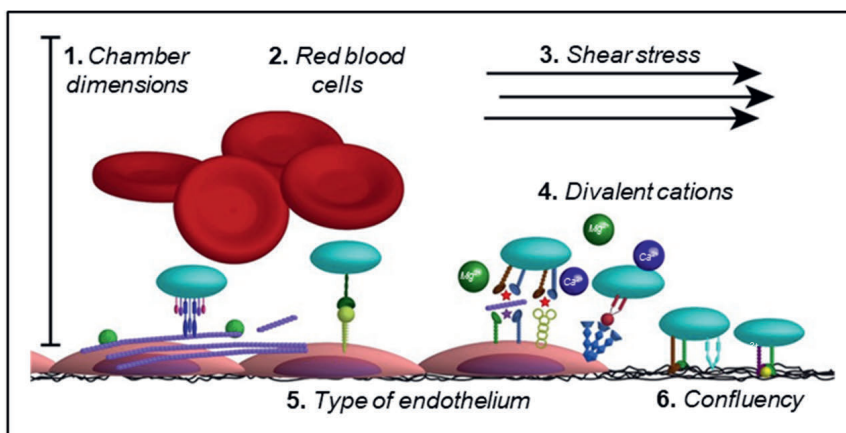


Figure 1. Key methodological variables in endothelial-lined flow chamber studies. Flexibility in flow chamber design has resulted in a range of different endothelial-lined flow chamber setups. Listed here are key variables between those studies: **(1)** Flow chamber dimensions: to achieve laminar flow, a height/width ratio of <0.2 is recommended. **(2)** Presence/absence of RBCs: RBCs are required for platelet margination and may influence the efficacy of certain antithrombotic agents, like dipyridamole. **(3)** Culturing of ECs under static or shear stress conditions: ECs change phenotype upon sensing mechanical stress; hence, culturing under shear stress is advised. **(4)** Presence/absence of Ca^{2+} and Mg^{2+} : physiological Ca^{2+} and Mg^{2+} levels are required for integrin function and for coagulation to take place. **(5)** Different EC sources: distinctive endothelial heterogeneity throughout the vasculature illustrates the importance of using an EC source appropriate to the research question. In addition, the expression level of several proteins that are involved in thrombus formation is affected by the passage number. **(6)** Confluency of EC layer: should be reported as a lack of confluency may trigger thrombus formation, because of exposure of subendothelial matrix components to the blood. Additional clarification is provided in the text. To enable comparison between studies, we encourage reporting the variables specified in this figure.

Status quo of endothelial-lined flow chamber studies: blood compartment

Flow chamber studies into mechanisms of platelet-endothelial interactions have been rapidly emerging over recent years. Although technical advances in microfluidics have increased flexibility in flow chamber design, this has also hampered standardization and comparison of results between studies.^{19,20} In this paragraph, key variables between flow chamber studies are listed, and it is explained how these variables could influence the platelet-endothelial interface (Figure 1). Strikingly, a major potential source of variation, flow channel dimension, is only reported in a minority of papers. Grosso modo platelets can undergo 2 types of interactions: platelet-platelet interactions and platelet-surface interactions. The transition between situations in which platelet-surface interactions or platelet-platelet interactions dominate is a function of channel size and aspect ratio (height/width) with values of <0.2 are being recommended to achieve constant shear stress, and thus laminar flow, across the middle of the adhesive surface.²⁰ Under these physiological conditions, red blood cells (RBCs) become centered in the middle of the vessel/flow chamber and push platelets towards the wall of the flow chamber (*i.e.* so-called platelet margination). Importantly, RBCs may also influence the efficacy of antithrombotic agents. For example, the antithrombotic effects of the

phosphodiesterase type 5 (PDE5) inhibitor dipyridamole are largely attributed to its inhibition of adenosine reuptake by RBCs and to a lesser extent to its inhibition of platelet PDE5.²¹ Hence, having RBCs present in the blood sample is of key importance to mimic the physiological process of platelet adhesion under flow, and, in general, superior to the use of platelet-rich plasma. The fact that there are no clear differences observed in study outcomes between studies with whole blood vs platelet-rich plasma (Table 1) does not impact the importance of having RBCs present, if only because several other factors also vary between these studies.

The type of anticoagulant used and in particular whether the anticoagulant does (e.g. citrate) or does not (e.g. hirudin, PPACK) remove divalent cations forms another potential source of variation. The adhesive properties of integrins $\alpha_2\beta_1$ and $\alpha_{IIb}\beta_3$ are quite sensitive to the extracellular levels of divalent cations, because of their Ca^{2+} and/ or Mg^{2+} binding domains, which control ligand binding.²² Indeed, Rataj et al.²³ reported reduced thrombus coverage in the presence of citrate when compared with heparin anticoagulated whole blood. Even with physiological Ca^{2+} and Mg^{2+} levels present (e.g. in heparin- anticoagulated blood), one has to be aware that, although integrin function is no longer impaired, the coagulation process is still blocked. As a consequence, the role of thrombin, a key protease in the coagulation cascade, and also a potent platelet activator, is not taken into account. Importantly, thrombin, and coagulation factors Xa, activated protein C, and the tissue factor/factor VIIa complex, also interact with PAR1 on the endothelium, thereby promoting the release of endothelial-derived VWF and the exposure of tissue factor and P-selectin at the endothelial surface.² Using a method where native non-anticoagulated whole blood was perfused directly from the vein of the donor through the flow chamber, Kirchhofer et al.²⁴ were the first to demonstrate that inhibition of thrombin led to greatly reduced platelet deposition, and fibrin deposition, on TNF- α -stimulated ECs under flow. Since then, to the best of our knowledge, only 2 groups have studied the contribution of the coagulation system to thrombus formation and/or channel occlusion in endothelium-lined flow chambers. Harris et al.²⁵ found a strong reduction in platelet surface area coverage and thrombus volume upon treatment of heparinized whole blood with the thrombin inhibitor bivalirudin, suggesting that anticoagulation with heparin did not suffice to block thrombin generation in this model where human blood was perfused over porcine ECs. Ciciliano et al.²⁶ recalcified citrated blood to allow coagulation to occur and observed reduced channel occlusion with hirudin and heparin in this setup. In contrast, in collagen-lined flow chambers the interplay between coagulation and platelets has been more extensively characterized, as reviewed elsewhere.⁵ The variables reported here (Figure 1) are not an exhaustive list, and other differences affect results, as reported elsewhere.²⁷⁻

Table 1. Reported involvement of platelet receptors and downstream signalling mediators in thrombus formation on inflamed or damaged endothelium

Target	Intervention	Flow chamber	Shear rate	EC source	EC treatment	Platelet source	Effect intervention on thrombus formation	Reference
α_s	CBL497 Ab	Parallel/plate	2.5 dynes/cm ²	HUVECs	Histamine	WPs, fixed	Platelet-VWF strings =	44*
α_a	Goh3 Ab	Parallel plate	150/s	HUVECs	Heat	WB	Platelet aggregate volume ↓	40
α_b	LM609 Ab	Parallel plate	2.5 dynes/cm ²	HUVECs	Histamine	WPs, fixed	Platelet-VWF strings = , VWF strings =	44*
α_β , α_β	Abciximab (7E3, ReoPro)	Parallel plate	1000/s	HUVECs	IFN- γ + TNF- α	WPs	Platelet SAC ↓	59
	Abciximab (7E3, ReoPro)	Parallel plate	50 dynes/cm ²	pPAECs	Serum	WB	Platelet SAC ↓	46
	Abciximab (7E3, ReoPro)	Parallel plate	750/s	HUVECs, fixated	TNF- α	WB	Platelet SAC ↓	34
	Abciximab (7E3, ReoPro)	Capillary, rectangular	100/s	pHUVECs	TNF- α + TGF- β	WPs + RBCs	Platelet SAC ↓	58
	Abciximab (7E3, ReoPro)	Bioflux 1000	5 dynes/cm ²	PAECs	Xenoactivation	WB	Platelet SAC, platelet aggregate volume ↓	25
	Abciximab (7E3, ReoPro)	Parallel plate	150/s	HUVECs	Heat	WB	Platelet aggregate volume ↓	40
	β_1 function neutralizing Ab	Capillary, rectangular	140/s	pHUVECs + pSMCs	TGF- β 1	WB	Platelet SAC ↓	47
α_β , β	Eptifibatid (Integrilin)	μ -slide VI	50/s	LECs	None	WB	Stable platelet-EC interactions = , platelet SAC ↑	71
	Eptifibatid (Integrilin)	Branching microchannel	1-4-, 10-40 dynes/cm ²	HUVECs	STX-2	WB	Platelet aggregate volume ↓, channel occlusion ↓	60
	Eptifibatid (Integrilin)	Branching microchannel	4 dynes/cm ²	HUVECs	FeCl ₃	WB	Channel occlusion ↓	26
	Lotrafiban	μ -slide VI	50/s	LECs	None	WB, mouse	Platelet SAC =	71
	MA-16N7C2 Ab	Parallel plate	24 dynes/cm ²	Ea.hy926	PLPC	WB, rec.†	Platelet translocation = , number of adhered platelets ↓	43
	P2 mAb	SPAA	170/s	HUVECs	None	PRP, ADP stimulated	Platelet SAC ↓	57
	P2 mAb	Cone and plate, adapted	250/s	pBAECs	None	PRP, TRAP-6 stimulated	Number of adhered platelets ↓	56
	RGDS peptide	Parallel plate	2.5 dynes/cm ²	HUVECs	Histamine	WPs, fixed	Platelet-VWF strings ↓, VWF strings ↓	44*
	RGDS peptide	SPAA	170/s	HUVECs	None	PRP, ADP stimulated	Platelet SAC ↓	57
	Ro 43-8857	SPAA	170/s	HUVECs	None	PRP, ADP stimulated	Platelet SAC ↓	57
	TAK-029	Not indicated	10/s	HBECS	None	PRP, ADP stimulated	Number of adhered platelets ↓	85
	TAK-029	Not indicated	10/s	HAECS	None	PRP, ADP stimulated	Number of adhered platelets ↓	86
ADAMTS13	ADAMTS13 function neutralizing pAb	Capillary, rectangular	400/s	pHUVECs	TNF- α + TGF- β	WPs + RBCs	VWF strings ↑, platelets in VWF strings ↑	58
C5	Ecuzimab	Bioflux200	3, 10 dynes/cm ²	pPAECs	Xenoactivation	PRP	Platelet SAC ↓	23
	Ecuzimab	Bioflux200	3, 10 dynes/cm ²	GTKO/hCD46-pPAECs	Xenoactivation	PRP	Platelet SAC ↓	23
CD36	FA6.152 mAb	Laboratory-Tek1	100/s	Ea.hy926	TNF- α	WB, rec.	Platelet SAC ↓	65
CD47	Agonist 4N1K	Laboratory-Tek1	100/s	Ea.hy926	TNF- α	WB	Platelet SAC ↑	65
	B6H12 mAb	Parallel plate, Laboratory-Tek1	100/s	Ea.hy926	TNF- α	WB	Platelet SAC ↓	65
	Cd47 ^{-/-}	Parallel plate	100/s	Ea.hy926	TNF- α	WB, mouse	Platelet SAC ↓	65
CLEC-2	Clec2 ^{+/+}	μ -slide VI	50/s	LECS	None	WB, mouse	Platelet SAC ↓	71
COX-1	Aspirin	Branching microchannel	4 dynes/cm ²	HUVECs	FeCl ₃	WB	Channel occlusion ↓	26
F-actin	Cytochalasin D	μ -slide VI	50/s	LECS	None	WB	Platelet SAC ↓	71

Table 1. (continued)

Target	Intervention	Flow chamber	Shear rate	EC source	EC treatment	Platelet source	Effect intervention on thrombus formation	Reference
GPIIb/IIIa	6D1 Ab	Parallel plate	2.5 dynes/cm ²	HUVECs	Histamine	WPs, fixed	Platelet-VWF strings ↓, VWF strings =	44*
	AK2, SZ2 mAb's	Parallel plate	2 dynes/cm ²	pHUVECs	Histamine	WPs + RBCs	Platelet translocation ↓	33
	AK2 mAb	Parallel plate	2.5 dynes/cm ²	pHUVECs	Histamine	WPs	Platelet-VWF strings ↓	39
	AK2 mAb	Branching microchannel	10-30 dynes/cm ²	HUVECs	Shear	WB, rec.	Platelet adhesion ↓	45
	ATA	Parallel plate	50 dynes/cm ²	pPAECs	Serum	WB	Platelet SAC ↓	46
	G19H10 Ab	Parallel plate	24 dynes/cm ²	Ea.hy926	PLPC	WB, rec. †	Platelet translocation ↓, number of adhered platelets ↓	43
PAR-1	GPIIb function blocking Ab	Parallel plate	150/s	HUVECs	Heat	WB	Platelet aggregate volume ↓	40
	GPIIb function neutralizing Ab	Capillary, rectangular	140/s	pHUVECs + pSMCs	TGF-β1	WB	Platelet SAC ↓	47
	GUR20-5 Ab	Not indicated	10/s	HBECS	None	PRP, ADP stimulated	Number of adhered platelets =	85
	GUR20-5 Ab	Not indicated	10/s	HAECS	None	PRP, ADP stimulated	Number of adhered platelets =	86
	IL4-R/iba	Branching microchannel	4 dynes/cm ²	HUVECs	FeCl ₃	WB, mouse	Channel occlusion ↓	26
	SZ2 mAb	Parallel plate	1000/s	HUVECs	IFN-γ + TNF-α	WPs	Platelet SAC ↓	59
PAR-1	Agonist TRAP-6	Capillary, rectangular	100/s	pHUVECs	TNF-α + TGF-β	WPs + RBCs	Platelet SAC ↓	58
	Agonist TRAP-6	Parallel plate	310/s	Ea.hy926	None	WB, rec.	Number of adhered platelets ↑	48
	Agonist TRAP-6	Parallel plate	24 dynes/cm ²	Ea.hy926	PLPC	WB, rec. †	Platelet translocation ↓, number of adhered platelets ↓	43
P2X ₁	Agonist ATP	Rectangular	Not indicated	BPAECs	None	WPs	Number of adhered platelets [(ATP < 5.0 nM), ↑ (ATP > 1.0 nM)]	64
PDE/AR	Agonist RBC derived ATP	Rectangular	Not indicated	BPAECs	None	WPs + RBCs	Number of adhered platelets ↓	64
	Gibenciamide	Rectangular	Not indicated	BPAECs	None	WPs + RBCs	Number of adhered platelets ↑	64
	Theophylline	Capillary, rectangular	140/s	pHUVECs	TGF-β1	WB	Platelet SAC ↓	47
P-selectin	Agonist soluble P-selectin	Parallel plate	2.5 dynes/cm ²	HUVECs	Histamine	WPs, fixed	Platelet-VWF strings ↓, VWF strings =	44*
	AK-6 mAb	Cone and plate, adapted	250/s	pBAECs	None	PRP, TRAP-6 stimulated	Number of adhered platelets ↓	56
Rac	CLB-Thromb/6 mAb	Parallel plate	24 dynes/cm ²	Ea.hy926	PLPC	WB, rec. †	Platelet translocation ↓, number of adhered platelets ↓	43
	pAb	Parallel plate	2 dynes/cm ²	pHUVECs	Histamine	WPs + RBCs	Platelet translocation ↓	33
	pAb	Parallel plate	2.5 dynes/cm ²	HUVECs	Histamine	WPs, fixed	Platelet-VWF strings =, VWF strings =	44*
	WASP12.2	Not indicated	6 dynes/cm ²	HUVECs	TNF-α	WPs	Number of adherent platelets ↓	50
	EHT1864	μ-slide VI	50/s	LECS	None	WB	Platelet SAC =	71
	SE5A5 mAb	Laboratory-Tek 1	100/s	Ea.hy926	TNF-α	WB, rec.	Platelet SAC =	65
Src	Dasatinib	μ-slide VI	50/s	LECS	None	WB	Stable platelet-EC interactions ↓, platelet SAC ↓	71
	Dasatinib	μ-slide VI	50/s	LECS	None	WB, mouse	Platelet SAC ↓	71
Syk	PRT060318	μ-slide VI	50/s	LECS	None	WB	Stable platelet-EC interactions ↓, platelet SAC =	71
	Syk ^{-/-}	μ-slide VI	50/s	LECS	None	WB, mouse	Platelet SAC ↓	71

Table 1. (continued)

Target	Intervention	Flow chamber	Shear rate	EC source	EC treatment	Platelet source	Effect intervention on thrombus formation	Reference
Thrombin	Bivalirudin	Bioflux 1000	5 dynes/cm ²	PAECs	Xenoactivation	WB	Platelet SAC ↓, platelet aggregate volume ↓	25
	Hirudin, heparin	Branching microchannel	4 dynes/cm ²	HUVECs	FeCl ₃	WB	Channel occlusion ↓	26
	Ro 46-6240, hirudin, heparin	Parallel plate	65/s	pHUVECs	TNF- α	WB	Number of platelet aggregates ↓	24
VCAM-1	1-4C3 Ab	Capillary, rectangular	100/s	pHUVECs	TNF- α + TGF- β	WPs 1	Platelet SAC =	58
	6G1 mAb	Parallel plate	2.5 dynes/cm ²	pHUVECs	Histamine	WPs	Platelet-VWF strings ↓	39
VWF	AJW-2 Ab	Parallel plate	24 dynes/cm ²	Ea.hy928	PLPC	WB, rec.†	Platelet translocation ↓, number of adhered platelets ↓	43
	AJW-2 Ab	Not indicated	24 dynes/cm ²	Aorta, rabbit	Cholesterol diet	WB, rec.†	Platelet translocation ↓ number of adhered platelets ↓	43
VWD type 3	VWD type 3	Branching microchannel	4 dynes/cm ²	HUVECs	FeCl ₃	WB, rec.	Channel occlusion ↓	26

All platelet sources are of human origin unless indicated otherwise. Decreased (\downarrow); no change (=); increased (\uparrow).

Ab, antibody; ADAMTS13, a disintegrin and metalloproteinase with a thrombospondin type 1 motif, member 13; AR, adenosine receptor; ATA, aurin tricarboxylic acid; ATP, adenosine triphosphate; BPAEC, bovine pulmonary artery endothelial cell; C5, complement component; CLEC-2, c-type lectinlike receptor 2; COX-1, cyclooxygenase 1; GTKO/hCD46-pPAEC, alpha1.3-galactosyltransferase deficient/human CD46 transgenic-primary porcine aortic endothelial cell; HUVEC, human umbilical vein endothelial cell; HUVEEC, human umbilical vein endothelial cell; H-AEC, human aortic endothelial cell; HBEC, human brain microvascular endothelial cell; HUVEC, human umbilical vein endothelial cell; HUVEEC, primary human umbilical vein endothelial cell; mAb, monoclonal antibody; pAb, polyclonal antibody; PAEC, porcine aortic endothelial cell; pBAEC, primary bovine aortic endothelial cell; pHUVEC, primary human umbilical vein endothelial cell; PLPC, palmitoyllysophosphatidylcholine; PLCy2, phospholipase γ 2; PMA, phorbol-12-myristate-13-acetate; pPAEC, primary porcine aortic endothelial cell; PRP, platelet-rich plasma; pSMC, primary smooth muscle cell; rec., reconstituted; RGDS, arginine glycine asparagine serine; SAC, surface area coverage; SIRP- α , signal regulatory protein α ; SPAA, stagnation point flow adhesion-aggregometer; STX-2, shiga toxin 2; TGF- β 1, transforming growth factor β 1; TNF- α , tumour necrosis factor α ; TRAP-6, thrombin receptor-activating peptide 6; VCAM-1, vascular cell adhesion molecule 1; VWD, von Willebrand disease; WB, whole blood; WP, washed platelet.

*No statistics applied.

†Spiked with TRAP-6-activated platelets.

Status quo of endothelial-lined flow chamber studies: endothelial compartment

Regarding the endothelial compartment, the following key aspects often vary between studies: culturing of ECs under shear vs static conditions, the type of stimulus used to trigger EC activation, the source and passage number of ECs, and the confluency of the EC layer (Figure 1). ECs sense mechanical stresses through several proteins that are also involved in the interaction of ECs with platelets and leukocytes, for example, $\beta 2$ and $\beta 3$ integrins, platelet and endothelial cell adhesion molecule 1, vascular endothelial cadherin, G-protein coupled receptors, and the cytoskeleton itself,³⁰ triggering a differential regulation of ~3% to 6% of endothelial genes.³¹ Following a shear stress transcriptional response, initiated by these receptors, 3 major types of responses can occur in ECs: (1) a detrimental, immediate response leading to the induction of endothelial activation; (2) a protective, chronic response causing suppression of endothelial activation, anti-inflammatory effectors, and morphologic adaptation to flow; or (3) a dysfunctional response to disturbed stresses leading to endothelial activation, inflammation, and atherogenesis.³² TNF- α is the most frequently used EC stimulus in flow chamber studies (Suppl. Table 1). In response, ECs release VWF and present several effector proteins on their membrane, such as E-selectin, P-selectin, intercellular adhesion molecule 1 (ICAM-1), VCAM-1, and tissue factor.^{33,34} Alternatively, PMA, TGF- $\beta 1$, STX-2, IFN- γ , cholesterol, FeCl₃, and heat have been used to activate or damage the endothelium (Suppl. Table 1). To our knowledge, no comprehensive comparison of cellular changes in ECs has been made between these agonists.

Of those genes that are influenced by the shear stress transcriptional response, the following non-exhaustive subset is involved in haemostasis and thrombosis: thrombomodulin, tissue factor, endothelial nitric oxide synthase, platelet and endothelial cell adhesion molecule 1, VCAM-1, and P-selectin.³¹ By and large, a pattern of protective antithrombotic changes can be seen when the ECs are cultured under physiological laminar flow patterns, while changes in flow profiles during the experiment are pro-thrombotic and pro-atherogenic.³¹ Without flow, the long-term shear induced alterations to EC protein expression and phenotype will likely not present.³⁰ Altogether, the previously mentioned points advocate for culturing ECs under flow conditions that are representative for the vessel and the underlying (patho)physiology. Of note, not only shear stress, but also the interaction of platelets³⁵ or platelet-derived microRNAs^{36,37} with ECs can modulate EC gene expression.

It is important to note that there is distinctive endothelial heterogeneity throughout the vasculature, including differences in tissue factor pathway inhibitor (predominantly in the capillaries), endothelial protein C receptor (large veins and arteries), endothelial nitric oxide synthase (found mostly arterial), and VWF (predominantly present in the veins under physiological conditions).³⁸ The study by Dong et al³⁹ represents one of few studies where different sources of ECs were

examined in flow studies in a quantitative manner. They showed that the number of ultra-long VWF strings is EC source dependent, with fewer ultra-large VWF strings forming on human coronary artery endothelial cells and human lung microvascular endothelial cells, both used after 4 to 5 passages, than on primary HUVECs and human umbilical artery endothelial cells. It remains to be determined whether the difference in passage number underlies the decreased ultra-large VWF strings formation in human coronary artery endothelial cells and human lung microvascular endothelial cells, or whether this is related to an inherent difference in VWF production.

Measurements of cell viability and confluence of the EC layer are another set of meaningful quality controls. Because platelets can interact with the extracellular matrix on which ECs are seeded, a lack of confluence can affect the outcome of the study. An example of the latter is provided by Sylman et al.,⁴⁰ who used heat to activate ECs and found that the large contribution of α_6 to platelet aggregate formation in their model was because of exposure of the laminin-rich matrix after receding of the EC upon heat treatment. In addition, it is of relevance to report the passage number of the ECs used in the flow studies, because the expression level of several proteins that are involved in thrombus formation, such as galectin 1,^{41,42} are affected by the number of passages. Altogether, a main aim of this review is to increase awareness of the variables that may cause variation in flow chamber studies and to facilitate comparison between studies by reporting these variables.

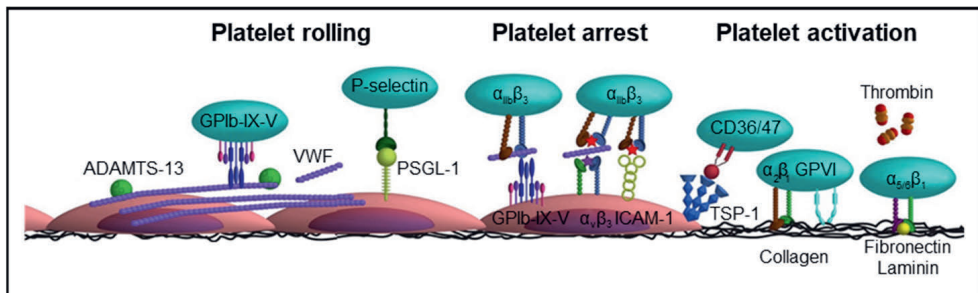


Figure 2. Schematic overview of the various interactions between platelet and endothelial surface molecules. Platelets interact with activated ECs via the following main mechanisms: **(1)** Platelet rolling via interaction of platelet GPIb-IX-V with endothelial-released VWF with a supporting role for the P-selectin/PSGL-1 axis. **(2)** Firm platelet adhesion to the endothelium via interaction of platelet $\alpha_{IIb}\beta_3$ with endothelial $\alpha_v\beta_3$ (via VWF, fibrinogen, fibronectin) and ICAM-1 (via fibrinogen). Alternatively, platelet $\alpha_{IIb}\beta_3$ can also interact with the endothelial GPIb-IX-V (via VWF). **(3)** A stimulatory role for thrombin and the thrombospondin-1 (TSP-1)/CD36 axis in platelet activation. More detailed information is provided in the text.

Mechanisms of platelet rolling over activated endothelium

To integrate the experimental data obtained from flow chamber studies into a unifying model of platelet-EC interaction, in this review, experimental data from flow studies were combined with knowledge obtained from *in vivo* thrombosis

studies. It is thought that the main mechanism of platelet rolling on the activated endothelium is mediated via interaction of platelet GPIb-IX-V complex with VWF,³⁵ with a supporting role for the P-selectin/PSGL-1 axis (Figure 2). Inhibition of GPIb α , in flow chamber experiments, resulted in a shear-dependent reduction in platelet translocation and binding to VWF strings^{33,39,43-45} and is accompanied by a reduction in platelet surface area coverage,^{46,47} aggregate volume,⁴⁰ and channel occlusion.²⁶ Similar results were obtained upon targeting the A1 domain of VWF,^{39,43} in the presence of VWF-free plasma²⁶ or upon desmopressin treatment of the endothelium.⁴⁸ This fits with the textbook knowledge that the contribution of platelet adhesion to immobilized VWF via GPIb-V-IX is considerably accelerated by high shear forces present in the arterial circulation, as a consequence of conformational changes in the immobilized VWF. Shear rate (per second) and shear stress (in dynes per square centimetre) are the 2 shear variables that are used in flow chamber studies. Shear rate is the rate at which adjacent layers of the blood are moving with respect to each other and increases while approaching the vessel wall. As platelet adhesion occurs at the vessel wall, wall shear rate is meant in this review when talking about shear rate. Shear stress is the (viscous) force of the blood applied on the vessel wall and is a linear function of the wall shear rate and the blood viscosity. For the major vessels of the human circulatory system, the wall shear rate can be compared with the shear stress (Figure 3). The variety in shear between the vessels is partly dependent on the diameter of the vessel (*i.e.* smaller blood vessels have a higher shear rate/stress than bigger blood vessels). An area for future research is to investigate whether platelets have a shear optimum when adhering to the endothelium and, if so, at which wall shear rate this optimum occurs.

In addition to VWF-GPIb, multiple *in vivo* and *in vitro* studies also show a role for both platelet PGSL-1 with endothelial P-selectin^{46,49} and platelet P-selectin with endothelial PSGL-1⁵⁰ in mediating platelet rolling and adhesion to activated endothelium. Antibodies against anti-P-selectin have been shown to reduce platelet translocation and binding to VWF strings,⁴⁴ platelet adhesion,⁵¹ and surface area covered⁴⁶ under both low shear (2.5 dynes/cm²) and high shear (50 dynes/cm², 1500/s) flow conditions (Table 1; Suppl. Table 2). Although platelets contain ~8900 copies of P-selectin per platelet,⁵² PSGL-1 was shown to be only present in small amounts on the platelet protein level.⁴⁹ Burkhardt et al.⁵² even failed to detect PGSL-1 in the human platelet proteome. Yet, the latter finding could be influenced by the fact that PSGL-1 is heavily glycosylated, which potentially hampers its digestion by trypsin, and hence the subsequent detection by mass spectrometry. PSGL-1 is functionally expressed, albeit at low levels, by ECs in certain organs under conditions of chronic inflammation.^{50,53} Furthermore, it has been suggested that activated platelets might also use the GPIb-IX-V complex as an alternative receptor for rolling over endothelial P-selectin.³³ Yet, to our knowledge, the latter study by Romo et al. received no follow up in literature so far, and a binding site for P-selectin on GPIb has not been reported. Moreover, inhibition of GPIb or P-selectin did not result in a complete inhibition of the adhesive potential of P-selectin or GPIb-expressing

Chinese hamster ovary cells.³³ Taken together, this points to a supporting role of the P-selectin/PSGL-1 axis in platelet-endothelium interaction, in particular under conditions where little VWF is present.

Mechanisms of platelet adhesion, activation, and thrombus formation on activated endothelium

Stable adhesion of platelets to the endothelium requires activation of integrins on the platelet and endothelial surface. A key player herein is platelet $\alpha_{IIb}\beta_3$ integrin (Table 1).⁵⁴ Its contribution to platelet adhesion and thrombus formation on activated endothelium was examined using a range of inhibitors that compete with the binding of VWF and fibrinogen to the integrin, often by (in)directly interacting with the RGD binding pockets of $\alpha_{IIb}\beta_3$.⁵⁵ Similar to blockage of GPIIb/IIIa, $\alpha_{IIb}\beta_3$ inhibition resulted in reduced platelet-containing VWF strings⁴⁴ accompanied by a reduction in platelet adhesion⁵⁶ and hence reduced platelet surface area coverage,^{25,34,46,47,57-59} platelet aggregate volume,⁴⁰ and channel occlusion^{26,60} (Table 1). Integrin $\alpha_{IIb}\beta_3$ interacts with the endothelium via the bridging molecules VWF, fibrinogen, and fibronectin, which can all bind to endothelial $\alpha_v\beta_3$ integrin. Inhibition of endothelial $\alpha_v\beta_3$ reduces stable platelet adhesion by ~50%, both under flowing⁶¹ and static conditions,^{62,63} suggesting the involvement of other receptors in mediation stable platelet-endothelial interactions. Indeed, endothelial ICAM-1, using fibrinogen as a bridging molecule, and endothelial GPIb-IX-V, via VWF, have also been shown to interact with platelet $\alpha_{IIb}\beta_3$ and mediate platelet adhesion (Figure 2).⁶²

Strikingly, the contribution of platelet receptors in the subsequent thrombus forming process has only investigated in a limited manner. So far, interventions into soluble platelet activation factors revealed the importance of the coagulation cascade, primarily via thrombin,²⁴⁻²⁶ but also of secondary feedback loops via cyclooxygenase 1²⁶ and of adenosine triphosphate-P2X₁ interaction⁶⁴ in mediating thrombus formation on activated endothelium. In addition, there appears to be a role for the TSP-1–CD36/CD47 axis in mediating platelet arrest.⁶⁵ Lagadec et al.⁶⁵ hypothesized that the interaction of TSP-1 with CD36 induces the exposition of the cell-binding domain of TSP-1, allowing its ligation with platelet CD47 and subsequent activation of platelet $\alpha_{IIb}\beta_3$ integrin. This fits with *in vitro* flow chamber and *in vivo* arterial thrombosis studies, which indicate a platelet activating and thrombus-stabilizing role for TSP-1, via CD36.^{66,67} Moreover, TSP-1 has also been shown to protect endothelium-bound VWF from ADAMTS13-mediated degradation, thereby further enhancing the dynamic recruitment of platelets into developing thrombi.⁶⁸ The observation that the TSP-1/CD36 interaction may also stimulate platelet activation by inhibition of the inhibitory cyclic adenosine monophosphate/cyclic guanosine monophosphate signalling pathways in platelets,^{69,70} and that TSP-1 is present in high amounts in the α -granules of platelets ($\pm 100,000$ copies/platelet),⁵² makes TSP-1 potentially a vital player in platelet activation and stable thrombus formation on inflamed endothelium.

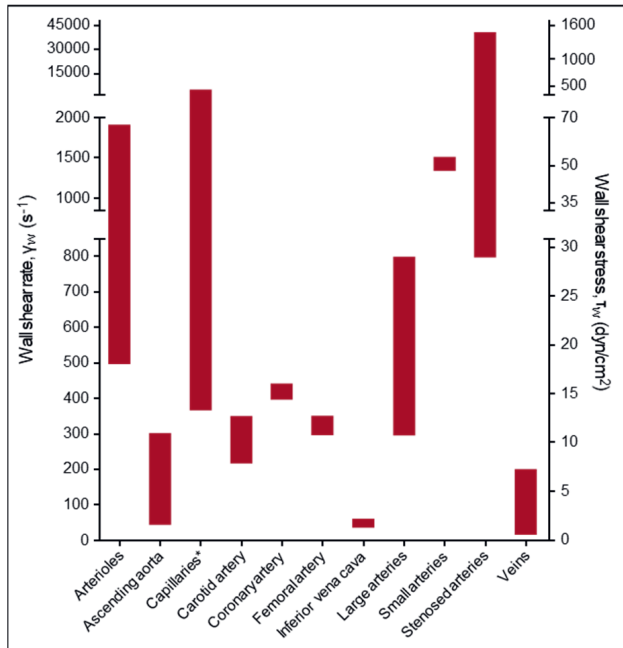


Figure 3. Wall shear rates and corresponding shear stresses in the vascular system. The data presented are from de Groot and Sixma⁸³ and Sakariassen et al.⁸⁴ assuming blood as a Newtonian fluid with a constant viscosity and a laminar flow. Asterisk indicates that shear stress is irrelevant because of microcirculatory blood flow.

Platelet interactions with ECs from lymphatic or xenogeneic origin

Beyond their well-known role as mediators of haemostasis and thrombosis, platelets are also involved in mouse embryonic lymphatic development. Intriguingly, platelet adhesion and activation to lymphatic ECs is regulated via a different mechanism to that in vascular ECs. Podoplanin, constitutively expressed by LECs but not present in vascular ECs, supports platelet arrest to LECs via interaction with platelet CLEC-2.⁷¹ The CLEC-2 receptor signals via a similar signalling pathway as GPVI,⁷ and inhibition of their downstream kinases Src and Syk reduces stable platelet-LEC interactions and platelet surface area coverage.⁷¹ Interestingly, although blockage of integrin $\alpha_{IIb}\beta_3$ did abolish aggregate formation on LECs, it also led to an increase in platelet surface area coverage. This latter is likely because of the fact that CLEC-2 levels in human platelets are much lower than those for $\alpha_{IIb}\beta_3$ (2000 vs 64,200–83,300 per platelet, respectively),⁵² and platelets thus preferentially bind to activated $\alpha_{IIb}\beta_3$, and form compact 3D aggregates, on LECs. Yet, upon blockage of $\alpha_{IIb}\beta_3$, platelets only adhere to podoplanin and form a homogeneous monolayer, which results in an increased surface area coverage. This example highlights that merely taking output parameters into account does not always adequately reflect the actual underlying process.

Endothelial-lined flow chamber studies have also been used as a model for xenograft rejection, showing an essential role for the complement system in platelet

interaction with ECs of xenogeneic origin.^{23,25,46} Whether perfusion of human blood over allogeneic ECs (*i.e.* from different individuals of the same species) also induces some activation of the complement system or not remains to be established. Briefly, Galbusera et al.⁴⁶ found that human serum induced porcine EC activation and thrombosis in a parallel plate flow chamber. The underlying mechanism involved complement-induced endothelial activation, with reactive oxygen species–triggered overexpression of endothelial-expressed P-selectin and $\alpha_v\beta_3$ as a consequence (Suppl. Table 2). This proposed mechanism was confirmed by Rataj et al.,²³ who demonstrated that blockage of complement factor 5 reduced platelet surface area coverage. In addition, Harris et al.²⁵ recently showed that galactose 1,3 α -galactose transferase–deficient porcine ECs resist hyperacute rejection and display a significant decrease in human platelet surface area coverage and aggregate volume when compared with wild-type porcine ECs. Combined, these findings from flow chamber studies on xenoactivation could be useful to assist with finding new strategies to control platelet activation and prevent xenograft rejection. This is relevant given the interest in xenotransplantation of pig organs into humans as a possible strategy to solve the current shortage of organs for human transplant.

Conclusion and future perspectives

Over recent years, technical advances have led to the development of a range of endothelial-lined flow chamber devices. In this review, we show that these devices hold promise in the field of haemostasis to provide insight into the main players in the cross talk between platelets, the coagulation system, leukocytes, and the endothelium. Although there is ample insight into the mechanisms underlying platelet rolling and arrest on activated endothelium (Figure 2), it remains obscure what happens after platelet adhesion. So far, the importance of the coagulation cascade, primarily via thrombin, and secondary feedback loops, among others via TSP-1, in mediating thrombus formation and stabilization on activated endothelium have been revealed. Of thrombi formed on collagen type I, it has been demonstrated that they consist of at least 3 platelet subpopulations: aggregating platelets with (reversible) integrin activation, pro-coagulant platelets exposing phosphatidylserine and binding coagulation factors, and contracting platelets with cell-cell contacts residing in the core of the thrombus.^{72,73} An open question is if, and to what extent, thrombus composition on activated endothelium differs from thrombus formation on collagen and between ECs from different vascular beds. Herein, an important technical challenge lies in including the coagulation system in endothelial-lined flow chamber studies in a controlled way. The study by Ciciliano et al.²⁶ is a solid attempt at this in recent years.

Recent technological advances in the flow chamber field partly stem from the high flexibility in design of microfluidics and have, among others, resulted in microfluidics that model the microvasculature^{60,74} or stenotic arteries.^{75,76} A multiparameter-based analysis of flow chamber experiments is another recent

development.⁷⁷ Overall, the different designs, setups, and analyses between flow chamber studies do not necessarily have to hamper comparison of experimental results, as long as key variables, such as flow channel dimensions, EC origin plus passage number, presence/absence of RBCs, and/or divalent cations Ca^{2+} and Mg^{2+} are routinely reported. Despite a good correlation between the experimental outcome of *in vitro* flow chamber experiments and *in vivo* arterial thrombosis studies,⁶ it is important to be aware of the characteristics of each model. For instance, the CLEC-2 ligand podoplanin is not present in vascular ECs but does become upregulated in the wall of the inferior vena cava during a murine model of deep vein thrombosis, modulating thrombosis.⁷⁸ In a vascular endothelial-lined flow chamber model this pro-thrombotic role of CLEC-2 would not be observed. Vice versa, flow chamber studies can provide insight into *in vivo* studies, for instance in the underlying mechanism of how FeCl_3 , a commonly used trigger of vascular damage, induces thrombosis.²⁶

Mechanistically, a rapidly emerging and in vogue topic is on the interactions of platelet-derived microparticles with the (activated) endothelium and the short- and long-term cellular effects of these interactions.⁷⁹ In addition, studies into the role of the glycocalyx in platelet-endothelial interactions,⁸⁰ post-thrombotic processes such as fibroblast infiltration into the thrombus,⁸¹ and platelet-dependent matrix degradation⁸² provide promising avenues to provide novel mechanistic insight.

In sum, in the short-term endothelial-lined flow chamber studies are suited to increase our knowledge of the mechanisms underlying platelet activation and thrombus formation on activated endothelium. In the long term, they hold promise for opening up new investigatory paths to find targets that are only involved in the interplay of vascular cells and haemostatic cells in pathological chronic conditions such as diabetes and atherosclerosis.

Acknowledgments

The authors are grateful to R. Koenen (Maastricht University) and M. T. Harper (Cambridge University, Cambridge, United Kingdom) for providing valuable suggestions and critical reading of the manuscript. This work was supported by grants from the Dutch Heart Foundation (2015T79) (D.M.C., T.G.M., and J.M.E.M.C.) and the Netherlands Organization for Scientific Research (NWO Vidi 016.156.421) (J.M.E.M.C.).

Authorship

Contribution: D.M.C., T.G.M., J.M.E.M.C. analysed literature and wrote the manuscript. Conflict-of-interest disclosure: The authors declare no competing financial interests. Correspondence: Judith M. E. M. Cosemans, Maastricht University, Universiteitssingel 50, 6200 MD Maastricht, The Netherlands; e-mail: judith.cosemans@maastrichtuniversity.nl

References

1. Smolenski A. Novel roles of cAMP/cGMP- dependent signaling in platelets. *J Thromb Haemost.* 2012;10(2):167-76.
2. Versteeg HH, Heemskerk JW, Levi M, et al. New fundamentals in hemostasis. *Physiol Rev.* 2013;93(1):327-58.
3. Weiss DJ. Comparative physiology of platelets from different species. In: Rao FHR, ed. *Handbook of Platelet Physiology and Pharmacology.* New York, NY: Springer;1999: 379-93.
4. Cosemans JM, Angelillo-Scherrer A, Mattheij NJ, et al. The effects of arterial flow on platelet activation, thrombus growth, and stabilization. *Cardiovasc Res.* 2013;99(2):342-52.
5. de Witt SM, Verdoold R, Cosemans JM, et al. Insights into platelet-based control of coagulation. *Thromb Res.* 2014;133 Suppl 2:S139-48.
6. de Witt SM, Nergiz-Ünal N, Feijge MA, et al. Genes in arterial thrombus formation: a comparison of in vivo and in vitro studies. *J Thromb Haemost.* 2013;11 Suppl 2:352-53.
7. Heemskerk JW, Mattheij NJ, Cosemans JM. Platelet-based coagulation: different populations, different functions. *J Thromb Haemost.* 2013;11(1):2-16.
8. Kalz J, ten Cate H, Spronk HM. Thrombin generation and atherosclerosis. *J Thromb Thrombolysis.* 2014;37(1):45-55.
9. Mastenbroek TG, van Geffen JP, Heemskerk JW, et al. Acute and persistent platelet and coagulant activities in atherothrombosis. *J Thromb Haemost.* 2015;13 Suppl 1:S272-80.
10. Weber C, Springer TA. Neutrophil accumulation on activated, surface-adherent platelets in flow is mediated by interaction of Mac-1 with fibrinogen bound to $\alpha_{IIb}\beta_3$ and stimulated by platelet-activating factor. *J Clin Invest.* 1997;100(8):2085-93.
11. Santoso S, Sachs UJ, Kroll H, et al. The junctional adhesion molecule 3 (JAM-3) on human platelets is a counterreceptor for the leukocyte integrin Mac-1. *J Exp Med.* 2002;196(5):679-91.
12. Wang Y, Sakuma M, Chen Z, et al. Leukocyte engagement of platelet glycoprotein Iba via the integrin Mac-1 is critical for the biological response to vascular injury. *Circulation.* 2005;112(19):2993-3000.
13. Zhao Z, Vajen T, Karshovska E, et al. Deletion of junctional adhesion molecule A from platelets increases early-stage neointima formation after wire injury in hyperlipidemic mice. *J Cell Mol Med.* 2017;21(8):1523-31.
14. Quinn KL, Henriques M, Tabuchi A, et al. Human neutrophil peptides mediate endothelial-monocyte interaction, foam cell formation, and platelet activation. *Arterioscler Thromb Vasc Biol.* 2011;31(9):2070-9.
15. von Hundelshausen P, Koenen RR, Sack M, et al. Heterophilic interactions of platelet factor 4 and RANTES promote monocyte arrest on endothelium. *Blood.* 2005;105(3):924-30.
16. van der Vorst EP, Döring Y, Weber C. Chemokines. *Arterioscler Thromb Vasc Biol.* 2015;35(11):e52-6.
17. Koenen RR. The prowess of platelets in immunity and inflammation. *Thromb Haemost.* 2016;116(4): 605-12.
18. Soehnlein O, Steffens S, Hidalgo A, et al. Neutrophils as protagonists and targets in chronic inflammation. *Nat Rev Immunol.* 2017;17(4):248-61.
19. Westein E, de Witt S, Lamers M, et al. Monitoring in vitro thrombus formation with novel microfluidic devices. *Platelets.* 2012;23(7):501-9.
20. McCarty OJ, Ku D, Sugimoto M, et al. Dimensional analysis and scaling relevant to flow models of thrombus formation: communication from the SSC of the ISTH. *J Thromb Haemost.* 2016;14(3):619-22.
21. Gesele P, Arnout J, Deckmyn H, et al. Mechanism of the antiplatelet action of dipyridamole in whole blood: modulation of adenosine concentration and activity. *Thromb Haemost.* 1986;55(1):12-8.
22. Cosemans JM, Iserbyt BF, Deckmyn H, et al. Multiple ways to switch platelet integrins on and off. *J Thromb Haemost.* 2008;6(8):1253-61.
23. Rataj D, Werwitzke S, Haarmeijer B, et al. Inhibition of complement component C5 prevents clotting in an ex vivo model of xenogeneic activation of coagulation. *Xenotransplantation.* 2016;23(2):117-27.
24. Kirchofer D, Tschopp TB, Hadváry P, et al. Endothelial cells stimulated with tumor necrosis factor- α express varying amounts of tissue factor resulting in in homogenous fibrin deposition in a native blood flow system. Effects of thrombin inhibitors. *J Clin Invest.* 1994;93(5): 2073-83.
25. Harris DG, Benipal PK, Cheng X, et al. III. Four-dimensional characterization of thrombosis in a live-cell, shear- flow assay: development and application to xenotransplantation. *PLoS One.* 2015;10(4):e0123015.

26. Ciciliano JC, Sakurai Y, Myers DR, et al. Resolving the multifaceted mechanisms of the ferric chloride thrombosis model using an interdisciplinary microfluidic approach. *Blood*. 2015;126(6):817-24.
27. Roest M, Reininger A, Zwaginga JJ, et al. Flow chamber-based assays to measure thrombus formation in vitro: requirements for standardization. *J Thromb Haemost*. 2011;9(11):2322-4.
28. Van Kruchten R, Cosemans JM, Heemskerk JW. Measurement of whole blood thrombus formation using parallel-plate flow chambers – a practical guide. *Platelets*. 2012;23(3):229-42.
29. Neeves KB, McCarty OJ, Reininger AJ, et al. Flow-dependent thrombin and fibrin generation in vitro: opportunities for standardization: communication from SSC of the ISTH. *J Thromb Haemost*. 2014;12(3):418-20.
30. Baeyens N, Bandyopadhyay C, Coon BG, et al. Endothelial fluid shear stress sensing in vascular health and disease. *J Clin Invest*. 2016;126(3):821-8.
31. Frueh J, Maimari N, Homma T, et al. Systems biology of the functional and dysfunctional endothelium. *Cardiovasc Res*. 2013;99(2): 334-41.
32. Resnick N, Yahav H, Shay-Salit A, et al. Fluid shear stress and the vascular endothelium: for better and for worse. *Prog Biophys Mol Biol*. 2003;81(3):177-99.
33. Romo GM, Dong JF, Schade AJ, et al. The glycoprotein Ib-IX-V complex is a platelet counterreceptor for P-selectin. *J Exp Med*. 1999;190(6):803-14.
34. Jain A, van der Meer AD, Papa AL, et al. Assessment of whole blood thrombosis in a microfluidic device lined by fixed human endothelium. *Biomed Microdevices*. 2016;18:73.
35. Massberg S, Brand K, Grüner S, et al. A critical role of platelet adhesion in the initiation of atherosclerotic lesion formation. *J Exp Med*. 2002;196(7):887-96.
36. Gidlof O, van der Brug M, Ohman J, et al. Platelets activated during myocardial infarction release functional miRNA, which can be taken up by endothelial cells and regulate ICAM1 expression. *Blood*. 2013;121(19):3908-17.
37. Laffont B, Corduan A, Plé H, et al. Activated platelets can deliver mRNA regulatory Ago2•microRNA complexes to endothelial cells via microparticles. *Blood*. 2013;122(2):253-61.
38. Aird WC. Endothelium and haemostasis. *Hamostaseologie*. 2015;35(1):11-6.
39. Dong JF, Moake JL, Nolasco L, et al. ADAMTS-13 rapidly cleaves newly secreted ultra-large von Willebrand factor multimers on the endothelial surface under flowing conditions. *Blood*. 2002;100(12):4033-9.
40. Sylman JL, Artzer DT, Rana K, et al. A vascular injury model using focal heat-induced activation of endothelial cells. *Integr Biol*. 2015;7(7):801-14.
41. Thijssen VL, Hulsmans S, Griffioen AW. The galectin profile of the endothelium: altered expression and localization in activated and tumor endothelial cells. *Am J Pathol*. 2008;172(2):545-53.
42. Romaniuk MA, Croci DO, Lapponi MJ, et al. Binding of galectin-1 to $\alpha_{IIb}\beta_3$ integrin triggers "outside-in" signals, stimulates platelet activation, and controls primary hemostasis. *FASEB J*. 2012;26(7):2788-98.
43. Theilmeyer G, Michiels C, Spaepen E, et al. Endothelial von Willebrand factor recruits platelets to atherosclerosis-prone sites in response to hypercholesterolemia. *Blood*. 2002;99(12):4486-93.
44. Huang J, Roth R, Heuser JE, et al. Integrin $\alpha_v\beta_3$ on human endothelial cells binds von Willebrand factor strings under fluid shear stress. *Blood*. 2009;113(7):1589-97.
45. Zheng Y, Chen J, López JA. Flow-driven assembly of VWF fibres and webs in in vitro microvessels. *Nat Commun*. 2015;6:7858.
46. Galbusera M, Buelli S, Gastoldi S, et al. Activation of porcine endothelium in response to xenogeneic serum causes thrombosis independently of platelet activation. *Xenotransplantation*. 2005;12(2):110-20.
47. Kuckleburg CJ, Yates CM, Kalia N, et al. Endothelial cell-borne platelet bridges selectively recruit monocytes in human and mouse models of vascular inflammation. *Cardiovasc Res*. 2011;91(1):134-41.
48. Calmer S, Ferkau A, Larmann J, et al. Desmopressin (DDAVP) improves recruitment of activated platelets to collagen but simultaneously increases platelet endothelial interactions in vitro. *Platelets*. 2014;25(1):8-15.
49. Frenette PS, Denis CV, Weiss L, et al. P-selectin glycoprotein ligand 1 (PSGL-1) is expressed on platelets and can mediate platelet-endothelial interactions in vivo. *J Exp Med*. 2000;191(8):1413-22.
50. da Costa Martins P, García-Vallejo JJ, van Thienen JV, et al. P-selectin glycoprotein ligand-1 is expressed on endothelial cells and mediates monocyte adhesion to activated endothelium. *Arterioscler Thromb Vasc Biol*. 2007;27(5):1023-9.
51. Terrisse AD, Puech N, Allart S, et al. Internalization of microparticles by endothelial cells promotes platelet/endothelial cell interaction under flow. *J Thromb Haemost*. 2010;8(12):2810-9.

52. Burkhardt JM, Vaudel M, Gambaryan S, et al. The first comprehensive and quantitative analysis of human platelet protein composition allows the comparative analysis of structural and functional pathways. *Blood*. 2012;120(15):e73-82.
53. Rivera-Nieves J, Burcin TL, Olson TS, et al. Critical role of endothelial P-selectin glycoprotein ligand 1 in chronic murine ileitis. *J Exp Med*. 2006;203(4):907-17.
54. Massberg S, Schürzinger K, Lorenz M, et al. Platelet adhesion via glycoprotein IIb integrin is critical for atheroprotection and focal cerebral ischemia: an in vivo study in mice lacking glycoprotein IIb. *Circulation*. 2005;112(8):1180-8.
55. Coller BS. $\alpha_{IIb}\beta_3$: structure and function. *J Thromb Haemost*. 2015;13(suppl 1):S17-25.
56. Dardik R, Savion N, Kaufmann Y, et al. Thrombin promotes platelet-mediated melanoma cell adhesion to endothelial cells under flow conditions: role of platelet glycoproteins P-selectin and GPIIb-IIIa. *Br J Cancer*. 1998;77(12):2069-75.
57. Reininger AJ, Korndörfer MA, Wurzinger LJ. Adhesion of ADP-activated platelets to intact endothelium under stagnation point flow in vitro is mediated by the integrin $\alpha_{IIb}\beta_3$. *Thromb Haemost*. 1998;79(5):998-1003.
58. Tull SP, Anderson SI, Hughan SC, et al. Cellular pathology of atherosclerosis: smooth muscle cells promote adhesion of platelets to cocultured endothelial cells. *Circ Res*. 2006;98(1):98-104.
59. Schulz C, Schäfer A, Stolla M, et al. Chemokine fractalkine mediates leukocyte recruitment to inflammatory endothelial cells in flowing whole blood: a critical role for P-selectin expressed on activated platelets. *Circulation*. 2007;116(7):764-73.
60. Tsai M, Kita A, Leach J, et al. In vitro modeling of the microvascular occlusion and thrombosis that occur in hematologic diseases using microfluidic technology. *J Clin Invest*. 2012;122(1):408-18.
61. Reininger AJ, Agneskirchner J, Bode PA, et al. c7E3 Fab inhibits low shear flow modulated platelet adhesion to endothelium and surface-absorbed fibrinogen by blocking platelet GP IIb/IIIa as well as endothelial vitronectin receptor—results from patients with acute myocardial infarction and healthy controls. *Thromb Haemost*. 2000;83(2):217-23.
62. Bombeli T, Schwartz BR, Harlan JM. Adhesion of activated platelets to endothelial cells: evidence for a GPIIb/IIIa-dependent bridging mechanism and novel roles for endothelial intercellular adhesion molecule 1 (ICAM-1), $\alpha_v\beta_3$ integrin, and GPIIb. *J Exp Med*. 1998;187(3):329-39.
63. Gawaz M, Neumann FJ, Dickfeld T, et al. Vitronectin receptor $\alpha_v\beta_3$ mediates platelet adhesion to the luminal aspect of endothelial cells: implications for reperfusion in acute myocardial infarction. *Circulation*. 1997;96(6):1809-18.
64. Karunarathne W, Ku CJ, Spence DM. The dual nature of extracellular ATP as a concentration-dependent platelet P2X₁ agonist and antagonist. *Integr Biol*. 2009;1(11-12):655-63.
65. Lagadec P, Dejoux O, Ticchioni M, et al. Involvement of a CD47-dependent pathway in platelet adhesion on inflamed vascular endothelium under flow. *Blood*. 2003;101(12):4836-43.
66. Nergiz-Ünal R, Lamers MM, Van Kruchten R, et al. Signaling role of CD36 in platelet activation and thrombus formation on immobilized thrombospondin or oxidized low-density lipoprotein. *J Thromb Haemost*. 2011;9(9):1835-46.
67. Kuijpers MJ, de Witt S, Nergiz-Ünal R, et al. Supporting roles of platelet thrombospondin-1 and CD36 in thrombus formation on collagen. *Arterioscler Thromb Vasc Biol*. 2014;34(6):1187-92.
68. Bonnefoy A, Daenens K, Feys HB, et al. Thrombospondin-1 controls vascular platelet recruitment and thrombus adherence in mice by protecting (sub)endothelial VWF from cleavage by ADAMTS13. *Blood*. 2006;107(3):955-64.
69. Isenberg JS, Romeo MJ, Yu C, et al. Thrombospondin-1 stimulates platelet aggregation by blocking the antithrombotic activity of nitric oxide/cGMP signaling. *Blood*. 2008;111(2):613-23.
70. Roberts W, Magwenzi S, Aburima A, et al. Thrombospondin-1 induces platelet activation through CD36-dependent inhibition of the cAMP/protein kinase A signaling cascade. *Blood*. 2010;116(20):4297-306.
71. Navarro-Núñez L, Pollitt AY, Lowe K, et al. Platelet adhesion to podoplanin under flow is mediated by the receptor CLEC-2 and stabilised by Src/Syk-dependent platelet signalling. *Thromb Haemost*. 2015;113(5):1109-20.
72. Munnix IC, Cosemans JM, Auger JM, et al. Platelet response heterogeneity in thrombus formation. *Thromb Haemost*. 2009;102(6):1149-56.
73. Ivanciu L, Stalker TJ. Spatiotemporal regulation of coagulation and platelet activation during the hemostatic response in vivo. *J Thromb Haemost*. 2015;13(11):1949-59.
74. Zheng Y, Chen J, Craven M, et al. In vitro microvessels for the study of angiogenesis and thrombosis. *Proc Natl Acad Sci USA*. 2012;109(24):9342-7.
75. Westein E, van der Meer AD, Kuijpers MJ, et al. Atherosclerotic geometries exacerbate pathological thrombus formation poststenosis in a von Willebrand factor-dependent manner. *Proc Natl Acad Sci USA*. 2013;110(4):1357-62.

76. Costa PF, Albers HJ, Linssen JEA, et al. Mimicking arterial thrombosis in a 3D-printed microfluidic in vitro vascular model based on computed tomography angiography data. *Lab Chip*. 2017;17(16):2785-92.
77. de Witt SM, Swieringa F, Cavill R, et al. Identification of platelet function defects by multi-parameter assessment of thrombus formation. *Nat Commun*. 2014;5:4257.
78. Payne H, Ponomaryov T, Watson SP, et al. Mice with a deficiency in CLEC-2 are protected against deep vein thrombosis. *Blood*. 2017;129(14):2013-20.
79. Edelstein LC. The role of platelet microvesicles in intercellular communication. *Platelets*. 2017;28(3):222-7.
80. Chappell D, Brettner F, Doerfler N, et al. Protection of glycocalyx decreases platelet adhesion after ischaemia/reperfusion: an animal study. *Eur J Anaesthesiol*. 2014;31(9):474-81.
81. Zhang YS, Davoudi F, Walch P, et al. Bioprinted thrombosis-on-a-chip. *Lab Chip*. 2016;16(21):4097-105.
82. Mastenbroek TG, Feijge MA, Kremers RM, et al. Platelet-associated matrix metalloproteinases regulate thrombus formation and exert local collagenolytic activity. *Arterioscler Thromb Vasc Biol*. 2015;35(12):2554-61.
83. de Groot PG, Sixma JJ. Perfusion chambers. In: Michelson AD, ed. *Platelets*. San Diego, CA:Academic Press; 2002:347-56
84. Sakariassen KS, Orning L, Turitto VT. The impact of blood shear rate on arterial thrombus formation. *Future Sci OA*. 2015;1(4):FSO30.
85. Tanahashi N, Fukuuchi Y, Tomita M, et al. Adhesion of adenosine diphosphate-activated platelets to human brain microvascular endothelial cells under flow in vitro is mediated via GPIIb/IIIa. *Neurosci Lett*. 2001;301(1):33-6.
86. Tomita Y, Tanahashi N, Tomita M, et al. Role of platelet glycoprotein IIb/IIIa in ADP-activated platelet adhesion to aortic endothelial cells in vitro: observation with video-enhanced contrast microscopy. *Clin Hemorheol Microcirc*. 2001;24(1):1-9.

Supplemental tables

Suppl. Table 1. Reported effect of endothelial cell treatment with inflammatory agents, or other damage, on EC-induced thrombus formation

EC treatment	Flow chamber	Shear rate	EC source	PII source	Effect EC treatment on thrombus formation	Ref
Cholesterol	Not indicated	24 dyn/cm ²	Aorta, rabbit	WB, rec.	Platelet translocation ↑, number of adhered platelets ↑	1
FeCl ₃	Branching microchannel	4 dyn/cm ²	HUVEC	WP, WB rec.	Channel occlusion ↑	2
Heat	Parallel plate	150 s ⁻¹	HUVEC	WB	Voltage-dependent ↑ in VWF strings and platelet aggregate volume	3
Histamin	Parallel plate	2.5, 10, 20 dyn/cm ²	HUVEC	WP, fixed	Shear-dependent formation of platelet-VWF strings, optimum at 10 dyn/cm ²	4‡
	Parallel plate	2 dyn/cm ²	pHUVEC	WP + RBC	Platelet translocation ↑	5
	Parallel plate	2.5, 20, 50 dyn/cm ²	pHUVEC	WP	Inverse shear-dependent formation of platelet-VWF strings	6
LPS	Parallel plate	650, 2600 s ⁻¹	pHUVEC	WB	Platelet coverage =	7
Microparticles	µ-slide VI	1500 s ⁻¹	HUVEC	WB	Platelet coverage ↑	8
PMA	Branching microchannel	10-30 dyn/cm ²	HUVEC	WB, rec.	Platelet adhesion ↑	9
STX-2	Branching microchannel	1-4, 10-40 dyn/cm ²	HUVEC	WB	Shear-dependent ↑ in platelet aggregate volume and channel occlusion	10
TGF-β1	Capillary, rectangular	140 s ⁻¹	HUVEC	WB	Platelet SAC ↑	11
Thrombin	Not indicated	10-50 s ⁻¹	HAEC	PRP	Number of adhered platelets ↑	12
	Not indicated	10 s ⁻¹	HBEC	PRP	Number of adhered platelets ↑	13
TNF-α	Parallel plate	750 s ⁻¹	HUVEC, fixed	WB	Platelet SAC ↑, expression of ICAM-1, VCAM-1, VWF, TF ↑	14
	Parallel plate	100 s ⁻¹	HUVEC	WB	Platelet SAC ↑	15
	Parallel plate	65 s ⁻¹	pHUVEC	WB	Number of platelet aggregates ↑	16
	Branching microchannel	1-4 dyn/cm ²	HLMVEC	WB	Velocity in channel ↓	10
	Branching microchannel	1-4 dyn/cm ²	HLMVEC	WB + TNF-α	Velocity in channel ↓	10
TNF-α + TGF-β	Capillary, rectangular	100, 400 s ⁻¹	pHUVEC	WP, WB rec.	Platelet SAC ↑ (100 s ⁻¹), = (400 s ⁻¹), stable platelet-EC interactions ↑ (100, 400 s ⁻¹)	17
TNF-α + IFN-γ	Parallel plate	1000 s ⁻¹	HUVEC	WP	Platelet SAC ↑	18
Serum, human	Parallel plate	50 dyn/cm ²	pPAEC	WB	Platelet SAC ↑	19
Shear	µ-slide VI	50, 150, 450, 1350 s ⁻¹	LEC	WB	Shear-dependent ↓ in platelet SAC	20
	Badimon	427, 853, 1280 s ⁻¹	Aorta, pig	WB	No adhered platelets	21

Abbreviations. Endothelial cells (EC); human aortic endothelial cells (HAEC); human brain microvascular endothelial cells (HBEC); human lung microvascular endothelial cells (HLMVEC); (primary) human umbilical vein endothelial cells ((p)HUVEC); interferon gamma (INF-γ); lipopolysaccharides (LPS); lymphatic endothelial cells (LEC); phorbol-12-myristate-13-acetate (PMA); platelet (PII); platelet-rich plasma (PRP); (primary) porcine aortic endothelial cells ((p)PAEC); reconstituted (rec); red blood cells (RBC); shiga toxin 2 (STX-2); transforming growth factor beta 1 (TGF-β1); tumour necrosis factor alpha (TNF-α); washed platelets (WP); whole blood (WB). All platelet sources are of human origin unless indicated otherwise. Decreased (↓); no change (=); increased (↑).

Suppl. Table 2. Reported involvement of endothelial cell receptors on thrombus formation performed in flow perfusion studies

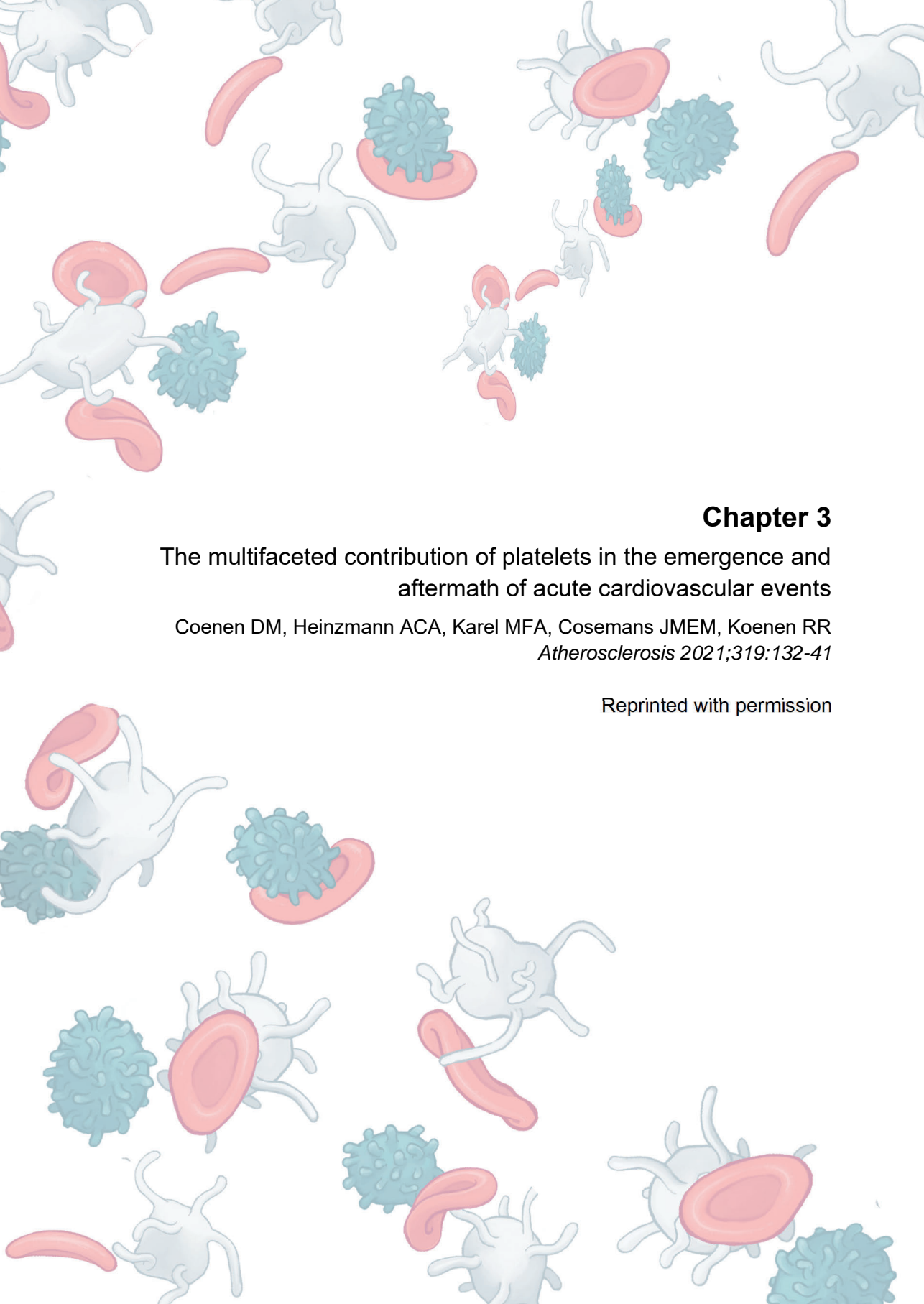
Target	Intervention	Flow chamber	Shear rate	EC source	EC treatment	Pit source	Effect intervention on thrombus formation	Ref
$\alpha_v\beta_3$	LM609 Ab	Parallel plate	50 dyn/cm ²	pPAEC	Serum	WB	Platelet SAC ↓	19
	Abciximab (TE3, Reopro)	SPAA	170 s ⁻¹	HUVEC	None	PRP, ADP stimulated	Platelet adhesion ↓	22
β_3	SZ21 Ab	μ -slide VI	50 s ⁻¹	LEC	None	WB	Platelet SAC =	20
GaIT	GaI-/-	Bioflux 1000	5 dyn/cm ²	PAEC	Xenoactivation	WB	Platelet SAC ↓, platelet aggregate volume ↓	23
	N/A	Bioflux 200	3, 10 dyn/cm ²	GTKO/hCD46-pPAEC	Xenoactivation	PRP	Platelet SAC ↓	24
GP1b α	anti-GP1b α Ab	μ -slide VI	1500 s ⁻¹	HUVEC	Microparticles	WB	Platelet adhesion ↓	8
CR1	sCR1	Parallel plate	50 dyn/cm ²	pPAEC	Serum	WB	Platelet SAC ↑	19
Lactadherin	Lactadherin Ab	μ -slide VI	1500 s ⁻¹	HUVEC	Microparticles	WB	Platelet adhesion ↑	8
PECAM-1	YR-131-12 Ab	μ -slide VI	50 s ⁻¹	LEC	None	WB	Platelet SAC =	20
PLC γ 2	U73122	μ -slide VI	50 s ⁻¹	LEC	None	WB	Platelet SAC =	20
P-selectin	anti-P-selectin Ab	Parallel plate	50 dyn/cm ²	pPAEC	Serum	WB	Platelet SAC ↓	19
	PSGL-1	Parallel plate	50 dyn/cm ²	pPAEC	Serum	WB	Platelet SAC ↓	19
PSGL-1	anti-P-selectin Ab	μ -slide VI	1500 s ⁻¹	HUVEC	Microparticles	WB	Platelet adhesion ↓	8
ROCK	anti-PSGL-1 Ab	Not indicated	6 dyn/cm ²	HUVEC	TNF- α	WP	Number of adherent platelets ↓	25
	Y27632	μ -slide VI	1500 s ⁻¹	HUVEC	Microparticles	WB	Platelet adhesion ↓	8
ROS	DMTU, PDTIC	Parallel plate	50 dyn/cm ²	pPAEC	Serum	WB	Platelet SAC ↓	19
	SOD	μ -slide VI	1500 s ⁻¹	HUVEC	Microparticles	WB	Platelet adhesion ↓	8
TSP-1	C6.7, A2.5 mAbs	Lab-Tek 1	100 s ⁻¹	Ea.hy926	TNF- α	WB, rec.	Platelet SAC ↓ (C6.7), = (A2.5)	15
VWF	Desmopressin	Parallel plate	310 s ⁻¹	Ea.hy926	None	WB, rec.	Number of adhered platelets ↑	26
	anti-VWF Ab	μ -slide VI	1500 s ⁻¹	HUVEC	Microparticles	WB	Platelet adhesion ↓	8

Abbreviations. Alpha 1.3-galactosyltransferase deficient/human CD46 transgenic-primary porcine aortic endothelial cells (GTKO/hCD46-pPAEC); complement component 5 (C5); complement receptor 1 (CR1); endothelial cell (EC); galactosyltransferase (GalT); human umbilical vein endothelial cells (HUVEC); intercellular adhesion molecule 1 (ICAM-1); lymphatic endothelial cells (LEC); monoclonal antibody (mAb); not applicable (N/A); platelet endothelial cell adhesion molecule 1 (PECAM-1); platelet (Plt); platelet-rich plasma (PRP); polyclonal antibody (pAb); (primary) porcine aortic endothelial cells (p)PAEC); rho- associated, coiled-coil containing protein kinase (ROCK); reconstituted (rec); reactive oxygen species (ROS); superoxide dismutase (SOD); thrombospondin-1 (TSP-1); tissue factor (TF); tumour necrosis factor alpha (TNF- α); vascular cell adhesion protein 1 (VCAM-1); von Willebrand factor (VWF); whole blood (WB). EC treatment pit source are of human origin unless indicated otherwise. Decreased (↓); no change (=); increased (↑).

Supplemental references

1. Theilmeier G, Michiels C, Spaepen E, et al. Endothelial von Willebrand factor recruits platelets to atherosclerosis-prone sites in response to hypercholesterolemia. *Blood*. 2002;99(12):4486-93.
2. Ciciliano JC, Sakurai Y, Myers DR, et al. Resolving the multifaceted mechanisms of the ferric chloride thrombosis model using an interdisciplinary microfluidic approach. *Blood*. 2015;126(6):817-24.
3. Sylman JL, Artzer DT, Rana K, et al. A vascular injury model using focal heat-induced activation of endothelial cells. *Integr Biol (Camb)*. 2015;7(7):801-14.
4. Huang J, Roth R, Heuser JE, et al. Integrin $\alpha_v\beta_3$ on human endothelial cells binds von Willebrand factor strings under fluid shear stress. *Blood*. 2009;113(7):1589-97.
5. Romo GM, Dong JF, Schade AJ, et al. The glycoprotein Ib-IX-V complex is a platelet counterreceptor for P-selectin. *J Exp Med*. 1999;190(6):803-14.
6. Dong JF, Moake JL, Nolasco L, et al. ADAMTS-13 rapidly cleaves newly secreted ultra-large von Willebrand factor multimers on the endothelial surface under flowing conditions. *Blood*. 2002;100(12):4033-9.
7. Clozel M, Kuhn H, Baumgartner HR. Procoagulant activity of endotoxin-treated human endothelial cells exposed to native human flowing blood. *Blood*. 1989;73(3):729-33.
8. Terrisse AD, Puech N, Allart S, et al. Internalization of microparticles by endothelial cells promotes platelet/endothelial cell interaction under flow. *J Thromb Haemost*. 2010;8(12):2810-9.
9. Zheng Y, Chen J, Craven M, et al. In vitro microvessels for the study of angiogenesis and thrombosis. *Proc Natl Acad Sci USA*. 2012;109(24):9342-7.
10. Tsai M, Kita A, Leach J, et al. In vitro modeling of the microvascular occlusion and thrombosis that occur in hematologic diseases using microfluidic technology. *J Clin Invest*. 2012;122(1):408-18.
11. Kuckleburg CJ, Yates CM, Kalia N, et al. Endothelial cell-borne platelet bridges selectively recruit monocytes in human and mouse models of vascular inflammation. *Cardiovasc Res*. 2011;91(1):134-41.
12. Itoh Y, Tomita M, Tanahashi N, et al. Platelet adhesion to aortic endothelial cells in vitro after thrombin treatment: observation with video-enhanced contrast microscopy. *Thromb Res*. 1998;91(1):15-21.
13. Tanahashi N, Fukuuchi Y, Tomita M, et al. Platelet adhesion to human brain microvascular endothelial cells in vitro: observation with video-enhanced contrast microscopy. *Neurosci Lett*. 1999;274(3):199-202.
14. Jain A, Graveline A, Waterhouse A, et al. A shear gradient-activated microfluidic device for automated monitoring of whole blood haemostasis and platelet function. *Nat Commun*. 2016;7:10176.
15. Lagadec P, Dejoux O, Ticchioni M, et al. Involvement of a CD47-dependent pathway in platelet adhesion on inflamed vascular endothelium under flow. *Blood*. 2003;101(12):4836-43.
16. Kirchofer D, Tschopp TB, Hadváry P, et al. Endothelial cells stimulated with tumor necrosis factor- α express varying amounts of tissue factor resulting in inhomogenous fibrin deposition in a native blood flow system: effects of thrombin inhibitors. *J Clin Invest*. 1994;93(5):2073-83.
17. Tull SP, Anderson SI, Hughan SC, et al. Cellular pathology of atherosclerosis: smooth muscle cells promote adhesion of platelets to cocultured endothelial cells. *Circ Res*. 2006;98(1):98-104.
18. Schulz C, Schäfer A, Stolla M, et al. Chemokine fractalkine mediates leukocyte recruitment to inflammatory endothelial cells in flowing whole blood: a critical role for P-selectin expressed on activated platelets. *Circulation*. 2007;116(7):764-73.
19. Galbusera M, Buelli S, Gastoldi S, et al. Activation of porcine endothelium in response to xenogeneic serum causes thrombosis independently of platelet activation. *Xenotransplantation*. 2005;12(2):110-20.
20. Navarro-Núñez L, Pollitt AY, Lowe K, et al. Platelet adhesion to podoplanin under flow is mediated by the receptor CLEC-2 and stabilised by Src/Syk-dependent platelet signalling. *Thromb Haemost*. 2015;113(5):1109-20.
21. Merhi Y, Lam JY, Lacoste LL, et al. Effects of thrombocytopenia and shear rate on neutrophil and platelet deposition on endothelial and medial arterial surfaces. *Arterioscler Thromb Vasc Biol*. 1993;13(7):951-7.
22. Reiningger AJ, Agneskirchner J, Bode PA, et al. c7E3 Fab inhibits low shear flow modulated platelet adhesion to endothelium and surface-absorbed fibrinogen by blocking platelet GP IIb/IIIa as well as endothelial vitronectin receptor-results from patients with acute myocardial infarction and healthy controls. *Thromb Haemost*. 2000;83(2):217-23.
23. Harris DG, Benipal PK, Cheng X, et al. III. Four-dimensional characterization of thrombosis in a live-cell, shear-flow assay: development and application to xenotransplantation. *PLoS One*. 2015;10(4):e0123015.

24. Rataj D, Werwitzke S, Haarmeijer B, et al. Inhibition of complement component C5 prevents clotting in an ex vivo model of xenogeneic activation of coagulation. *Xenotransplantation*. 2016;23(2):117-27.
25. da Costa Martins P, García-Vallejo JJ, van Thienen JV, et al. P-selectin glycoprotein ligand-1 is expressed on endothelial cells and mediates monocyte adhesion to activated endothelium. *Arterioscler Thromb Vasc Biol*. 2007;27(5):1023-9.
26. Calmer S, Ferkau A, Larmann J, et al. Desmopressin (DDAVP) improves recruitment of activated platelets to collagen but simultaneously increases platelet endothelial interactions in vitro. *Platelets*. 2014;25(1):8-15.



Chapter 3

The multifaceted contribution of platelets in the emergence and aftermath of acute cardiovascular events

Coenen DM, Heinzmann ACA, Karel MFA, Cosemans JMEM, Koenen RR
Atherosclerosis 2021;319:132-41

Reprinted with permission

Abstract

Atherosclerosis is an underlying cause of a broad array of cardiovascular diseases characterized by plaques, arterial wall thickening initiated by hyperlipidaemia, pro-inflammatory signals, endothelial dysfunction and the influx of inflammatory cells. By still incompletely characterized mechanisms, these plaques can destabilize or erode, leading to thrombosis and blood vessel occlusion and becomes clinically manifest as angina pectoris, myocardial infarction (MI) or stroke.

Among the several blood cell types that are involved in the development of atherosclerosis, the role of platelets during the thrombotic occlusion of ruptured or eroded plaques is well established and clinically exploited as evident by the extensive use of platelet inhibitors. However, there is increasing evidence that platelets are also involved in the earlier stages of atheroma development by exhibiting pro-inflammatory activities. The scope of this review is to describe the role of platelets in the initiation and propagation stages of atherosclerosis and beyond; in atherothrombotic complications.

1. Contribution of platelets to the early onset of atherosclerotic lesions

The development of atherosclerosis starts already at an early age as local vascular inflammation and fatty streaks, some of which progress over time to become clinically relevant atheromas at a later stage in life.¹ Under the inflammatory conditions present during early athero- genesis, the endothelial cells of the vessel wall express certain adhesion molecules, e.g. ICAM-1, and release vWF, which makes them permissive for transient and stable interactions with (activated) platelets. Activated platelets are thought to promote the onset of plaque formation or progression in multiple ways, which can be categorized in I) depositing chemokines on the inflamed endothelium and thereby recruiting leukocytes, II) binding to the endothelium and triggering an inflammatory response in endothelial cells, III) binding to and activating leukocytes, IV) releasing extracellular vesicles (EVs) (Figure 1A).

1.1 Inflammatory interactions of platelets with endothelial cells

Rolling of platelets over endothelial cells is mainly mediated by von Willebrand factor (VWF),² which is released from the Weibel-Palade bodies of activated endothelial cells, and by platelets themselves. It can be conceived that VWF retained on the vessel wall binds to passing platelets via the platelet GPIb-IX-V complex, which might in turn serve as a bridge to facilitate leukocyte recruitment (see below).³ Deletion of VWF leads to a reduction of atherosclerotic plaque formation in mice.⁴ Interaction between platelet P-selectin and endothelial PSGL-1 supports platelet rolling over the inflamed endothelium. Whilst rolling, platelets deposit the chemokines CCL5 (RANTES) or CXCL4 (platelet factor 4) onto the endothelium, which increases recruitment of monocytes by 2- to 3-fold⁵ and neutrophils to carotid arteries of mice.⁶ Platelet-specific genetic deletion, or pharmacologic blockade of P-selectin was shown to result in a reduced deposition

of CCL5 by platelets on endothelial cells and on the vessel wall.^{6,7} However, the exact role of how P-selectin mediates CCL5 deposition is unclear. Deposited CCL5 can also undergo interactions with other inflammatory factors, e.g. with human neutrophil peptide 1 (HNP1), which potentiates the vascular recruitment of classical monocytes⁸ and with CCL17 to attract T cells to sites of inflammation.⁹ Heteromeric interactions of CCL5 and CXCL4 further enhance monocyte recruitment.¹⁰ Inhibition of the interactions of CCL5 with CXCL4, CCL17, and HNP1 by specifically designed synthetic peptides leads to a reduction of leukocyte recruitment *in vitro*, and to a reduced plaque formation when administered to mice in models of atherosclerosis (CXCL4 and CCL17)^{9,10} or to decreased myocardial tissue damage when given to mice in models of heart ischemia reperfusion (CXCL4, HNP1).^{8,11}

Firm platelet adhesion to the endothelium occurs via interaction of platelet $\alpha_{IIb}\beta_3$ with endothelial $\alpha_v\beta_3$ and ICAM-1, as reviewed in detail by Coenen et al..¹² Of note, mice double deficient in *ApoE* and α_{IIb} display attenuated atherosclerosis in the carotid artery and aorta when compared to *ApoE* knockout mice.¹³ Yet, there are several other receptors mediating the platelet-endothelial interface with a key role for the cell-bound cytokine CD154 (CD40 ligand) and its receptor CD40 in leukocyte recruitment and endothelial inflammation.¹⁴ Both are present in platelets; CD154 is presented surface-bound after platelet activation and also released in a soluble form, whereas CD40 is constitutively expressed in a membrane-bound fashion.^{14,15} A recent study highlighted an involvement of CD154 and ultra-large multimers of VWF (UL-VWF) in the platelet-mediated recruitment of monocytes to the vessel wall.¹⁶ Stimulation of endothelial cells with sCD154 or activated platelets under high shear flow conditions led to a release of UL-VWF, which served as a substrate for monocyte adhesion *in vitro* and *in vivo*. In addition, perfusing plasma from patients with cardiovascular disease over activated endothelial cells was found to lead to an increased length of secreted UL-VWF, with an increase of adherent platelets, compared to controls.¹⁶ Moreover, during early plaque development, platelet CD154 can induce endothelial inflammation by trans-interactions with endothelial CD40.¹⁷ Interestingly, cis-interactions of CD154 with platelet-CD40 leads to proteolytic release of soluble CD154 (sCD154).¹⁴ By serving as an activating ligand for integrin $\alpha_{IIb}\beta_3$ on platelets, sCD154 was shown to exert stabilizing autocrine functions during arterial thrombus formation.¹⁵ In a later study by Lievens and colleagues, the role of CD154 in thrombus stabilization was confirmed and platelet CD154 appeared to stimulate atherogenesis.¹⁸ Repeated injections with activated wild type platelets into hyperlipidaemic mice resulted in accelerated plaque development, an effect that was far less prominent after injections with CD154-deficient platelets,¹⁸ similar to observations with P-selectin-deficient platelets.⁷ Unlike CD154, CD40 was not found to play a role in thrombus stabilization, but platelet-CD40 was also found to play a role in atherosclerotic plaque development and phenotype,¹⁹ an observation that appears to be somewhat at odds with its previously described function in regulating CD154 activity,¹⁴ and asks for further investigation.

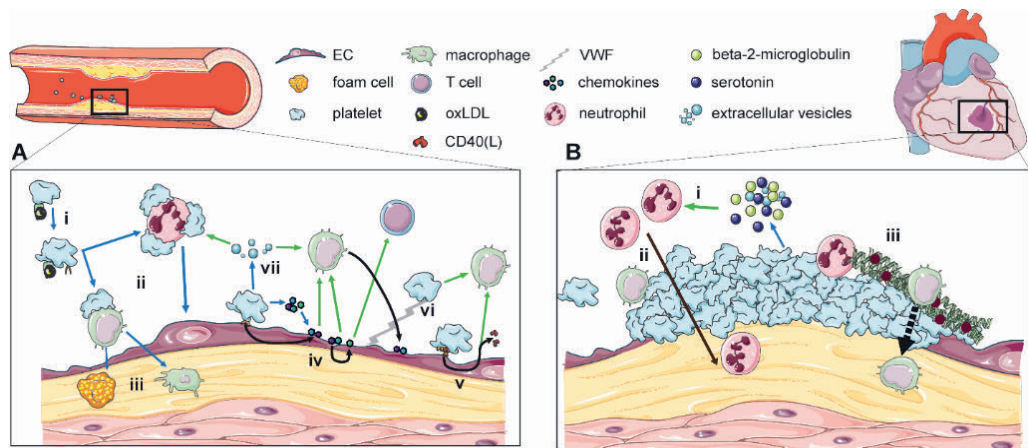


Figure 1. Platelet-related mechanisms in atherosclerosis and atherothrombotic ischemic events. (A) Platelets can support atherogenic vascular inflammatory processes by **i**) binding to oxidized low-density lipoprotein (oxLDL), causing platelet activation and accelerating foam cell formation, **ii**) binding to and activating leukocytes, and **iii**) supporting the influx and differentiation of monocytes/macrophages, **iv**) depositing chemokines on the inflamed endothelium and thereby recruiting leukocytes, **v**) binding to the endothelium and triggering an inflammatory response in endothelial cells, **vi**) bridging leukocytes to the endothelium by binding to von Willebrand factor (VWF), **vii**) releasing extracellular vesicles. **(B)** Platelets can support ischemic thrombo-inflammatory processes by **i**) releasing inflammatory mediators that act on monocytes and neutrophils, **ii**) directly facilitating leukocyte recruitment and infiltration at the site of injury, **iii**) stimulating the release of neutrophil extracellular traps that can serve as a substrate for the coagulation reaction and for leukocyte recruitment.

An open question with potential relevance for the role of platelets in plaque development is whether platelets can leave the blood vessel and enter surrounding tissues, e.g. plaques. Although platelets do not appear to exit the vessel when bound to transmigrating leukocytes,²⁰ platelets are able to actively migrate towards the chemokines CXCL12 and CXCL14 in chemotaxis experiments.^{21,22} In addition, platelets have been found outside of blood vessels in inflamed or ischemic tissues,²³ yet it is unclear whether they actively migrate outside blood vessels in a self-supported fashion. However, platelets have been shown to enter the plaque interior through leaky microvessels.²⁴ As outlined below, platelets might contribute to the formation of foam cells. At later stages, they might disintegrate into microvesicles, which can influence macrophage and smooth muscle cells phenotype (see section 1.3). However, isolated microvesicles from human plaques have been found to be of diverse cellular origins, except from platelets.²⁵

1.2 Platelet-leukocyte interactions

Although platelet-leukocyte interactions appear to be involved in pathologic inflammation and thrombosis, they also appear to serve physiologic functions, for instance in host defence. Activated platelets can bind to monocytes, neutrophils and lymphocytes and can increase their adhesiveness to inflamed endothelial cells or exposed sub-endothelial cells (for further reference please consult: ²⁶⁻²⁹).

Given their ability to interact with many molecular and cellular partners, platelets have been shown to serve as a bridge from the leukocyte to the vessel wall.³⁰⁻³² Such mechanisms might lead to an increased accelerated influx of mononuclear cells into the developing plaque. During dyslipidaemia, an important role for the formation of platelet-leukocyte adhesion might be played by oxidized low-density lipoprotein (oxLDL), which can directly activate platelets through the CD36 receptor.^{33,34} Besides increasing platelet adhesiveness to immobilized substrates, binding of oxLDL to platelets leads to pro-inflammatory activation, increasing adhesion to neutrophils and monocytes and enhancing leukocyte extravasation and foam cell formation.^{35,36} Thus, changes in plasma under pathologic conditions might modulate platelet-endothelial and platelet-leukocyte interactions.

Platelet-leukocyte interactions are receiving increasing attention as possible interventional target. Pharmacologic and genetic manipulation of platelet-monocyte interactions by altering or blocking the binding site on macrophage antigen 1 (Mac-1, CD11b/CD18) for glycoprotein 1b α (GP1b α) led to reduced thrombosis in carotid arteries and cremaster arterioles in mice, without affecting hemostasis.³⁷ A similar approach was followed for the interaction of Mac-1 with CD154, using a blocking peptide or a novel antibody that specifically blocks the binding site for CD154 on Mac-1.^{38,39} Blocking the Mac-1 – CD154 interaction led to a reduced leukocyte recruitment, inflammation and decreased atherosclerotic plaque formation, without affecting normal host defence. As opposed to the Mac-1– GP1b α pair, the exact role of Mac-1 – CD154 interaction for platelet-leukocyte interplay remains to be pinpointed. Platelet adhesion to endothelial cells can thus support monocyte recruitment, and several studies have indicated an involvement of chemokines. For example, the membrane-bound chemokines CX3CL1 (fractalkine) and CXCL16, expressed on vascular cells, are involved in the interaction of monocytic cells with endothelial cells. Interestingly, inhibition of platelet adhesion also led to a reduction of adherent monocytes to inflamed endothelial cells.⁴⁰ Multiple complementary mechanisms might be involved. For example, expression of CX3CL1 on activated endothelial cells might directly activate platelets, leading to the expression of P-selectin, facilitating the capture of monocytes.^{40,41} Further, CX3CL1 supports the interaction of VWF with GPIb α .⁴² In addition to CX3CL1, CXCL16 exerts a similar supportive function in the recruitment of platelets and monocytes to the vessel wall.^{43,44}

It has to be noted that although a large number of studies have shown that platelets interact with endothelium during vascular inflammation and atherogenesis and serve as a bridge for leukocytes to the larger arterial and venous vessel wall, less evidence is present on whether platelets also serve this role in a microvascular context. Although the effects of the pharmacological compounds used cannot be clearly ascribed to a single cell type, the phosphodiesterase inhibitor cilostazol and aspirin were shown to reduce platelet-leukocyte aggregation in the injured microvasculature of mice.^{45,46}

1.3 Release of extracellular vesicles and miRNA transfer

Next to the release of chemokines and other bioactive substances, platelets can also release EVs upon activation (the authors refer to ref. ¹⁵¹ for a comprehensive overview). These EVs have the potential to modulate biologic processes distal from the site of platelet activation.^{47,48} So far, platelet-derived EVs have been demonstrated to enhance the recruitment of monocytes and neutrophils to the vessel wall during inflammation,^{49,50} deposit chemokines that trigger the recruitment of monocytes;⁵¹ directly promote monocyte differentiation into macrophages;⁵¹ alter macrophage genotype and function;^{53,54} induce proliferation and transformation of smooth muscle cells to a pro-inflammatory phenotype,⁵⁵ upon infiltrating the bone marrow, modulate the behaviour of megakaryocytes to alter thrombopoiesis during inflammation.⁵⁶ Although these observations might be explained by the action of proteins and lipids carried by EVs, a number of interesting studies have also pointed towards nucleic acids, notably microRNAs (miR), as molecular effectors. Platelets are a main contributor to the plasma pool of circulating miRNAs and contain miRNAs linked to atherosclerosis. The miRNAs-126, -223, 191-5p and -320b have been found to be transferred from platelets and their EVs to endothelial cells.⁵⁷⁻⁵⁹ MiRNA-126 – the most abundant miRNA in platelets⁶⁰ – controls VCAM-1 expression, which is linked to endothelial dysfunction.⁶¹ Platelet miRNA223 can regulate endothelial gene expression and appears to have quiescence promoting effect on endothelial cells,⁵⁹ e.g. via downregulating ICAM-1 expression.^{58,62} Also, miRNA320b can downregulate ICAM-1 and miRNA191-5 inhibits endothelial cell apoptosis and angiogenesis (see expert review by Elgheznawy and Fleming⁵⁹). It should be noted that *in vitro* experiments are the basis of the findings above, and that evidence supporting functional transfer of platelet-derived miRNA *in vivo* is still scarce. Interestingly, miRNA223 is downregulated in patients with diabetes mellitus type.^{63,64}

1.4 Platelet hyperreactivity as risk factor for atherosclerotic cardiovascular disease

Increased activity of platelets, defined as a lowered activation threshold and/or a refractiveness towards antiplatelet therapy, is considered a risk factor for atherosclerosis and major cardiovascular events.⁶⁵ Interestingly, (treatment-resistant) platelet hyperreactivity is often observed in patients with diabetes.⁶⁶ Hyperglycaemia is a hallmark of (uncontrolled) diabetes and this has been shown to increase platelet activity in a number of ways. For example, dysregulated calcium signalling in platelets during diabetes leads to increased activity of the protease calpain-1.⁶⁷ This results in the degradation of particular proteins that regulate platelet activity e.g. platelet endothelial cell adhesion molecule-1 (CD31), which is a negative regulator of platelet function.⁶⁸

Being a systemic metabolic disease, diabetes also affects metabolic processes within platelets. The high availability of glucose leads to an increased activity of the polyol pathway and to oxidative stress. The enzyme aldose reductase is the starting point of the polyol pathway, which is activated after stimulation of

platelets with collagen, leading to oxidative stress and to an increased release of the autocrine platelet activator thromboxane A₂.⁶⁹ In a follow-up study, the oxidative stress caused by the increased activity of aldose reductase was shown to lead to mitochondrial dysfunction and to apoptosis in platelets, as characterized by exposure of phosphatidylserine on the platelet outer membrane.⁷⁰ Interestingly, this was linked to increased thrombus size in a model of arterial thrombosis.

Mitochondria play an important role in platelet function,⁷¹ and there is rich evidence in literature that platelet activity is tightly linked to mitochondrial (dys)function (recent examples e.g. refs. ^{71,73}). Platelet hyperreactivity associated with mitochondrial dysfunction was also observed during ageing in mice.⁷⁴ This finding was explained by increased circulating levels of tumour necrosis factor- α (TNF- α), which is associated with ageing. In the bone marrow, TNF- α skewed the polarization of hematopoietic progenitor cells towards megakaryocytes, leading to enhanced production of hyperreactive platelets with more mitochondria that had altered metabolic function. Although it is unknown whether this mechanism contributes to the risk for adverse cardiovascular events associated with platelet hyperreactivity in humans, the study demonstrates that an inflammatory state can be propagated by the production of platelets with a hyperreactive and potentially pro-inflammatory phenotype.⁷⁴

Another mechanism for increased platelet reactivity is an increased relative number of so-called reticulated platelets, young platelets that contain more α - and dense granules and mitochondria and have an increased reactivity compared with older platelets.^{75,76} A recent study in mice indicated that high glucose levels led to increased platelet production by the bone marrow megakaryocytes, with the circulating platelets having a high fraction of reticulated platelets.⁷⁷ This hyperglycaemia-induced thrombocytosis might contribute to the hyperreactivity observed with diabetes. In addition, reticulated platelets might be less sensitive to antiplatelet therapy, which might contribute to the increased risk for ischemic events in patients with diabetes.⁷⁸ However, the sensitivity of reticulated platelets to platelet inhibitors might depend on the compound and the contribution of this young platelet fraction to resistance to antiplatelet therapy is currently still incompletely clarified.⁷⁹⁻

81

Besides diabetes, platelet hyperreactivity and continuous platelet activation are observed in myelodysplastic syndromes such as polycythaemia vera and essential thrombocythemia.⁸² Considered a risk factor (or precursor) for these syndromes is clonal haematopoiesis of indeterminate potential (CHIP), which is characterized by the clonal expansion of bone marrow cells carrying particular gene mutations that occur and accumulate during a human lifespan (notably in the genes coding for *TET2*, *ASXL1*, *DNMT3A*).⁸³ Although the occurrence of CHIP by itself is generally not accompanied by symptoms, it is associated with a strongly increased risk for developing myelodysplastic syndromes and cancer,⁸³ and intriguingly, also atherosclerotic cardiovascular disease.⁸⁴ Many of the gene mutations that are linked to CHIP also affect the activation state of blood cells in general and of platelets in

particular. For example, an increased platelet activation state and increased amounts of circulating platelet-monocyte and platelet-neutrophil complexes were observed in carriers of the JAK2V617F mutation,⁸⁵ which might contribute to an increased risk for thrombosis in these individuals.⁸² Although future research is necessary to clarify the relation between CHIP and platelet hyperreactivity, it is tempting to speculate that platelets might contribute to the increased cardiovascular risk observed in CHIP carriers. An overview of the gene mutations that may contribute to CHIP in relation to platelet function is provided elsewhere.⁸⁶

Table 1. Expression levels of human and mouse platelet proteins involved in atherosclerosis and vascular inflammation.

Protein class/name	Platelet copy number		Protein accession number ^C	
	Human ^a	Mouse ^b	Human	Mouse
Chemokines				
PF4; CXCL4	563,000	274,032	P02776	Q9Z126
PF4var; CXCL4L1	352,000	–	P10720	–
PBP; CXCL7	479,000	176,316	P02775	Q9EQI5
RANTES; CCL5	4,500	n.d.	P13501	P30882
TARC; CCL17	n.d.	n.d.	Q92583	F6R5P4/Q9WUZ6
Glycoproteins				
GPIIb/IIIa	49,000	157,581	P13224	P56400
GPIX	32,400	63,503	P14770	O88186
GPV	30,200	35,620	P40197	O08742
GPIb/IX/V	18,900	46,154	P07359	O35930
Platelet GP4; CD36	16,700	n.d.	P16671	Q08857/Q9QZU3
PSGL-1	n.d.	n.d.	Q14242	Q62170
Other				
β2M	19,600	34,170	P61769	P01887
JAM-A	13,300	14,860	Q9Y624	O88792
PECAM-1; CD31	9,400	5,566	P16284	Q08481
P-selectin; CD62P	8,900	35,970	P16109	Q01102
Neutrophil defensin 1; HNP1	3,100	–	P59665	–
TNFRSF5; CD40	1,300	n.d.	P25942	P27512
CD40L; CD154	1,600	n.d.	P29965	P27548

Derived from a: ¹³⁶, b: ¹³⁷, c: www.uniprot.org.

PF4, platelet factor 4; PF4var, platelet factor 4 variant; C(X)CL, C-(X)-C motif chemokine ligand; PBP, platelet basic protein; RANTES, regulated on activation, normal T cell expressed and secreted; TARC, thymus and activation regulated chemokine; GP, glycoprotein; PSGL-1, P-selectin glycoprotein ligand 1; β2M, β-2 microglobulin; JAM-A, junctional adhesion molecule A; PECAM-1, platelet-endothelial cell adhesion molecule-1; HNP1, human neutrophil peptide 1, neutrophil defensin 1; TNFRSF5, Tumour necrosis factor receptor superfamily member 5; CD, cluster of differentiation; CD40L, CD40 ligand.

'n.d.' not detectable according to refs. ¹³⁶ or ¹³⁷.

'–' gene not present in mouse.

A high platelet reactivity is also observed in mice with a genetic deletion of the junctional adhesion molecule (JAM)-A, leading to markedly reduced activation thresholds due to enhanced outside-in signalling through the α_{IIb}β₃ integrin.^{87,88} In our study, this platelet hyperreactivity was exploited to investigate its role in atherosclerotic plaque development. We observed that hyperreactive *JAM-A*^{-/-} platelets released more CCL5 and CXCL4 into the blood. They also interacted more

strongly with leukocytes and with a dysfunctional vascular endothelium than their wild type counterparts. Hyperlipidaemic mice with hyperreactive platelets showed accelerated development of atherosclerosis⁸⁹ and also increased neointima formation after wire-injury.⁹⁰ As the majority of experimental studies investigating the role of platelets in vascular disease were performed using loss-of-function mutations in platelets,⁹¹ the above study demonstrated that a gain-of-platelet function can result in increased plaque formation. The platelet-derived molecules involved in atherosclerosis and vascular inflammation are summarized in Table 1 and the platelet-related mechanisms discussed in this section are summarized in Table 2.

1.5 Translation mouse data to human

Although there is a large body of data from animal models in the different stages of plaque development,^{91,92} this is yet incompletely translated to humans. The evidence for a role of platelets in atherogenesis in humans is limited and largely indirect, which might be attributed to the fact that experimental options are far more abundant in animal models. Several platelet-derived chemokines and growth factors are detectable in atherosclerotic plaques.^{93,94} Persistent platelet activation has been reported in association with major cardiovascular risk factors that accelerate atherogenesis.⁹⁵ A relationship between increased platelet activation markers and the extent of carotid intima/media thickness, a marker of plaque size, has been described.^{96,97} In addition, platelet reactivity was associated with plaque morphology as determined by intravascular ultrasound.⁹⁸ Although these studies do not provide as solid an experimental link between platelet function and atherosclerosis as genetic or pharmacologic mouse studies, they do provide evidence for a role of platelets in plaque development in humans. The recent clinical trials CANTOS,⁹⁹ COLCOT¹⁰⁰ and LoDoCo2¹⁰¹ have convincingly demonstrated that inflammation plays an important role in the pathophysiology of cardiovascular diseases. Suppression of inflammation significantly reduced the risk for adverse events *e.g.* myocardial infarction. It is unclear whether lowering inflammation would also have effects on platelet functions. To address such questions, indicators of the inflammatory functions of platelets could be measured within the course of similar future study set ups *e.g.* circulating platelet-leukocyte complexes, circulating platelet-derived microvesicles and platelet protein and nucleic acid content.

Table 2. Platelet-related atherogenic mechanisms.

Factor	Interactions	Mechanism	Reference
Platelet-EC interactions			
CCL5	CXCL4, CCL17, HNP1	↑ leukocyte no., ↑ plaque formation, ↑ myocardial tissue damage	8, 9
CD62P	unknown on platelets	↑ platelet-endothelial interactions, ↑ cytokine secretion, ↑ plaque	17, 138-140
CD154	CD40, αIIbβ3 integrin	↑ endothelial inflammation, ↑ autocrine thrombus stability, ↑ plaque, ↑ monocyte no.	14-16, 18, 19
CD40		= thrombus stability, ↑ plaque development, plaque phenotype	19
VWF	Platelet GPIIb	↑ platelet-EC interaction, ↑ leukocyte no., ↑ plaque	2-4
UL-VWF	Platelet GPIIb	↑ monocyte no., ↑ platelet adhesion	16
oxLDL	Platelet CD36	↑ platelet activation, ↑ platelet-leukocyte interactions, ↑ foam cell formation	33-36
Mac-1 (CD11b/CD18)	Platelet GPIIb	↑ thrombosis, = hemostasis	37
Mac-1 (CD11b/CD18)	Platelet CD154	↑ leukocyte recruitment, ↑ inflammation, ↑ plaque, = host defense	38, 39
PSGL-1	Platelets	↑ polarized neutrophil migration, ↑ inflammation, ↑ immune defense	141
TLR4	LPS	= aggregation/granule release, ↑ platelet-neutrophil interaction, ↑ NETs, ↑ IL-1β synthesis	118, 142, 143
Bacteria	GPIIb, αIIbβ3, VWF	↓ mortality in sepsis, ↑ development of non-alcoholic liver disease	144, 145
Extracellular vesicles	Leukocytes	↑ monocyte/neutrophil no., ↑ chemokine deposition, ↑ monocyte differentiation	47, 49-54
Extracellular vesicles	Smooth muscle cells	↑ pro-inflammatory SMC proliferation and transformation	55
Extracellular vesicles		Bone marrow infiltration, megakaryocyte behavior, thrombopoiesis alteration	56
miRNAs	EC, SMC	↑ ICAM-1 expression, altered EC protein expression, SMC phenotypic switch	57, 58, 146, 147
Platelet hyper-reactivity			
Mitochondria	Neutrophils, EC	↑ neutrophil activation, ↑ NETs, ↑ inflammatory responses, ↑ tissue repair	148-150
Mitochondrial function		↑ platelet activation	72, 73
Diabetes, hyperglycemia		↑ platelet activity, dysregulated calcium signaling, ↑ calpain-1, ↑ protein degradation	66-68, 77
Diabetes, hyperglycemia		↑ platelet production (thrombocytosis), ↑ reticulated platelets	75
Diabetes, hyperglycemia		↑ polyol pathway activity, ↑ oxidative stress, ↑ thromboxane A2 release	69
Diabetes, hyperglycemia		↑ mitochondrial dysfunction, ↑ platelet apoptosis, ↑ arterial thrombus size	70
Oxidative stress		↑ platelet activity, ↑ mitochondrial dysfunction, ↑ circulating TNFα	74
Ageing		↑ progenitor cell polarization to megakaryocytes, ↑ hyperreactive platelet production	74
TNFα		↑ clonal expansion of bone marrow cells, ↑ platelet activation, ↑ platelet-leukocyte complexes	82-85
CHIP		↑ outside-in signaling, ↑ CCL5/CXCL4 release, ↑ atherosclerosis development	87-90
JAM-A deficiency	αIIbβ3 integrin		

2. Contribution of platelets to atherothrombosis and vascular remodelling

2.1 Platelets in atherothrombosis development

Opposed to the aforementioned processes of atherosclerosis development, the role of platelets in subsequent thrombus formation is well-studied and established.¹⁰²⁻¹⁰⁴ Traditionally, a plaque was described as either being stable or vulnerable, where the latter is more prone to rupture. Plaque rupture releases thrombogenic and pro-inflammatory substances thereby stimulating platelet activation and the formation of platelet-rich thrombi.^{102,103,105} It is thought that the primary mechanisms of atherothrombosis after plaque rupture are similar to those of thrombus formation in a healthy, non-atherosclerotic vessel.^{103,106} In brief, platelets can adhere to exposed collagen and VWF via their GPVI and GPIb α receptors, respectively, followed by $\alpha_{IIb}\beta_3$ integrin-dependent platelet aggregation. Subsequently, platelets release their granular and vesicular contents, evoking positive feedback loops via the soluble agonists ADP and thromboxane A₂ (TxA₂).¹⁰²

2.2 Platelets in plaque rupture and plaque erosion

The conception and importance of plaque rupture and subsequent processes as described above are recently being debated by Quillard et al. and Libby et al., who emphasize the importance of not only plaque rupture, but of plaque erosion as a cause of acute coronary syndromes.^{107,108} Contrasting with the common vision of the past years,¹⁰² they state that plaque rupture results in a 'red' fibrin-rich thrombus, whereas the 'white' platelet-rich thrombus is being formed after plaque erosion.¹⁰⁷⁻¹⁰⁹ The proposed mechanism in plaque erosion involves the damage and activation of the endothelial cells, resulting in the exposure of extracellular matrix and subendothelial compounds to the blood.¹⁰⁷ As discussed in more detail in our previous work, interactions of platelets with activated endothelium are distinct from the aforementioned thrombotic processes.¹² Interestingly, *in vivo* evidence of the role of platelets in atherothrombosis is either predominantly based on models of plaque rupture or no clear distinction is made between rupture, erosion and healing.^{103,104}

Plaque disruptions are often asymptomatic and followed by plaque healing. Even though this disruption of the plaque is nonfatal, it contributes to plaque progression and narrowing of the lumen.¹¹⁰ Recent studies have focused on the mechanism of atherosclerotic plaque healing and its potential importance, as healed plaques are associated with long-term clinical stability, while impaired healing with recurrent acute coronary syndromes.^{111,112} Given their importance in wound healing, it appears plausible that platelets also play a role in the healing of ruptured plaques. However, this notion has not yet been investigated.

2.3 Platelet-leukocyte interaction in atherothrombosis

Various vascular diseases, including atherosclerosis and ischemic stroke, are thought to be associated with thrombosis as well as inflammation, creating a

state of so-called thrombo-inflammation, in which not only platelets, the coagulation system and inflamed endothelial cells are of importance, but also leukocytes.¹¹³ The chemokine NAP-2 (CXCL7) derived from platelets, regulates leukocyte shape change and forms a chemotactic gradient within the thrombus, guiding leukocytes through the thrombus to the site of vascular injury.¹¹⁴ Thrombin was shown to be a major player in leukocyte attraction, as it promotes P-selectin expression on mouse platelets through cleavage of platelet PAR4,¹¹⁵ allowing interaction of leukocyte PSGL-1 with platelet P-selectin. However, it was also demonstrated that fibrin in thrombi can potentially act as a physical shield and reservoir for thrombin and hence limit the amount of intravascular leukocyte migration.¹¹⁵

Neutrophils play a key role in acute and chronic inflammation, through their release of granule contents and NETs, which can trigger blood coagulation. Furthermore, NETs are involved in many pathological inflammatory processes, e.g. thrombosis and atherosclerosis.^{116,117} This is demonstrated in animal models and in patients. For example, the formation of NETs was shown to be increased by activated platelets¹¹⁸ and NETosis was found to be involved in the pathophysiology of MI.^{11,119} Furthermore, NETs are found in atherosclerotic lesions and in coronary thrombi removed from AMI patients.^{120,121} It is thought that NETs distribute thrombosis by serving as a scaffold for adherent platelets, erythrocytes, and fibrin.^{122,123} Furthermore, NETs in thrombi might increase inflammation thereby increasing cell death, plaque instability and impairing regression.^{122,124} Taken together, platelets attract neutrophils into arterial thrombi, the neutrophils can exacerbate the inflammatory reaction and propagate thrombosis by the formation of NETs.

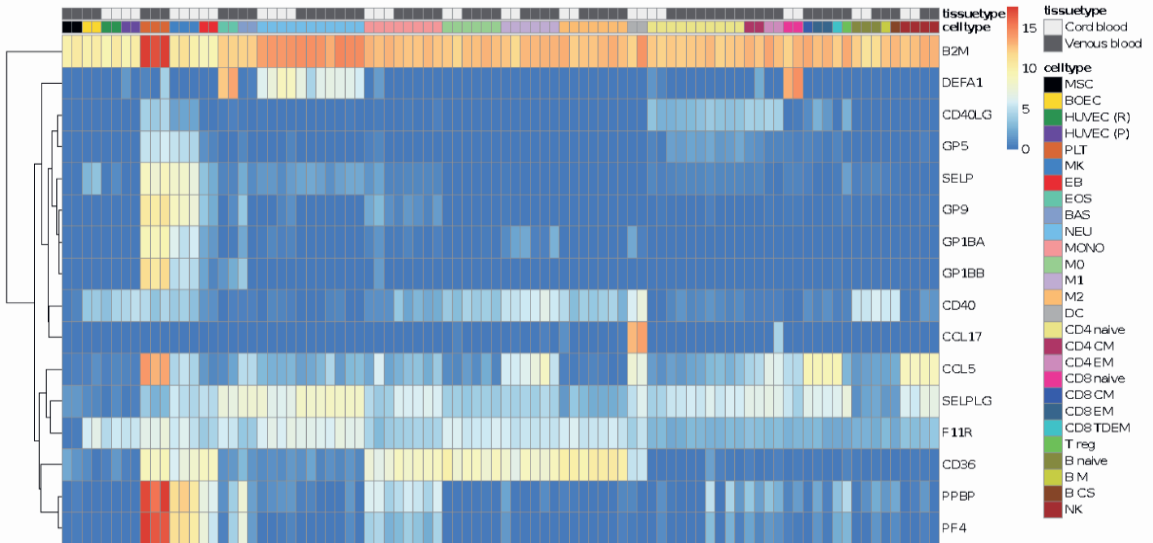


Figure 2. Hematopoietic cell-specific RNA expression of human genes involved in atherosclerosis. Orange colour marks platelet cell type RNA expression relative to other hematopoietic cell populations (log₂ fpkm). Red indicates high relative expression and blue indicates low relative expression. Data source and further information on: <https://blueprint.haem.cam.ac.uk/mRNA/>.

Table 3. Platelet-related mechanisms in myocardial infarction.

Factor	Interactions	Mechanism	Reference
Thrombin	PAR4	↑ leukocyte no.	115
CXCL7	CXCR1/2	↑ leukocyte shape change/migration	114
Fibrin		↑ leukocyte migration	115
NETs	Activated platelets, erythrocytes, fibrin	↑ monocyte no./activation, ↑ inflammation, ↓ plaque stability, ↑ lesion size	11, 116, 119-122, 124
β2M		↑ pro-inflammatory monocytes, ↓ pro-reparative monocytes	125
Serotonin		↑ neutrophil infiltration/degranulation, ↑ infarct size, ↓ cardiac function	127-130
FcγRIIa			131
C3	α _v β ₃ integrin	↑ platelet activation, coagulation, thrombosis	132-134
CD62P	PSGL-1	platelet-leukocyte interaction, leukocyte rolling	126

2.4 Complement and platelet-secreted factors in MI

Platelet-secreted factors are involved in the initiation and progression of atherosclerosis, may serve as a bridge between platelets and other cells, and contribute to the subsequent development of atherothrombotic diseases such as MI and stroke. Among these factors is β-2 microglobulin (β2M), a subunit of the major histocompatibility complex 1, which plasma levels are increased immediately after an MI. Increased levels of β2M resulted in the mobilization and differentiation of pro-inflammatory monocytes, which occurs through a non-canonical TGFβ signalling. Interestingly, platelets are a major source of β2M, and a recent study demonstrated that platelet-derived β2M (plt-β2M) was responsible for mediating this effect.¹²⁵ In plt-β2M-deficient mice, increased classical TGFβ signalling occurred, inducing the dominance of a pro-reparative monocyte phenotype. This had implications for cardiac repair after ischemia, since *plt-β2M*^{-/-} mice showed an early reparative response after experimental MI. Thus, β2M levels might control TGFβ-signalling and thereby the fraction of classical and reparatory monocytes.¹²⁵

Platelets and endothelial cells express P-selectin upon activation, which facilitates transient and stable interactions with leukocytes, and might thus serve as an interesting target for therapeutic intervention. In the SELECT-ACS trial, a blocking anti-P-selectin monoclonal antibody, inclacumab, was administered to patients with acute coronary syndrome scheduled for coronary angiography and/or percutaneous intervention.¹²⁶ Compared to placebo controls, patients receiving inclacumab showed decreased markers of myocardial damage, indicating that P-selectin blockade might be beneficial for the treatment of acute ischemic events.¹²⁶

Platelets contain and store serotonin (5-hydroxytryptamine, 5-HT) in their dense granules and platelet-derived serotonin is associated with myocardial ischemia and reperfusion injury and with a worsened outcome.^{127,128} Platelet serotonin has been shown to mediate neutrophil infiltration in states of acute inflammation or tissue damage.¹²⁹ During MI, platelets release high amounts of serotonin, leading to increased neutrophil infiltration into ischemic tissue. Mice lacking platelet serotonin had decreased infarct size and improved cardiac function after experimental MI. Serotonin caused degranulation of both mouse and human neutrophils. Interestingly, administration of selective serotonin reuptake inhibitors (SSRIs) depleted serotonin from platelets and this also reduced myocardial damage after MI in mice. In humans, serotonin levels correlated with neutrophil activation

parameters and the use of SSRIs lowered neutrophil CD11b expression and circulating levels of myeloperoxidase.¹³⁰

Next to small molecules present in platelet releasates, the expression of the gamma globulin receptor FcγRIIIa and the complement system on platelets are associated with MI and stroke.^{131,132} The complement system consists of three pathways with complement factor C3 in the centre, which is cleaved into C3a and C3b. The inflammatory function of the complement system in general¹³³ and in particular C3b¹³⁴ has been linked to platelet activation, coagulation and thrombosis. In a recent study, complement C3aR and C3a have been shown to be involved in the pathophysiology of MI through activation of integrin $\alpha_{IIb}\beta_3$.¹³² Thus, complement factors might serve as interesting targets for the treatment of MI and stroke.

In general, it can be appreciated that platelet-secreted factors are interesting targets in atherothrombotic diseases, as proteomic and network analysis revealed differentially released proteins from platelets in patients with acute coronary syndrome and stable angina pectoris.¹³⁵ The platelet-related mechanisms discussed in this section are schematically represented in Figure 2 and summarized in Table 3.

3. Concluding remarks

In this review article, the multifaceted role of platelets in the development of atherosclerosis and its subsequent acute clinical consequences have been discussed. Being best known for their acute thrombotic properties among physicians and investigators, therapeutics have been primarily directed against molecules and receptors that mediate platelet activation and aggregation. However, since platelets also have a role in wound healing, the role of these compounds in the recovery of vascular and/or ischemic damage has not yet been assessed. As outlined in this article, platelets harbour many different therapeutic opportunities that are interesting to pursue. Notably, the inflammatory responses facilitated by platelets, primarily located in the vasculature, might be dampened by specific inhibitors that do not affect the haemostatic potential of platelets. As platelets are supportive rather than executive immune cells, this could have less risk to be accompanied by immunologic side effects than directly targeting leukocytes. Therapeutic targeting of inflammatory platelet functions might not only be beneficial for the longer-term prevention of plaque formation, but also offer chances for the manipulation of the repair reaction during the acute phase of MI or stroke.

Highlights

- Platelets have an essential role in haemostasis and are also critically involved in major thrombotic events e.g. myocardial infarction and stroke.
- Antiplatelet therapy is primarily directed against the haemostatic function of platelets.

- Platelets have many roles in the development of atherosclerosis and vascular inflammation preceding major thrombotic events.
- Platelets are also involved in post-ischemic inflammation.
- These functions are reviewed in this paper and presented as interesting therapeutic targets.

Financial support

This work was supported by the Netherlands Foundation for Scientific Research (ZonMW VIDI 016.126.358 to R.R.K. and ZonMW VIDI 91716421 to J.M.E.M.C.), the Landsteiner Foundation for Blood Transfusion Research (LSBR Nr. 1638 to R.R.K.) and by the Dutch Heart Foundation (2015T79 to DMC and J.M.E.M.C.).

Declaration of competing interest

The authors declare that they have no known competing financial interests or personal relationships that could have appeared to influence the work reported in this paper.

Acknowledgements

The digital artwork was composed using elements of the Servier Medical Art collection, distributed under Creative Commons Attribution 3.0 Unported License.

References

1. Libby P, Buring JE, Badimon L, et al. Atherosclerosis. *Nat Rev Dis Primers*. 2019;5(1):56.
2. Andre P, Denis CV, Ware J, et al. Platelets adhere to and translocate on von Willebrand factor presented by endothelium in stimulated veins. *Blood*. 2000;96(10):3322-8.
3. Theilmeier G, Michiels C, Spaepen E, et al. Endothelial von Willebrand factor recruits platelets to atherosclerosis-prone sites in response to hypercholesterolemia. *Blood*. 2002; 99(12):4486-93.
4. Methia N, Andre P, Denis CV, et al. Localized reduction of atherosclerosis in von Willebrand factor-deficient mice. *Blood*. 2001;98(5):1424-8.
5. von Hundelshausen P, Weber KS, Huo Y, et al. RANTES deposition by platelets triggers monocyte arrest on inflamed and atherosclerotic endothelium. *Circulation*. 2001;103(13):1772-7.
6. Drechsler M, Megens RT, van Zandvoort M, et al. Hyperlipidemia-triggered neutrophilia promotes early atherosclerosis. *Circulation*. 2010;122(18):1837-45.
7. Huo Y, Schober A, Forlow SB, et al. Circulating activated platelets exacerbate atherosclerosis in mice deficient in apolipoprotein E. *Nat Med*. 2003; 9(1):61-7.
8. Alard JE, Ortega-Gomez A, Wichapong K, et al. Recruitment of classical monocytes can be inhibited by disturbing heteromers of neutrophil HNP1 and platelet CCL5. *Sci Transl Med*. 2015; 7(317):317ra196.
9. von Hundelshausen P, Agten SM, Eckardt V, et al. Chemokine interactome mapping enables tailored intervention in acute and chronic inflammation. *Sci Transl Med*. 2017; 9(384):eaah6650.
10. Koenen RR, von Hundelshausen P, Nesselmeier IV, et al. Disrupting functional interactions between platelet chemokines inhibits atherosclerosis in hyperlipidemic mice. *Nat Med*. 2009; 15(1):97-103.
11. Vajen T, Koenen RR, Werner I, et al. Blocking CCL5-CXCL4 heteromerization preserves heart function after myocardial infarction by attenuating leukocyte recruitment and NETosis. *Sci Rep*. 2018; 8(1):10647.
12. Coenen DM, Mastenbroek TG, Cosemans J. Platelet interaction with activated endothelium: mechanistic insights from microfluidics. *Blood*. 2017;130(26):2819-28.

13. Massberg S, Schurzinger K, Lorenz M, et al. Platelet adhesion via glycoprotein IIb integrin is critical for atheroprotection and focal cerebral ischemia: an in vivo study in mice lacking glycoprotein IIb. *Circulation*. 2005;112(8):1180-8.
14. Henn V, Steinbach S, Buchner K, et al. The inflammatory action of CD40 ligand (CD154) expressed on activated human platelets is temporally limited by coexpressed CD40. *Blood*. 2001; 98(4):1047-54.
15. Andre P, Prasad KS, Denis CV, et al. CD40L stabilizes arterial thrombi by a β_3 integrin-dependent mechanism. *Nat Med*. 2002; 8(3):247-52.
16. Popa M, Tahir S, Elrod J, et al. Role of CD40 and ADAMTS13 in von Willebrand factor-mediated endothelial cell-platelet-monocyte interaction. *Proc Natl Acad Sci USA*. 2018; 115(24):E5556-65.
17. Henn V, Slupsky JR, Grafe M, et al. CD40 ligand on activated platelets triggers an inflammatory reaction of endothelial cells. *Nature*. 1998;391(6667):591-4.
18. Lievens D, Zerneck A, Seijkens T, et al. Platelet CD40L mediates thrombotic and inflammatory processes in atherosclerosis. *Blood*. 2010; 116(20):4317-27.
19. Gerdes N, Seijkens T, Lievens D, et al. Platelet CD40 exacerbates atherosclerosis by transcellular activation of endothelial cells and leukocytes. *Arterioscler Thromb Vasc Biol*. 2016;36(3):482-90.
20. van Gils JM, da Costa Martins PA, Mol A, et al. Transendothelial migration drives dissociation of platelet-monocyte complexes. *Thromb Haemost*. 2008;100(2):271-9.
21. Witte A, Rohlfing AK, Dannenmann B, et al. The chemokine CXCL14 mediates platelet function and migration via direct interaction with CXCR4. *Cardiovasc Res*. 2020;cva0080.
22. Kraemer BF, Borst O, Gehring EM, et al. PI3 kinase-dependent stimulation of platelet migration by stromal cell-derived factor 1 (SDF-1). *J Mol Med (Berl)*. 2010;88(12):1277-88.
23. Schleicher RI, Reichenbach F, Kraft P, et al. Platelets induce apoptosis via membrane-bound FasL. *Blood*. 2015;126(12):1483-93.
24. van Lammeren GW, Pasterkamp G, de Vries JP, et al. Platelets enter atherosclerotic plaque via intraplaque microvascular leakage and intraplaque hemorrhage: a histopathological study in carotid plaques. *Atherosclerosis*. 2012;222(2):355-9.
25. Leroyer AS, Isobe H, Leseche G, et al. Cellular origins and thrombogenic activity of microparticles isolated from human atherosclerotic plaques. *J Am Coll Cardiol*. 2007;49(7):772-7.
26. Rainger GE, Chimen M, Harrison MJ, et al. The role of platelets in the recruitment of leukocytes during vascular disease. *Platelets*. 2015;26(6):507-20.
27. Schrottmaier WC, Mussbacher M, Salzmann M, et al. Platelet-leukocyte interplay during vascular disease. *Atherosclerosis*. 2020;307:109-20.
28. Rayes J, Bourne JH, Brill A, et al. The dual role of platelet-innate immune cell interactions in thrombo-inflammation. *Res Pract Thromb Haemost*. 2020;4(1):23-35
29. Martinod K, Deppermann C. Immunothrombosis and thromboinflammation in host defense and disease. *Platelets*. 2020;1-11.
30. da Costa Martins P, van den Berk N, Ulfman LH, et al. Platelet-monocyte complexes support monocyte adhesion to endothelium by enhancing secondary tethering and cluster formation. *Arterioscler Thromb Vasc Biol*. 2004;24(1):193-9.
31. Kuckleburg CJ, Yates CM, Kalia N, et al. Endothelial cell-borne platelet bridges selectively recruit monocytes in human and mouse models of vascular inflammation. *Cardiovasc Res*. 2011;91(1):134-41.
32. Schulz C, von Bruhl ML, Barocke V, et al. EMMPRIN (CD147/basigin) mediates platelet-monocyte interactions in vivo and augments monocyte recruitment to the vascular wall. *J Thromb Haemost*. 2011;9(5):1007-19.
33. Assinger A, Koller F, Schmid W, et al. Specific binding of hypochlorite-oxidized HDL to platelet CD36 triggers proinflammatory and procoagulant effects. *Atherosclerosis*. 2010;212(1):153-60.
34. Nergiz-Unal R, Lamers MM, van Kruchten R, et al. Signaling role of CD36 in platelet activation and thrombus formation on immobilized thrombospondin or oxidized low-density lipoprotein. *J Thromb Haemost*. 2011;9(9):1835-46.
35. Badrnya S, Butler LM, Soderberg-Naucleer C, et al. Platelets directly enhance neutrophil transmigration in response to oxidized low-density lipoprotein. *Thromb Haemost*. 2012;108(4):719-29.
36. Badrnya S, Schrottmaier WC, Kral JB, et al. Platelets mediate oxidized low-density lipoprotein-induced monocyte extravasation and foam cell formation. *Arterioscler Thromb Vasc Biol*. 2014;34(3):571-80.
37. Wang Y, Gao H, Shi C, et al. Leukocyte integrin Mac-1 regulates thrombosis via interaction with platelet GPIIb. *Nat Commun*. 2017;8:15559.

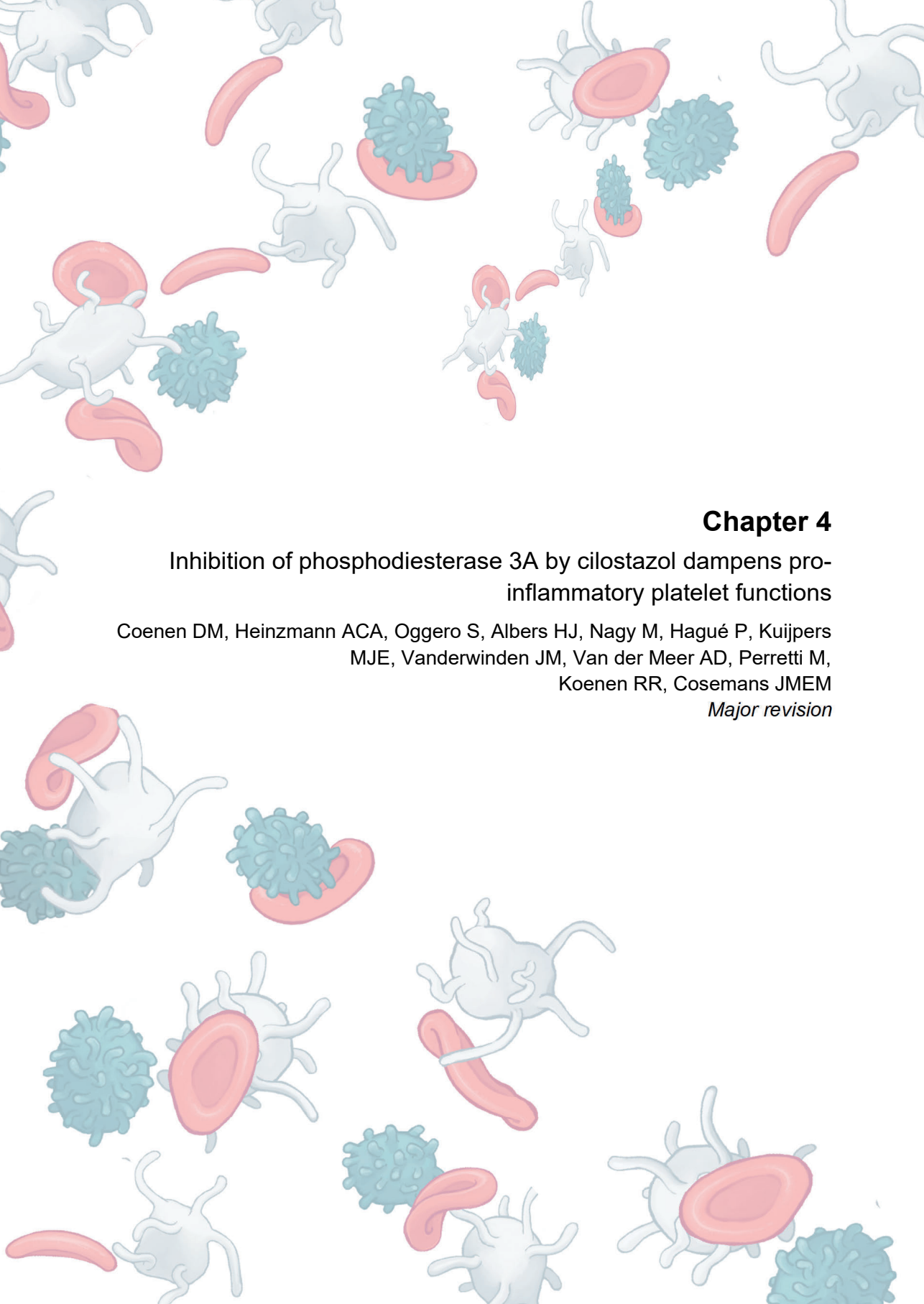
38. Wolf D, Hohmann JD, Wiedemann A, et al. Binding of CD40L to Mac-1's I-domain involves the EQLKKSRTL motif and mediates leukocyte recruitment and atherosclerosis—but does not affect immunity and thrombosis in mice. *Circ Res*. 2011;109(11):1269-79.
39. Wolf D, Anto-Michel N, Blankenbach H, et al. A ligand-specific blockade of the integrin Mac-1 selectively targets pathologic inflammation while maintaining protective host-defense. *Nat Commun*. 2018;9(1):525.
40. Schulz C, Schafer A, Stolla M, et al. Chemokine fractalkine mediates leukocyte recruitment to inflammatory endothelial cells in flowing whole blood: a critical role for P-selectin expressed on activated platelets. *Circulation*. 2007;116(7):764-73.
41. Postea O, Vasina EM, Cauwenberghs S, et al. Contribution of platelet CX(3)CR1 to platelet-monocyte complex formation and vascular recruitment during hyperlipidemia. *Arterioscler Thromb Vasc Biol*. 2012;32(5):1186-93.
42. Meyer dos Santos S, Klinkhardt U, Scholich K, et al. The CX3C chemokine fractalkine mediates platelet adhesion via the von Willebrand receptor glycoprotein Ib. *Blood*. 2011; 117(18):4999-5008.
43. Meyer dos Santos S, Blankenbach K, Scholich K, et al. Platelets from flowing blood attach to the inflammatory chemokine CXCL16 expressed in the endothelium of the human vessel wall. *Thromb Haemost*. 2015;114(2):297-312.
44. Linke B, Meyer dos Santos S, Picard-Willems B, et al. CXCL16/CXCR6-mediated adhesion of human peripheral blood mononuclear cells to inflamed endothelium. *Cytokine*. 2019;122:154081.
45. Higashiyama M, Hokari R, Kurihara C, et al. Indomethacin-induced small intestinal injury is ameliorated by cilostazol, a specific PDE-3 inhibitor. *Scand J Gastroenterol*. 2012;47(8-9):993-1002.
46. Iba T, Kidokoro A, Fukunaga M, et al. Comparison of the protective effects of type III phosphodiesterase (PDE3) inhibitor (cilostazol) and acetylsalicylic acid on intestinal microcirculation after ischemia reperfusion injury in mice. *Shock*. 2006;26(5):522-6.
47. Morel O, Toti F, Hugel B, et al. Procoagulant microparticles: disrupting the vascular homeostasis equation? *Arterioscler Thromb Vasc Biol*. 2006;26(12):2594-604.
48. Vajen T, Mause SF, Koenen RR. Microvesicles from platelets: novel drivers of vascular inflammation. *Thromb Haemost*. 2015;114(2):228-36.
49. Chimen M, Evryviadou A, Box CL, et al. Appropriation of GPIb α from platelet-derived extracellular vesicles supports monocyte recruitment in systemic inflammation. *Haematologica*. 2020;105(5):1248-61.
50. Kuravi SJ, Harrison P, Rainger GE, et al. Ability of platelet-derived extracellular vesicles to promote neutrophil-endothelial cell interactions. *Inflammation*. 2019;42(1):290-305.
51. Mause SF, von Hundelshausen P, Zernecke A, et al. Platelet microparticles: a transcellular delivery system for RANTES promoting monocyte recruitment on endothelium. *Arterioscler Thromb Vasc Biol*. 2005;25(7):1512-8.
52. Vasina EM, Cauwenberghs S, Feijge MA, et al. Microparticles from apoptotic platelets promote resident macrophage differentiation. *Cell Death Dis*. 2011;2(9):e211.
53. Sadallah S, Eken C, Martin PJ, et al. Microparticles (ectosomes) shed by stored human platelets downregulate macrophages and modify the development of dendritic cells. *J Immunol*. 2011;186(11):6543-52.
54. Laffont B, Corduan A, Rousseau M, et al. Platelet microparticles reprogram macrophage gene expression and function. *Thromb Haemost*. 2016;115(2):311-23.
55. Vajen T, Benedikter BJ, Heinzmann ACA, et al. Platelet extracellular vesicles induce a pro-inflammatory smooth muscle cell phenotype. *J Extracell Vesicles*. 2017;6(1):1322454.
56. French SL, Butov KR, Allaeyts I, et al. Platelet-derived extracellular vesicles infiltrate and modify the bone marrow during inflammation. *Blood Adv*. 2020;4(13):3011-23.
57. Laffont B, Corduan A, Ple H, et al. Activated platelets can deliver mRNA regulatory Ago2•microRNA complexes to endothelial cells via microparticles. *Blood*. 2013;122(2):253-61.
58. Gidlöf O, van der Brug M, Ohman J, et al. Platelets activated during myocardial infarction release functional miRNA, which can be taken up by endothelial cells and regulate ICAM1 expression. *Blood*. 2013;121(19):3908-17, S1-26.
59. Elgheznavy A, Fleming I. Platelet-enriched MicroRNAs and cardiovascular homeostasis. *Antioxidants Redox Signal*. 2018;29(9):902-21.
60. Sunderland N, Skroblin P, Barwari T, et al. MicroRNA biomarkers and platelet reactivity: the clot thickens. *Circ Res*. 2017;120(2):418-435.
61. Fish JE, Santoro MM, Morton SU, et al. miR-126 regulates angiogenic signaling and vascular integrity. *Dev Cell*. 2008;15(2):272-84.
62. Li J, Tan M, Xiang Q, et al. Thrombin-activated platelet-derived exosomes regulate endothelial cell expression of ICAM-1 via microRNA-223 during the thrombosis-inflammation response. *Thromb Res*. 2017;154:96-105.

63. Elghezawy A, Shi L, Hu J, et al. Dicer cleavage by calpain determines platelet microRNA levels and function in diabetes. *Circ Res*. 2015;117(2):157-65.
64. Fejes Z, Poliska S, Czimmerer Z, et al. Hyperglycaemia suppresses microRNA expression in platelets to increase P2RY12 and SELP levels in type 2 diabetes mellitus. *Thromb Haemost*. 2017;117(3):529-42.
65. Breet NJ, van Werkum JW, Bouman HJ, et al. Comparison of platelet function tests in predicting clinical outcome in patients undergoing coronary stent implantation. *J Am Med Assoc*. 2010;303(8):754-62.
66. Ferreiro JL, Angiolillo DJ. Diabetes and antiplatelet therapy in acute coronary syndrome. *Circulation*. 2011;123(7):798-813.
67. Randriamboavonjy V, Pistrosch F, Bolck B, et al. Platelet sarcoplasmic endoplasmic reticulum Ca^{2+} -ATPase and μ -calpain activity are altered in type 2 diabetes mellitus and restored by rosiglitazone. *Circulation*. 2008;117(1):52-60.
68. Falati S, Patil S, Gross PL, et al. Platelet PECAM-1 inhibits thrombus formation in vivo. *Blood*. 2006;107(2):535-41.
69. Tang WH, Stitham J, Gleim S, et al. Glucose and collagen regulate human platelet activity through aldose reductase induction of thromboxane. *J Clin Invest*. 2011;121(11):4462-76.
70. Tang WH, Stitham J, Jin Y, et al. Aldose reductase-mediated phosphorylation of p53 leads to mitochondrial dysfunction and damage in diabetic platelets. *Circulation*. 2014;129(15):1598-609.
71. Melchinger H, Jain K, Tyagi T, et al. Role of platelet mitochondria: life in a nucleus-free zone. *Front Cardiovasc Med*. 2019;6:153.
72. Baaten CCFMJ, Moenen FCJ, Henskens YMC, et al. Impaired mitochondrial activity explains platelet dysfunction in thrombocytopenic cancer patients undergoing chemotherapy. *Haematologica*. 2018;103(9):1557-67.
73. Bennett JA, Mastrangelor MA, Ture SK, et al. The choline transporter Slc44a2 controls platelet activation and thrombosis by regulating mitochondrial function. *Nat Commun*. 2020;11(1):3479.
74. Davizon-Castillo P, McMahon B, Aguila S, et al. TNF- α -driven inflammation and mitochondrial dysfunction define the platelet hyperreactivity of aging. *Blood*. 2019;134(9):727-40.
75. Hille L, Lenz M, Vlachos A, et al. Ultrastructural, transcriptional, and functional differences between human reticulated and non-reticulated platelets. *J Thromb Haemost*. 2020;18(8):2034-2046.
76. Bongiovanni D, Santamaria G, Klug M, et al. Transcriptome analysis of reticulated platelets reveals a prothrombotic profile. *Thromb Haemost*. 2019;119(11):1795-1806.
77. Kraakman MJ, Lee MK, Al-Sharea A, et al. Neutrophil-derived S100 calcium-binding proteins A8/A9 promote reticulated thrombocytosis and atherogenesis in diabetes. *J Clin Invest*. 2017;127(6):2133-47.
78. Guthikonda S, Alviar CL, Vaduganathan M, et al. Role of reticulated platelets and platelet size heterogeneity on platelet activity after dual antiplatelet therapy with aspirin and clopidogrel in patients with stable coronary artery disease. *J Am Coll Cardiol*. 2008;52(9):743-9.
79. Verdoia M, Pergolini P, Rolla R, et al. Impact of immature platelet fraction on platelet reactivity during prasugrel maintenance treatment. *Platelets*. 2019;30(7):915-22.
80. Mijovic R, Kovacevic N, Zarkov M, et al. Reticulated platelets and antiplatelet therapy response in diabetic patients. *J Thromb Thrombolysis*. 2015;40(2):203-10.
81. Stratz C, Nuhrenberg T, Valina CM, et al. Impact of reticulated platelets on the antiplatelet effect of the intravenous P2Y₁₂-receptor inhibitor cangrelor. *Thromb Haemost*. 2018;118(2):362-8.
82. Barbui T, Finazzi G, Falanga A. Myeloproliferative neoplasms and thrombosis. *Blood*. 2013;122(13):2176-84.
83. Steensma DP, Bejar R, Jaiswal S, et al. Clonal hematopoiesis of indeterminate potential and its distinction from myelodysplastic syndromes. *Blood*. 2015;126(1):9-16.
84. Jaiswal S, Libby P. Clonal haematopoiesis: connecting ageing and inflammation in cardiovascular disease. *Nat Rev Cardiol*. 2020;17(3):137-44.
85. Arellano-Rodrigo E, Alvarez-Larran A, Reverter JC, et al. Increased platelet and leukocyte activation as contributing mechanisms for thrombosis in essential thrombocythemia and correlation with the JAK2 mutational status. *Haematologica*. 2006;91(2):169-75.
86. Veninga A, de Simone I, Heemskerk JWM, et al. Clonal haematopoietic mutations linked to platelet traits and the risk of thrombosis or bleeding. *Haematologica*. 2020;105(8):2020-31.
87. Naik MU, Caplan JL, Naik UP. Junctional adhesion molecule-A suppresses platelet integrin $\alpha_{IIb}\beta_3$ signaling by recruiting Csk to the integrin-c-Src complex. *Blood*. 2014;123(9):1393-402.
88. Naik MU, Stalker TJ, Brass LF, et al. JAM-A protects from thrombosis by suppressing integrin $\alpha_{IIb}\beta_3$ -dependent outside-in signaling in platelets. *Blood*. 2012;119(14):3352-60.
89. Karshovska E, Zhao Z, Blanchet X, et al. Hyperreactivity of junctional adhesion molecule A-deficient platelets accelerates atherosclerosis in hyperlipidemic mice. *Circ Res*. 2015;116(4):587-99.

90. Zhao Z, Vajen T, Karshovska E, et al. Deletion of junctional adhesion molecule A from platelets increases early-stage neointima formation after wire injury in hyperlipidemic mice. *J Cell Mol Med*. 2017;21(8):1523-31.
91. von Hundelshausen P, Schmitt MM. Platelets and their chemokines in atherosclerosis-clinical applications. *Front Physiol*. 2014;5:294.
92. Kessler T, Schunkert H, von Hundelshausen P. Novel approaches to fine-tune therapeutic targeting of platelets in atherosclerosis: a critical appraisal. *Thromb Haemost*. 2020;120(11):1492-1504.
93. Coppinger JA, Cagney G, Toomey S, et al. Characterization of the proteins released from activated platelets leads to localization of novel platelet proteins in human atherosclerotic lesions. *Blood*. 2004;103(6):2096-104.
94. Pitsilos S, Hunt J, Mohler ER, et al. Platelet factor 4 localization in carotid atherosclerotic plaques: correlation with clinical parameters. *Thromb Haemost*. 2003;90(6):1112-20.
95. Davi G, Patrono C. Platelet activation and atherothrombosis. *N Engl J Med*. 2007;357(24):2482-94.
96. Koyama H, Maeno T, Fukumoto S, et al. Platelet P-selectin expression is associated with atherosclerotic wall thickness in carotid artery in humans. *Circulation*. 2003;108(5):524-9.
97. Fateh-Moghadam S, Li Z, Ersel S, et al. Platelet degranulation is associated with progression of intima-media thickness of the common carotid artery in patients with diabetes mellitus type 2. *Arterioscler Thromb Vasc Biol*. 2005;25(6):1299-303.
98. Yun KH, Mintz GS, Witzensbichler B, et al. Relationship between platelet reactivity and culprit lesion morphology: an assessment from the ADAPT-DES intravascular ultrasound substudy. *JACC Cardiovasc Imaging*. 2016;9(7):849-854.
99. Ridker PM, Everett BM, Thuren T, et al. Antiinflammatory therapy with canakinumab for atherosclerotic disease. *N Engl J Med*. 2017;377(12):1119-31.
100. Tardig JC, Kouz S, Waters DD, et al. Efficacy and safety of low-dose colchicine after myocardial infarction. *N Engl J Med*. 2019;381(26):2497-505.
101. Nidorf SM, Fiolet ATL, Mosterd A, et al. Colchicine in patients with chronic coronary disease. *N Engl J Med*. 2020;383(19):1838-47.
102. Jackson SP. Arterial thrombosis—insidious, unpredictable and deadly. *Nat Med*. 2011;17(11):1423-36.
103. Mastenbroek TG, van Geffen JP, Heemskerk JW, et al. Acute and persistent platelet and coagulant activities in atherothrombosis. *J Thromb Haemost*. 2015;13 Suppl 1:S272-80.
104. Karel M, Hechler B, Kuijpers M, et al. Atherosclerotic plaque injury-mediated murine thrombosis models: advantages and limitations. *Platelets*. 2020;31(4):439-46.
105. Libby P. Mechanisms of acute coronary syndromes and their implications for therapy. *N Engl J Med*. 2013;368(21):2004-13.
106. Versteeg HH, Heemskerk JW, Levi M, et al. New fundamentals in hemostasis. *Physiol Rev*. 2013;93(1):327-58.
107. Libby P, Pasterkamp G, Crea F, et al. Reassessing the mechanisms of acute coronary syndromes. *Circ Res*. 2019;124(1):150-60.
108. Quillard T, Franck G, Mawson T, et al. Mechanisms of erosion of atherosclerotic plaques. *Curr Opin Lipidol*. 2017;28(5):434-41.
109. Sato Y, Hatakeyama K, Yamashita A, et al. Proportion of fibrin and platelets differs in thrombi on ruptured and eroded coronary atherosclerotic plaques in humans. *Heart*. 2005;91(4):526-30.
110. Burke AP, Kolodgie FD, Farb A, et al. Healed plaque ruptures and sudden coronary death: evidence that subclinical rupture has a role in plaque progression. *Circulation*. 2001;103(7):934-40.
111. Vergallo R, Crea F. Atherosclerotic plaque healing. *N Engl J Med*. 2020;383(9):846-57.
112. Vergallo R, Porto I, D'Amario D, et al. Coronary atherosclerotic phenotype and plaque healing in patients with recurrent acute coronary syndromes compared with patients with long-term clinical stability: an in vivo optical coherence tomography study. *JAMA Cardiol*. 2019;4(4):321-9.
113. van der Meijden PEJ, Heemskerk JWM. Platelet biology and functions: new concepts and clinical perspectives. *Nat Rev Cardiol*. 2019;16(3):166-79.
114. Ghasemzadeh M, Kaplan ZS, Alwis I, et al. The CXCR1/2 ligand NAP-2 promotes directed intravascular leukocyte migration through platelet thrombi. *Blood*. 2013;121(22):4555-66.
115. Kaplan ZS, Zarpellon A, Alwis I, et al. Thrombin-dependent intravascular leukocyte trafficking regulated by fibrin and the platelet receptors GPIb and PAR4. *Nat Commun*. 2015;6:7835.
116. Laridan E, Martinod K, De Meyer SF. Neutrophil extracellular traps in arterial and venous thrombosis. *Semin Thromb Hemost*. 2019;45(1):86-93.
117. von Bruhl ML, Stark K, Steinhart A, et al. Monocytes, neutrophils, and platelets cooperate to initiate and propagate venous thrombosis in mice in vivo. *J Exp Med*. 2012;209(4):819-35.

118. Clark SR, Ma AC, Tavener SA, et al. Platelet TLR4 activates neutrophil extracellular traps to ensnare bacteria in septic blood. *Nat Med.* 2007;13(4):463-9.
119. Savchenko AS, Borissoff JI, Martinod K, et al. VWF-mediated leukocyte recruitment with chromatin decondensation by PAD4 increases myocardial ischemia/reperfusion injury in mice. *Blood.* 2014;123(1):141-8.
120. de Boer OJ, Li X, Teeling P, et al. Neutrophils, neutrophil extracellular traps and interleukin-17 associate with the organisation of thrombi in acute myocardial infarction. *Thromb Haemost.* 2013;109(2):290-7.
121. Mangold A, Alias S, Scherz T, et al. Coronary neutrophil extracellular trap burden and deoxyribonuclease activity in ST-elevation acute coronary syndrome are predictors of ST-segment resolution and infarct size. *Circ Res.* 2015;116(7):1182-92.
122. Mangold A, Hofbauer TM, Ondracek AS, et al. Neutrophil extracellular traps and monocyte subsets at the culprit lesion site of myocardial infarction patients. *Sci Rep.* 2019;9(1):16304.
123. Pertiwi KR, van der Wal AC, Pabittei DR, et al. Neutrophil extracellular traps participate in all different types of thrombotic and haemorrhagic complications of coronary atherosclerosis. *Thromb Haemost.* 2018;118(6):1078-87.
124. Josefs T, Barrett TJ, Brown EJ, et al. Neutrophil extracellular traps promote macrophage inflammation and impair atherosclerosis resolution in diabetic mice. *JCI Insight.* 2020;5(7):e134796.
125. Hilt ZT, Pariser DN, Ture SK, et al. Platelet-derived β 2M regulates monocyte inflammatory responses. *JCI Insight.* 2019;4(5):e122943.
126. Tardiff JC, Tanguay JF, Wright SR, et al. Effects of the P-selectin antagonist inclacumab on myocardial damage after percutaneous coronary intervention for non-ST-segment elevation myocardial infarction: results of the SELECT-ACS trial. *J Am Coll Cardiol.* 2013;61(20):2048-55.
127. Shimizu Y, Minatoguchi S, Hashimoto K, et al. The role of serotonin in ischemic cellular damage and the infarct size-reducing effect of sarpogrelate, a 5-hydroxytryptamine-2 receptor blocker, in rabbit hearts. *J Am Coll Cardiol.* 2002;40(7):1347-55.
128. Vikenes K, Farstad M, Nordrehaug JE. Serotonin is associated with coronary artery disease and cardiac events. *Circulation.* 1999; 100(5):483-9.
129. Duerschmied D, Suidan GL, Demers M, et al. Platelet serotonin promotes the recruitment of neutrophils to sites of acute inflammation in mice. *Blood.* 2013;121(6):1008-15.
130. Mauler M, Herr N, Schoenichen C, et al. Platelet serotonin aggravates myocardial ischemia/reperfusion injury via neutrophil degranulation. *Circulation.* 2019;139(7):918-31.
131. Schneider DJ, McMahon SR, Ehle GL, et al. Assessment of cardiovascular risk by the combination of clinical risk scores plus platelet expression of Fc γ R11a. *Am J Cardiol.* 2020;125(5):670-2.
132. Sauter RJ, Sauter M, Reis ES, et al. Functional relevance of the anaphylatoxin receptor C3aR for platelet function and arterial thrombus formation marks an intersection point between innate immunity and thrombosis. *Circulation.* 2018;138(16):1720-35.
133. Subramaniam S, Jurk K, Hobohm L, et al. Distinct contributions of complement factors to platelet activation and fibrin formation in venous thrombus development. *Blood.* 2017;129(16):2291-302.
134. Hamad OA, Nilsson PH, Wouters D, et al. Complement component C3 binds to activated normal platelets without preceding proteolytic activation and promotes binding to complement receptor 1. *J Immunol.* 2010;184(5):2686-92.
135. Maguier PB, Parsons ME, Szklanna PB, et al. Comparative platelet releasate proteomic profiling of acute coronary syndrome versus stable coronary artery disease. *Front Cardiovasc Med.* 2020;7:101.
136. Burkhart JM, Vaudel M, Gambaryan S, et al. The first comprehensive and quantitative analysis of human platelet protein composition allows the comparative analysis of structural and functional pathways. *Blood.* 2012;120(15):e73-82.
137. Zeiler M, Moser M, Mann M. Copy number analysis of the murine platelet proteome spanning the complete abundance range. *Mol Cell Proteomics.* 2014;13(12):3435-45.
138. Frenette PS, Denis CV, Weiss L, et al. P-selectin glycoprotein ligand 1 (PSGL- 1) is expressed on platelets and can mediate platelet-endothelial interactions in vivo. *J Exp Med.* 2000;191(8):1413-22.
139. Massberg S, Enders G, Leiderer R, et al. Platelet-endothelial cell interactions during ischemia/reperfusion: the role of P-selectin. *Blood.* 1998;92(2):507-15.
140. Weyrich AS, McIntyre TM, McEver RP, et al. Monocyte tethering by P-selectin regulates monocyte chemotactic protein-1 and tumor necrosis factor- α secretion. Signal integration and NF- κ B translocation. *J Clin Invest.* 1995;95(5):2297-303.
141. Sreeramkumar V, Adrover JM, Ballesteros I, et al. Neutrophils scan for activated platelets to initiate inflammation. *Science.* 2014;346(6214):1234-8.
142. Andonegui G, Kerfoot SM, McNagny K, et al. Platelets express functional Toll-like receptor-4. *Blood.* 2005;106(7):2417-23.

143. Brown GT, Narayanan P, Li W, et al. Lipopolysaccharide stimulates platelets through an IL-1 β autocrine loop. *J Immunol.* 2013;191(10):5196-203.
144. Wong CH, Jenne CN, Petri B, et al. Nucleation of platelets with blood-borne pathogens on Kupffer cells precedes other innate immunity and contributes to bacterial clearance. *Nat Immunol.* 2013;14(8):785-92.
145. Malehmir M, Pfister D, Gallage S, et al. Platelet GPIb α is a mediator and potential interventional target for NASH and subsequent liver cancer. *Nat Med.* 2019;25(4):641-55.
146. Risitano A, Beaulieu LM, Vitseva O, et al. Platelets and platelet-like particles mediate intercellular RNA transfer. *Blood.* 2012;119(26):6288-95.
147. Zeng Z, Xia L, Fan X, et al. Platelet-derived miR-223 promotes a phenotypic switch in arterial injury repair. *J Clin Invest.* 2019;129(3):1372-86.
148. Boudreau LH, Duchez AC, Cloutier N, et al. Platelets release mitochondria serving as substrate for bactericidal group IIA-secreted phospholipase A2 to promote inflammation. *Blood.* 2014;124(14):2173-83.
149. Puhm F, Afonyushkin T, Resh U, et al. Mitochondria are a subset of extracellular vesicles released by activated monocytes and induce type I IFN and TNF responses in endothelial cells. *Circ Res.* 2019;125(1):43-52.
150. Mahrouf-Yorgov M, Augeul L, Da Silva CC, et al. Mesenchymal stem cells sense mitochondria released from damaged cells as danger signals to activate their rescue properties. *Cell Death Differ.* 2017;24(7):1224-38.
151. Konkoth A, Saraswat R, Dubrou C, et al. Multifaceted role of extracellular vesicles in atherosclerosis. *Atherosclerosis.* 2020;S0021-9150(20)31500-8.



Chapter 4

Inhibition of phosphodiesterase 3A by cilostazol dampens pro-inflammatory platelet functions

Coenen DM, Heinzmann ACA, Oggero S, Albers HJ, Nagy M, Hagué P, Kuijpers MJE, Vanderwinden JM, Van der Meer AD, Perretti M, Koenen RR, Cosemans JMEM
Major revision

Abstract

Objective: Platelets possess not only haemostatic, but also inflammatory properties, which combined are thought to play a detrimental role in thrombo-inflammatory diseases such as acute coronary syndromes and stroke. Phosphodiesterase 3 and -5 inhibitors have demonstrated efficacy in secondary prevention of arterial thrombosis, partially mediated by their anti-platelet action. Yet, it is unclear whether such inhibitors also affect platelet-inflammatory functions. Here, we aimed to examine the effect of the PDE3A inhibitor cilostazol and the PDE5 inhibitor tadalafil on platelet function in various aspects of thrombo-inflammation.

Approach and results: Cilostazol, but not tadalafil, delayed *ex vivo* platelet-dependent fibrin formation under whole blood flow over type I collagen at 1000 s⁻¹. Using whole blood from *Pde3a* deficient mice, we confirmed the inhibitory effect of cilostazol on PDE3A. Interestingly, cilostazol specifically reduced the release of phosphatidylserine- (PS) positive extracellular vesicles (EVs) from human platelets while not affecting total EV release. Both cilostazol and tadalafil reduced the interaction of human platelets with inflamed endothelium under arterial flow and the release of the chemokines CCL5 and CXCL4 from platelets. Moreover, cilostazol, but not tadalafil, reduced monocyte recruitment and platelet-monocyte interaction *in vitro*.

Conclusions: In conclusion, this study demonstrated yet unrecognized roles for platelet PDE3A and platelet PDE5 in platelet pro-coagulant and pro-inflammatory responses.

Introduction

In atherosclerosis and its major clinical presentation, myocardial infarction and stroke, there is a strong crosstalk between inflammatory and thrombotic processes. For instance, platelets are considered to promote atherogenesis by recruiting leukocytes to the inflamed endothelium (via chemokines) and by triggering an inflammatory response in endothelial cells through direct interaction or with released extracellular vesicles (EVs).¹ Prevention of (recurrent) cardiovascular events predominantly comprises therapy with platelet activation inhibitors, such as aspirin and clopidogrel, or dual pathway inhibition with a low dose anticoagulant on top of aspirin.² Despite this comprehensive treatment, a quarter of the yearly arising strokes and myocardial infarcts is reoccurring,^{3,4} highlighting a need for new or additional treatment options.

In contrast to standard anti-platelet and anti-coagulant drugs, which dampen platelet- or coagulant activity, phosphodiesterase (PDE) inhibitors act by promoting vasodilation and platelet inhibitory pathways.⁵ The PDEs 2, 3 and 5 are expressed in platelets and hydrolyse cAMP (PDE2, PDE3) and cGMP (PDE2, PDE3, PDE5) to adenosine monophosphate and guanosine monophosphate, respectively, thereby lowering the threshold for platelet activation.⁵ Whereas PDE2 inhibitors are still under preclinical development, the PDE3A inhibitor cilostazol (IC₅₀ PDE3 inhibition: 0.2 μM)

is prescribed to alleviate symptoms of intermittent claudication in patients with peripheral artery disease and for secondary stroke prevention.⁶⁻⁸ Of note, cilostazol, as opposed to aspirin and clopidogrel, does not influence bleeding time.^{9,10} The PDE5 inhibitor dipyridamole was formerly used as a standard treatment for secondary stroke treatment in combination with aspirin, but current guidelines now advise monotherapy with aspirin or with clopidogrel.¹¹⁻¹⁴ Dipyridamole (IC₅₀ PDE5 inhibition: 0.9 μM) is known for its antithrombotic action. However, the platelet inhibiting function of dipyridamole does not only rely on its action via PDE5, but also on the blockage of adenosine reuptake.¹⁵ In contrast to dipyridamole, tadalafil (IC₅₀ PDE5 inhibition: 1.8 nM), sildenafil (IC₅₀ PDE5 inhibition: 5.22 nM), and vardenafil (IC₅₀ PDE5 inhibition: 0.7 nM) have a high specificity in only inhibiting PDE5 and these compounds are used for the treatment of erectile dysfunction.⁵ Tadalafil and sildenafil are also beneficial in pulmonary arterial hypertension.¹⁶ The effect of PDE3 inhibition on haemostatic or thrombotic platelet activation and aggregation has been explored widely, but research on the platelet pro-inflammatory function of cilostazol is limited. Moreover, research about PDE5 inhibition with its specific inhibitor tadalafil with regard to a thrombotic or inflammatory state is scarce.

Here we examine the effect of the PDE3A inhibitor cilostazol and the PDE5 inhibitor tadalafil on platelet function in various aspects of thrombo-inflammation.

Methods

Data are available upon reasonable request from the corresponding author. Reagents and detailed methods of all procedures are provided in the Data Supplement.

Blood collection

Human blood was obtained from healthy donors after full informed consent in compliance with the Declaration of Helsinki. Studies were approved by the local Medical Ethics Committee. Users of antiplatelet and/or anticoagulant medication were excluded. Regarding the flow experiments under inflammatory conditions, human whole blood was kindly provided by the Experimental Centre for Technical Medicine (ECTM) at the University of Twente.

Mice

Animal experiments were approved by the Ethics Committee for Animal Well-Being of the Faculty of Medicine, Université Libre de Bruxelles (ULB), protocol LA1230331-621N, in line with the regional and national regulations and the EU directives. All experiments were performed in accordance with relevant guidelines and regulations. Mice were bred and maintained under standard husbandry conditions and regular diet in the animal facility of the Faculty of Medicine, ULB. Genotyping was performed as described.¹⁷ Male and female C57BL/6 wild type (WT) and *Pde3a*^{-/-} mice between 10 and 26 weeks old were anaesthetized by

intraperitoneal injection with 800 µl avertin, which was standard procedure approved by the Ethical Committee for the procurement of biological materials for *ex vivo* studies. The effects of the anaesthesia were verified by checking the foot reflex. No post-anaesthetic effects were present as the mice were directly euthanized by cervical dislocation after blood collection on 3.2% sodium citrate via retro-orbital puncture.

Cell culture

Human umbilical vein endothelial cells (HUVECs) were cultured in ECGM medium (PromoCell) in a humidified atmosphere with 5% CO₂ at 37 °C. HUVECs between passage 5 and 7 were used.

Human acute monocytic leukaemia (THP-1) cells were cultured in RPMI-1640 Glutamax medium supplemented with 20% FCS and 1% penicillin/streptomycin in a humidified atmosphere with 5% CO₂ at 37 °C. THP-1 cells between passage 5 and 16 were used.

Statistical analysis

Flow perfusion experiments over collagen were analysed with a two-way ANOVA, except for time to fibrin formation with the pharmacological intervention, which was tested with an ordinary one-way ANOVA. Flow perfusion experiments over inflamed endothelium and the experiments regarding THP-1 migration, cAMP/cGMP levels and VASP phosphorylation were analysed with a Kruskal-Wallis test. THP-1 adhesion was evaluated with a Wilcoxon matched-pairs signed rank test. Statistical testing for remaining experiments was performed using an ordinary one-way ANOVA. Correction for multiple comparisons was achieved with Dunnett's, Dunns, Sidak's and Holm-Sidak's post-hoc testing. All data was statistically analysed with Graphpad Prism 8.4.3.

Results

Function of PDE3A and PDE5 in the activation of human and mouse platelets

To determine the effects of cilostazol and tadalafil on platelet activation markers, washed human platelets were incubated with increasing concentrations of these compounds prior to stimulation with the collagen-analogue CRP (0.3 µg/ml) and analysed by flow cytometry (Figure 1A). In suspension, cilostazol dose-dependently inhibited platelet integrin $\alpha_{IIb}\beta_3$ activation and secretion of platelet α - and dense granules (Figure 1B). Tadalafil significantly inhibited platelet integrin activation at 5 nM and above, while secretion of α -granules was only decreased at 20 and 50 nM. Dense granule secretion was not affected at these concentrations (Figure 1C). In resting or CRP-stimulated washed platelets, incubation with cilostazol or with tadalafil neither led to significantly altered cAMP and cGMP levels nor to altered phosphorylation of VASP at serine-157 or -239 (Suppl. Table 1 and Suppl. Figure 1).

Surprisingly, in platelets from WT or *Pde3a*^{-/-} (knockout; KO) mice measured with flow cytometry, integrin $\alpha_{IIb}\beta_3$ activation and α -granule secretion were unaltered upon stimulation of diluted whole blood with increasing doses of the platelet agonists ADP, AYPGKF (PAR4) or CRP (GPVI) (Suppl. Figure 2). There were no indications of platelet pre-activation as activation markers of unstimulated platelets levels were < 3 % (Suppl. Figure 2).

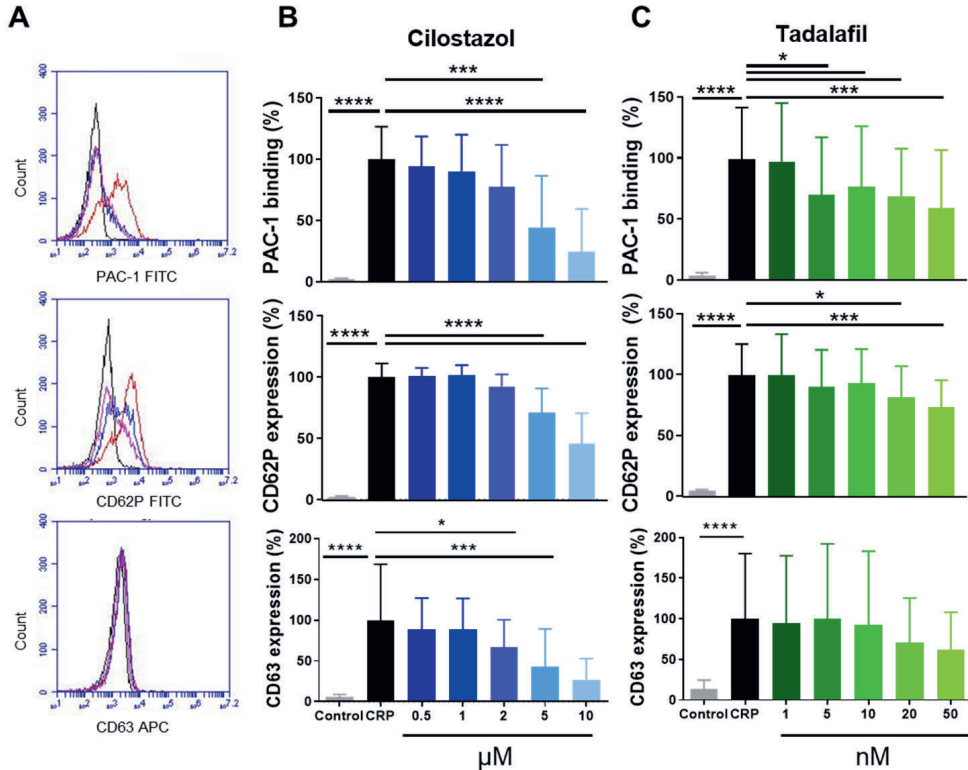


Figure 1. PDE3A and PDE5 inhibition dose-dependently decreases platelet integrin activation and granule secretion. Washed platelets were activated with collagen-related peptide (CRP, 0.3 $\mu\text{g}/\text{ml}$) and platelet integrin $\alpha_{IIb}\beta_3$ activation (PAC-1: $65.68 \pm 17.42\%$) and platelet α -granule secretion (CD62P: $72.74 \pm 8.17\%$), δ -granule secretion (CD63: $20.36 \pm 13.97\%$) were measured by flow cytometry (A). Dose-dependent decrease by PDE3A (B) and PDE5 (C) inhibition. Shown are data in duplicate in percentage normalized against the activated platelets without inhibitor. Corresponding vehicle controls were included for every condition. Histograms: black is control, red is CRP, pink is cilostazol (5 μM), blue is tadalafil (10 nM). Mean + S.D., $n = 5-7$, * $p < 0.05$, *** $p < 0.001$, **** $p < 0.0001$. Statistics: ordinary one-way ANOVA followed by Holm-Sidak's multiple comparisons test. CRP, collagen-related peptide.

PDE3A, but not PDE5, inhibition delays platelet-dependent coagulation, while maintaining initial haemostatic thrombus formation in human and mouse platelets

Haemostatic platelet thrombus formation involves reciprocal interaction between platelets and coagulation factors.¹⁸ To our knowledge, we are first to assess the role of PDE3A and PDE5 on *in vitro* platelet thrombus formation under

coagulating conditions using pharmacological inhibitors and blood from mice deficient for *Pde3a*. Of note, global *Pde5a* KO mice are embryonically lethal and no conditional *Pde5a* KO mouse models exist.¹⁹

Upon perfusion, human platelets adhered instantaneously to the collagen I and tissue factor surface and formed large and fibrin-rich thrombi with an average time to fibrin formation of 302 seconds. Platelet-collagen interaction as such was not affected by cilostazol (50 μ M, 95-98% protein-bound in plasma) or tadalafil (100 nM, 94% protein-bound in plasma) as the integrated feature size, which reflects platelet surface area coverage with respect to large thrombi and smaller platelet clusters,²⁰ was unaltered (Figure 2A, B). Interestingly, cilostazol, but not tadalafil, significantly increased time to fibrin formation to 384 seconds ($p=0.03$, Figure 2C). Surface area coverage of the platelet activation markers fibrin(ogen), CD62P and CD63 was unaltered (Suppl. Figure 3).

In a similar experimental setup, blood from *Pde3a* KO mice was compared to that of WT mice (Figure 2D-F). Mouse thrombi were analysed based on their morphologic appearance, in which the integrated feature size was significantly decreased with blood *Pde3a* KO mice upon perfusion over the collagen type I surface, in the absence of tissue factor ($p=0.05$, Figure 2F). When coagulation was stimulated by including tissue factor in the collagen type I surface, the differences between WT and KO mice were abolished (Figure 2F). No phenotypic differences of thrombi were observed between genotypes (Suppl. Figure 4). To expand the experimental window for picking up an effect of PDE3 inhibition in mice, iloprost was added to the blood, which causes a raise in cAMP levels. In our hands, such experimental window is smaller in mouse platelets when compared to human platelets as mouse platelets are more easily activated with as a consequence lower basal cAMP levels. Interestingly, the time to fibrin formation was increased in blood from *Pde3a* KO in comparison to blood from WT mice, in the presence of iloprost (Figure 2G). When investigating the activation markers of adherent platelets, surface area coverage of JON/A, CD62P, or annexin V was found to be uniform among WT and *Pde3a* deficient mice (Suppl. Figure 3). Altogether, these data suggest a promoting role for PDE3A, but not PDE5, in platelet-dependent fibrin formation, with platelet-collagen interaction under flow ranging from mildly inhibited to unaltered depending on the extent of coagulation.

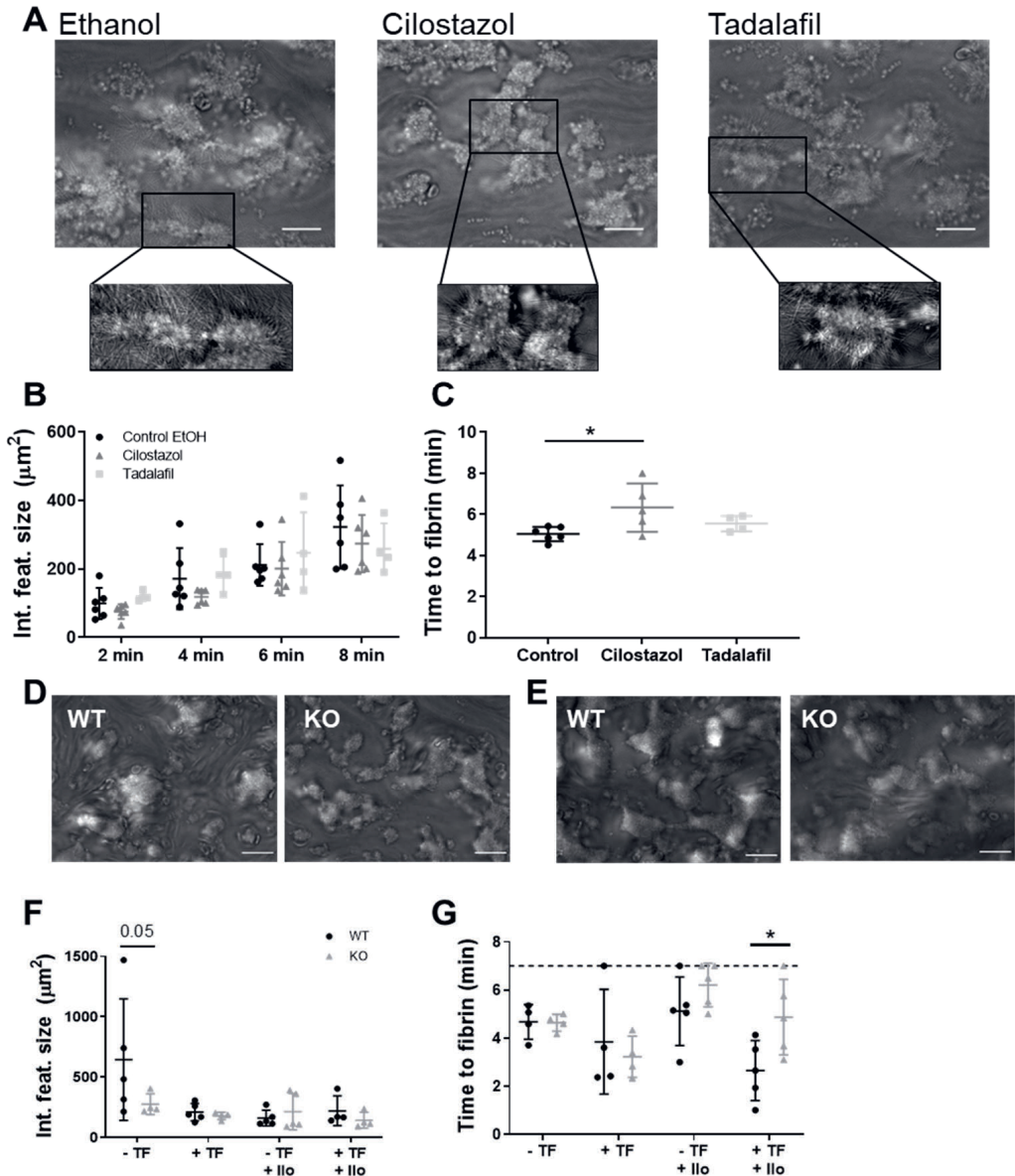


Figure 2. Effects of PDE-inhibition or genetic deletion on platelet-dependent coagulation under flow over collagen. Recalcified citrate-anti-coagulated human (A-C) or mouse (D-G) blood was perfused over a collagen type I surface or a combined collagen type I plus tissue factor surface for 7 (mouse) or 8 (human) min at a wall shear rate of 1000 s^{-1} . (A) Representative brightfield images after 8 minutes of blood perfusion without inhibitor (0.1% ethanol) or in the presence of cilostazol ($50 \mu\text{M}$) or tadalafil (100 nM). Quantitative analysis of integrated feature size (B) and time to fibrin formation (C). Representative brightfield images of blood perfusion of WT mice and *Pde3a*^{-/-} mice over collagen type I without (D) or with (E) tissue factor in the absence of iloprost under coagulating conditions. Quantitative analysis of integrated feature size (F) and time to fibrin (G). Scale is $20 \mu\text{m}$. Mean \pm S.D., $n = 4-6$ (human) or $4-5$ (mouse), * $p < 0.05$. Statistics: two-way ANOVA followed by Dunnett's (B) or Sidak's (F, G) multiple comparisons test. Time to fibrin formation (human) was tested by ordinary one-way ANOVA followed by Holm-Sidak's multiple comparisons test (C). Ilo, iloprost; KO, knockout; TF, tissue factor; WT, wild type.

PDE3A and PDE5 inhibition decreases platelet adhesion to inflamed endothelial cells

Next, we investigated the role of PDE3A under thrombo-inflammatory conditions, first specifically in platelet-endothelial interactions, in which different receptors are involved than in platelet interactions with vascular matrix components.^{21,22} Healthy endothelial cells ensure platelet quiescence, among others via the secretion of prostacyclin and nitric oxide,²³ and indeed, no platelet adhesion was visible during and after whole blood perfusion over untreated endothelial cells (data not shown). Inflammatory conditions were created by overnight or 4-hour stimulation of HUVECs with TNF- α (10 ng/ml), which gave similar results (data not shown). Whole blood perfusion over inflamed endothelial cells resulted in the adhesion of single platelets, which clustered but remained a single layer of platelets (Figure 3A). Pre-treatment of blood from healthy volunteers with cilostazol reduced platelet adhesion on the inflamed endothelium, already at a dosage which is 10-fold lower (5 μ m, Figure 3B) than used for the platelet-collagen interaction experiments (Figure 2). Interestingly, incubation with 10 nM tadalafil, which is 10-fold lower dose than the one used for platelet-collagen interaction under flow (Figure 2), inhibited platelet-endothelial interaction to a similar extent as cilostazol. These data suggest that pharmacological inhibition of PDE3A and PDE5 inhibits interactions of platelets with inflamed endothelium.

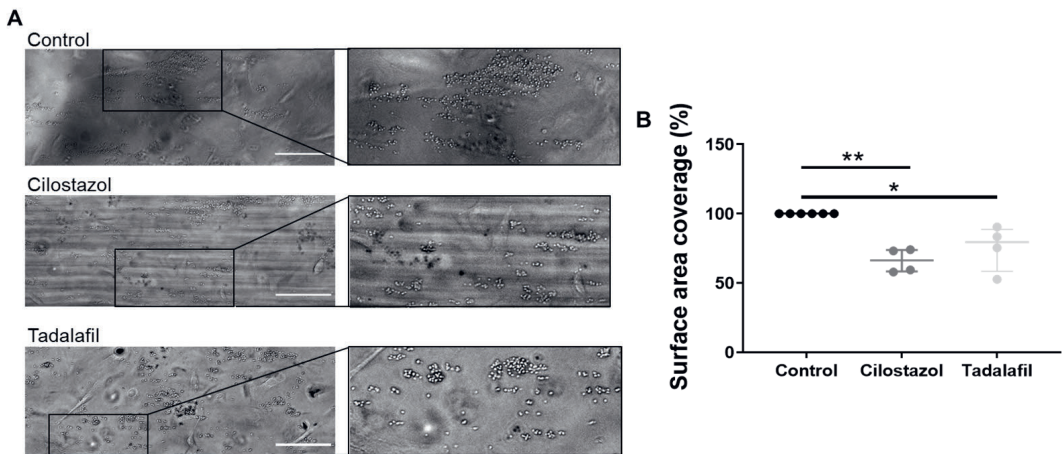


Figure 3. Platelet adhesion on inflamed endothelium is decreased upon PDE3A or -5 inhibition. Recalcified citrate-anti-coagulated human blood was perfused over HUVECs treated with 10 ng/ml TNF- α for 10 minutes at a wall shear rate of 1000 s^{-1} . **(A)** Representative brightfield images after 10 minutes of blood perfusion without inhibitor (0.1% ethanol) or in the presence of cilostazol (5 μ M) or tadalafil (10 nM). Quantitative analysis of platelet surface area coverage **(B)** in percentage normalized against whole blood perfusion without inhibitor. Scale is 100 μ m. Interquartile range, $n = 4-6$, * $p < 0.05$, ** $p < 0.01$. Statistics: Kruskal-Wallis test followed by Dunn's multiple comparisons test.

Monocyte migration to and adhesion on platelets is reduced by inhibition of PDE3A but not of PDE5

In the context of (thrombo-)inflammation, platelets facilitate monocyte activation and migration into the endothelium via chemotaxis and via direct interaction with monocytes.^{1,24} Platelet-induced monocyte migration was studied with a chemotaxis chamber (Figure 4). Washed platelets already induced migration of THP-1 cells without the addition of a platelet agonist (Figure 4A, B), which is suggestive of platelet activation in the well. Platelet activation with CRP shows a positive trend ($p=0.11$) to further increased THP-1 cell migration. Cilostazol ($5 \mu\text{M}$) pre-treatment diminished the CRP-induced chemotaxis, whereas PDE5 inhibition with tadalafil showed no effect (Figure 4B). Subsequently, we studied the effect of PDE3A inhibition on monocyte adhesion to a platelet monolayer, formed on a collagen type I surface, under flow conditions. Inhibition of PDE3A caused a relatively small, but significant ($p=0.04$), reduction in THP-1 adhesion to platelets (Figure 4C, D). Taken together, inhibition of PDE3A and thus increasing cAMP in platelets decreases both platelet-induced monocyte migration as well as adhesion of monocytes on platelets.

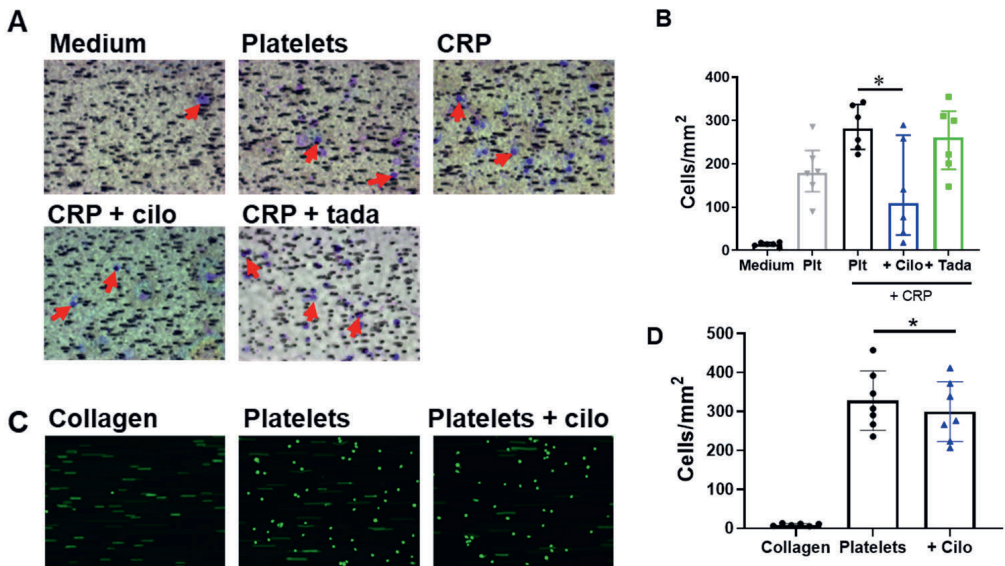


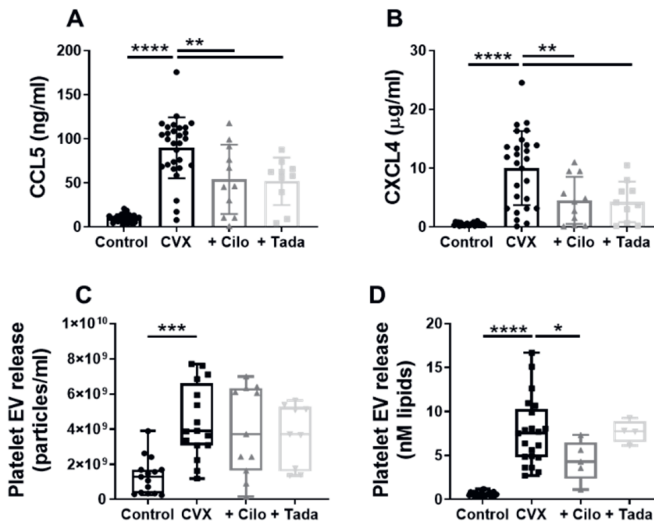
Figure 4. PDE3A inhibition decreases platelet-induced migration and platelet-induced adhesion of THP-1 cells under flow. Representative images (A) and quantitative analysis (B) of THP-1 cell migration to medium, and to washed platelets, untreated or additionally stimulated with CRP and inhibited with cilostazol ($5 \mu\text{M}$) or tadalafil (10 nM). Red arrows indicate THP-1 cells. Representative images (C) or quantitative analysis (D) of THP-1 adhesion to collagen alone, and to washed platelets in the absence or presence of cilostazol ($5 \mu\text{M}$). Interquartile range (B), mean \pm S.D. (D), $n = 6$ (A, B) or 7 (C, D), * $p < 0.05$. Statistics: Kruskal-Wallis test followed by Dunn's multiple comparisons test (B) and Wilcoxon matched-pairs signed rank test (D). Cilostazol; CRP, collagen-related peptide; plt, platelets; tada, tadalafil.

Platelet chemokine- and pro-coagulant EV release are regulated by PDE3A and partly by PDE5

Platelet chemokines promote leukocyte recruitment to the inflamed endothelium.^{1,24} We examined the effect of PDE3A and PDE5 inhibition on the release of the chemokines CCL5 (RANTES) and CXCL4 (platelet factor 4) by platelets. Convulxin- or thrombin-activated platelets secreted a substantial amount of CCL5 and CXCL4 (Figure 5A, B, $p < 0.0001$, Suppl. Figure 5). Both cilostazol and tadalafil reduced this chemokine release (Figure 5A, B, $p < 0.01$, Suppl. Figure 5), implicating a thus far unexplored role for PDE3A and -5 signalling in the secretion of pro-inflammatory factors from platelets.

Platelet-derived EV play an important role in both haemostasis and inflammation and other cardiovascular diseases.^{25,26} NTA was used to measure total platelet EV release. Stimulation of platelets with convulxin or thrombin resulted in a 3.3-fold and 2.4-fold increase of EV release, respectively (Suppl. Figure 5C, D, $p < 0.01$). Neither cilostazol (5 μM) nor tadalafil (10 nM) affected the total platelet EV release induced by convulxin (Figure 5C) or thrombin (Suppl. Figure 5). Cells can shed various EV subtypes, among which pro-coagulant EV have gained considerable attention.²⁷ Pro-coagulant (PS-positive) platelet EV release, determined with a prothrombinase-based assay and expressed as the amount of lipids (nM), was increased after platelet stimulation with convulxin (12.2-fold, Figure 5D, $p < 0.01$, Suppl. Figure 5D) or with thrombin (5.9-fold, Suppl. Figure 5, $p < 0.001$). PDE5 inhibition was not associated with altered pro-coagulant EV release. Importantly, cilostazol significantly decreased pro-coagulant EV release induced by convulxin (Figure 5D, $p = 0.02$), whereas it showed a tendency of reduction of pro-coagulant EVs after platelet stimulation with thrombin ($p = 0.08$) (Suppl. Figure 5).

Taken together, the above findings suggest that the pathways of pro-inflammatory platelet functions are regulated through the actions of PDE3A and PDE5, although potentially in different ways.



< **Figure 5. Effect of PDE3A and -5 inhibition on convulxin-induced chemokine and extracellular vesicle release by platelets.** Washed platelets were stimulated with convulxin (100 ng/ml) without or with cilostazol (5 μ M) or tadalafil (10 nM), and the release of chemokines CCL5 (A) and CXCL4 (B), and of total (C) and pro-coagulant (D) platelet extracellular vesicle (EV) was measured. (A, B) Mean \pm S.D., $n = 27-29$ (control, CVX) or $10-11$ (cilo, tada). (C, D) Interquartile range, $n = 15-16$ (control, CVX; NTA), $9-11$ (cilo, tada; NTA), $21-22$ (control, CVX; PTase), $4-5$ (cilo, tada; PTase), * $p < 0.05$, ** $p < 0.01$, *** $p < 0.001$, **** $p < 0.0001$. Statistics: ordinary one-way ANOVA followed by Dunnett's (A, B) or Holm-Sidak's (C, D) multiple comparisons test. Cilo, cilostazol; CVX, convulxin; NTA, nanoparticle tracking analysis; PTase, prothrombinase; tada, tadalafil.

Discussion

Platelets are increasingly considered to not only have a main role in haemostasis and thrombosis, but also to be important in other conditions, such as vascular inflammation.^{28,29} In so-called thrombo-inflammatory diseases, mechanisms of thrombosis and inflammation are intertwined, and can elicit and amplify one another. Here we report yet unrecognized roles for PDE3A and PDE5 in platelet pro-coagulant and pro-inflammatory responses. We found that PDE3A, but not PDE5, promotes platelet-dependent coagulation, through the delay of platelet-dependent fibrin formation and the reduction of pro-coagulant platelet EV release. With respect to pro-inflammatory responses, we observed that PDE3A and PDE5 promote platelet-chemokine release and the interaction of platelets with inflamed endothelium. Platelet PDE3A also promotes monocyte recruitment and platelet-monocyte interaction.

Both pharmacologic inhibition of PDE3A and -5 led to an unaltered platelet surface area coverage, platelet integrin activation, and granule secretion on collagen type I under flow. This might seem in contrast to previous studies that found reduced thrombus volume and platelet aggregation under shear flow.³⁰⁻³⁶ However, these studies were performed in the absence of coagulation. The experimental setting in our study encompassed coagulating conditions, which is an important difference in methodology, since thrombus formation and coagulation are interconnected by the interaction of platelets with coagulation factors.¹⁸ For example, thrombin generated on the platelet thrombi, being a potent agonist, might dampen the effects of cilostazol on integrin activation, secretion and thrombus formation. Of note, cilostazol did reduce integrin activation and secretion of α - and dense granules of washed platelets under non-coagulating conditions, which is in agreement with others.³⁷⁻³⁹

Our pharmacological studies were complemented by *ex vivo* perfusion using whole blood from *Pde3a*-deficient mice. *Pde3a*-deficient platelets displayed normal integrin activation and thrombus formation, but an increased time to fibrin formation under coagulating conditions. These results correspond to the pharmacologic PDE3A inhibition using cilostazol in human platelets and suggest that this delay in fibrin formation can be attributed to direct actions on PDE3A enzyme activity and not by *e.g.* blockage of adenosine reuptake, as observed with dipyridamole. Yet, in contrast to treatment of human platelets with cilostazol, we found integrin $\alpha_{IIb}\beta_3$ activation and CD62P expression in flow cytometry to be unaltered in *Pde3a* KO

platelets after stimulation with various platelet agonists. This might reflect differences in responses of the washed human platelets compared to those in diluted mouse whole blood. Nevertheless, the findings raise the question on the role of PDE3A in activation of mouse platelets versus human platelets. One explanation might be different amounts of the enzymes in platelets; human platelets have on average 1,400 copies of PDE3A and 10,900 copies PDE5 per platelet,⁴⁰ and mouse platelets contain 3,400 copies of PDE3A and 50,382 of PDE5.⁴¹ Evidence on the role of PDE3A in murine platelet activation is scarce in literature. One study reported that cAMP concentrations in resting *Pde3a*-deficient platelets was twice as high as in WT counterparts, which would suggest that these *Pde3a*^{-/-} platelets have a higher activation threshold.⁴²

Previous studies have largely focused on the role of cilostazol on the (non-inflamed) endothelium with respect to platelet-endothelium interaction, but such data are lacking for tadalafil. Cilostazol was found to directly act on the endothelium by inducing NO production,⁴³ and by suppressing expression of endothelial P-selectin and intercellular adhesion molecule-1 (ICAM-1),⁴⁴ which will dampen platelet activation and platelet-endothelial interaction.²¹ Our findings demonstrate that cilostazol and tadalafil reduce the adhesion of platelets in whole blood to activated endothelial cells under arterial shear conditions. As endothelial cells also contain PDE3A and PDE5 and both inhibitors are present during the perfusion experiments, a role for endothelial PDE3/PDE5 in the reduced platelet-endothelium interaction with cilostazol and tadalafil cannot be excluded a priori. However, this would involve an instantaneous alteration of expressed receptors for platelet adhesion in activated endothelial cells, which is rather unlikely. Our findings with cilostazol extend those by Fukuoka et al.,⁴⁵ who found that cilostazol inhibits platelet-endothelial cell interaction in murine cerebral microvessels after transient bilateral common carotid artery occlusion using infusion of labelled platelets obtained from a donor mouse. Of note, it is unclear from the article whether these donor platelets were also treated with cilostazol or not. In addition, elevation of cAMP in platelets by cilostazol was shown to reduce initial platelet accumulation at sites of laser-induced endothelial injury *in vivo*.⁴⁶ Taken together, our data suggest that platelet PDE3A and PDE5 do not only regulate thrombotic platelet responses, but also platelet function under inflammatory conditions.

During the past years, the importance of platelets in vascular inflammation and inflammatory diseases has been recognized, in which not only platelet-endothelial interactions are involved, but also the interplay between platelets and leukocytes.^{47,48} Migration and adhesion of monocytes towards and onto platelets was decreased upon PDE3A inhibition, although the inhibiting effects observed for monocyte adhesion were not as pronounced as for monocyte migration. Our findings extend earlier work in which a similar reduction by cilostazol treatment in binding of monocytes to collagen-activated platelets was observed, albeit under static conditions in a flow cytometer.³⁷ Importantly, we show that platelet PDE3A inhibition resulted in a strong reduction of the release of chemokines CCL5 and CXCL4, which

is in agreement with the reduction in α -granule release by PDE3 inhibition. These chemokines promote the adhesion of monocytes to endothelial cells.^{49,50} Interestingly, PDE5 inhibition decreased the release of CCL5 and CXCL4, while leaving monocyte migration unaffected. Beyond monocyte recruitment, CCL5 and in particular CXCL4 are also involved in neutrophil recruitment and activation, T cell differentiation, and injury responses of vascular smooth muscle cells.⁵¹⁻⁵⁴ Thus, the inhibition of CCL5 and CXCL4 release from platelets might be beneficial for the prevention of these pathological effects. In summary, cilostazol inhibits monocyte recruitment to and adhesion on platelets, presumably via the reduced release of CCL5 and CXCL4.

In our study, neither cilostazol nor tadalafil altered total platelet EV levels measured by nanoparticle tracking analysis. Conflicting reports exist about the effect of cilostazol on platelet EV release.⁵⁵ No role of PDE3A inhibition in platelet EV release was found when this was measured with an ELISA.^{56,57} In contrast, cilostazol decreased total platelet EV levels determined with flow cytometry.^{36,39,58-61} The lack of consistent effects of cilostazol on EV release is presumably related to the method of characterization, emphasizing the need for standardization.²⁶ Platelet extracellular vesicles exert pro-coagulant properties.^{62,63} The increased pro-coagulant activity in stroke and myocardial infarct patients is characterized by phosphatidylserine- (PS) or tissue factor expressing cells and extracellular vesicles.⁶⁴⁻⁶⁶ We are the first to distinguish between total EV levels and the number of pro-coagulant EVs in the context of phosphodiesterase inhibition. We found reduced pro-coagulant (PS-positive) extracellular vesicle release by cilostazol but not by tadalafil. Interestingly, acetylsalicylic acid had no effect on either total EV release in stroke patients nor pro-inflammatory or pro-coagulant EV release.⁶⁷ A remaining question is to what extent and how our pro-coagulant EV fraction differs from our total EV fraction and therefore, an important next step would be to fully characterize the platelet extracellular vesicles using fluorescent markers to obtain an advanced perspective of distinct EV subtypes, in healthy subjects and in various platelet-associated diseases.

Taken together, our findings demonstrate that the PDE3A inhibitor cilostazol not only delays platelet-dependent fibrin formation and platelet pro-coagulant EV release, but it also dampens platelet-mediated inflammatory responses. It would be of particular interest to examine whether cilostazol treatment also affects platelet (pro-coagulant) EVs in patients and whether the EV level is associated with (reduced) thrombotic events.

Highlights

- We identified novel roles for platelet PDE3A and PDE5 in promoting pro-coagulant and pro-inflammatory platelet functions.
- PDE3A inhibition with cilostazol reduces pro-coagulant extracellular vesicle release.

- Release of the chemokines CCL5 and CXCL4 is decreased by either cilostazol or the PDE5 inhibitor tadalafil.
- Our findings add mechanistic insight substantiating a beneficial effect of cilostazol in thrombo-inflammatory diseases.

Acknowledgements

Acknowledgements: We want to acknowledge Dr. Joel Moss and Steven Hockman from the NIH/NHLBI, who kindly granted us the permission to use the *Pde3a* knockout mice, originating from the lab of Prof. Dr. Vincent Manganiello (deceased).

Sources of funding: This work was supported by the Dutch Heart Foundation [2015T79 to D.M.C and J.M.E.M.C.]; the Netherlands Organization for Scientific Research [NWO Vidi 91716421 to J.M.E.M.C.]; the European Research Council [ERC Advanced 'VESCEL' to H.J.A.]; and the European Union [Horizon 2020 Marie Skłodowska-Curie 'EVOLUTION' No. 675111 to S.O. and M.P.].

Disclosures: none declared.

References

1. Coenen DM, Heinzmann ACA, Karel MFA et al. The multifaceted contribution of platelets in the emergence and aftermath of acute cardiovascular events. *Atherosclerosis*. 2021;319:132-41.
2. Weitz JI, Angiolillo DJ, Geisler T, et al. Dual pathway inhibition for vascular protection in patients with atherosclerotic disease: rationale and review of the evidence. *Thromb Haemost*. 2020;120:1147-58.
3. Benjamin EJ, Virani SS, Callaway CW, et al. Heart disease and stroke statistics-2018 update: a report from the American Heart Association. *Circulation*. 2018;137:e67-492.
4. World Health Organization. Cardiovascular diseases (cvds); [https://www.who.int/en/news-room/fact-sheets/detail/cardiovascular-diseases-\(cvds\)](https://www.who.int/en/news-room/fact-sheets/detail/cardiovascular-diseases-(cvds)). 2017.
5. Gresele P, Momi S, Falcinelli E. Anti-platelet therapy: phosphodiesterase inhibitors. *Br J Clin Pharmacol*. 2011;72:634-46.
6. Gerhard-Herman MD, Gornik HL, Barrett C, et al. 2016 AHA/ACC guideline on the management of patients with lower extremity peripheral artery disease: a report of the American College of Cardiology/American Heart Association task force on clinical practice guidelines. *J Am Coll Cardiol*. 2017;69:e71-126.
7. Noma K, Higashi Y. Cilostazol for treatment of cerebral infarction. *Expert Opin Pharmacother*. 2018;19:1719-26.
8. Toyoda K, Uchiyama S, Yamaguchi T, et al. Dual antiplatelet therapy using cilostazol for secondary prevention in patients with high-risk ischaemic stroke in Japan: a multicentre, open-label, randomised controlled trial. *The Lancet Neurology*. 2019;18:539-48.
9. Tamai Y, Takami H, Nakahata R, et al. Comparison of the effects of acetylsalicylic acid, ticlopidine and cilostazol on primary hemostasis using a quantitative bleeding time test apparatus. *Haemostasis*. 1999;29:269-76.
10. Wilhite DB, Comerota AJ, Schmieder FA, et al. Managing pad with multiple platelet inhibitors: the effect of combination therapy on bleeding time. *Journal of Vascular Surgery*. 2003;38:710-3.
11. Florescu C, Mustafa ER, Tarteia EA, et al. Antiplatelet therapy in secondary ischemic stroke prevention - a short review. *Rom J Morphol Embryol*. 2019;60:383-7.
12. Erdman MK, Leary MC. Antiplatelet agents. *Primer on cerebrovascular diseases*. 2017:874-81.
13. Bath PM, Woodhouse LJ, Appleton JP, et al. Antiplatelet therapy with aspirin, clopidogrel, and dipyridamole versus clopidogrel alone or aspirin and dipyridamole in patients with acute cerebral ischaemia (TARDIS): a randomised, open-label, phase 3 superiority trial. *Lancet*. 2018;391:850-9.
14. Powers WJ, Rabinstein AA, Ackerson T, et al. Guidelines for the early management of patients with acute ischemic stroke: 2019 update to the 2018 guidelines for the early management of acute ischemic stroke: a guideline for healthcare professionals from the American Heart Association/American Stroke Association. *Stroke*. 2019;50:e344-418.
15. Gresele P, Zoja C, Deckmyn H, et al. Dipyridamole inhibits platelet aggregation in whole blood. *Thromb Haemost*. 1983;50:852-6.

16. Parikh V, Bhardwaj A, Nair A. Pharmacotherapy for pulmonary arterial hypertension. *J Thorac Dis.* 2019;11:S1767-81.
17. Masciarelli S, Horner K, Liu C, et al. Cyclic nucleotide phosphodiesterase 3A-deficient mice as a model of female infertility. *J Clin Invest.* 2004;114:196-205.
18. Swieringa F, Spronk HMH, Heemskerk JWM, et al. Integrating platelet and coagulation activation in fibrin clot formation. *Res Pract Thromb Haemost.* 2018;2:450-60.
19. Zhang M, Takimoto E, Hsu S, et al. Myocardial remodeling is controlled by myocyte-targeted gene regulation of phosphodiesterase type 5. *J Am Coll Cardiol.* 2010;56:2021-30.
20. de Witt SM, Swieringa F, Cavill R, et al. Identification of platelet function defects by multi-parameter assessment of thrombus formation. *Nat Commun.* 2014;5:4257.
21. Coenen DM, Mastenbroek TG, Cosemans J. Platelet interaction with activated endothelium: mechanistic insights from microfluidics. *Blood.* 2017;130:2819-28.
22. Versteeg HH, Heemskerk JW, Levi M, et al. New fundamentals in hemostasis. *Physiol Rev.* 2013;93:327-58.
23. Smolenski A. Novel roles of cAMP/cGMP-dependent signaling in platelets. *J Thromb Haemost.* 2012;10:167-76.
24. Rayes J, Bourne JH, Brill A, et al. The dual role of platelet-innate immune cell interactions in thrombo-inflammation. *Res Pract Thromb Haemost.* 2020;4:23-35
25. Vajen T, Mause SF, Koenen RR. Microvesicles from platelets: Novel drivers of vascular inflammation. *Thromb Haemost.* 2015;114:228-36.
26. Dickhout A, Koenen RR. Extracellular vesicles as biomarkers in cardiovascular disease; chances and risks. *Front Cardiovasc Med.* 2018;5:113.
27. Gasecka A, Nieuwland R, Budnik M, et al. Randomized controlled trial protocol to investigate the antiplatelet therapy effect on extracellular vesicles (AFFECT EV) in acute myocardial infarction. *Platelets.* 2018:1-7.
28. Franco AT, Corken A, Ware J. Platelets at the interface of thrombosis, inflammation, and cancer. *Blood.* 2015;126:582-8.
29. Koenen RR. The prowess of platelets in immunity and inflammation. *Thromb Haemost.* 2016;116:605-12.
30. Yagi H, Yamaguchi N, Shida Y, et al. Cilostazol down-regulates the height of mural platelet thrombi formed under a high-shear rate flow in the absence of ADAMTS13 activity. *Eur J Pharmacol.* 2012;691:151-5.
31. Minami N, Suzuki Y, Yamamoto M, et al. Inhibition of shear stress-induced platelet aggregation by cilostazol, a specific inhibitor of cGMP-inhibited phosphodiesterase, in vitro and ex vivo. *Life Sciences.* 1997;61:PL383-9.
32. Nakamura T, Uchiyama S, Yamazaki M, et al. Synergistic effect of cilostazol and dipyridamole mediated by adenosine on shear-induced platelet aggregation. *Thromb Res.* 2007;119:511-6.
33. Onoda K, Ohashi K, Hashimoto A, et al. Inhibition of platelet aggregation by combined therapy with aspirin and cilostazol after off-pump coronary artery bypass surgery. *Ann Thorac Cardiovasc Surg.* 2008;14:230-7.
34. Ryu KH, Han HY, Lee SY, et al. Ginkgo biloba extract enhances antiplatelet and antithrombotic effects of cilostazol without prolongation of bleeding time. *Thromb Res.* 2009;124:328-34.
35. Tanigawa T, Nishikawa M, Kitai T, et al. Increased platelet aggregability in response to shear stress in acute myocardial infarction and its inhibition by combined therapy with aspirin and cilostazol after coronary intervention. *Am J Cardiol.* 2000;85:1054-9.
36. Yamazaki M, Uchiyama S, Xiong Y, et al. Effect of remnant-like particle on shear-induced platelet activation and its inhibition by antiplatelet agents. *Thromb Res.* 2005;115:211-8.
37. Ito H, Miyakoda G, Mori T. Cilostazol inhibits platelet-leukocyte interaction by suppression of platelet activation. *Platelets.* 2004;15:293-301.
38. Lee SY, Kang MJ, Cha JK. Cilostazol reduces PAC-1 expression on platelets in ischemic stroke. *J Clin Neurol.* 2008;4:148-52.
39. Nomura S, Inami N, Iwasaka T, et al. Platelet activation markers, microparticles and soluble adhesion molecules are elevated in patients with arteriosclerosis obliterans: therapeutic effects by cilostazol and potentiation by dipyridamole. *Platelets.* 2004;15:167-72.
40. Burkhart JM, Vaudel M, Gambaryan S, et al. The first comprehensive and quantitative analysis of human platelet protein composition allows the comparative analysis of structural and functional pathways. *Blood.* 2012;120:e73-82.
41. Zeiler M, Moser M, Mann M. Copy number analysis of the murine platelet proteome spanning the complete abundance range. *Mol Cell Proteomics.* 2014;13:3435-45.
42. Sun B, Li H, Shakur Y, et al. Role of phosphodiesterase type 3A and 3B in regulating platelet and cardiac function using subtype-selective knockout mice. *Cell Signal.* 2007;19:1765-71.

43. Hashimoto A, Miyakoda G, Hirose Y, et al. Activation of endothelial nitric oxide synthase by cilostazol via a cAMP/protein kinase A- and phosphatidylinositol 3-kinase/Akt-dependent mechanism. *Atherosclerosis*. 2006;189:350-7.
44. Hase Y, Okamoto Y, Fujita Y, et al. Cilostazol, a phosphodiesterase inhibitor, prevents no-reflow and hemorrhage in mice with focal cerebral ischemia. *Exp Neurol*. 2012;233:523-33.
45. Fukuoka T, Hayashi T, Hirayama M, et al. Cilostazol inhibits platelet-endothelial cell interaction in murine microvessels after transient bilateral common carotid artery occlusion. *J Stroke Cerebrovasc Dis*. 2014;23:1056-61.
46. Sim DS, Merrill-Skoloff G, Furie BC, et al. Initial accumulation of platelets during arterial thrombus formation in vivo is inhibited by elevation of basal cAMP levels. *Blood*. 2004;103:2127-34.
47. Projahn D, Koenen RR. Platelets: key players in vascular inflammation. *J Leukoc Biol*. 2012;92:1167-75.
48. van Gils JM, Zwaginga JJ, Hordijk PL. Molecular and functional interactions among monocytes, platelets, and endothelial cells and their relevance for cardiovascular diseases. *J Leukoc Biol*. 2009;85:195-204.
49. von Hundelshausen P, Koenen RR, Sack M, et al. Heterophilic interactions of platelet factor 4 and RANTES promote monocyte arrest on endothelium. *Blood*. 2005;105:924-30.
50. Vajen T, Koenen RR, Werner I, et al. Blocking CCL5-CXCL4 heteromerization preserves heart function after myocardial infarction by attenuating leukocyte recruitment and NETosis. *Sci Rep*. 2018;8:10647.
51. Rossaint J, Herter JM, Van Aken H, et al. Synchronized integrin engagement and chemokine activation is crucial in neutrophil extracellular trap-mediated sterile inflammation. *Blood*. 2014;123:2573-84.
52. Gerdes N, Zhu L, Ersoy M, et al. Platelets regulate CD4⁺ T-cell differentiation via multiple chemokines in humans. *Thromb Haemost*. 2011;106:353-62.
53. Shi G, Field DJ, Long X, et al. Platelet factor 4 mediates vascular smooth muscle cell injury responses. *Blood*. 2013;121:4417-27.
54. Drechsler M, Megens RT, van Zandvoort M, et al. Hyperlipidemia-triggered neutrophilia promotes early atherosclerosis. *Circulation*. 2010;122:1837-45.
55. Rosinska J, Lukasik M, Kozubski W. The impact of vascular disease treatment on platelet-derived microvesicles. *Cardiovasc Drugs Ther*. 2017;31:627-44.
56. Ichijo M, Ishibashi S, Ohkubo T, et al. Elevated platelet microparticle levels after acute ischemic stroke with concurrent idiopathic thrombocytopenic purpura. *J Stroke Cerebrovasc Dis*. 2014;23:587-9.
57. Shirafuji T, Hamaguchi H, Kanda F. Measurement of platelet-derived microparticle levels in the chronic phase of cerebral infarction using an enzyme-linked immunosorbent assay. *Kobe J Med Sci*. 2008;54:E55-61.
58. Chen Y, Xiao Y, Lin Z, et al. The role of circulating platelets microparticles and platelet parameters in acute ischemic stroke patients. *J Stroke Cerebrovasc Dis*. 2015;24:2313-20.
59. Nomura S, Imamura A, Okuno M, et al. Platelet-derived microparticles in patients with arteriosclerosis obliterans. *Thromb Res*. 2000;98:257-68.
60. Nomura S, Shouzu A, Omoto S, Hayakawa T, Kagawa H, Nishikawa M, Inada M, Fujimura Y, Ikeda Y, Fukuhara S. Effect of cilostazol on soluble adhesion molecules and platelet-derived microparticles in patients with diabetes. *Thromb Haemost*. 1998;80:388-392.
61. Omoto S, Nomura S, Shouzu A, et al. Significance of platelet-derived microparticles and activated platelets in diabetic nephropathy. *Nephron*. 1999;81:271-7.
62. Cauwenberghs S, Feijge MA, Harper AG, et al. Shedding of procoagulant microparticles from unstimulated platelets by integrin-mediated destabilization of actin cytoskeleton. *FEBS Lett*. 2006;580:5313-20.
63. Tans G, Rosing J, Thomassen MC, et al. Comparison of anticoagulant and procoagulant activities of stimulated platelets and platelet-derived microparticles. *Blood*. 1991;77:2641-8.
64. Muller I, Klocke A, Alex M, et al. Intravascular tissue factor initiates coagulation via circulating microvesicles and platelets. *FASEB J*. 2003;17:476-8.
65. Sims PJ, Wiedmer T, Esmon CT, et al. Assembly of the platelet prothrombinase complex is linked to vesiculation of the platelet plasma membrane. Studies in Scott syndrome: an isolated defect in platelet procoagulant activity. *J Biol Chem*. 1989;264:17049-57.
66. Yao Z, Wang L, Wu X, et al. Enhanced procoagulant activity on blood cells after acute ischemic stroke. *Transl Stroke Res*. 2017;8:83-91.
67. Rosinska J, Maciejewska J, Narozny R, et al. Association of platelet-derived microvesicles with high on-treatment platelet reactivity in convalescent ischemic stroke patients treated with acetylsalicylic acid. *Wiad Lek*. 2019;72:1426-36.

Supplemental methods

Reagents

Cilostazol (Cas no. 73963-72-1) was ordered from Tebu Bio (Le-Perray-en-Yvelines, France) and tadalafil (Cas no. 171596-29-5) from Merck (Kenilworth, NJ, USA). Iloprost was bought in the hospital pharmacy of Maastricht University Medical Centre+ (MUMC+, Maastricht, The Netherlands) and sodium nitroprusside (SNP) from Janssen Pharmaceutica (Beerse, Belgium). Apyrase was obtained from Merck (Kenilworth, NJ, USA). Cross-linked collagen-related peptide (CRP) was purchased from CambCol Laboratories (Cambridge, UK), convulxin from Enzo (Zandhoven, Belgium), thrombin from Haematologic Technologies (Essex Junction, VT, USA) and collagen type I (HORM collagen) from Takeda (Tokio, Japan). 2-methylthio adenosine diphosphate (2-MeS-ADP) was bought from Santa Cruz Biotechnology (Dallas, TX, USA) and Ala-Tyr-Pro-Gly-Lys-Phe (AYPGKF) from Bachem Biosciences (Bubendorf, Switzerland). The monoclonal antibodies (mAbs) PAC-1, JON/A, anti-CD62P and anti-CD63 were purchased from Becton Dickinson (Franklin Lakes, NJ, USA), Emfret (Eibelstadt, Germany), Becton Dickinson (PE, Franklin Lakes, NJ, USA)/Beckman Coulter (FITC, Brea, CA, USA) and ITK Biologend (San Diego, CA, USA), respectively. The mAbs against vasodilator-stimulated phosphoprotein (VASP) (phospho-Ser 157 and phospho-Ser 239) were purchased from Biomol (Hamburg, Germany). Fluorescently labelled fibrinogen and annexin V were purchased from Invitrogen Life Technologies (ThermoFisher, Waltham, MA, USA). Tissue factor was ordered from Innovin (London, UK), D-Phe-Pro-Arg-chloromethylketone (PPACK) from Merck (Kenilworth, NJ, USA) and fragmin from Pfizer (New York, NY, USA). Calcium and magnesium were purchased from Merck (Kenilworth, NJ, USA) and Ambion (ThermoFisher, Waltham, MA, USA). Saponin and formaldehyde were purchased from Merck (Kenilworth, NJ, USA). Human umbilical vein endothelial cells (HUVECs) were purchased from Lonza (Basel, Switzerland), THP-1 cells were from Leibniz-Institut DSMZ (ACC 16, Braunschweig, Germany), Endothelial Cell Growth Medium (ECGM) from Promocell (Heidelberg, Germany) and RPMI-1640 glutamax medium, fetal calf serum and penicillin/streptomycin were purchased from Gibco, Thermo Fisher (Waltham, MA, USA). Tumour necrosis factor- α (TNF- α) was purchased from Merck (Kenilworth, NJ, USA).

Platelet isolation

Blood was drawn on 3.2% sodium citrate (Vacurette, Greiner bio-one). Whole blood was centrifuged at 240 g for 15 minutes without break to obtain platelet-rich plasma (PRP). Washed platelets were prepared by addition of 1:10 acid citrate dextrose (ACD, 80 mM trisodium citrate, 52 mM citric acid and 183 mM glucose) to the PRP and centrifugation at 2230 g for 2 minutes. Subsequently, the platelet pellet was resuspended in Hepes buffer pH 6.6 (10 mM Hepes, 136 mM NaCl, 2.7 mM KCl, 2 mM MgCl₂, 0.1% glucose and 0.1% bovine serum albumin (BSA)). After addition of 0.1 U/ml apyrase and ACD (1:15), the platelet suspension was

centrifuged again at 2230 g for 2 minutes. The final platelet pellet was suspended in Hepes buffer pH 7.45. Platelet count was measured using a Sysmex XP-300 (Sysmex).

Platelet activation with flow cytometry

Human washed platelets (50×10^6 platelets/ml) were incubated with a range of concentrations of cilostazol or tadalafil for 20 minutes. Next, the platelets were activated with collagen-related peptide (CRP; $0.3 \mu\text{g/ml}$) in the presence of 2 mM CaCl_2 for 15 minutes and $\alpha_{\text{IIb}}\beta_3$ integrin activation and α - and dense granule secretion were measured with PAC-1 (FITC, 1:20), anti-CD62P (FITC, 1:10) and anti-CD63 (APC, 1:20) antibodies with an Accuri C6 flow cytometer (Beckton Dickinson).

Mouse blood was diluted 25 times in Thyroid Hepes buffer pH 7.45 (5 mM Hepes, 136 mM NaCl, 2.7 mM KCl, 0.42 mM NaH_2PO_4 , 2 mM MgCl_2 , 0.1% glucose and 0.1% BSA) with addition of 20 μM PPACK and 20 U/ml fragmin. Diluted blood was incubated for 4 minutes with 5 nM iloprost and activated with a concentration range of AYPGKF (50 μM , 75 μM and 100 μM), CRP (0.5 $\mu\text{g/ml}$, 1 $\mu\text{g/ml}$ and 10 $\mu\text{g/ml}$) or 2-MeS-ADP (0.01 μM and 0.1 μM) in the presence of 2 mM CaCl_2 for 10 minutes. $\alpha_{\text{IIb}}\beta_3$ integrin activation and α -granule secretion were measured with JON/A (PE, 1:10) and anti-CD62P (FITC, 1:10) antibodies with an Accuri C6 flow cytometer.

cAMP/cGMP measurements

Washed platelets (200×10^6 platelets/ml) were incubated with cilostazol (5 μM) or tadalafil (10 nM) for 20 minutes or iloprost (10 nM) and sodium nitroprusside (SNP, 0.1 μM) for 2 minutes. Subsequently, the platelets were activated with CRP (0.3 $\mu\text{g/ml}$) in the presence of 2 mM CaCl_2 for 15 minutes. Ice-cold ethanol was added after which the samples were directly snap frozen in liquid nitrogen and stored at -80°C until continuation of the assay. After thawing and centrifugation at 350 g for 10 minutes, the samples were dried under nitrogen at 56°C and dissolved in assay buffer. cAMP and cGMP were measured using the Amersham Biotrak Enzymeimmunoassay (EIA) System (GE Healthcare Life Sciences) according to the manufacturer's instructions.

VASP phosphorylation with flow cytometry

Washed platelets (100×10^6 platelets/ml) were incubated with cilostazol (5 μM) or tadalafil (10 nM) for 20 minutes or iloprost (10 nM) and SNP (0.1 μM) for 2 minutes. Subsequently, the platelets were activated with CRP (0.3 $\mu\text{g/ml}$) in the presence of 2 mM CaCl_2 for 15 minutes. Fixation was performed with 2% formaldehyde in phosphate-buffered saline (PBS) with 0.2% BSA for 15 minutes and the platelets were permeabilised with 0.1% saponin in PBS with 0.2% BSA after two centrifuge steps at 2230 g for 2 minutes and in between washing with PBS with 0.2% BSA. The fixated and permeabilised platelets were stained with anti-p-VASP S157

and S239 (FITC, 1:100) antibodies and analysed with an Accuri C6 flow cytometer (Beckton Dickinson).

Collagen-mediated whole blood thrombus formation under flow

GPVI-mediated thrombus formation under flow was performed using a parallel plate flow chamber (3,000 x 50 μm) as described by de Witt et al. and Brouns et al.^{1,2} Human blood was incubated with cilostazol (50 μM), tadalafil (100 nM) or vehicle (0.1% ethanol) for ten minutes. Recalcified blood (f.c. 6.3 mM CaCl_2 and 3.2 mM MgCl_2 [human] or 7.5 mM CaCl_2 and 3.5 mM MgCl_2 [mouse]) was perfused for eight minutes at 1000 s^{-1} over microspots that were coated with 50 $\mu\text{g}/\text{ml}$ collagen type I and, where indicated, post-coated after one hour with 500 pM tissue factor. Because in our hands mouse platelets can more easily be activated than human platelets, the stable prostacyclin analogue iloprost (5 nM) was added as an extra condition in the murine perfusion experiments. Human blood was stained with fluorescently labelled fibrinogen (Alexa Fluor 546, 1:200) and with anti-CD62P (FITC, 1:40) and anti-CD63 (APC, 1:50) antibodies and murine blood with JON/A (PE, 1:20), anti-CD62P (FITC, 1:40) antibodies and annexin V (Alexa Fluor 647, 1:200). Brightfield and fluorescence images were taken during perfusion with an EVOS FL microscope with 60x magnification. Time to fibrin formation was determined by visual inspection of the formation of fibrin fibres from platelet thrombi. Analysis of the images was performed with Fiji ImageJ software. Images were scored based on morphology, contraction and multilayer.

Platelet activation on and interaction with inflamed endothelium

Platelet activation on and interaction with inflamed endothelium was examined using polydimethylsiloxane (PDMS) flow chambers (300 x 50 μm), made by standard soft lithography techniques. A mold was fabricated by patterning channel-like structures in SU-8 negative photoresist (Microchem) on a silicon wafer using photolithography. PDMS base and curing agent (Sylgard 184) were mixed at a 10/1 ratio (w/w) and degassed for 2h. The degassed PDMS was poured on the wafer and baked overnight at 60 $^{\circ}\text{C}$. After the curing step the PDMS slab was removed from the wafer resulting in embossed channels in the PDMS slab. In- and outlets were made using a 1 mm biopsy puncher (Integra Miltex). Subsequently, the flow chambers were made by plasma treatment (Femto Science Cute, O_2 plasma 50 W at 50 kHz and 40 seconds exposure) of the PDMS structures and a glass slide (Thermo Scientific) followed by bonding of the two layers. The channels were coated with a 100 $\mu\text{g}/\text{ml}$ collagen type I (Corning, rat tail) solution in PBS for 30 minutes, after which HUVECs were seeded by introducing 10 μl cell suspension with a concentration of 15×10^6 cells/ml in ECGM medium (PromoCell). After 30-minute incubation, this step was repeated whilst incubating top-side down to coat both the bottom and the top of each channel. When confluency was reached, the cells were treated overnight or for 4 hours with TNF- α (10 ng/ml).

Recalcified blood (f.c. 6.32 mM CaCl₂ and 3.16 mM MgCl₂), incubated with cilostazol (5 µM), tadalafil (10 nM) or vehicle (0.1% ethanol) for ten minutes and stained with 1 µg/ml DiOC₆, was perfused over the inflamed endothelial cell layer for ten minutes at 1000 s⁻¹. Subsequently, the channels were rinsed with HEPES buffer (supplemented with 200 mM CaCl₂, 1 µg/ml heparin, 1% glucose and 1% BSA) and stained with anti-CD62P (PE, 1:40) and anti-CD63 (APC, 1:50) antibodies. Brightfield and fluorescence images were taken with an EVOS FL microscope with 20x magnification. Analysis of the images was performed with Fiji ImageJ software.

THP-1 cell migration

Washed platelets (250x10⁶ platelets/ml) were incubated with cilostazol (5 µM) or tadalafil (10 nM) for 20 minutes and activated with CRP (1.5 µg/ml) in the presence of 2 mM CaCl₂ for 15 minutes and applied to the bottom well of a 12-well chemotaxis chamber (Neuro Probe). A polycarbonate membrane filter of 25 by 80 mm with 5 µm pores and a silicon gasket were carefully applied to prevent air bubbles and the top 12-wells plate was placed. THP-1 cells (1x10⁶ cells/L) were added in the upper wells and the complete chamber was incubated at 37 °C with 5% CO₂. After 90 minutes, the chamber was disassembled and non-migrated cells and debris on top of the filter was carefully removed. Subsequently, the filter was stained using a Diff-Quick staining (Eberhard Lehmann GmbH) and five representative images per well were made with a Leica DM2000 microscope with 40x objective. Analysis of the images was performed with Fiji ImageJ software.

THP-1 cell adhesion

Adhesion of THP-1 cells to a platelet monolayer was determined as previously described,³ with minor adjustments. Briefly, a glass coverslip was coated with Horm collagen (50 µg/ml) for 1 hour at room temperature. Subsequently, the coverslip was blocked for 30 minutes with 1% BSA in HEPES buffer pH 7.45 and mounted into an Ibidi sticky-Slide VI 0.4. The channels were incubated with washed platelets (20x10⁶ platelets/ml, isolated as described above) for 1 hour at 37 °C. After removing non-adherent platelets and blocking the channel with 5% BSA in HEPES buffer pH 7.45 for 30 minutes at room temperature, platelets were inhibited with 5 µM cilostazol for 20 minutes at 37 °C. Fluorescent labelling and perfusion of leukocytes was performed at a shear rate of 0.2 dynes/cm² (0.2 ml/min).

Platelet extracellular vesicle (EV) release

Platelets were isolated from whole blood as described above with minor modifications. To obtain PRP, 1:15 ACD was added to the blood and this was centrifuged at 350 g for 15 minutes without break. The PRP was supplemented with ACD (1:10) and centrifuged at 1200 g for 15 minutes. The platelet pellet was resuspended in HEPES buffer pH 6.6 (with 0.2% glucose and 0.5% BSA) and centrifuged again at 1200 g for 15 minutes after addition of 1:10 ACD. The final

platelet pellet was suspended in Hepes buffer pH 7.45 (with 0.2% glucose and 0.5% BSA).

Washed platelets (200×10^6 platelets/ml) were incubated with cilostazol (5 μM), tadalafil (10 nM) or vehicle (0.1% ethanol) for ten minutes at 37 °C, and stimulated with convulxin (100 ng/ml) or thrombin (5 nM) for 30 minutes at 37 °C. After centrifugation at 2520 g for 5 minutes, the supernatant was passed through a 0.8 μm hydrophilic Minisart syringe filter (Sartorius) to a fresh tube and centrifuged at 20,000 g for 1 hour at 4 °C. The supernatant was stored for chemokine analysis and the EV pellet was resuspended in Hepes buffer pH 7.5, snap frozen in liquid nitrogen and stored at -80 °C for further examination.

Chemokine analysis

CCL5 (RANTES) and CXCL4 (platelet factor 4) concentrations in platelet supernatant were measured using an enzyme-linked immunosorbent assay (ELISA) kit from R&D systems according to the manufacturer's instructions. The biotinylated goat anti-human detection antibody for CCL5 was made in-house from sera of goats immunized with human CCL5 at Eurogentec sarl (Seraing, Belgium).

Platelet EV analysis

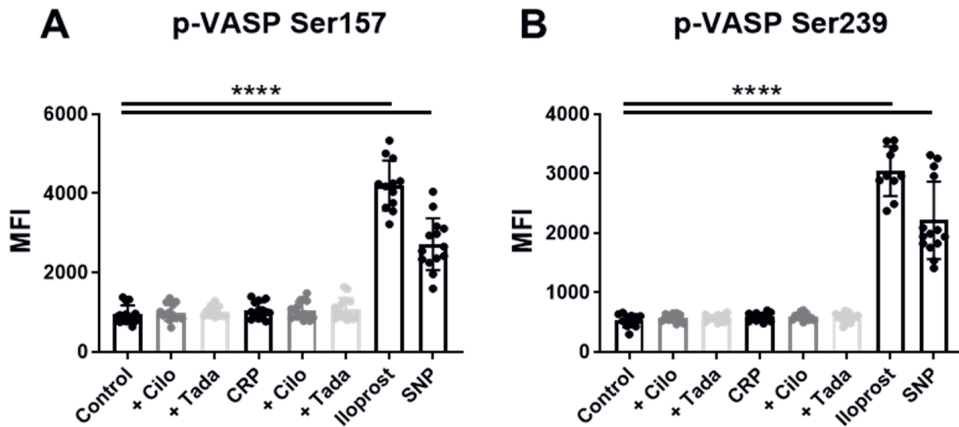
Platelet EV concentration was measured with nanoparticle tracking analysis (NTA) using the Nanosight NS300 (Malvern Panalytical). NTA determines concentration and size of particles based on their Brownian motion.⁴ Samples were diluted 1:20 in Hepes buffer pH 7.45 without BSA and measured under static conditions with a 488 nm laser and a camera level of 13. Three videos of 60 seconds each were captured per sample. Hepes buffer pH 7.45 with 0.5% BSA was measured to correct for the dissolvent of the samples.

Additionally, pro-coagulant platelet EV release was analysed with a prothrombinase-based assay. In this assay, formation of thrombin on a lipid surface is measured as described.⁵ Here, the membrane of the platelet EV served as the lipid surface. Briefly, the prothrombinase complex consisted of purified bovine coagulation factors Xa (0.05 nM) and Va (1 nM) in Hepes buffer pH 7.7 (25 mM Hepes, 150 mM NaCl, 5 mM CaCl_2 and 0.5% BSA). Indicated amounts of platelet phospholipids or EV were incubated for 10 minutes at 37 °C. Human prothrombin (500 nM, Haematologic Technologies) was added and subsamples were added to cold buffer pH 7.9 (50 mM Tris, 20 mM EDTA and 175 mM NaCl). Subsequently, thrombin substrate P2238 (Pepscan) was added and subsamples were measured in a plate reader every 30 seconds for 15 minutes at wavelengths of 405 nm and 490 nm at 37 °C. The lipid concentration was calculated from changes in the absorbance, compared to the lipid calibration curve.

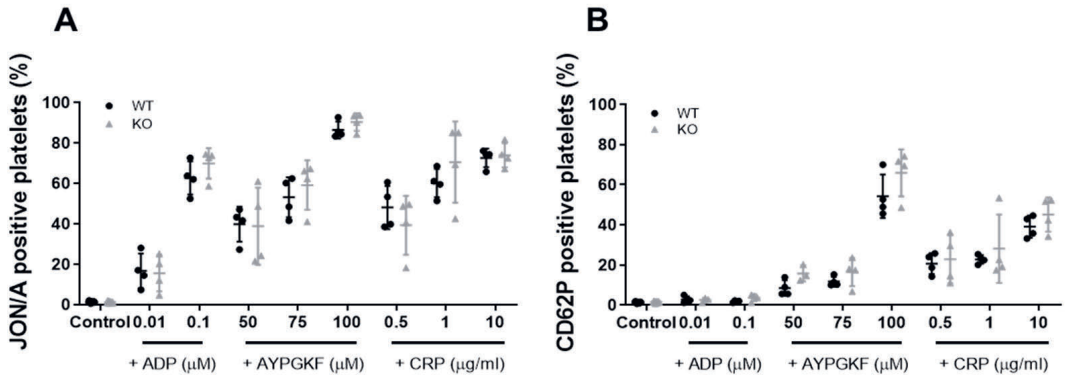
Supplemental table and figures**Supplemental Table 1. Effects of PDE-inhibition on platelet cAMP and cGMP levels.**

	cAMP		cGMP	
	- CRP	+ CRP	- CRP	+ CRP
Control	1 ± 0.22	0.77 ± 0.17	1 ± 0.15	1.06 ± 0.57
Cilostazol	1.15 ± 0.21	1.05 ± 0.25	1.23 ± 0.42	1.47 ± 0.78
Tadalafil	1.08 ± 0.24	1.06 ± 0.23	1.38 ± 0.47	1.16 ± 0.65
Iloprost	9.92 ± 1.60**		0.68 ± 0.35	
SNP	1.34 ± 0.37		7.4 ± 2.72	

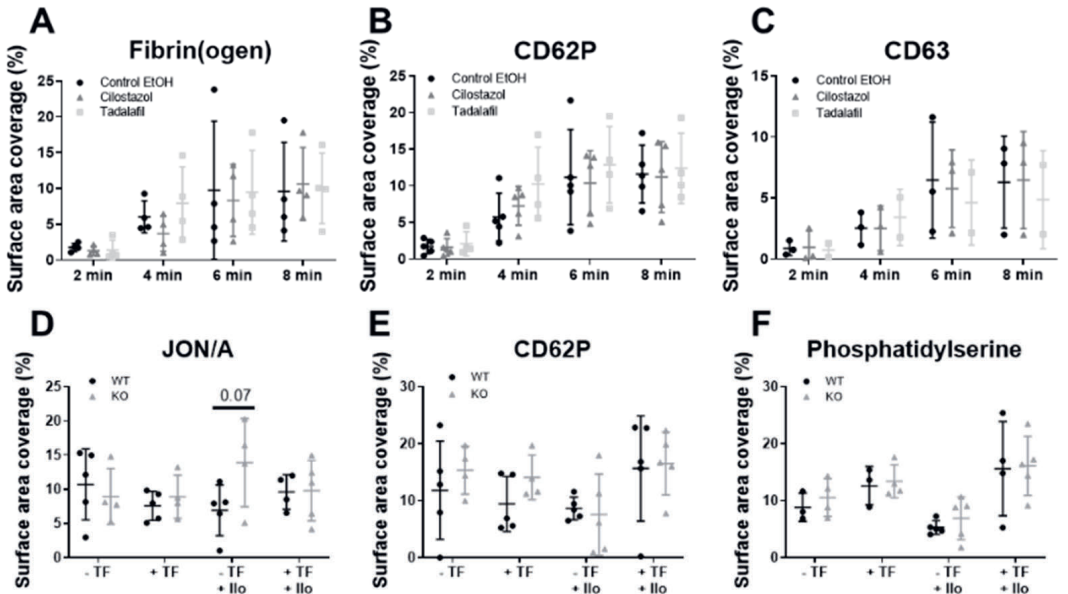
Fold change of cAMP and cGMP levels of washed platelets, untreated or additionally stimulated with the agonist CRP (0.3 µg/ml) or the PDE inhibitors cilostazol (5 µM), tadalafil (10 nM) or the endothelium-like secretory products iloprost (10 nM) or sodium nitroprusside (0.1 µM). Mean ± S.E.M., $n = 3-10$, ** $p < 0.01$. Statistics: Kruskal-Wallis test followed by Dunn's multiple comparisons test. CRP, collagen-related peptide; SNP, sodium nitroprusside.



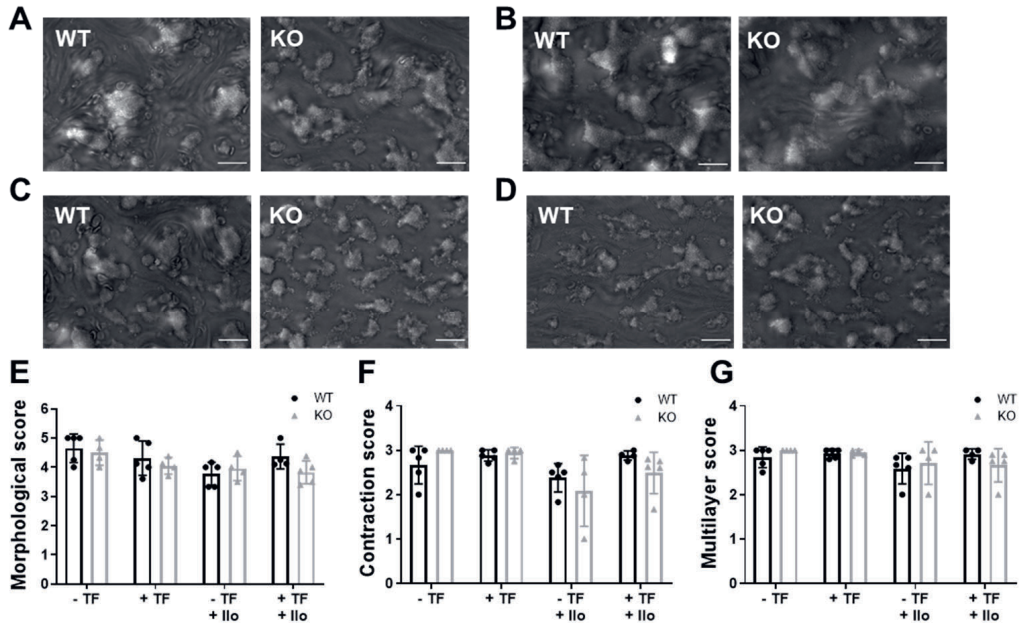
Supplemental Figure 1. Effects of PDE-inhibition on VASP phosphorylation. Phosphorylation level, shown as median fluorescence intensity (MFI), of the VASP serine residue 157 (**A**) and the VASP serine residue 239 (**B**) is increased by the endothelium-like secretory products iloprost (10 nM) and sodium nitroprusside (0.1 µM). Interquartile range, $n = 6$, **** $p < 0.0001$. Statistics: Kruskal-Wallis test followed by Dunn's multiple comparisons test. Cilo, cilostazol (5 µM); CRP, collagen-related peptide (0.3 µg/ml); SNP: sodium nitroprusside; tada, tadalafil (10 nM).



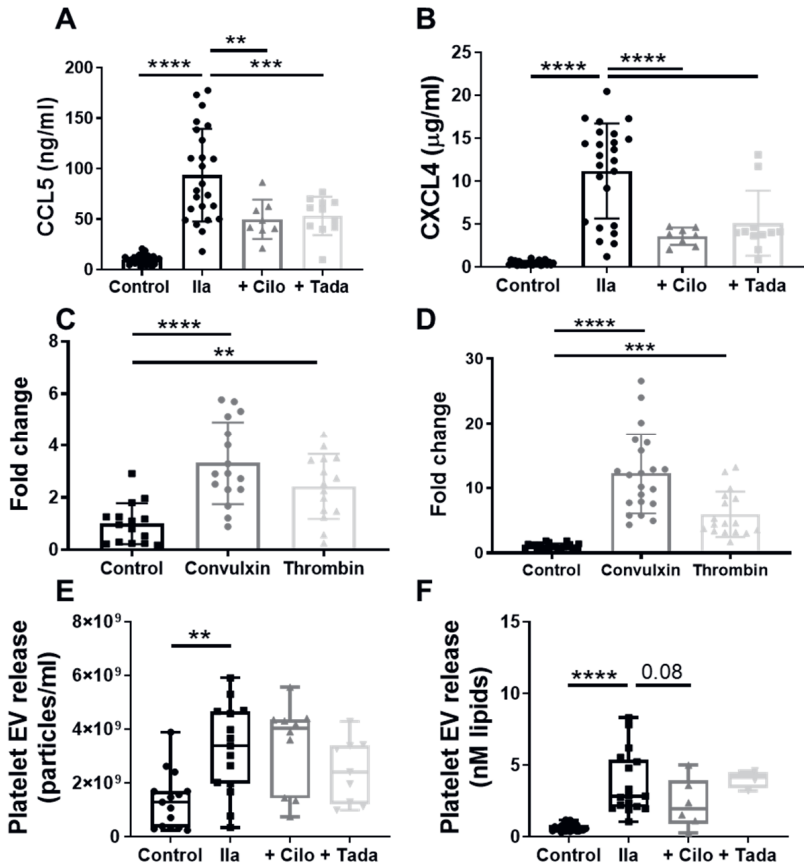
Supplemental Figure 2. Platelets from *Pde3a*^{-/-} mice show normal $\alpha_{IIb}\beta_3$ integrin activation and α -granule secretion. Platelet integrin $\alpha_{IIb}\beta_3$ activation (A) and platelet α -granule secretion (B) were unaffected in *Pde3a*^{-/-} mice compared with WT mice. Statistics: two-way ANOVA followed by Holm-Sidak's multiple comparisons test. Mean + S.D., *n* = 4. KO, knockout; WT, wild type.



Supplemental Figure 3. Effects of PDE-inhibition or genetic deletion on platelet activation markers under flow over collagen under coagulating conditions. Recalcified citrate-anti-coagulated human (A-C) or mouse (D-F) blood was perfused over a collagen type I surface or a combined collagen type I plus tissue factor surface for 7 (mouse) or 8 (human) min at a wall shear rate of 1000 s^{-1} . Human blood was perfused without inhibitor (0.1% ethanol) or in the presence of cilostazol (50 μM) or tadalafil (100 nM). Quantitative analysis of surface area coverage of AF546-fibrin(ogen) (A), α -granule secretion (FITC-anti-CD62P) (B) and δ -granule secretion (APC-anti-CD63) (C) (human) and $\alpha_{IIb}\beta_3$ activation (PE-JON/A) (D), α -granule secretion (FITC-anti-CD62P) (E) and phosphatidylserine (PS) exposure (AF647-annexin A5) (F) (mouse). Mean \pm S.D., *n* = 2-5 (human) or 4-5 (mouse). Statistics: two-way ANOVA followed by Dunnett's (A-C) or Sidak's (D-F) multiple comparisons test. Ilo, iloprost; KO, knockout; TF, tissue factor; WT, wild type.



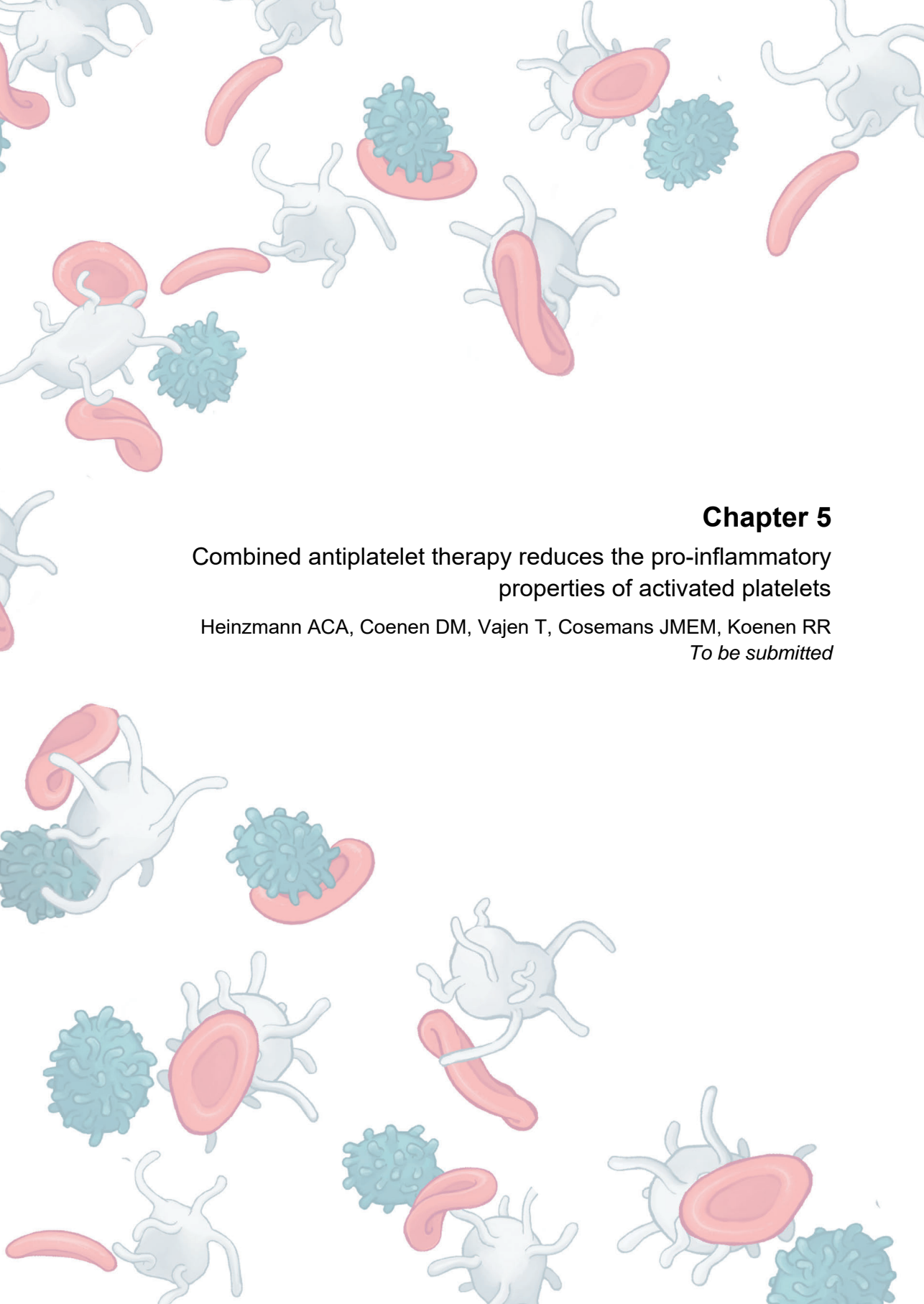
Supplemental Figure 4. *Pde3a*^{-/-} mice show normal platelet thrombus formation depending on morphology, contraction, and multilayer. Recalcified citrate-anti-coagulated mouse blood was perfused over a collagen type I surface or a combined collagen type I plus tissue factor surface at a wall shear rate of 1000 s⁻¹. Representative images of blood perfusion of WT mice and *Pde3a*^{-/-} mice over collagen type I without (A, C) or with (B, D) tissue factor under coagulating conditions in the absence (A, B) or presence (C, D) of iloprost (5 nM). Quantitative analysis of morphological score (from 0: no or hardly any adhered platelets to 5: large size thrombi) (E), contraction score (from 0: no contraction to 3: fully contracted) (F) and multilayer score (from 0: no multilayer to 3: large fully multilayered thrombi) (G). Scale is 20 μm. Mean ± S.D., n = 4-5. Statistics: two-way ANOVA followed by Sidak's multiple comparisons test. Ilo, iloprost; KO, knockout; TF, tissue factor; WT, wild type.



Supplemental Figure 5. Influence of PDE3A and -5 inhibition on thrombin-induced chemokine and extracellular vesicle release by platelets. Washed platelets were stimulated with thrombin (5 nM) without or with cilostazol (5 µM) or tadalafil (10 nM), and the release of chemokines CCL5 (A) and CXCL4 (B), and of total (C, E) and pro-coagulant (D, F) platelet extracellular vesicle (EV) was measured. (A, B) Mean ± S.D., $n = 24-27$ (control, Ila) or 8-11 (cilo, tada). (C, D) Mean + S.D., $n = 15-16$ (C), 17-22 (D). (E, F) Interquartile range, $n = 15$ (control, Ila; NTA), 9-10 (cilo, tada; NTA), 17-22 (control, Ila; PTase), 4-6 (cilo, tada; PTase), ** $p < 0.01$, *** $p < 0.001$, **** $p < 0.0001$. Statistics: ordinary one-way ANOVA followed by Dunnett's (A-D) or Holm-Sidak's (E, F) multiple comparisons test. Cilo, cilostazol; Ila, thrombin; NTA, nanoparticle tracking analysis; PTase, prothrombinase; tada, tadalafil.

Supplemental references

- de Witt SM, Swieringa F, Cavill R et al. Identification of platelet function defects by multi-parameter assessment of thrombus formation. *Nat Commun*. 2014;5:4257.
- Brouns SLN, van Geffen JP, Campello E, et al. Platelet-primed interactions of coagulation and anticoagulation pathways in flow-dependent thrombus formation. *Sci Rep*. 2020;10:11910.
- Vajen T, Heinzmann ACA, Dickhout A, et al. Laminar flow-based assays to investigate leukocyte recruitment on cultured vascular cells and adherent platelets. *J Vis Exp*. 2018.
- Dragovic RA, Gardiner C, Brooks AS, et al. Sizing and phenotyping of cellular vesicles using nanoparticle tracking analysis. *Nanomedicine*. 2011;7:780-8.
- Vasina EM, Cauwenberghs S, Staudt M, et al. Aging- and activation-induced platelet microparticles suppress apoptosis in monocytic cells and differentially signal to proinflammatory mediator release. *Am J Blood Res*. 2013;3:107-23.



Chapter 5

Combined antiplatelet therapy reduces the pro-inflammatory properties of activated platelets

Heinzmann ACA, Coenen DM, Vajen T, Cosemans JMEM, Koenen RR
To be submitted

Abstract

The cause of atherothrombosis is rupture or erosion of atherosclerotic lesions, leading to myocardial infarction or stroke. Here, platelet activation plays a major role, leading to the release of bioactive molecules, e.g. chemokines and coagulation factors, and to platelet clot formation. Several antiplatelet therapies have been developed for secondary prevention of cardiovascular events, in which anticoagulant drugs are often combined. Besides playing a role in haemostasis, platelets are also involved in inflammation. However, it is unclear whether current antiplatelet therapy also affects platelet immune functions. In this study, the possible anti-inflammatory effects of antiplatelet medications were investigated on chemokine release using ELISA and on the chemotaxis of THP-1 cells towards platelet releasates.

We found that antiplatelet medication acetylsalicylic acid (ASA) led to reduced chemokine (C-C motif) ligand 5 (CCL5) and chemokine (C-X-C motif) ligand 4 (CXCL4) release from platelets, while leukocyte chemotaxis was not affected. Depending on the agonist, $\alpha_{IIb}\beta_3$ - and P2Y₁₂-inhibitors also affected CCL5 or CXCL4 release. The combination of ASA with a P2Y₁₂ inhibitor or a phosphodiesterase inhibitor did not provide an additive reduction on CCL5 or CXCL4 release. Interestingly, these combinations did reduce leukocyte chemotaxis. This study provides evidence that combined therapy of ASA and a P2Y₁₂ or PDE3 inhibitor can decrease the inflammatory leukocyte recruiting potential of the releasate of activated platelets.

Introduction

Atherothrombosis, a result of atherosclerotic plaque rupture or erosion, leads to acute coronary syndromes (ACS), ischemic strokes and cardiovascular deaths and contributes to the global burden of premature mortality and morbidity.¹ Platelet activation plays a central role in atherothrombosis, which in turn leads to the release of pro-thrombotic and pro-inflammatory factors and amplifies activation of the coagulation cascade.^{2,3} Although the importance of platelets in the acute phase of cardiovascular disease (CVD) is undisputed, their relevance for the development of atherosclerosis is incompletely understood. Many studies have highlighted functions of platelets beyond haemostasis.⁴ For example, platelets can bridge leukocytes to the inflamed vessel wall,⁵⁻⁷ they release extracellular vesicles with pro-inflammatory activity^{8,9} and they can induce the release of neutrophil extracellular traps.^{10,11} In addition, platelets also release chemokines from α -granules upon activation.^{12,13}

Chemokines are a group of small chemotactic cytokines that orchestrate cell trafficking and play important roles in immune responses, inflammation, angiogenesis, and cell differentiation.¹⁴ The CC- and CXC-chemokines are the largest subfamilies. Among the most abundant CC-chemokines in platelets is CCL5 (RANTES, +/- 4,500 copies per platelet).¹⁵ Platelet activation leads to CCL5 release

from the α -granules and CCL5 can also be deposited on inflamed endothelium and leading to subsequent monocyte arrest.¹³ CXCL4 (platelet factor 4) is the most abundant CXC chemokine in platelets (355,000 copies per platelet).¹⁵ CXCL4 is a largely platelet-specific chemokine and, similar to CCL5, stored in α -granules. Binding of CCL5 to CXCL4 increases monocyte arrest to endothelial cells under flow.^{16,17} Besides facilitating CCL5-induced monocyte arrest, CXCL4 has several reported physiologic functions, e.g. modifying differentiation of T-cells and macrophages, activation of smooth muscle cells, inhibition of apoptosis of neutrophils and monocytes, and increasing oxLDL uptake.¹⁸

Control of platelet reactivity is essential for the secondary prevention of adverse cardiovascular events.^{19,20} After myocardial infarction, "dual antiplatelet therapy", i.e. combined treatment with the cyclooxygenase inhibitor acetylsalicylic acid (aspirin) and with purinergic receptor P2Y₁₂ antagonists, e.g. clopidogrel, prasugrel or ticagrelor is recommended. For immediate platelet effects, the intravenous P2Y₁₂ antagonist cangrelor or $\alpha_{IIb}\beta_3$ antagonists are available. Finally, cilostazol is a phosphodiesterase 3 (PDE3) inhibitor and is implemented as a treatment for patients with peripheral arterial disease (PAD).²¹ Of note, all platelet inhibition strategies bear a non-negligible risk of severe bleeding complications. In addition, a substantial number of patients does not optimally respond to antiplatelet therapy.²²

During antiplatelet therapy, a reduction of inflammation was observed in patients.²³ However, it is unclear whether this is due to direct effects of antiplatelet therapy on platelets or indirect, non-platelet dependent effects.²³ The aim of this study is to investigate the influence of common antiplatelet drugs on inflammatory functions of platelets and whether this influence is distinct from their established anti-haemostatic effects. Specifically, the effects of common antiplatelet medications were investigated on the release of chemokines by platelets from healthy donors and on the chemotactic properties of platelets towards mononuclear cells. This study provides additional evidence that the anti-inflammatory effects seen in clinical trials might originate from platelets, depending on the pathway of platelet activation.

Materials and methods

Platelet isolation and activation

Blood was collected from healthy volunteers and two patients with Glanzmann thrombasthenia, with established deficiency in integrin $\alpha_{IIb}\beta_3$,²⁴ with a 21 Gauge needle (vacutainer precision glide, BD) into citrate tubes (9 ml coagulation sodium citrate 3.2% vacuette®, Greiner Bio-One, Kremsmünster, Austria). Platelet-rich plasma (PRP) was obtained by centrifugation of blood at 350 g for 15 min. Washed platelets were obtained by centrifugation of PRP at 1240 g for 15 min, and a wash step with platelet buffer pH 6.6 (10 mM HEPES buffer, 2 mM CaCl₂, 136 mM NaCl, 2.7 mM KCl, 2 mM MgCl₂ supplemented with 0.5% BSA and 0.2% glucose). All centrifugation steps were performed in presence of anticoagulant acid citrate

buffer (80 mM trisodium citrate, 52 mM citric acid and 183 mM glucose), to prevent platelet activation during isolation procedure. After pelleting, platelets were resuspended in platelet buffer pH 7.45 (10 mM HEPES buffer, 2 mM CaCl₂, 136 mM NaCl, 2.7 mM KCl, 2 mM MgCl₂ supplemented with 0.5% BSA and 0.2% glucose) at a concentration of 2x10⁸ platelets/ml. The use of human subjects was approved after full informed consent by the local Maastricht ethics committee (METC), and studies were performed accordance with the declaration of Helsinki.

Washed platelets (2x10⁸/ml) were activated with different agonists, 100 ng/ml convulxin (CVX, Enzo Life Sciences, Lausen, Switzerland), 50 μM TRAP-6 (AnaSpec Inc. California, USA), or 5 nM thrombin (Haematologic Technologies New Hampshire, USA) for 30 min at 37°C. Platelets were pre-incubated for 5 min at 37 °C with inhibitors prior to activation, as described. Integrin α_{IIb}β₃ ligand binding was blocked with 10 nM tirofiban (CAS 144494-65-5, Correvio Int. Geneve, Switzerland) or eptifibatid (Integrilin, CAS 188627-80-7, GlaxoSmithKline, Brentford, UK). P2Y₁₂ was inhibited with cangrelor (CAS 163706-06-7, Novartis, Basel, Switzerland), PDE3 with cilostazol (73963-72-1, Tebu Bio, Le Perray-en-Yvelines, France) and thromboxane A₂ generation with aspirin (ASA (100 mg, CAS 50-78-2, Bayer, Leverkusen, Germany). Activated platelets were spun down by centrifugation at 300 g for 5 min, after which the supernatant was filtered with PK50 MiniSart sterile 0.8 μm filters (Sartorius, Göttingen, Germany) and centrifugated for 1 hr at 20 000 g. Samples were collected and snap frozen into liquid nitrogen and stored at -80°C until analyses.

Chemokine determination

Washed platelets (2x10⁸/ml) were activated as described and after time points (5, 15, 30 and 60 min) chemokine samples were collected. Secretion of chemokine CCL5 was determined by an in-house Enzyme-Linked Immune Sorbent Assay (ELISA), while CXCL4 secretion was determined by an ELISA kit from R&D Systems (according to manufacturer's instructions). For CCL5, samples were diluted into PBS with 1% BSA, and incubated for 2 h at room temperature in a Maxisorb 96 wells plate (Nunc), coated with CCL5 capture antibody (R&D Systems, Minnesota, USA). After washing with PBS buffer containing 0.05% Tween-20, a second antibody (biotin-labelled goat anti-human CCL5 mAb, home-made) was added, and incubated for 2 hours at room temperature. For detection, incubation with HRP-labelled streptavidin (R&D Systems Minnesota, USA) was performed in the dark for 20 min at room temperature. A TMB substrate kit (KPL Inc. Massachusetts, USA) was used and colour development was measured at 450 nm and 550 nm wavelength. Data analysis was performed with a 4-parameter logistic fit calculation.

Cell migration assay

Assessment of THP-1 cell migration towards a chemoattractant, a 12-well Boyden chemotaxis chamber (NeuroProbe, Gaithersburg, Germany) with a 5 μm

pore polycarbonate membrane (NeuroProbe, Gaithersburg, Germany) was used. The chemoattractant are the supernatants after platelet activation. Donor samples were pooled per condition and diluted 4 times in RPMI 1% FBS medium (Gibco Thermo Fisher Scientific, Massachusetts, USA). Chemoattractants were added to the lower compartment of the chamber. THP-1 cells in a concentration of $1 \times 10^6/\text{mL}$ cells were added to the upper compartment of the chamber. After incubation of 1.5 hours at 37°C , the membrane was cleared of non-migrated cells and the membrane was stained with Diff-Quick stain (Eberhard Lehmann GmbH, Berlin, Germany). Stained membrane was imaged with light microscopy (Leica), and cells were counted manually in 5 fields per well and expressed as cells/mm^2 . This migration assay was repeated at least 4 times per condition.

Statistical analysis

Experiments were performed using platelets from at least 3 different blood donors. Experimental data were represented as median with interquartile range. Statistical analysis was performed with the Kruskal-Wallis test with Dunns correction. Significance of differences of a p-value <0.05 were considered significant. Statistical analysis was performed with Graphpad Prism software version 9.0.0.

Results

Release of chemokines from activated platelets is not dependent on activation pathway

Platelet activation leads to release of their content e.g. coagulation and growth factors, chemokines, and of extracellular vesicles. In this study, a focus lies on the release of the chemokines CXCL4 and CCL5. Platelet activation by convulxin (GPVI agonist), thrombin (PAR-1 and -4 agonist), and TRAP-6 (PAR-1 agonist) led to comparable levels of released chemokine (Figure 1A-B). Intriguingly, there was a notable donor-to-donor difference regarding chemokine release by activated platelets (Figure 1A-B). Already after 5 min of platelet activation, maximum levels of CCL5 and CXCL4 were observed with both convulxin- and thrombin-stimulation (Figure 1C-D). These findings indicate that activated platelets release chemokines rapidly upon stimulation of GPVI or PAR-1/-4 receptors.

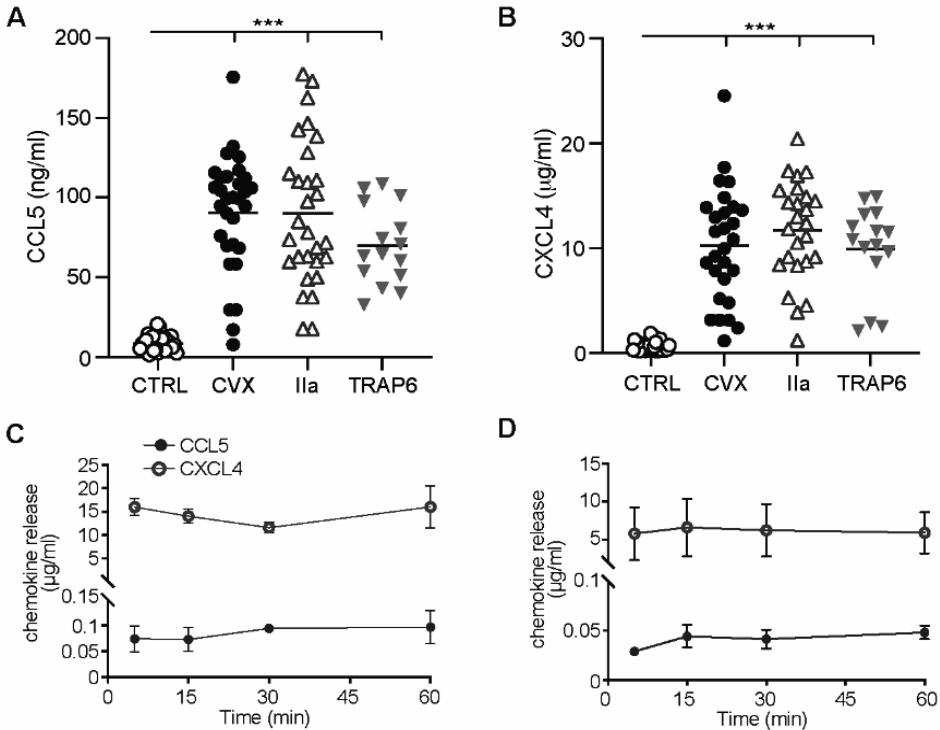


Figure 1. Different platelet activation pathways have no influence on chemokine release. Washed platelets ($2 \times 10^8/\text{ml}$) were activated with convulxin (CVX, 100 ng/ml), thrombin (Ila, 5 nM), or TRAP-6 (50 μM) for 30 min at 37°C. Platelets were removed and chemokines CCL5 (A) and CXCL4 (B) were determined with ELISA. Chemokine release was followed in time after convulxin (C) and thrombin (D) activation. White circles represent no stimulated platelets, black circles represent convulxin activation and white triangles represent thrombin activation, gray triangles represents TRAP-6 activation. CTRL: $n = 31$, CVX: $n = 29$, Ila: $n = 29$, and TRAP-6: $n = 15$. Median with interquartile range (A, B), Mean \pm SE (C, D). *** $p < 0.001$, Kruskal-Wallis with Dunn's test.

Impact of platelet aggregation inhibitors on CCL5 and CXCL4 release by platelets

Some clinical studies suggested that inhibition of $\alpha_{\text{IIb}}\beta_3$ integrin, responsible for platelet aggregation, reduces the inflammatory response in patients.²³ To investigate whether platelet aggregation inhibitors can also inhibit chemokine release, washed platelets were incubated with eptifibatide or tirofiban for 5 min prior to platelet activation with convulxin or thrombin. The release of CCL5 was not significantly reduced after antiplatelet treatment (Figure 2A-B). Interestingly, whereas eptifibatide hardly showed an effect, the release chemokine CXCL4 was decreased by over 50% after treatment with tirofiban (Figure 2C-D). This difference in CCL5 and CXCL4 release was also observed in platelets isolated from patients with Glanzmann thrombasthenia, who have defective $\alpha_{\text{IIb}}\beta_3$ integrins (Figure 2A-C). These data suggest that the chemokines CCL5 and CXCL4 are released by differential pathways. Taken together, these findings imply that inhibition of integrin $\alpha_{\text{IIb}}\beta_3$ only has minor effects on chemokine release from activated platelets.

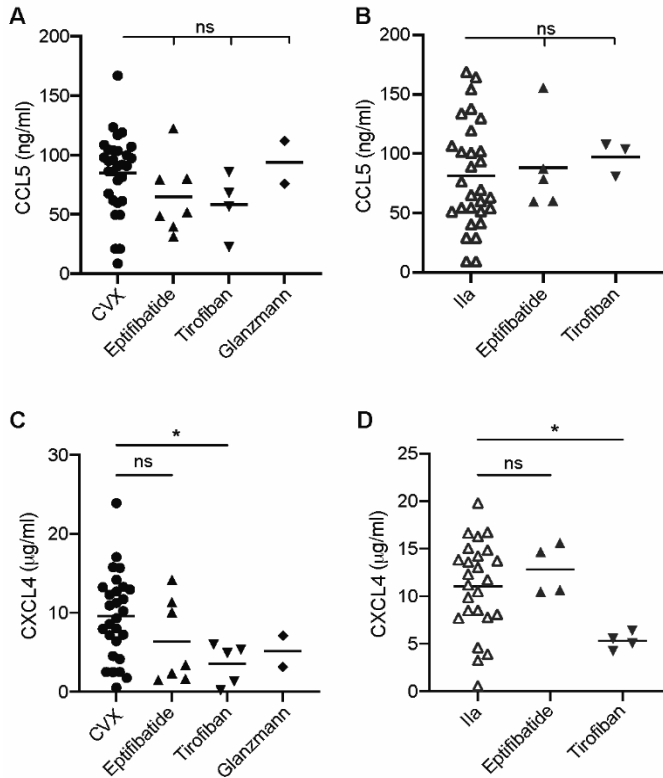


Figure 2. Effects of antiplatelet drugs against $\alpha_{IIb}\beta_3$ on chemokine release. Washed platelets (2×10^9 /ml) were incubated with indicated compounds, 5 min prior to platelet activation and chemokine release was determined. CCL5 release after convulxin (A) and thrombin (B) activation and CXCL4 release after convulxin (C) and thrombin (D) activation. Platelets isolated from individuals with Glanzmann thrombasthenia were activated with convulxin (A, C) and chemokines were determined as described. Black circles represent convulxin activation and white triangles represent thrombin activation. CTRL: $n = 29$, eptifibatide: $n = 7$, tirofiban: $n = 4$, and Glanzmann: $n = 2$. Median with interquartile range. * $p < 0.05$, Kruskal-Wallis with Dunn's test.

Single or dual antiplatelet therapy influences CCL5 and CXCL4 release

ASA and P2Y₁₂ inhibitors are commonly prescribed antiplatelet drugs for the secondary prevention of major adverse cardiovascular events.^{25,26} Platelet inhibition with ASA did not show a significant effect on CCL5 release from convulxin-activated platelets, whereas CCL5 release after thrombin activation was reduced (Figure 3A). Interestingly, unlike CCL5, CXCL4 chemokine was reduced after stimulation of convulxin or thrombin (Figure 3B). Similar to ASA, the release of CCL5 was not affected by cangrelor after stimulation of the GPVI pathway using convulxin (Figure 4A). However, CCL5 release was reduced by cangrelor after stimulation of the PAR-1/PAR-4 pathway with thrombin (Figure 4B). The release of CXCL4 was reduced by cangrelor after stimulation with thrombin and a downward trend ($p = 0.1$) was observed upon stimulation with convulxin (Figure 4C-D). Combined treatment of platelets with both ASA and cangrelor did not further increase the overall inhibition of chemokine release (Figure 4A-D).

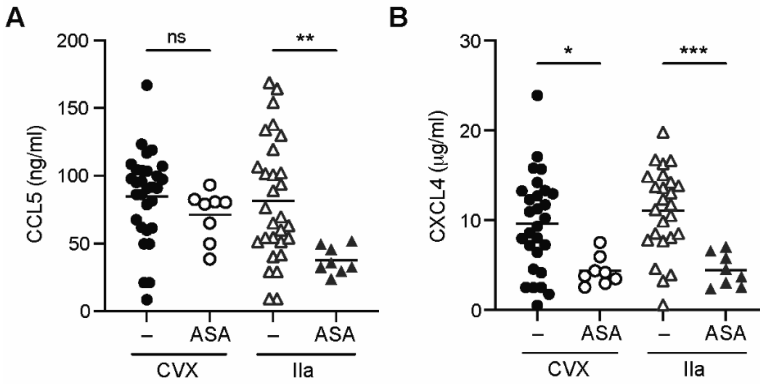


Figure 3. Effect of ASA on chemokine release. Washed platelets (2×10^8 /ml) from healthy volunteers exposed to ASA ($50 \mu\text{M}$) were activated and CCL5 (A) and CXCL4 (B) release was determined as described. Circles represent convulxin activation and triangles represent thrombin activation. CTRL: $n = 29$, and ASA: $n = 8$. Median with interquartile range. * $p < 0.05$, ** $p < 0.01$, *** $p < 0.001$, Kruskal-Wallis with Dunn's test.

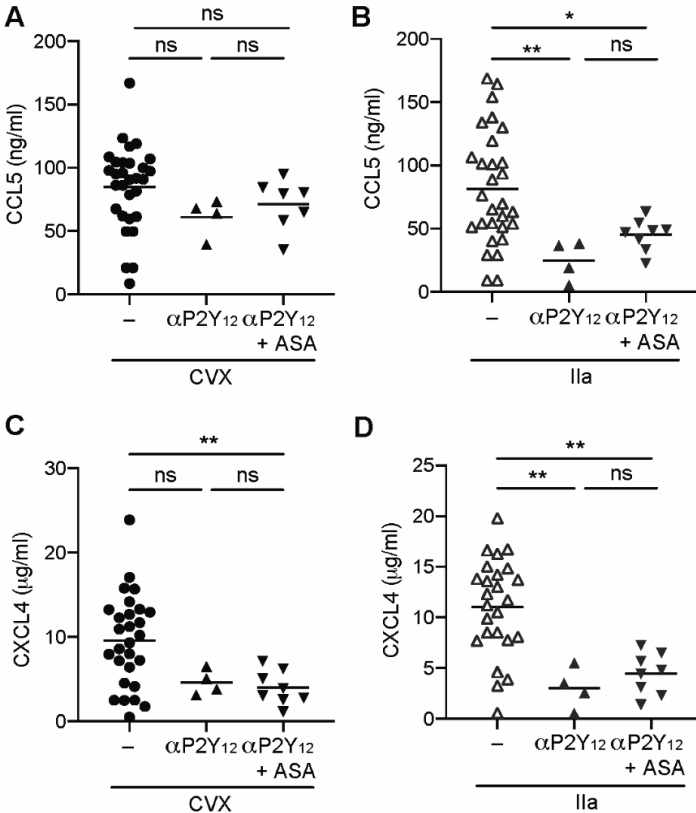


Figure 4. Effects of P2Y₁₂ inhibition on chemokine release. Washed platelets (2×10^8 /ml) from healthy volunteers exposed to ASA ($50 \mu\text{M}$) were activated and CCL5 (A, B) and CXCL4 (C, D) release was determined as described. Prior to activation, platelets were incubated with P2Y₁₂ inhibitor cangrelor for 5 min. Black circles represent convulxin activation and white triangles represent thrombin activation. CTRL: $n = 29$, P2Y₁₂: $n = 4$, and P2Y₁₂ + ASA: $n = 8$. Median with interquartile range. * $p < 0.05$, ** $p < 0.01$, Kruskal-Wallis with Dunn's test.

Impact of combined cilostazol and ASA treatment on CCL5 and CXCL4 release from activated platelets

Inhibition of platelet cAMP via PDE3 with cilostazol was shown to have an inhibiting effect on chemokine CCL5 and CXCL4 release upon stimulation with convulxin or thrombin in our recent study (chapter 4 of this thesis). To investigate whether cilostazol has an additional effect on CCL5 and CXCL4 release from ASA-treated platelets, these platelets were incubated with cilostazol for 10 min prior to platelet activation. This only resulted in a minimal decrease of chemokine release compared to ASA alone (Figure 5), except when CCL5 release was measured after triggering with convulxin (Figure 5A). Here, addition of cilostazol resulted in a stronger decrease of CCL5 release than ASA alone (Figure 5A). The combination of cilostazol with cangrelor had no additional effect on the release of CCL5 and CXCL4 (Figure 6). These data suggest that combined treatment of platelets with ASA and cilostazol does not potentiate the inhibition of chemokine release after platelet activation.

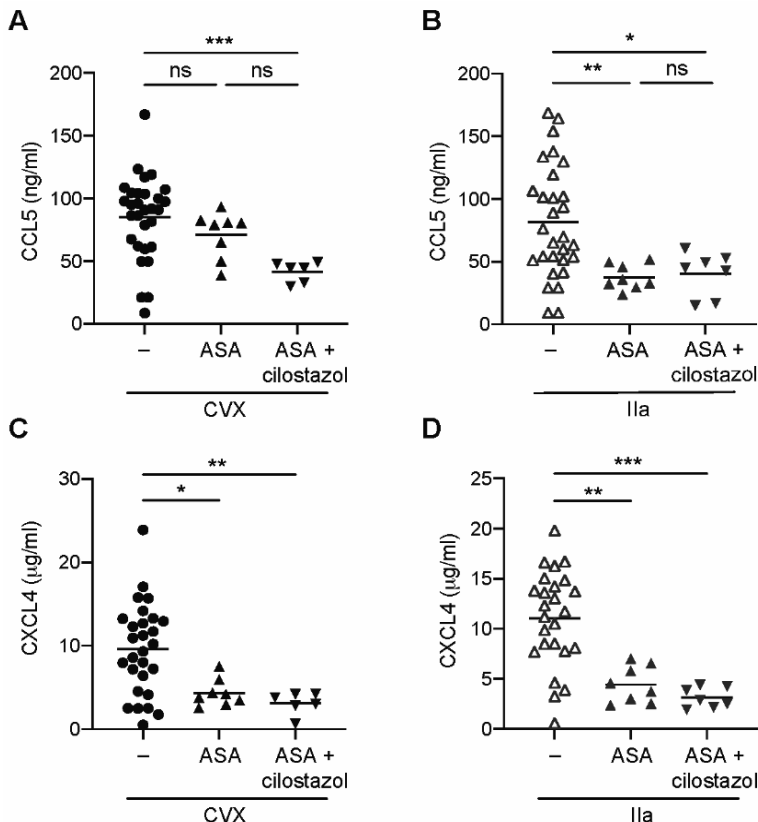


Figure 5. Dual treatment with ASA + cilostazol treatment has no additional effects on chemokine release. Washed platelets (2×10^8 /ml) from healthy volunteers exposed to ASA ($50 \mu\text{M}$) were activated and CCL5 (A, B) and CXCL4 (C, D) release was determined as described. Platelets were incubated 10 min prior to activation with the PDE3 inhibitor cilostazol. Black circles represent convulxin activation and white triangles represent thrombin activation. Ctrl: $n = 29$, ASA: $n = 8$, and ASA + Cilo: $n = 6$. Median with interquartile range. * $p < 0.05$, ** $p < 0.01$ and *** $p < 0.001$, Kruskal-Wallis with Dunn's test.

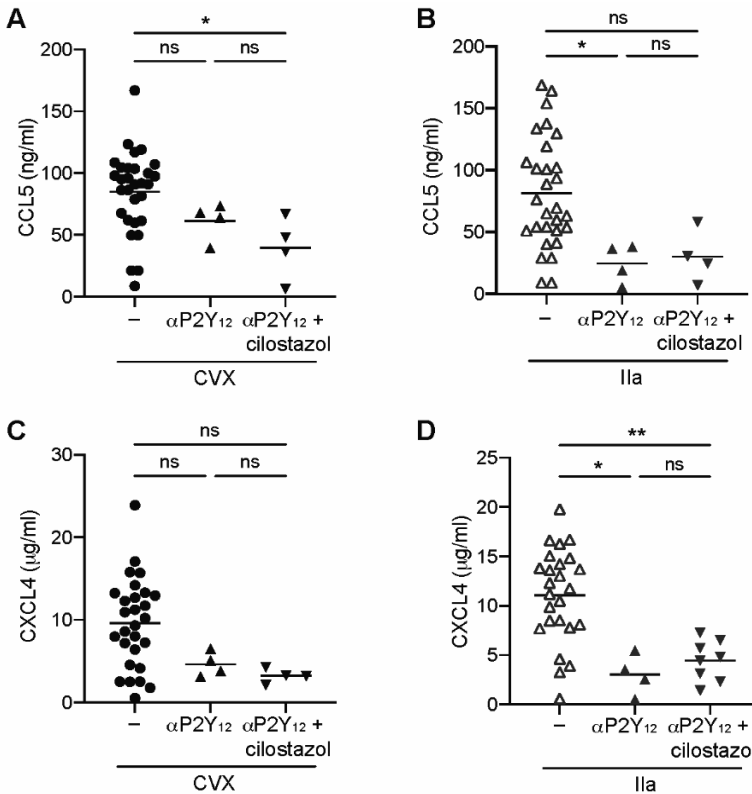


Figure 6. Combination treatment with cangrelor + cilostazol treatment has no additional effects on chemokine release. Washed platelets (2×10^9 /ml) from healthy volunteers were pre-treated with P2Y₁₂ inhibitor cangrelor 5 min before activation and CCL5 (A, B) and CXCL4 (C, D) release was determined as described. Platelets were incubated 10 min prior to activation with the PDE3 inhibitor cilostazol. Black circles represent convulxin activation and white triangles represent thrombin activation. Ctrl: $n = 29$, P2Y₁₂: $n = 4$, and P2Y₁₂ + Cilo: $n = 4$. Median with interquartile range. * $p < 0.05$, ** $p < 0.01$ and *** $p < 0.001$, Kruskal-Wallis with Dunn's test.

Combined treatment of platelets with aspirin and cangrelor or cilostazol inhibits chemotaxis of monocytic cells.

Chemokines CCL5 and CXCL4 are involved in various immune pathways, for example migration and adhesion of leukocytes. To investigate the possible effects of antiplatelet drugs on platelet-induced leukocyte migration, a Boyden chemotaxis chamber was used to assess the migration of monocytic THP1 cells towards platelet supernatants. Releasates of platelets activated with convulxin induced a more pronounced chemotactic response than those induced after activation with thrombin (Figure 7). Platelet activation after exposure to ASA or tirofiban did not lead to a reduced migration with both agonist (Figure 7A). Interestingly, the chemotactic potential of platelets releasate was reduced after inhibition with cangrelor, but only when activated with convulxin (Figure 7B). This inhibition was more pronounced when cangrelor was combined with ASA (Figure 7B). Inhibition of platelets with cilostazol alone led to a slight decrease of migration, which could be further reduced by a combination with ASA (Figure 7C). The

combination of cangrelor and cilostazol had no effect of the migration of monocytic cells (Figure 7D). Taken together, this data suggests that combined therapy of ASA and α P2Y₁₂ or PDE3 inhibitor can decrease the inflammatory leukocyte recruiting potential of the releasate of activated platelets.

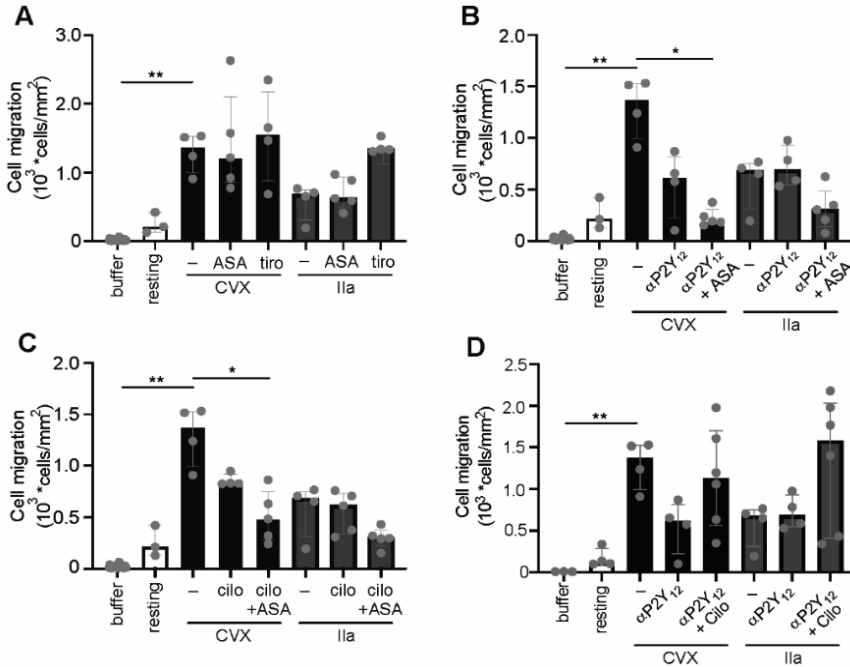


Figure 7. Chemoattractant properties of activated platelets and the effects of antiplatelet drugs. Migration of monocytic cells ($1 \times 10^6/\text{mL}$) was induced in a 12-well chemotaxis chamber for 90 min at 37 °C. Buffer, or supernatants of resting or activated washed platelets was added in the bottom compartment. If applicable, platelets were activated by convulxin or thrombin without or with ASA or tirofiban (A), cangrelor (α P2Y₁₂) or ASA + P2Y₁₂ (B), Cilostazol (cilo) or ASA + Cilo (C), P2Y₁₂ or P2Y₁₂ + cilo (D). $n = 4$. Median with interquartile range. * $p < 0.05$, Kruskal-Wallis with Dunn's test.

Discussion

In this study, we investigated the effect of antiplatelet medication on platelet-chemokine release and platelet releasate-induced chemotaxis. We focused on convulxin and thrombin as these agonists potently trigger protein kinase C activation, which is critical for platelet granule secretion²⁷ as chemokines CCL5 and CXCL4 reside in α -granules.¹³ We could confirm previous observations that chemokine release is a rapid response after platelet activation and occurs nearly instantaneously within 5 min after activation.^{28,29} Interestingly, although activation with convulxin and thrombin led to similar amounts of CCL5 and CXCL4 released along with a similar time course, the release of CCL5 induced by convulxin appeared to be more resistant to antiplatelet compounds than the release of CXCL4. A clear reduction of CXCL4 release was observed after treatment of platelets with tirofiban. This effect was less pronounced when eptifibatide was used. Interestingly, there was

no reduction of CCL5 release after incubation with any $\alpha_{IIb}\beta_3$ inhibitor, neither was CCL5 or CXCL4 release reduced in platelets from the two Glanzmann patients. However, tirofiban appeared to not interfere with other chemoattractants released by platelets, as it did not influence migration of monocytic cells. It should be taken into account that the $\alpha_{IIb}\beta_3$ antagonists on the market are both structurally and functionally different, which lead to different outcome in different studies. For example, abciximab is a humanized fab fragment of the monoclonal 7e3, the cyclic peptide eptifibatid is not specific to $\alpha_{IIb}\beta_3$ integrin, but also binds to $\alpha_M\beta_2$ and to $\alpha_v\beta_3$, and tirofiban is considered to be specific for $\alpha_{IIb}\beta_3$ integrin and binds to the RGD binding site on the integrin, which might lead to neoepitopes.^{23,30,31} In animal models, blockade or genetic deletion of $\alpha_{IIb}\beta_3$ reduced platelet interactions with the endothelium and with leukocytes.^{32,33} This was also observed in models with human platelets and endothelial cells³⁴ and in patients with acute coronary syndrome.^{35,36} In our study, we investigated platelet-releasate induced leukocyte migration but did not study direct interaction of platelet (-chemokines) with leukocytes and/or the endothelium. With regard to the findings in this study, it can be stated that depending on which platelet-derived chemokines are investigated, there is an anti-inflammatory effect of these drugs.

ASA is well known for its anti-platelet and anti-inflammatory effects. ASA irreversibly acetylates cyclooxygenases (COX) -1 and -2, thereby inhibiting the production of thromboxane A_2 (TXA₂) via COX-1, leading to inhibition of platelet aggregation and decreased vasoconstriction.³⁷ A low dose (81-100 mg²³) of ASA has anti-inflammatory effects, by triggering the synthesis of arachidonic acid metabolites leading to blockade of the expression of CXCL8 in macrophages and endothelial cells^{23,38}). In this study, we have observed that ASA significantly decreased chemokine release through the thrombin-induced pathway (PAR-1/PAR-4), and to a lesser extent after activation with convulxin. Despite the observed reduction of chemokine release, the anti-inflammatory response of ASA was not reflected in the migration of monocytes in this study, which was unaffected by ASA. This may suggest that ASA mediates its anti-inflammatory response mainly in a platelet-independent manner.

A resistance of patients towards ASA leads to suboptimal antiplatelet therapy.²² This issue is addressed for example by combining ASA with a second antiplatelet drug, e.g. P2Y₁₂ receptor inhibitors (clopidogrel, ticagrelor, prasugrel). Unlike for clopidogrel, ticagrelor and cangrelor have less data available on their influence on circulating markers of inflammation in patients, although ticagrelor more efficiently reduced CXCL8 levels in healthy volunteers than clopidogrel.³⁹ Clopidogrel was shown to reduce inflammatory markers in CVD patients, and it can interfere with leukocyte-platelet interactions, although it is unclear whether this is due to vascular or antiplatelet effects.⁴⁰⁻⁴² Furthermore, clopidogrel reduced CCL5 plasma levels both in animals and in patients.⁴³⁻⁴⁵ All P2Y₁₂ antagonists appear to interfere with the interaction of platelets with monocytes and with neutrophils^{41,42} although all may have platelet independent effects, as stated above. We have

observed that treatment of platelets with cangrelor showed a similar effect as with ASA. The chemokine release induced by thrombin is inhibited, whereas chemokine release induced by convulxin was less well inhibited by cangrelor. Inhibition of platelets with cangrelor alone did not lead to a reduced migration of monocytic cells. Although cangrelor in combination with ASA did not lead to a further reduction of chemokine release compared with ASA or cangrelor alone, the combination of both compounds almost eliminated the attraction of monocytic cells by platelet supernatant. A possible explanation for this observation might be that the combination of ASA and cangrelor can inhibit the release of several chemoattractants from platelets.

So far, this study has focussed on the effect of antiplatelet medications and combinations on the inflammatory properties of platelets. Interestingly, we have observed differential protein and extracellular vesicle secretion patterns after platelet activation throughout this, and in other studies.^{46,47} In this study, we have observed differential CCL5 and CXCL4 release under the influence of different antiplatelet medications. This would suggest that these chemokines are differently packaged inside the α -granule of platelets and that their differential release is governed by autocrine feedback activation mechanisms. Although differential packaging and release of granule content has been described previously in literature, it remains controversial whether this is a physiologic regulatory principle^{48,49} or a stochastically occurring process.^{50,51} Support for the latter comes from studies that show that platelet secretion depends on several factors, e.g. cargo solubility, granule shape, and/or granule-plasma membrane fusion routes.⁵⁰ In addition, α -granule proteins were found to be stochastically stored in the granules into subdomains.⁵¹ Others did find evidence for a functional separation of α -granule content and of their release depending on the context of platelet activation.^{48,49} Unlike the previous studies, this study also took the effects of inhibitors of platelet activation and activation into account, thereby revealing a differential release of α -granule content.

The PDEs -3 and -5 regulate the cAMP- and cGMP-dependent signalling pathways in platelets, and the PDE3 inhibitor cilostazol was shown to inhibit platelet aggregation and the release of P-selectin, CXCL4 and platelet-derived growth factor in previous studies (reviewed in ⁵²). In this study, the combination of ASA and cilostazol did not further inhibit chemokine release after platelet activation compared to ASA alone. However, when combined, monocyte recruitment was decreased, which suggests that the combination of ASA and cilostazol can inhibit the release of chemoattractants from platelets.

In summary, on basis of our findings we can conclude that the majority of antiplatelet drugs influence the release of inflammatory mediators, chemokines in this study, from activated platelets. Although ASA, P2Y₁₂ receptor inhibitors and PDE3 inhibitors also have an effect on the vasculature and leukocytes, they are also able to reduce inflammation in a platelet-dependent manner e.g. by modulating interactions of platelets with other immune cells,^{41,42} and by inhibition of platelet secretion through the thrombin activation pathway (this study). Interestingly,

chemokine release from platelets can be effectively reduced by specific combinations of medications. Dual therapy with ASA and a P2Y₁₂ receptor inhibitor or with cilostazol shows promising effects in reducing the pro-inflammatory properties of platelets. The reduction of inflammation by targeting of chemokine release during the antiplatelet treatment of atherothrombosis could be supplemented with an anticoagulant, e.g. rivaroxaban (direct anti-factor Xa inhibitor) to further combat cardiovascular inflammation while minimizing the risk for bleeding complications.

Key findings

- Combined therapy of ASA and α P2Y₁₂ or a PDE3 inhibitor decreases platelets pro-inflammatory potential of leukocyte recruitment.
- Secretion triggered via PAR-1/-4 is the most affected by anti-platelet medications.
- As single therapy, cangrelor and ASA are comparable in the reduction of platelets pro-inflammatory chemokine release.

References

1. Herrington W, Lacey B, Sherliker P, et al. Epidemiology of Atherosclerosis and the Potential to Reduce the Global Burden of Atherothrombotic Disease. *Circ Res*. 2016;118:535-46.
2. Jackson SP. Arterial thrombosis-insidious, unpredictable and deadly. *Nat Med*. 2011;17:1423-36.
3. Viles-Gonzalez JF, Fuster V, Badimon JJ. Atherothrombosis: a widespread disease with unpredictable and life-threatening consequences. *Eur Heart J*. 2004;25:1197-207.
4. Smyth SS, McEver RP, Weyrich AS, et al. Platelet functions beyond hemostasis. *J Thromb Haemost*. 2009;7:1759-66.
5. da Costa Martins P, van den Berk N, Ulfman LH, et al. Platelet-monocyte complexes support monocyte adhesion to endothelium by enhancing secondary tethering and cluster formation. *Arterioscler Thromb Vasc Biol*. 2004;24:193-9.
6. Kuckleburg CJ, Yates CM, Kalia N, et al. Endothelial cell-borne platelet bridges selectively recruit monocytes in human and mouse models of vascular inflammation. *Cardiovasc Res*. 2011;91:134-41.
7. Schrottmaier WC, Mussbacher M, Salzmann M, et al. Platelet-leukocyte interplay during vascular disease, *Atherosclerosis*. 2020;307:109-120.
8. Vajen T, Mause SF, Koenen RR. Microvesicles from platelets: novel drivers of vascular inflammation. *Thromb Haemost*. 2015;114:228-36.
9. Konkoth A, Saraswat R, Dubrou C, et al. Multifaceted role of extracellular vesicles in atherosclerosis, *Atherosclerosis*. 2020;S0021-9150(20)31500-8.
10. Maugeri N, Campana L, Gavina M, et al. Activated platelets present high mobility group box 1 to neutrophils, inducing autophagy and promoting the extrusion of neutrophil extracellular traps. *J Thromb Haemost*. 2014;12:2074-88.
11. Vajen T, Koenen RR, Werner I, et al. Blocking CCL5-CXCL4 heteromerization preserves heart function after myocardial infarction by attenuating leukocyte recruitment and NETosis. *Sci Rep*. 2018;8:10647.
12. Gleissner CA. Macrophage phenotype modulation by CXCL4 intherosclerosis. *Front Physiol*. 2012;3:1.
13. von Hundelshausen P, Schmitt MM. Platelets and their chemokines in atherosclerosis-clinical applications. *Front Physiol*. 2014;5:294.
14. Fernandez EJ, Lolis E. Structure, function, and inhibition of chemokines. *Annu Rev Pharmacol Toxicol*. 2002;42:469-99.

15. Burkhart JM, Vaudel M, Gambaryan S, et al. The first comprehensive and quantitative analysis of human platelet protein composition allows the comparative analysis of structural and functional pathways. *Blood*. 2012;120:e73-82.
16. von Hundelshausen P, Koenen RR, Sack M, et al. Heterophilic interactions of platelet factor 4 and RANTES promote monocyte arrest on endothelium. *Blood*. 2005;105:924-30.
17. Koenen RR, von Hundelshausen P, Nesmelova IV, et al. Disrupting functional interactions between platelet chemokines inhibits atherosclerosis in hyperlipidemic mice. *Nat Med*. 2009;15:97-103.
18. Coenen DM, Heinzmann ACA, Karel MFA, et al. The multifaceted contribution of platelets in the emergence and aftermath of acute cardiovascular events. *Atherosclerosis*. 2021;319:132-41.
19. Gurbel PA, Fox KAA, Tantry US, et al. Combination antiplatelet and oral anticoagulant therapy in patients with coronary and peripheral artery disease. *Circulation*. 2019;139:2170-85.
20. Piepoli MF, Hoes AW, Agewall S, et al. 2016 European guidelines on cardiovascular disease prevention in clinical practice: the sixth joint task force of the European Society of Cardiology and other societies on cardiovascular disease prevention in clinical practice (constituted by representatives of 10 societies and by invited experts) developed with the special contribution of the European Association for Cardiovascular Prevention & Rehabilitation (EACPR). *Eur Heart J*. 2016;37:2315-81.
21. Tsigkou V, Siasos G, Rovos K, et al. Peripheral artery disease and antiplatelet treatment. *Curr Opin Pharmacol*. 2018;39:43-52.
22. Sibbing D, Byrne RA, Bernlochner I, et al. High platelet reactivity and clinical outcome - fact and fiction. *Thromb Haemost*. 2011;106:191-202.
23. Muller KA, Chatterjee M, Rath D, et al. Platelets, inflammation and anti-inflammatory effects of antiplatelet drugs in ACS and CAD. *Thromb Haemost*. 2015;114:498-518.
24. Rosado JA, Meijer EM, Hamulyak K, et al. Fibrinogen binding to the integrin $\alpha_{IIb}\beta_3$ modulates store-mediated calcium entry in human platelets. *Blood*. 2001;97:2648-56.
25. Parker WAE, Storey RF. Novel approaches to P2Y₁₂ inhibition and aspirin dosing. *Platelets*. 2020;1-8.
26. Floyd CN. Dual antiplatelet therapy in coronary artery disease: comparison between ACC/AHA 2016 and ESC 2017 guidelines. *Eur Cardiol*. 2020;15:1-3.
27. Konopatskaya O, Gilio K, Harper MT, et al. PKC α regulates platelet granule secretion and thrombus formation in mice. *J Clin Invest*. 2009;119:399-407.
28. Blanchet X, Cesarek K, Brandt J, et al. Inflammatory role and prognostic value of platelet chemokines in acute coronary syndrome. *Thromb Haemost*. 2014;112:1277-87.
29. van Holten TC, Bleijerveld OB, Wijten P, et al. Quantitative proteomics analysis reveals similar release profiles following specific PAR-1 or PAR-4 stimulation of platelets. *Cardiovasc Res*. 2014;103:140-6.
30. Collier BS. $\alpha_{IIb}\beta_3$: structure and function. *J Thromb Haemost*. 2015;13 Suppl 1:S17-25.
31. Lambrechts K, de Maistre S, Abraini JH, et al. Tirofiban, a glycoprotein IIb/IIIa antagonist, has a protective effect on decompression sickness in rats: is the crosstalk between platelet and leukocytes essential? *Front Physiol*. 2018;9:906.
32. Kupatt C, Habazettl H, Hanusch P, et al. c7E3Fab reduces postischemic leukocyte-thrombocyte interaction mediated by fibrinogen. Implications for myocardial reperfusion injury. *Arterioscler Thromb Vasc Biol*. 2000;20:2226-32.
33. Massberg S, Brand K, Gruner S, et al. A critical role of platelet adhesion in the initiation of atherosclerotic lesion formation. *J Exp Med*. 2002;196:887-96.
34. May AE, Kalsch T, Massberg S, et al. Engagement of glycoprotein IIb/IIIa ($\alpha_{IIb}\beta_3$) on platelets upregulates CD40L and triggers CD40L-dependent matrix degradation by endothelial cells. *Circulation*. 2002;106:2111-7.
35. May AE, Neumann FJ, Gawaz M, et al. Reduction of monocyte-platelet interaction and monocyte activation in patients receiving antiplatelet therapy after coronary stent implantation. *Eur Heart J*. 1997;18:1913-20.
36. Neumann FJ, Zohlhofer D, Fakhoury L, et al. Effect of glycoprotein IIb/IIIa receptor blockade on platelet-leukocyte interaction and surface expression of the leukocyte integrin Mac-1 in acute myocardial infarction. *J Am Coll Cardiol*. 1999;34:1420-6.
37. Undas A, Brummel-Ziedins K, Mann KG. Why does aspirin decrease the risk of venous thromboembolism? On old and novel antithrombotic effects of acetyl salicylic acid. *J Thromb Haemost*. 2014;12:1776-87.
38. Otto GP, Sossdorf M, Boettel J, et al. Effects of low-dose acetylsalicylic acid and atherosclerotic vascular diseases on the outcome in patients with severe sepsis or septic shock. *Platelets*. 2013;24:480-5.

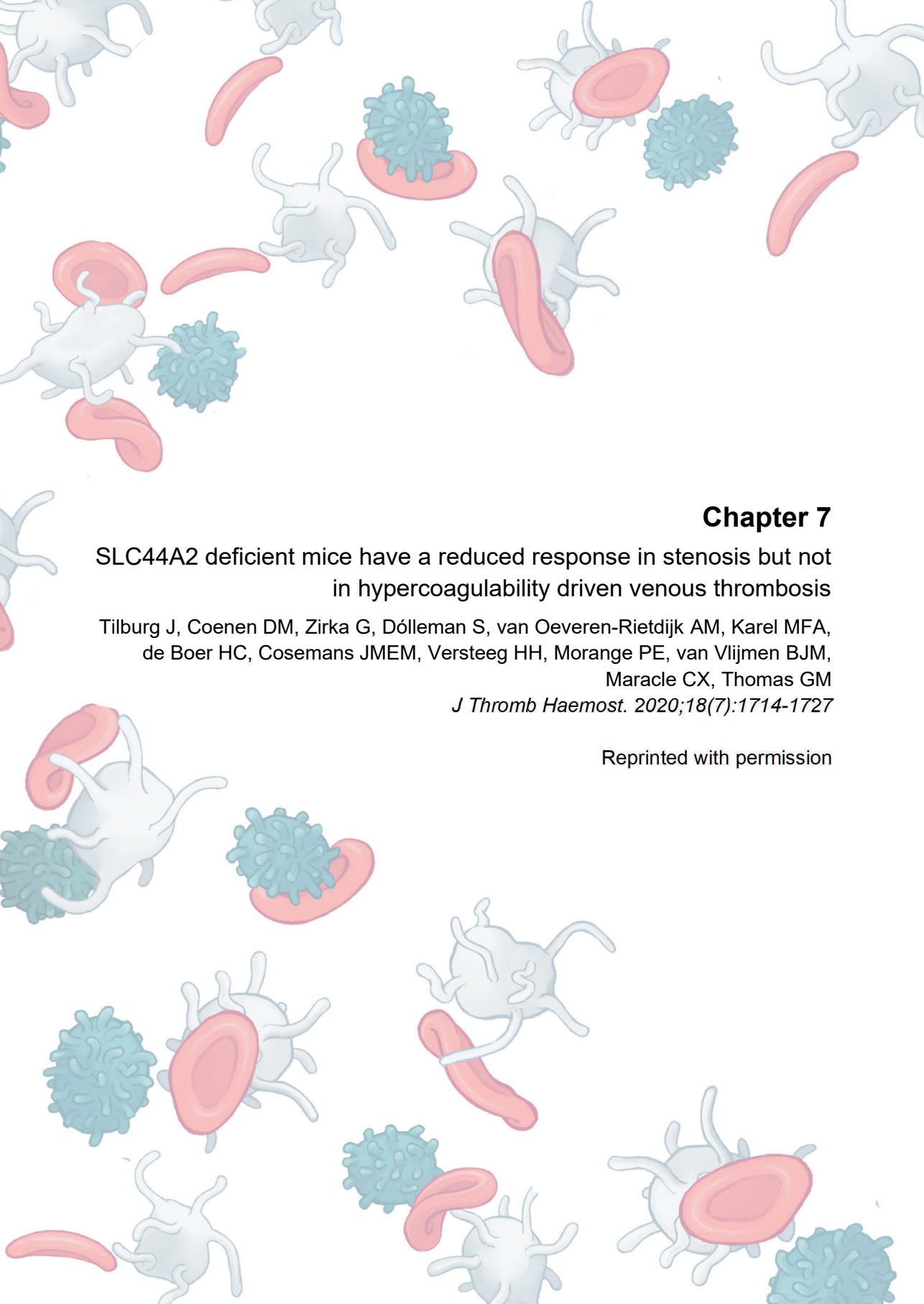
39. Thomas MR, Outteridge SN, Ajjan RA, et al. Platelet P2Y₁₂ inhibitors reduce systemic inflammation and its prothrombotic effects in an experimental human model. *Arterioscler Thromb Vasc Biol.* 2015;35:2562-70.
40. Schafer A, Fraccarollo D, Pfortsch S, et al. Clopidogrel improves endothelial function and NO bioavailability by sensitizing adenylyl cyclase in rats with congestive heart failure. *Basic Res Cardiol.* 2011;106:485-94.
41. Schrottmaier WC, Kral JB, Badrnya S, et al. Aspirin and P2Y₁₂ inhibitors in platelet-mediated activation of neutrophils and monocytes. *Thromb Haemost.* 2015;114:478-89.
42. Thomas MR, Storey RF. Effect of P2Y₁₂ inhibitors on inflammation and immunity. *Thromb Haemost.* 2015;114:490-7.
43. Coimbra LS, Steffens JP, Rossa C Jr., et al. Clopidogrel enhances periodontal repair in rats through decreased inflammation. *J Clin Periodontol.* 2014;41:295-302.
44. Harding SA, Sarma J, Din JN, et al. Clopidogrel reduces platelet-leucocyte aggregation, monocyte activation and RANTES secretion in type 2 diabetes mellitus. *Heart.* 2006;92:1335-7.
45. Meyer A, Weithaeuser A, Steffens D, et al. Inhibition of platelet function with clopidogrel is associated with a reduction of inflammation in patients with peripheral artery disease. *Cardiovasc Revasc Med.* 2016;17:169-75.
46. Dickhout A, Tullemans BME, Heemskerk JWM, et al. Galectin-1 and platelet factor 4 (CXCL4) induce complementary platelet responses in vitro. *PLoS One.* 2021;16:e0244736.
47. Heinzmann ACA, Karel MFA, Coenen DM, et al. Complementary roles of platelet $\alpha_{IIb}\beta_3$ integrin, phosphatidylserine exposure and cytoskeletal rearrangement in the release of extracellular vesicles. *Atherosclerosis.* 2020;310:17-25.
48. Chatterjee M, Huang Z, Zhang W, et al. Distinct platelet packaging, release, and surface expression of proangiogenic and antiangiogenic factors on different platelet stimuli. *Blood.* 2011;117:3907-11.
49. Italiano JE Jr., Richardson JL, Patel-Hett S, et al. Angiogenesis is regulated by a novel mechanism: pro- and antiangiogenic proteins are organized into separate platelet α granules and differentially released. *Blood.* 2008;111:1227-13.
50. Jonnalagadda D, Izu LT, Whiteheart SW. Platelet secretion is kinetically heterogeneous in an agonist-responsive manner. *Blood.* 2012;120:5209-16.
51. Kamykowski J, Carlton P, Sehgal S, et al. Quantitative immunofluorescence mapping reveals little functional coclustering of proteins within platelet α -granules. *Blood.* 2011;118:1370-3.
52. Gresele P, Momi S, Falcinelli E. Anti-platelet therapy: phosphodiesterase inhibitors. *Br J Clin Pharmacol.* 2011;72:634-46.



Chapter 6

Plasma measurements of endothelial-, leukocyte- and platelet (dys)function in HFpEF patients

Coenen DM, Weerts J, Barandiarán Aizpurua MA, Schroen B, van Empel VPM, Cosemans JMEM
Preliminary report



Chapter 7

SLC44A2 deficient mice have a reduced response in stenosis but not in hypercoagulability driven venous thrombosis

Tilburg J, Coenen DM, Zirka G, Dólleman S, van Oeveren-Rietdijk AM, Karel MFA, de Boer HC, Cosemans JMEM, Versteeg HH, Morange PE, van Vlijmen BJM, Maracle CX, Thomas GM
J Thromb Haemost. 2020;18(7):1714-1727

Reprinted with permission

Abstract

Background: Genome wide association studies (GWAS) identified *SLC44A2* as a novel susceptibility gene for venous thrombosis (VT) and previous work established that *SLC44A2* contributed to clot formation upon vascular injury.

Objective: To further investigate the role of *SLC44A2* in VT by utilizing *SLC44A2* deficient mice (*Slc44a2*^{-/-}) in two representative disease models.

Methods: Mice were included in a hypercoagulability model driven by siRNA-mediated hepatic gene silencing of anticoagulants *Serpinc1* (antithrombin) and *Proc* (protein C) and a flow restriction (stenosis) model induced by partial ligation of the inferior vena cava.

Results: In the hypercoagulability model, no effect in onset was observed in *Slc44a2*^{-/-} animals; however, a drop in plasma fibrinogen and von Willebrand factor coinciding with an increase in blood neutrophils was recorded. In the neutrophil dependent stenosis model after 48 hours, *Slc44a2*^{-/-} mice had significantly smaller thrombi both in length and weight with less platelet accumulation as a percentage of the total thrombus area. During the initiation of thrombosis at 6 hours post-stenosis, *Slc44a2*^{-/-} mice also had smaller thrombi both in length and weight, with circulating platelets remaining elevated in *Slc44a2*^{-/-} animals. Platelet activation and aggregation under both static- and venous and arterial shear conditions were normal for blood from *Slc44a2*^{-/-} mice.

Conclusions: These studies corroborate the original GWAS findings and establish a contributing role for *SLC44A2* during the initiation of VT, with indications that this may be related to platelet-neutrophil interaction. The precise mechanism however remains elusive and warrants further investigation.

1. Introduction

Venous thrombosis (VT) is a major contributor to the global health burden with a number of well-characterized genetic determinants identified, that are all linked to coagulation pathways.¹ A recent meta-analysis of 12 genome wide association studies (GWAS) identified a novel susceptibility locus for VT within the *SLC44A2* gene which had never been linked to coagulation and/or haemostasis before.² The association between *SLC44A2* and thrombotic events has been next reported in a second GWAS study, confirming *SLC44A2* as being a unique contributor to thrombotic disease.³

The solute carrier family 44 member 2 protein (*SLC44A2*)⁴ is a presumed choline transporter based on its sequence; however, functional evidence remains limited.⁵ We previously characterized *SLC44A2* deficient mice (*Slc44a2*^{-/-}) by evaluating several parameters of haemostasis including thrombin generation, transcriptional profiling of coagulation related genes, plasma levels of coagulation factors, von Willebrand factor (VWF) antigen plasma levels, multimerization, and localization within vessels, in addition to recording responses to vascular injury.^{6,7} We established that *Slc44a2*^{-/-} have relatively normal haemostasis with the

exception of a reduced level of circulating plasma VWF (~20%). These mice have also an impaired response to laser injury of the cremaster arterioles, with significantly less platelet accumulation measured at the site of injury in the C57BL/6 background.

In the present study we delineate the importance of SLC44A2 in VT by utilizing *Slc44a2*^{-/-} mice in two different VT models; the hypercoagulability small interfering ribonucleic acid (siRNA)-induced model and the flow restriction (stenosis) model. In the first model, mice are injected with siRNA targeting hepatic expression of the anticoagulants *Proc* (protein C) and *Serpinc1* (antithrombin), thereby creating a state of hypercoagulability and resulting in the formation of pronounced blood clots within the large veins in and around the mandibular area of the head.⁸ In the second model thrombus formation is induced by reduction in blood flow of the inferior vena cava (IVC) by approximately 90%, thereby activating the local endothelium and the recruitment of immune cells.⁹

2. Methods

2.1 Mice

Mice deficient for SLC44A2 (*Slc44a2*^{-/-}) were previously generated¹⁰ and introduced on a C57BL/6J background.^{7,10} *Slc44a2*^{-/-} and littermate controls (*Slc44a2*^{+/+}) were genotyped using ear biopsy DNA as described.¹¹ Experimental animal procedures were approved by local animal welfare committees at the Leiden University Medical Center and Aix-Marseille University. All experiments were performed blinded for genotype.

2.2 Spontaneous thrombosis following silencing of antithrombin and protein C

Female *Slc44a2*^{-/-} and *Slc44a2*^{+/+} mice 6 weeks of age were intravenously injected with siRNAs targeting antithrombin (si*Serpinc1*: #S62673; Ambion) and protein C (si*Proc*: #S72192) complexed with invivofectamine 3.0 (Invitrogen) as previously described.⁸ A dose of 80 nmol of si*Serpinc1* and si*Proc* per kg of body weight in study one and 60 nmol in study two was used. The endpoint was reached once 50% of all mice displayed previously described typical clinical features.⁸ Blood was collected 24 hours pre-injection via tail cut using dipotassium ethylenediaminetetraacetic (K2EDTA) acid coated vials (Sarstedt). Blood was also collected from the IVC with 11 μmol/L sodium citrate upon sacrifice and under anaesthesia induced by subcutaneous injection of ketamine (100 mg/kg), xylazine (12.5 mg/kg), and atropine (125 μg/kg). Cell counts were assessed by SysmexXT-2000iV (Sysmex Europe GMBH).

2.3 Thrombosis following stenosis of the IVC

Male *Slc44a2*^{-/-} and *Slc44a2*^{+/+} mice 11 to 12 weeks of age underwent partial ligation of the IVC as previously described,^{9,11} with all side branches below the renal veins completely ligated. A 50 μL blood sample was collected from the

periorbital eye plexus directly before the collection surgery and stabilized with 0.5 mol/L K2EDTA. Cell counts were assessed by Sysmex XN 3000 instrument.

2.4 Plasma analysis

VWF antigen levels were determined by enzyme-linked immunosorbent assay (ELISA) with anti-human VWF (DAKO A082) as described.¹² Fibrinogen levels were measured by ELISA according to the manufacturer's protocol, with the exception of using 1 mol/L H2SO4 and half the reaction volume (MGF-EIA, Stago). Extracellular DNA was quantified using the Quant-iT PicoGreen DNA Assay Kit (ThermoFisher Scientific).

2.5 Liver analysis

RNA was isolated from liver using RNA-Bee (Tel-Test, Inc) and subsequently cDNA was synthesized according to manufacturer's protocol (SuperScript II Reverse Transcriptase, Thermo Fisher). Liver transcript levels of *Slc44a2*, *Serpinc1*, and *Proc* were determined by quantitative polymerase chain reaction (qPCR).¹³ IVC RNA was isolated using the RNeasy microkit (Qiagen 74034). cDNA was synthesized and transcript levels of *Slc44a2*, *Ccl2*, *Cxcl1*, *Cxcl5*, *Il6*, *Selplg*, and *Vcam1* were quantified by qPCR. β -actin (*Actb*) was used as reference gene (primers Table S1 in supporting information). Fibrin in liver (and also lungs) was determined by immunoblotting using the mouse monoclonal 59D8 anti-fibrin antibody as previously described.¹⁴

2.6 Histology

Following removal, thrombi were measured, weighed, and frozen in optimum cutting temperature (OCT; Tissue Tek). Serial cryo sections from the medial region of the thrombi were made at 10 μ m. Immunohistochemical staining was performed as described¹¹ using anti-Ly6G (Biolegend #127602; 1:1000 dilution), anti-citrullinated histone H3 (CitH3; Abcam #ab5103; 1:300 dilution), anti-VWF (DAKO #A0082; 1:4000 dilution; Abcam # ab11713; 1:50 dilution), anti-glycoprotein Ib (GPIb; Emfret #R300; 1:2000 dilution) and anti-tissue factor (TF; in-house re-source, 1:2000 dilution) antibodies. The corresponding secondaries were anti-Rat IgG horseradish peroxidase (HRP) conjugated (Abcam #ab205720; 125 μ g/mL) or anti-Rabbit IgG HRP conjugated (DAKO # P039901-2; 125 μ g/mL) and signal was visualized using Vector NovaRED (Vector Laboratories #SK4800). Immunofluorescence staining was performed as before¹¹ using the fluorophore-conjugated secondaries anti-rabbit 488 (#A-11008), anti-rat 568 (#A-11077), anti-sheep 647 (#A-21448) (Invitrogen, all at 1:750 dilution). Microscopic images were taken using the Panoramic MIDI Slide Scanner and Caseviewer software (3Dhistech). Quantifications were calculated using the Fiji ImageJ program.¹⁵ Per mouse, when a thrombus was available, one stained section from the medial region was used for comparison.

2.7 Reactive oxygen species production

Citrated blood was collected via tail cut and leukocyte activation was measured *ex vivo* in 25 μ L blood incubated with anti-CD11b (BD Pharmingen; clone M1/70), anti-B220 (eBioscience; clone RA3-6B2), and anti-Ly6G (eBioscience, clone 1A8) for 30 minutes on ice. Erythrocytes were then lysed using 0.155 mol/L NH_4Cl , 0.01 mol/L KHCO_3 , 0.1 mmol/L ethylenediaminetetraacetic acid (EDTA) for 10 minutes at 20°C and remaining cells were incubated with DHR-123 (ThermoFischer, #D23086, 1:1000, 10 minutes, 37°C) and stimulated or not with phorbol myristate acetate (PMA; 2 μ g/mL, Sigma P8139, 10 minutes, 37°C). Fluorescence was measured on an LSR II flow cytometer (BD Bioscience).

2.8 Platelet aggregation

Citrated blood was collected via IVC and centrifuged at 313 g for 3 minutes at room temperature using a soft break. Platelet rich plasma layer (PRP) and one third of the erythrocytes layer was collected and separately centrifuged at 704 g for 15 seconds using soft break. Platelet counts were determined by Sysmex and adjusted with platelet poor plasma (PPP). PRP was further diluted into HEPES:Tyrode pH 7.3 and rested for 30 minutes before measurements. PRP was then incubated with 1.2 mmol/L thrombin receptor activating peptide 4 (TRAP4; Bachem, #4035529-005) or 24 μ mol/L adenosine diphosphate (ADP; HART biological). Aggregation was measured for 15 minutes on a Thrombo-Aggregometer (SD Medical, #TA-8V) against PPP.

2.9 Platelet perfusion

Platelet adhesion and activation following perfusion over coverslip coated with VWF-binding peptide (50 μ g/mL, Dept. of Biochemistry, Cambridge University) or collagen type I (50 μ g/mL, HORM collagen, Takeda) was assessed as described before.¹⁶ Citrated whole blood was re-calcified with 7.5 mmol/L CaCl_2 and 3.75 mmol/L MgCl_2 in the presence of D-phenylalanyl-prolyl-arginyl chloromethyl ketone (PPACK; 53 μ mol/L, Calbiochem) and heparin (5 U/mL), labelled with 0.5 μ g/mL DiOC₆ (AnaSpec). Analysis of fluorescence images was performed with pre-defined scripts in Fiji software.^{15,17}

2.10 Platelet activation by flow cytometry

Citrated tail blood was diluted 25 times in Tyrode HEPES pH 7.45 (5 mmol/L HEPES, 136 mmol/L NaCl, 2.7 mmol/L KCl, 0.42 mmol/L NaH_2PO_4 , 2 mmol/L MgCl_2 , 0.1% glucose and 0.1% bovine serum albumin) in the presence of PPACK (20 μ mol/L) and fragmin (20 U/mL, Pfizer). The blood was activated for 10 minutes with various concentrations of cross-linked collagen-related peptide (CRP-XL, from Cambridge University), 2-methylthio- adenosine-5'-diphosphate (2-MeSADP, BioConnect), or the protease activated receptor 4 (PAR4) agonist AYPGKF. Platelets were labelled with anti-GPIIb/IIIa (JON/A; Emfret, PE, 1:10 dilution) and

anti-P-selectin (CD62P; Emfret, FITC, 1:10 dilution), and activation measured with an Accuri C6 flow cytometer (Becton Dickinson).

2.11 Statistics

For phenotype free survival, differences were calculated using the Mantel-Cox log rank test method. Spearman's correlation was used to compute *r* and determine correlation between immunohistochemical stains. Reactive oxygen species (ROS) production and platelet aggregation were evaluated by *t*-test. Changes in platelet binding under perfusion and platelet activation with flow cytometry were determined by two-way analysis of variance. Statistical testing for the remaining readouts were calculated using the Mann-Whitney rank-sum test. All calculations were performed using the Prism statistical program, version 8 (GraphPad).

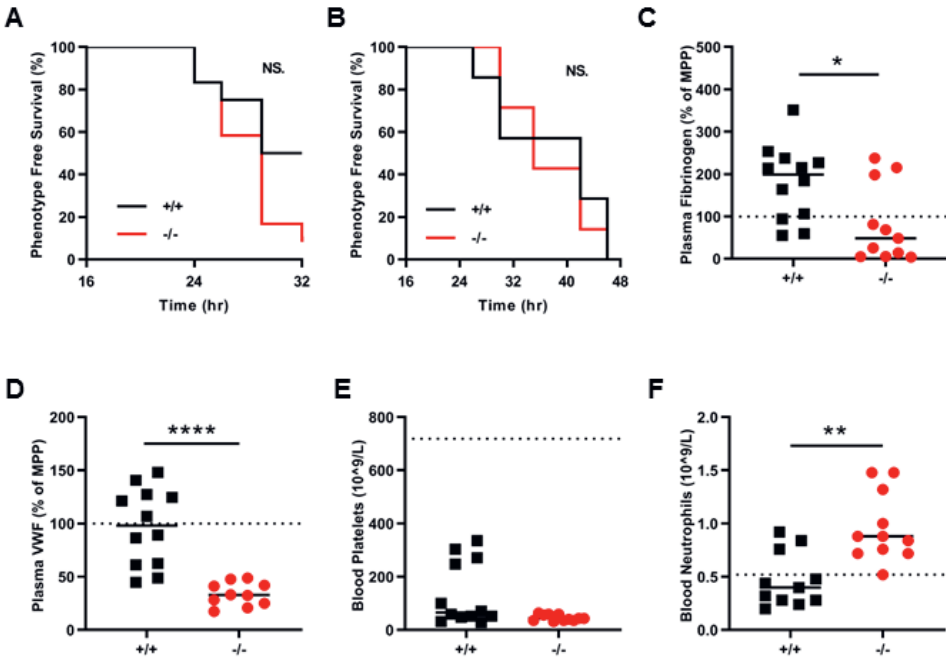


Figure 1. Hypercoagulability mediated venous thrombosis through siRNAs targeting *Serpinc1* and *Proc* in *SLC44A2* deficient mice. (A) Phenotype free survival in *SLC44A2* deficient mice (*Slc44a2*^{-/-}, -/-) and littermate wild type controls (*Slc44a2*^{+/+}, +/+) shown as percentage following injection with 80 nmol/kg siRNA (*n* = 12 per group). (B) Phenotype free survival following injection with 60 nmol/kg siRNA (*n* = 6 per group). The following blood parameters were measured after treatment with 80 nmol/kg siRNA: (C) Plasma fibrinogen levels 32 hours post-treatment expressed as a percentage of MPP (mouse pool plasma), (D) plasma VWF (von Willebrand factor) levels 32 hours post-treatment expressed as a percentage of MPP (mouse pool plasma), (E) blood platelet counts at time of sacrifice. For reference platelet levels of *Slc44a2*^{+/+} before siRNA treatment are represented by the dotted line (mean cell counts). (F) Circulating neutrophil levels at time of sacrifice. For reference platelet levels of *Slc44a2*^{+/+} mice before siRNA treatment are represented by the dotted line (mean cell counts). Statistical analysis for phenotype free survival determined using Mantel-Cox test. Solid line represents median value. Statistical differences were evaluated using Mann-Whitney rank-sum test (NS = non-significant; *signifies *p*<0.05; **signifies *p*<0.01; ****signifies *p*<0.0001).

3. Results

3.1 SLC44A2 does not alter onset in a model of hypercoagulability driven VT

In order to determine whether SLC44A2 had an effect on thrombus formation driven by hypercoagulability, we induced a hypercoagulable state in SLC44A2 deficient mice (*Slc44a2*^{-/-}) and wild type control (*Slc44a2*^{+/+}) through siRNA-mediated knockdown of hepatic expression of the anticoagulants antithrombin (*Serpinc1*) and protein C (*Proc*). Venous thrombosis and related features in this model are same for male and female mice, but well characterized particularly for female mice.^{8,18} We thus used female mice here. After 24 hours, mice from both groups began to present typical features coinciding with thrombotic coagulopathy, *i.e.* oedema of mandibular area and bleeding around the eye. At the time of sacrifice, 32 hours post-siRNA treatment, 50% of *Slc44a2*^{+/+} (6/12) and 92% of *Slc44a2*^{-/-} mice (11/12) had developed the observable phenotype (Figure 1A), but this difference in onset was not significant. Both groups lost approximately 8% of their original body weight (Figure S1 in supporting information). To validate the incidence over a more protracted timeline, we repeated the study using a lower dose of siRNA. Again no significant difference could be observed with 43% of *Slc44a2*^{+/+} (3/7) and 29% of *Slc44a2*^{-/-} mice (2/7) developing the phenotype 32 hours post injection (Figure 1B). All mice were affected at the collection point of 46 hours. Upon sacrifice, knockdown of hepatic *Serpinc1* and *Proc* was confirmed and was 70% and 98% lower, respectively, as compared to untreated control mice. This was comparable between genotypes (Figure S2 in supporting information), although *Proc* levels were lower ($p=0.0024$) in *Slc44a2*^{-/-}, measured at 1% of control versus 3.6% in *Slc44a2*^{+/+}.

In addition to macrovascular thrombosis in the head the deposition of fibrin in the lungs and liver typically occurs in this model.^{8,18} Accordingly, fibrin was detected in both the lungs and liver of the *Slc44a2*^{+/+} mice and was comparable to *Slc44a2*^{-/-} mice (Figure S3 in supporting information). Fibrinogen levels in the plasma were lowered in the *Slc44a2*^{-/-} mice as compared to *Slc44a2*^{+/+} ($p=0.0129$, Figure 1C). We confirmed the previously described reduction in circulating VWF of ~20% in *Slc44a2*^{-/-} mice before siRNA treatment ($p=0.0211$, Figure S4 in supporting information).⁷ Remarkably, upon sacrifice following thrombosis, this difference in VWF was even more pronounced as measured antigen levels were 66% lower in *Slc44a2*^{-/-} mice as compared to *Slc44a2*^{+/+} ($p<0.0001$, Figure 1D). No differences in blood cell counts prior to injection and following siRNA treatment were observed. Platelet consumption is associated with thrombosis in this model and even though four *Slc44a2*^{+/+} mice did not develop an observable thrombus, corresponding with higher amounts of blood platelets, there was no significant difference in platelet levels following treatment between genotypes (Figure 1E). Interestingly, a significant increase in blood neutrophils ($p=0.0017$, Figure 1F) was recorded in the *Slc44a2*^{-/-} mice upon sacrifice. However, the formation of thrombi in this model was previously

demonstrated to occur independently of VWF or neutrophils.¹⁸ Thus, even with such changes, SLC44A2 does not affect thrombosis incidence in this model.

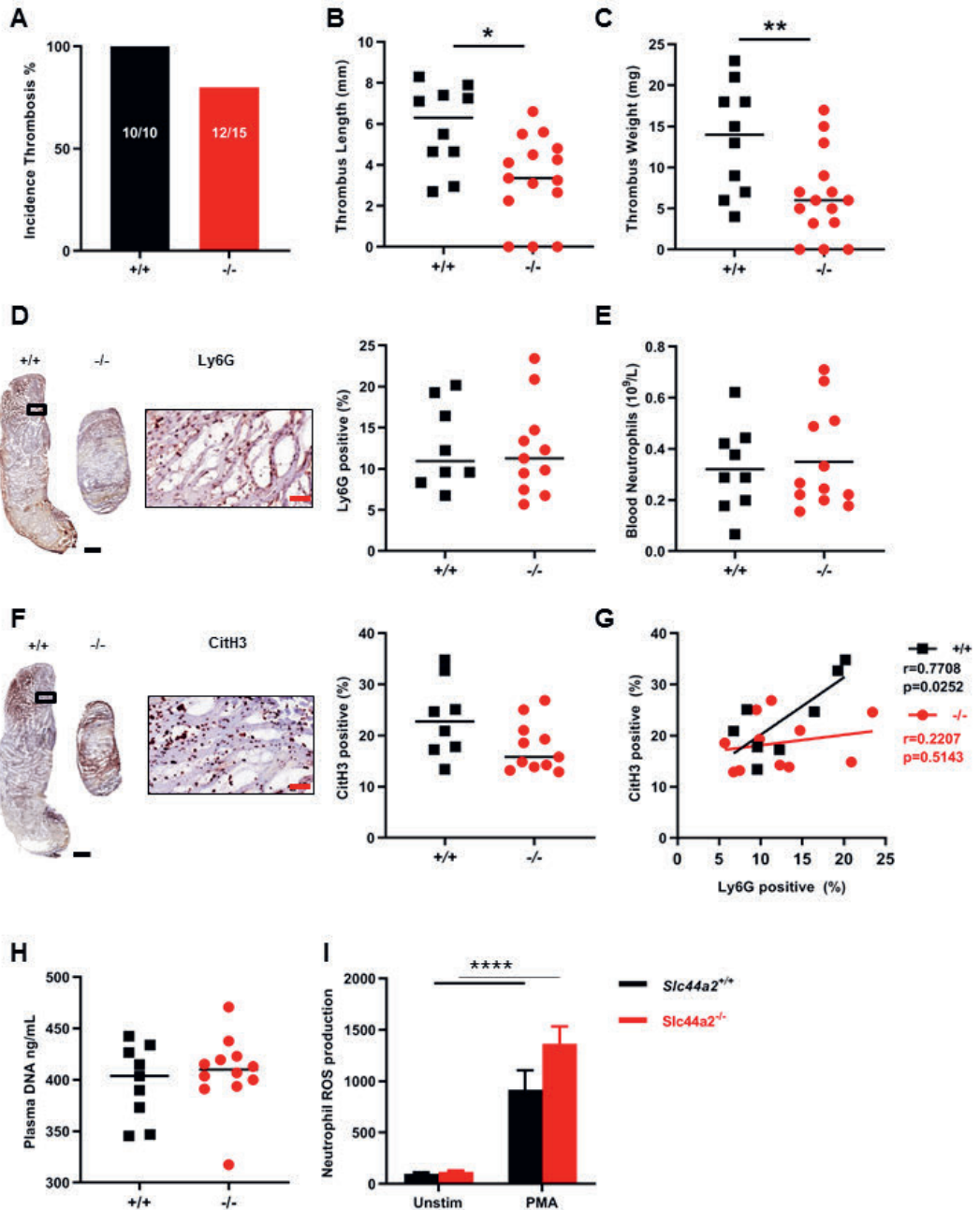


Figure 2. Venous thrombosis in SLC44A2 deficient mice following 48 hours stenosis of the inferior vena cava (IVC). (A) Incidence of thrombosis after 48 hours in wild type (*Slc44a2*^{+/+}, +/+) (*n* = 10) or SLC44A2 deficient mice (*Slc44a2*^{-/-}, -/-) (*n* = 15), shown as percentage (%). (B) Length and (C) weight of thrombi formed at 48 hours. (D) Immunohistochemical (IHC) staining of neutrophil marker Ly6G in a representative thrombus from a *Slc44a2*^{+/+} and *Slc44a2*^{-/-}, with high

magnification from *Slc44a2*^{+/+} (location is indicated by the black box; left) and quantification of positive area as a percentage of total thrombus area (right, +/+ *n* = 8, -/- *n* = 11). (E) Blood neutrophil counts at time of sacrifice (48 hours; +/+ *n* = 9, -/- *n* = 12). (F) IHC staining of the NETosis marker citrullinated histone H3 (CitH3) in a representative thrombus of a *Slc44a2*^{+/+} and *Slc44a2*^{-/-}, with high magnification from *Slc44a2*^{+/+} (location is indicated by the black box; left) and quantification of positive area as a percentage of total thrombus area (right, +/+ *n* = 8, -/- *n* = 11). (G) Correlation plot between LY6G and CitH3 staining (+/+, *n* = 8; -/-, *n* = 11). (H) Plasma DNA level at time of sacrifice (48 hours; ng/mL; +/+, *n* = 9; -/-, *n* = 11). (I) Reactive oxygen species (ROS) produced by *Slc44a2*^{+/+} or *Slc44a2*^{-/-} neutrophils *ex vivo* following activation of whole blood with 2 µg/mL phorbol 12-myristate 13-acetate (PMA), quantified by FACS analysis, expressed in median fluorescence index (MFI; *n* = 5). (Note on numbers: blood samples that became coagulated or thrombi that were damaged during sectioning were not included for subsequent analysis.) Black bars equal 500 µm. Red bars equal 50 µm. Solid line represents median value. Statistical differences for ROS production were evaluated by *t*-test and for remaining biological readouts, the Mann-Whitney rank-sum test (*signifies *p*<0.05; **signifies *p*<0.01; ****signifies *p*<0.0001).

3.2 *Slc44a2*^{-/-} mice have reduced thrombosis following 48 hours of stenosis

We continued by using a model demonstrated to be dependent on neutrophils and VWF: the flow restriction (stenosis) model of deep vein thrombosis (DVT).^{11,19,20} Male mice, littermates of the female mice used in the previous model, were used in respect of the “3R’s” rule for more ethical use of animals and to maintain the same environmental exposure and breeding sources for mice included in the different VT models.²¹ In this model the blood flow was reduced by approximately 90%, with blood stasis activating the local endothelium and driving inflammation-mediated thrombosis.⁹ Following 48 hours, 100% of the *Slc44a2*^{+/+} mice (10/10) and 80% of the *Slc44a2*^{-/-} mice (12/15) developed a thrombus (Figure 2A). The thrombi formed in *Slc44a2*^{-/-} mice were significantly smaller both in length (-43%, *p*=0.0120) and weight (-52%, *p*=0.0099; Figure 2B-C). Mice heterozygous for SLC44A2 (*Slc44a2*^{+/-}) were found to have 100% incidence (7/7) with median thrombus measurements for length and weight falling between those of the *Slc44a2*^{+/+} and *Slc44a2*^{-/-} groups (Figure S5 in supporting information), suggesting a dose-dependent effect of SLC44A2 on VT. No differences in thrombi neutrophil density were visible (Ly6G staining, Figure 2D) and the levels of circulating blood neutrophils at the time of sacrifice were also similar (Figure 2E). To determine whether neutrophil extracellular trap release (NETosis) was affected, we evaluated CitH3 staining into the obtained thrombi. A trend was observed for lower CitH3 in the *Slc44a2*^{-/-} mice (*p*=0.0908; Figure 2F) and the positive correlation found between the neutrophil and CitH3 staining (*r*=0.7708; *p*=0.0252) in *Slc44a2*^{+/+} was absent in *Slc44a2*^{-/-} animals (*r*=0.2207; *p*=0.5143; Figure 2G) suggesting reduced NETosis within thrombi in absence of SLC44A2. However, no signs of systemic decrease in plasma DNA levels could be found 48 hours after stenosis (Figure 2H). Additionally, *ex vivo* production of reactive oxygen species (ROS) by stimulated neutrophils was not different between neutrophils deficient or not for SLC44A2 (Figure 2I). Together these data demonstrate a role for SLC44A2 in stenosis driven thrombosis and suggest a possible effect on NETosis at the site of thrombosis.

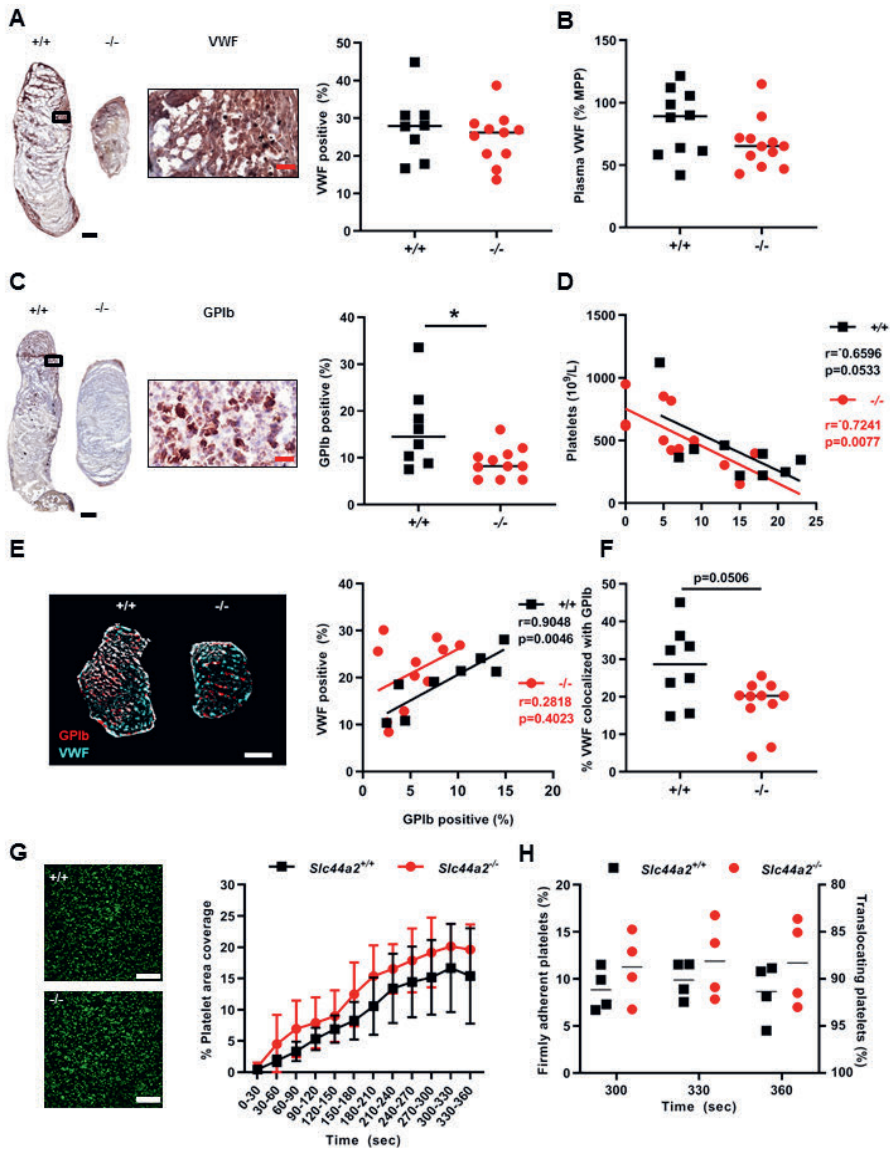


Figure 3. von Willebrand factor (VWF) and platelet characteristics of SLC44A2 deficient mice following 48 hours stenosis and ex vivo under flow conditions. (A) Immunohistochemical (IHC) staining of VWF in thrombus of a representative wild type (*Slc44a2*^{+/+}, +/+) and SLC44A2 deficient mice (*Slc44a2*^{-/-}, -/-), with high magnification from *Slc44a2*^{+/+} (location is indicated by the black box; left) and quantification (right) of positive area as a percentage of total thrombus area in *Slc44a2*^{+/+} (n = 8) or *Slc44a2*^{-/-} mice (n = 11). **(B)** Plasma VWF levels after 48 hours stenosis expressed as a percentage of MMP (mouse pool plasma; +/+ n = 9, -/- n = 12). **(C)** IHC staining of glycoprotein Ib (GPIb) in thrombus of a representative *Slc44a2*^{+/+} and *Slc44a2*^{-/-}, with high magnification from *Slc44a2*^{+/+} (location is indicated by the black box; left) and quantification (right) of positive area as a percentage of total thrombus area (+/+ n = 8, -/- n = 11). **(D)** Correlation plot between thrombus weight and circulating blood platelets (+/+ n = 9, -/- n = 12). **(E)** Immunofluorescent co-stain of GPIb (red) and VWF (cyan) on thrombus sections (left) with correlation plot (right; +/+ n = 8; -/- n = 11). **(F)** Percentage of VWF positive area colocalized with GPIb. **(G)** Representative images of DiOC₆-labeled platelets of a wild type (*Slc44a2*^{+/+}, +/+) control (up) and a SLC44a2 deficient mouse (*Slc44a2*^{-/-}, -/-; down) on a surface coated with VWF-binding

peptide. Scale bar is 20 μm . **(H)** Percentage of stable platelet area coverage over a 30 second time period in field view within heparinized and D-phenylalanyl-prolyl-arginyl chloromethyl ketone (PPACK) treated whole blood flowing over slides coated with a murine VWF binding peptide at venous shear rate (150 s^{-1}) over time ($n = 5$ per group). (Note on numbers: blood samples that became coagulated or thrombi that were damaged during sectioning were not included for subsequent analysis.) **(I)** Percentage platelets displaying a firm or transient interaction with VWF-binding peptide determined by a method described by Meyer dos Santos et al.¹⁷ Black and white bars equal 500 μm . Red bar equals 50 μm . Statistical differences between for platelet perfusion were evaluated by two-way analysis of variance and for remaining biological readouts, the Mann-Whitney rank-sum test. Coefficient r calculated using Spearman's correlation (*signifies $p < 0.05$)

3.3 *Slc44a2*^{-/-} mice have less platelet accumulation after 48 hours stenosis

Previously, we determined that *Slc44a2*^{-/-} have a reduced level of circulating plasma VWF antigen when compared to *Slc44a2*^{+/+}.⁷ To investigate whether the VWF release from the endothelium was reduced in SLC44A2 deficient mice, this discharge was stimulated using intraperitoneal injection of 2 mg/kg lipopolysaccharides (LPS), a dose inducing Weibel-Palade body release. VWF plasma levels were increased following LPS injection; however, in time we observed no differences in VWF levels between *Slc44a2*^{+/+} and *Slc44a2*^{-/-} mice (Figure S6 in supporting information). This suggests that smaller thrombi in *Slc44a2*^{-/-} mice are not likely due to reduced levels of available VWF following stenosis. We also found that VWF distribution within thrombi was comparable between the two genotypes by constituting approximately 30% of the thrombus area (Figure 3A) and that plasma VWF at 48 hours post-stenosis was not significantly different between groups ($p = 0.2030$; Figure 3B). When we focused on platelets, platelet counts could be correlated to thrombus size both in *Slc44a2*^{+/+} and *Slc44a2*^{-/-} mice as platelet accumulation is a major determinant of thrombus size at 48 hour-stenosis (Figure 3D). Remarkably though, the proportion of platelet marker GPIb-positive area was significantly reduced ($p = 0.0259$) in thrombi from *Slc44a2*^{-/-} mice (Figure 3C). As VWF and GPIb are established binding partners,²² we evaluated the relationship of the two proteins on serial sections. VWF was strongly associated with GPIb in *Slc44a2*^{+/+} mice ($r = 0.9004$; $p = 0.0023$); however, this association was absent in *Slc44a2*^{-/-} ($r = -0.3471$; $p = 0.2956$; Figure S7 in supporting information). We then verified these relationships on the same thrombus section by confocal microscopy. We measured a clear association between VWF and GPIb in the *Slc44a2*^{+/+} group ($r = 0.9048$; $p = 0.0046$) and none within the *Slc44a2*^{-/-} ($r = 0.2818$; $p = 0.4023$) (Figure 3E). Moreover, the area of VWF that co-localized with GPIb was reduced in the *Slc44a2*^{-/-} animals (-36% , $p = 0.0506$; Figure 3F). As this indicated a possible altered interaction between GPIb and VWF, we evaluated the binding potential of platelets to VWF under venous flow (150 s^{-1}) *ex vivo* using slides coated with a murine VWF binding peptide and perfused with whole blood. We observed a comparable increase of platelet binding with a final mean surface area coverage of 15.4% (5.6%-22.2%) by *Slc44a2*^{+/+} platelets and 19.7% (17.2%-25.6%) by *Slc44a2*^{-/-} platelets after 6 minutes ($p = 0.9122$; Figure 3G). When we further dissect between firmly adherent and translocating platelets we also did not observe differences, indicating that also stable binding of platelets is unaffected by SLC44A2 (Figure 3H). To evaluate

whether platelets under arterial flow have altered adherence, whole blood was perfused over collagen at 1000 s^{-1} , also here no differences were observed (Figure S8 in supporting information). Based on these findings, platelet accumulation is reduced in thrombi from *Slc44a2*^{-/-} mice at 48 hours and this is not related to VWF availability. Additionally, perfusion studies revealed that platelet-VWF interactions did not seem to be affected in *Slc44a2*^{-/-} mice.

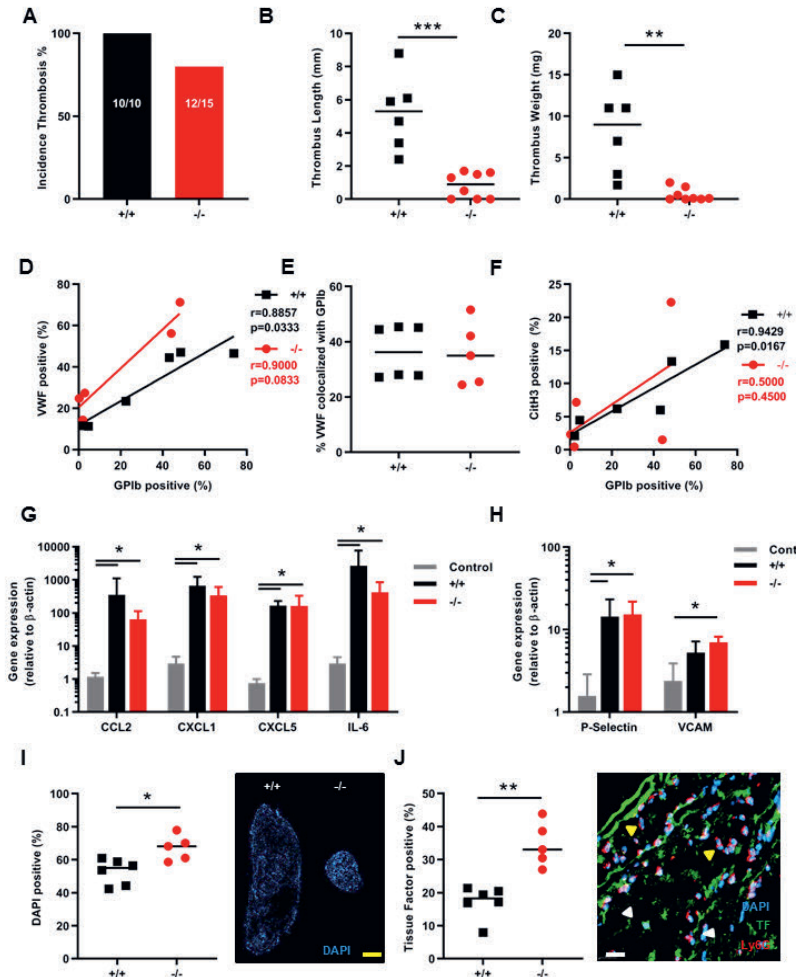


Figure 4. Thrombosis in SLC44A2 deficient mice following 6 hours stenosis of the inferior vena cava (IVC). (A) Incidence of thrombosis after 6 hours in mice wild type (+/+, $n = 6$) or SLC44A2 deficient mice (-/-, $n = 8$), shown as percentage. (B) Length and (C) weight of thrombi formed at 6 hours. (D) Correlation plot of GPIb and VWF immunostaining on thrombus sections (+/+, $n = 6$; -/-, $n = 5$). (E) Percentage of VWF positive area co-localized with GPIb. (F) Correlation plot of GPIb and citrullinated histone H3 immunostaining on thrombus sections. (G) Transcript levels of inflammatory molecules produced by the local IVC in *Slc44a2*^{+/+} (+/+, $n = 6$) or *Slc44a2*^{-/-} (-/-, $n = 5$) for SLC44A2 collected at 6 hours post-stenosis as compared to non-ligated control C57BL/6J mice ($n = 3$); chemokine (C-C motif) ligand 2 (*Ccl2*), chemokine (C-X-C motif) ligand 1 (*Cxcl1*), *Cxcl5*, interleukin-6 (*Il6*). (H) IVC expression of mRNA transcripts encoding adhesion molecules; P-selectin and vascular cell adhesion molecule 1 (VCAM1) following 6 hours stenosis. Bars represent mean values with standard deviation (error bars). (I) Nuclear stain (DAPI) of leukocytes in thrombi from *Slc44a2*^{+/+} and *Slc44a2*^{-/-} mice (top left) with quantification as a percentage of total thrombus

area (+/+ $n=6$; -/- $n=5$). (J) Quantification of immunofluorescent (IF) staining of tissue factor (TF; left) as a percentage of total thrombus area. Representative image of IF co-stain by confocal microscopy of neutrophil marker Ly6G, TF, and nuclear stain (DAPI; right panel). Yellow arrows indicate Ly6G positive cells and white arrows indicate TF positive cells. Yellow bar equals 500 μm and white bar equals 20 μm . Statistical differences were evaluated using Mann-Whitney rank-sum test (*signifies $p<0.05$; **signifies $p<0.01$; ***signifies $p<0.001$).

3.4 Thrombosis in *Slc44a2*^{-/-} mice is reduced at 6 hours post-stenosis

To gain further insight into the role of SLC44A2 during the initiation phase of thrombosis, thrombosis was measured 6 hours post IVC ligation. At this time point 100% of the *Slc44a2*^{+/+} (6/6) and 62.5% of the *Slc44a2*^{-/-} mice formed thrombi (5/8) (Figure 4A). The thrombi from the *Slc44a2*^{-/-} mice were again smaller both in length (-83%, $p=0.0007$) and weight (-99%, $p=0.0013$; Figure 4B-C). As before, we observed that *Slc44a2*^{+/-} mice (incidentally included) fell in between with 75% incidence (3/4) and median values of length and weight halfway in between those of the *Slc44a2*^{+/+} and *Slc44a2*^{-/-} (Figure S9 in supporting information). An independent experiment executed by a different operator, in a different facility, substantiated these findings, with significant effects of genotype on thrombus weight ($p=0.0020$) and length ($p=0.0010$), and again no effect on incidence (Figure S10 in supporting information). Evaluation of the thrombi revealed large variability within each group for GPIb staining with high and low subsets for both *Slc44a2*^{+/+} and *Slc44a2*^{-/-}, leading to no significant differences with regard to platelet density (Figure S11A in supporting information). Similarly, no differences could be detected with regard to VWF staining (Figure S11B). We found again a correlation between the VWF and GPIb staining in *Slc44a2*^{+/+} mice ($r=0.8857$; $p=0.0333$) that persisted this time in *Slc44a2*^{-/-} ($r=0.9000$; $p=0.0833$; Figure 4D). The percentage of VWF that co-localized with GPIb was also comparable between the groups (Figure 4E). These data indicate that the early binding of platelets to VWF is unaltered. Additional quantification determined no differences in thrombus density in neutrophils (Ly6G staining) and NETs (CitH3 staining; Figure S11C-D). The CitH3-positive area was found to be strongly correlated with GPIb levels in *Slc44a2*^{+/+} mice ($r=0.9429$; $p=0.0167$), but not in the *Slc44a2*^{-/-} animals ($r=0.5000$; $p=0.4500$; Figure 4F), which was not observed at the 48-hour time point (Figure S12 in supporting information).

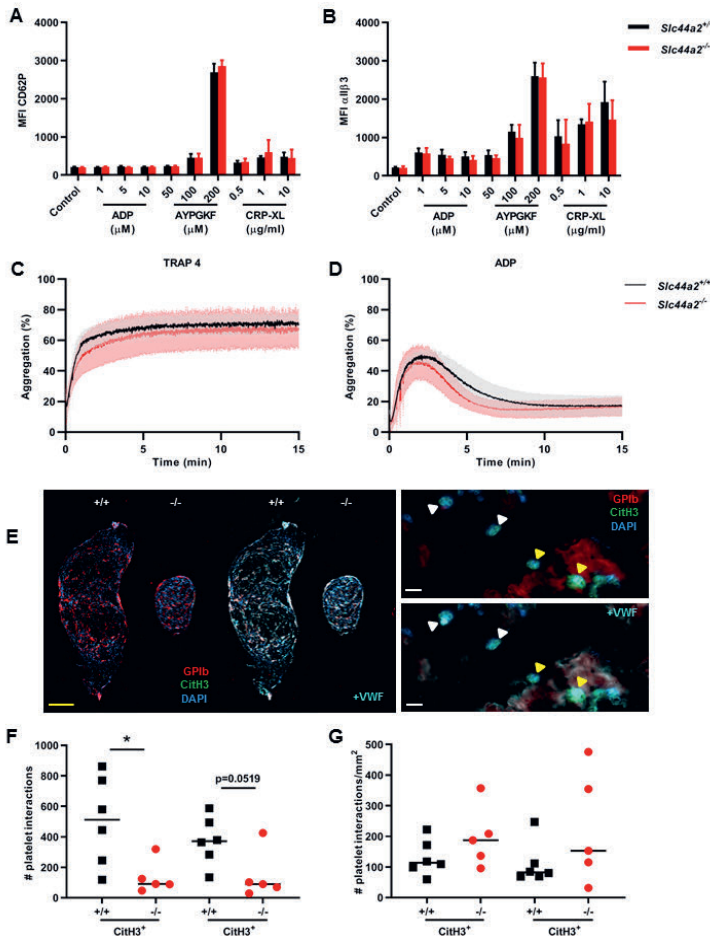
Stenosis is followed by an acute response from the local endothelium marked by upregulation of inflammatory cytokines and adhesion markers.⁹ Transcript levels of cytokines CCL2, CXCL1, CXCL5, and IL-6 in the IVC 6 hours post-stenosis were increased compared to control untreated IVC ($p<0.05$), which was in line with previous reports.⁹ However, there were no differences in transcript levels between genotypes (Figure 4G). The same observations were made for the transcripts coding for the adhesion molecules P-selectin and VCAM-1, which are central to immune cell interactions with the endothelium ($p<0.05$; Figure 4H). These data indicate a normal inflammatory response by the endothelium in *Slc44a2*^{-/-} mice after stenosis.

In this model endothelial activation is followed by recruitment of immune cells to the site of stenosis. Leukocytes incorporated into the thrombi can be visualized using a nuclear stain because platelets and erythrocytes are enucleated cells. Interestingly, when the thrombi were stained with 4',6-diamidino-2-phenylindole (DAPI), the density of DAPI-positive leukocytes was significantly elevated in the *Slc44a2*^{-/-} mice (% , p=0.0303; Figure 4I). This was not observed at 48 hours post-stenosis (Figure S13 in supporting information). As we established there was no difference in Ly6G positive cell composition (Figure S11C); this observation suggests that the increased leukocytes are likely not neutrophils. TF production by leukocytes is another critical step in this model and we observed a two-fold increase in TF immunostaining density in thrombi from the *Slc44a2*^{-/-} animals (p=0.0043; Figure 4J). Interestingly, the nucleated cells that co-localized with TF were mainly Ly6G negative (Figure 4J) while all nucleated cells were Ly6C positive (Figure S14 in supporting information) indicating that these are likely monocytes, which was previously reported to be the main source of TF in this model.⁹ Together these data demonstrate that SLC44A2 is important during the initiation of thrombosis, but not for endothelial activation in this VT model.

3.5 Platelet activation, aggregation, and neutrophil interactions are unaltered in *Slc44a2*^{-/-} platelets

We established that SLC44A2 deficiency has a pronounced effect on stenosis-driven thrombosis, coinciding with reduced platelet accumulation after 2 days without any noticeable effect on platelet/VWF co-localization. We hypothesized that SLC44A2 may be involved after platelet adhesion to the vessel wall in subsequent stages of platelet activation. We observed that the consumption of platelets from circulation had not yet occurred in the *Slc44a2*^{-/-} mice at 6 hours post-stenosis. As a result, the levels of circulating platelets differ between *Slc44a2*^{+/+} and *Slc44a2*^{-/-} after stenosis (p=0.0061; Figure S15 in supporting information). The upregulation of membrane protein P-selectin (CD62P) is a key step during platelet activation,²³ whereas a feature of later stages of platelet activation is the binding of platelets to fibrinogen via the $\alpha_{IIb}\beta_3$ integrins. When we look at the percentage positive platelets for CD62P exposure as well as $\alpha_{IIb}\beta_3$ activation after stimulation with different concentrations of ADP, PAR4 agonist and collagen-related peptide CRP-XL, we observed a significantly lowered exposure in *Slc44a2*^{-/-} platelets under some conditions (Figure S16 in supporting information). When we, however, analyzed the median fluorescence intensity of both CD62P and $\alpha_{IIb}\beta_3$ we did not find an effect of SLC44A2 (Figure 5A-B). To determine if SLC44A2 had an effect on platelet-platelet interactions, we measured platelet aggregation using PRP following activation using TRAP-4 (strong stimulus) and ADP (weak stimulus). We did not detect any significant differences in platelet aggregation in *Slc44a2*^{-/-} (Figure 5C-D). This is in line with our previous observation, using washed platelets, in which platelet aggregation induced by thrombin or collagen was unaffected.⁷ Together, this is suggestive of a normal response by *Slc44a2*^{-/-} platelets.

In addition to the primary role of platelets in haemostasis, they can also activate neutrophils and stimulate NETosis²⁴ as neutrophils and NETs can activate and recruit platelets.^{20,25,26} To evaluate whether SLC44A2 influenced murine platelet-neutrophil interactions, we perfused recalcified whole blood at venous shear rates (150 s^{-1}) over slides coated with a VWF capturing peptide. Under these conditions, we did not observe neutrophil binding to the platelets that adhered to the slides; however, the rapid formation of fibrin and coagulation of the blood also made the analysis challenging. We then used a different approach and analysed platelet-leukocyte interactions within the thrombi of the mice obtained 6 hours after stenosis. Here we could clearly distinguish leukocytes adjacent to platelets and record if they were either positive or negative for CitH3 (Figure 5E, left panel). We noticed that areas positive for GPIb strongly overlapped with VWF expression (Figure 5E, right panel) as we saw earlier (Figure 4D). Quantification of the total number of platelet-leukocyte interactions revealed that more platelets were found interacting with CitH3 positive cells in *Slc44a2*^{+/+} mice than in *Slc44a2*^{-/-} mice (Figure 5F); however, this difference was not significant when thrombus size was taken into account (Figure 5G).



< Figure 5. Characterization of platelets in SLC44A2 deficient mice. Percentage of cells positive for (A) exposed P-selectin (CD62P) or (B) activated integrin $\alpha_{IIb}\beta_3$ following activation with ADP (1, 5, 10 $\mu\text{mol/L}$), protease-activated receptor 4 (PAR4) agonist AYPGKF (50, 100, 200 $\mu\text{mol/L}$) or collagen related peptide (CRP-XL; 0.5, 1 or 10 $\mu\text{g/mL}$) as determined by flow cytometry and quantified as the percentage of cells staining positive (%) in wild type (*Slc44a2*^{+/+}, *n* = 5) or SLC44A2 deficient mice (*Slc44a2*^{-/-}, *n* = 5). Platelet aggregation following stimulation with (C) 1.2 mmol/L thrombin receptor activating peptide 4 (TRAP-4) or (D) 24 $\mu\text{mol/L}$ adenosine diphosphate (ADP) in *Slc44a2*^{+/+} and *Slc44a2*^{-/-}. (E) Immunofluorescent co-stain of thrombi from *Slc44a2*^{+/+} and *Slc44a2*^{-/-} of nuclei (DAPI; blue), platelet marker GPIb (red), and citrullinated histone H3 (CitH3; green) with and without additional visualization of staining with VWF (cyan; left). Higher magnification indicates leukocyte-platelet interactions (yellow triangles) and leukocytes positive for CitH3 without platelet interactions (white triangles) with (right bottom) and without (right top) additional visualization of VWF. Yellow bar represents 500 μm , white bar represents 10 μm . (F) Quantification of nucleated cells in contact with platelets either positive or negative for CitH. (G) Number of platelet interactions with leukocytes per mm² of thrombus. Statistical differences for flow cytometry were calculated using two-way analysis of variance (shown as mean with standard deviation [SD]) and for aggregometry, *t*-test (shown with mean and SD). For platelet-leukocyte quantifications, statistical differences were evaluated using Mann-Whitney rank-sum test (*signifies *p*<0.05; **signifies *p*<0.01).

4. Discussion

Genomic studies can be a powerful tool for identifying novel factors that contribute to pathophysiology.^{27,28} *SLC44A2* is the first gene outside of the coagulation cascade found to be associated with VT risk.^{2,3} VT is influenced both by inflammation and coagulation.²⁹ During inflammation, endothelial cells and neutrophils will play a major role in the initiation phase of thrombosis, whereas hypercoagulability will mostly influence the propagation phase.⁹ Here we used SLC44A2 deficient mice in two independent models of VT. We have substantiated the genomic data from the GWAS and established a functional role for SLC44A2 in stenosis-, but not in hypercoagulability-, driven thrombosis. The absence of a role for SLC44A2 in thrombosis driven by hypercoagulability supports the notion that SLC44A2 does not interfere with the coagulation system. This is in agreement with our previous finding that SLC44A2 does not influence mouse haemostasis (including coagulation) under normal conditions⁷ and also with the observation that variation in SLC44A2 did not associate with haemostasis phenotypes included in the GWAS.² For stenosis-driven thrombosis we observed that SLC44A2 deficiency affects thrombus size after 6 and 48 hours of blood flow restriction in mice. This is interesting because in contrast to the hypercoagulability model, the stenosis model is inflammation driven, indicating a role for SLC44A2 in inflammation-regulated thrombosis. This suggests that neutrophil recruitment and/or activation could be altered in *Slc44a2*^{-/-} mice. Our data do not permit us to conclude on a possible reduction in neutrophil adhesion to the vessel wall in absence of SLC44A2 but they could still suggest a possible reduction in NETosis and platelet accumulation in this model. The percentage of platelets activated *ex vivo* was slightly reduced under specific conditions; the median fluorescence index (MFI) of platelet activation markers however was not affected, leading us to conclude that the overall platelet activation is unaffected. Moreover, aggregation and thrombus formation *in vitro/ex vivo* were found to be normal for

blood from SLC44A2 deficient mice, which is suggestive of normal haemostatic function of *Slc44a2*^{-/-} platelets. Despite the normal haemostatic function of platelets, altogether, these studies establish a contributing role for SLC44A2 during the initiation of VT.

The function of SLC44A2 is poorly understood, although there is emerging data that describe ways it may be modulating thrombosis. SLC44A2 is suggested to be a binding partner of VWF and this interaction on neutrophils led to agglutination when in the presence of plasma containing anti-SLC44A2 antibodies (HNA3A), thereby inducing transfusion related acute lung injury (TRALI).³⁰ Additionally, findings presented at the European Congress on Thrombosis and Hemostasis 2018 demonstrated that a specific allelic variant of SLC44A2, also associated with VT, plays a role in neutrophil binding to VWF which leads to NETosis after priming with TNF- α .³¹ Most recently, it was shown that platelets primed by VWF display activated integrin $\alpha_{IIb}\beta_3$ (but not CD62P), which can then bind neutrophil SLC44A2 and mediate NETosis under venous flow.³² Based on these findings, the role of SLC44A2 is supposedly limited to neutrophil biology and NET release; however, the suggested binding partner differs. One theory suggests a direct interaction with VWF and the other with platelet integrin $\alpha_{IIb}\beta_3$ following adherence to VWF. Combining all these findings would implicate SLC44A2 as a binding partner of two elements involved in thrombosis, one being VWF and the other platelet integrin $\alpha_{IIb}\beta_3$, with both binding to SLC44A2 on neutrophils.

Neutrophils are known to be a major driver of venous thrombosis in the stenosis model.⁹ Therefore it is tempting to speculate that SLC44A2 on neutrophils is responsible for the underlying effects of this protein on thrombus formation. In the current study, upon stenosis we observe a trend for less CitH3 within the *Slc44a2*^{-/-} thrombi at 48 hours, which is in line with the notion that SLC44A2 deficient neutrophils are less active in the production of NETs. However, we demonstrated that neutrophil activation is still occurring in these mice both *in vivo* and *ex vivo*, as determined by CitH3 staining, plasma DNA levels, and ROS production. It is possible that the observed reduced platelet incorporation into *Slc44a2*^{-/-} thrombi at 48 hours is due to slightly less NETosis as this process promotes platelet aggregation through the interaction of NET bound cathepsin G with platelet P2Y₁₂ and $\alpha_{IIb}\beta_3$ receptors.^{26,33}

Alternatively, platelet activation can also drive NET production through the presentation of high mobility group box 1 (HMGB1)³⁴ or CD62P.³⁵ This would support our observation of increased CitH3 expression with increasing platelet levels in thrombi following 6 hours stenosis in the *Slc44a2*^{+/+} mice. Importantly, though, we did observe direct contact of platelets with CitH3 positive leukocytes within the thrombi of both groups at 6 hours, implying that platelets deficient for SLC44A2 can still activate neutrophils, even when they are also lacking SLC44A2. Interestingly, the lost correlation of GPIb and VWF at 48 hours is in line with the previous finding of reduced platelet accumulation following laser injury of the cremaster arterioles.⁷ This may, however, still be related to neutrophil activation as it was demonstrated to also contribute to clot formation in this model.³⁶

To better address the importance of SLC44A2 in platelets versus neutrophils, a more dynamic system would be useful such as intra-vital microscopy combined with live cell imaging of the cell types following stenosis.⁹ Furthermore, as SLC44A2 is expressed by many cell types central to thrombosis including endothelial cells, leukocytes, platelets, and erythrocytes, cell transfer experiments or cell-specific knock-outs may also be necessary when dissecting out the contributions of certain compartments or cell types. In particular neutrophil and platelet specific *Slc44a2* knockouts would be of interest for future investigations as our data, in addition to the findings from others,³⁰⁻³² points toward SLC44A2 involvement on these two cell types as being relevant to VT pathophysiology. With the existence of mice carrying a conditional allele for *Slc44a2*, these studies are certainly feasible. We do not find evidence that SLC44A2 is important for endothelial activation following stenosis. Notably, in the present study we used female mice for the hypercoagulability model and male mice for the stenosis model, which was in part because it allowed comparison with previous published studies using these models. Future work using a cell-specific approach may include both sexes, allowing detection of possible sex-specific effects, which was not possible in the present study.

In conclusion, by utilizing a murine representation of DVT, we were able to corroborate the recent genomic studies identifying SLC44A2 as a susceptibility gene for VT and establish that SLC44A2 is key during the initiation of thrombosis with indications that this may be related to platelet-neutrophil interaction, either directly and/ or indirectly. The precise mechanism however remains elusive and warrants further investigation.

Essentials

- SLC44A2 does not affect onset in a murine model of venous thrombosis driven by hypercoagulability.
- Mice lacking SLC44A2 have less severity of venous thrombosis in the stenosis model following 6 and 48 hours.
- There is significantly less platelet accumulation in thrombi of SLC44A2 deficient mice at 48 hours post-stenosis.

Acknowledgements

The authors thank Dr Pavan K. Kommareddi, Thankam S. Nair, and Dr Thomas E. Carey (Kresge Hearing Research Institute, Department of Otolaryngology/Head and Neck Surgery, University of Michigan, Ann Arbor, MI, USA) for the floxed *Slc44a2* mouse embryos used to generate the mice on a C57BL/6J background and Dr Charles Esmon (University of Oklahoma Health Sciences Center, Oklahoma City, OK, USA) for providing the 59D8 fibrin antibody. Also, we thank Lieke van den Heijkant for assisting with the hypercoagulability model.

Conflicts of interest

The authors declare no competing financial interests.

Author contributions

Experimental design: JT, DMC, GZ, SD, HCdB, JMEMC, HHV, PEM, BJMvV, CXM, GMT. Performed experiments and analysed data: JT, DMC, GZ, SD, MFAK, HCdB, JMEMC, BJMvV, CXM, GMT. Wrote the paper: JT, BJMvV, CXM, GMT. All authors commented on manuscript drafts.

Funding information

This work was supported by Trombosestichting Nederland (#2015-4), the Landsteiner Foundation for Blood Transfusion Research (#1503), the Dutch Heart Foundation (2015T79), the Netherlands Organization for Scientific Research (NWO Vidi 91716421), a European Molecular Biology Organization Short-Term Fellowship (EMBO #7468), a European Society of Cardiology First Contact Initiative grant and by a French ANR grant (ANR-17-CE14-0003-01).

References

1. Raskob GE, Angchaisuksiri P, Blanco AN, et al. Thrombosis: a major contributor to global disease burden. *Arterioscler Thromb Vasc Biol.* 2014;34:2363-71.
2. Germain M, Chasman DI, de Haan H, et al. Meta-analysis of 65,734 individuals identifies TSPAN15 and SLC44A2 as two susceptibility loci for venous thromboembolism. *Am J Hum Genet.* 2015;96:532-42.
3. Hinds DA, Buil A, Ziemek D, et al. Genome-wide association analysis of self-reported events in 6135 individuals and 252 827 controls identifies 8 loci associated with thrombosis. *Hum Mol Genet.* 2016;25:1867-74.
4. Nair TS, Kozma KE, Hoefling NL, et al. Identification and characterization of choline transporter-like protein 2, an inner ear glycoprotein of 68 and 72 kDa that is the target of antibody-induced hearing loss. *J Neurosci.* 2004;24:1772-9.
5. Iwao B, Yara M, Hara N, et al. Functional expression of choline transporter like-protein 1 (CTL1) and CTL2 in human brain microvascular endothelial cells. *Neurochem Int.* 2016;93:40-50.
6. Tilburg J, Michaud SA, Maracle CX, et al. Plasma protein signatures of a murine venous thrombosis model and Slc44a2 knockout mice using quantitative-targeted proteomics. *Thromb Haemost.* 2020; 120:423–6.
7. Tilburg J, Adili R, Nair TS, et al. Characterization of hemostasis in mice lacking the novel thrombosis susceptibility gene Slc44a2. *Thromb Res.* 2018;171:155-9.
8. Safdar H, Cheung KL, Salvatori D, et al. Acute and severe coagulopathy in adult mice following silencing of hepatic antithrombin and protein C production. *Blood.* 2013;121:4413-6.
9. von Bruhl ML, Stark K, Steinhart A, et al. Monocytes, neutrophils, and platelets cooperate to initiate and propagate venous thrombosis in mice in vivo. *J Exp Med.* 2012;209:819-35.
10. Kommareddi P, Nair T, Kakaraparthi BN, et al. Hair cell loss, spiral ganglion degeneration, and progressive sensorineural hearing loss in mice with targeted deletion of Slc44a2/Ctl2. *J Assoc Res Otolaryngol.* 2015;16:695-712.
11. Brill A, Fuchs TA, Savchenko AS, et al. Neutrophil extracellular traps promote deep vein thrombosis in mice. *J Thromb Haemost.* 2012;10:136-44.
12. Tjernberg P, Vos HL, Castaman G, et al. Dimerization and multimerization defects of von Willebrand factor due to mutated cysteine residues. *J Thromb Haemost.* 2004;2:257-65.
13. Cleuren AC, Van der Linden IK, De Visser YP, et al. 17 α -Ethinylestradiol rapidly alters transcript levels of murine coagulation genes via estrogen receptor α . *J Thromb Haemost.* 2010;8:1838-46.
14. Visser YP, Walther FJ, el Laghmani H, et al. Apelin attenuates hyperoxic lung and heart injury in neonatal rats. *Am J Respir Crit Care Med.* 2010;182:1239-50.

15. Schindelin J, Arganda-Carreras I, Frise E, et al. Fiji: an opensource platform for biological-image analysis. *Nat Methods*. 2012;9:676-82.
16. de Witt SM, Swieringa F, Cavill R, et al. Identification of platelet function defects by multi-parameter assessment of thrombus formation. *Nat Commun*. 2014;5:4257.
17. Meyer dos Santos S, Klinkhardt U, Schneppenheim R, et al. Using ImageJ for the quantitative analysis of flow-based adhesion assays in real-time under physiologic flow conditions. *Platelets*. 2010;21:60-6.
18. Heestermans M, Salloum-Asfar S, Streef T, et al. Mouse venous thrombosis upon silencing of anticoagulants depends on tissue factor and platelets, not FXII or neutrophils. *Blood*. 2019;133:2090-9.
19. Brill A, Fuchs TA, Chauhan AK, et al. von Willebrand factor-mediated platelet adhesion is critical for deep vein thrombosis in mouse models. *Blood*. 2011;117:1400-7.
20. Martinod K, Demers M, Fuchs TA, et al. Neutrophil histone modification by peptidylarginine deiminase 4 is critical for deep vein thrombosis in mice. *Proc Natl Acad Sci USA*. 2013;110:8674-9.
21. Alvarado CM, Diaz JA, Hawley AE, et al. Male mice have increased thrombotic potential: sex differences in a mouse model of venous thrombosis. *Thromb Res*. 2011;127:478-86.
22. Bockenstedt P, Greenberg JM, Handin RI. Structural basis of von Willebrand factor binding to platelet glycoprotein Ib and collagen. Effects of disulfide reduction and limited proteolysis of polymeric von Willebrand factor. *J Clin Invest*. 1986;77:743-9.
23. Stenberg PE, McEver RP, Shuman MA, et al. A platelet α -granule membrane protein (GMP-140) is expressed on the plasma membrane after activation. *J Cell Biol*. 1985;101:880-6.
24. Zucoloto AZ, Jenne CN. Platelet-neutrophil interplay: insights into neutrophil extracellular trap (NET)-driven coagulation in infection. *Front Cardiovasc Med*. 2019;6:85.
25. Darbousset R, Thomas GM, Mezouar S, et al. Tissue factor-positive neutrophils bind to injured endothelial wall and initiate thrombus formation. *Blood*. 2012;120:2133-43.
26. Fuchs TA, Brill A, Duerschmied D, et al. Extracellular DNA traps promote thrombosis. *Proc Natl Acad Sci USA*. 2010;107:15880-5.
27. Visscher PM, Wray NR, Zhang Q, et al. 10 Years of GWAS discovery: biology, function, and translation. *Am J Hum Genet*. 2017;101:5-22.
28. Tregouet DA, Morange PE. What is currently known about the genetics of venous thromboembolism at the dawn of next generation sequencing technologies. *Br J Haematol*. 2018;180:335-45.
29. Branchford BR, Carpenter SL. The role of inflammation in venous thromboembolism. *Front Pediatr*. 2018;6:142.
30. Bayat B, Tjahjono Y, Berghofer H, et al. choline transporter-like protein-2: new von Willebrand factor-binding partner involved in antibody-mediated neutrophil activation and transfusion-related acute lung injury. *Arterioscler Thromb Vasc Biol*. 2015;35:1616-22.
31. Zirka G, Robert P, Legendre P, et al. HNA-3a Expressed by CTL-2 is a crucial epitope for neutrophil adhesion and activation on VWF European Congress on Thrombosis and Haemostasis (ECTH). Marseille, France, 2018.
32. Constantinescu-Bercu A, Frontini M, Salles-Crawley I, Woollard K, Crawley J. Activated $\alpha_{IIb}\beta_3$ on platelets mediates flow-dependent NETosis via SLC44A2. *Elife*. 2020;9:e53353.
33. Elaskalani O, Abdol Razak NB, Metharom P. Neutrophil extracellular traps induce aggregation of washed human platelets independently of extracellular DNA and histones. *Cell Commun Signal*. 2018;16:24.
34. Maugeri N, Campana L, Gavina M, et al. Activated platelets present high mobility group box 1 to neutrophils, inducing autophagy and promoting the extrusion of neutrophil extracellular traps. *J Thromb Haemost*. 2014;12:2074-88.
35. Etulain J, Martinod K, Wong SL, et al. P-selectin promotes neutrophil extracellular trap formation in mice. *Blood*. 2015;126:242-6.
36. Wang Y, Gao H, Shi C, et al. Leukocyte integrin Mac-1 regulates thrombosis via interaction with platelet GPIIb. *Nat Commun*. 2017;8:15559.

Supplemental table and figures

Table S1 qPCR primer sequences used for (coagulation) gene profiling of lung and liver.

Gene	Forward Primer	Reverse Primer
<i>Actb</i>	AGGTCATCACTATTGGCAACGA	CCAAGAAGGAAGGCTGGAAAA
<i>Slc44a2</i>	CGGAAGGACGCAGTCTATGG	AGGAAGAGCAACACACAGCA
<i>Serpinc1</i>	CCCTGGCCGACTTCACAA	TTTTGCAGTGCCTGTGCTACA
<i>Proc</i>	GCGTGGAGGGCACCAA	CCCTGCGTCGCAGATCAT
<i>Ccl2</i>	TTAAAAACCTGGATCGGAACCAA	GCATTAGCTTCAGATTTACGGGT
<i>Cxcl1</i>	CTGGGATTCACCTCAAGAACATC	CAGGGTCAAGGCAAGCCTC
<i>Cxcl5</i>	GTTCCATCTCGCCATTTCATGC	GCGGCTATGACTGAGGAAGG
<i>Il6</i>	TAGTCCTTCCTACCCCAATTTCC	TTGGTCCTTAGCCACTCCTTC
<i>Selplg</i>	ACCGTGGTCATGCTAGAGAGA	ACTGAGGTTAGACTCCACTGTG
<i>Vcam1</i>	AGTTGGGGATTTCGGTTGTTCT	CCCCTCATTCTTACCACCC

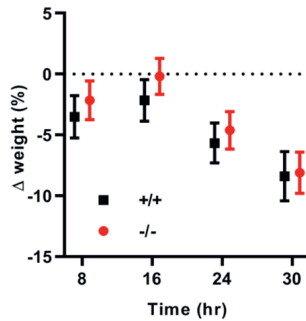


Figure S1. Comparable levels of weight loss in the hypercoagulability model of thrombosis. Weight loss over time following treatment with siRNA targeting the anticoagulants antithrombin and protein C as a percentage of total weight of SLC44A2 deficient (-/-) and wild type control mice (+/+) represented as mean with SD ($n = 12$ per group).

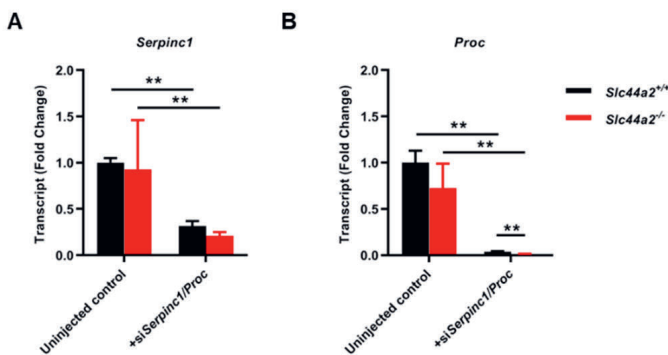


Figure S2. Confirmation of knockdown of *Serpinc1* and *Proc* at the transcriptional level. Liver gene transcript levels of (A) *Serpinc1* and (B) *Proc* after siRNA-mediated hepatic knockdown of *Serpinc1* and *Proc* ($n = 12$ per group) and un-injected controls ($n = 4$) in SLC44A2 deficient (*Slc44a2*^{-/-}) and wild type control mice (*Slc44a2*^{+/+}). The comparative threshold cycle method with β -actin as internal control was used for quantification and normalization. The mean is represented as fold change compared to un-injected *Slc44a2*^{-/-} and *Slc44a2*^{+/+} mice. Error bars represent the difference between $2^{\Delta\Delta Ct}$. Statistical differences were evaluated using Mann-Whitney rank-sum test (** signifies $p < 0.01$).

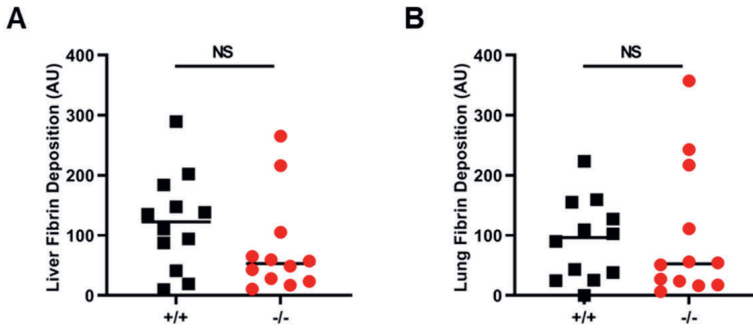


Figure S3. Fibrin deposition in peripheral organs following treatment with siRNA. Deposition of fibrin in arbitrary units (AU) in liver (A) and lungs (B) of SLC44A2 deficient (*Slc44a2*^{-/-}) and wild type control mice (*Slc44a2*^{+/+}) following treatment with siRNA targeting the anticoagulants antithrombin and protein C (*n* = 12 per group). Black lines represent median value. Statistical differences were evaluated using Mann-Whitney rank-sum test.

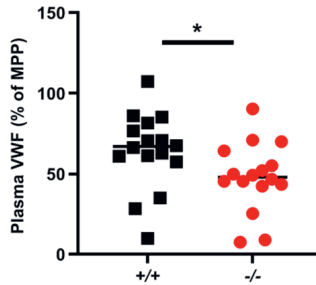


Figure S4. Plasma VWF levels before treatment with siRNA. Plasma VWF (Von Willebrand Factor) levels before siRNA treatment expressed as a percentage of MPP (mouse pool plasma) in SLC44A2 deficient mice (*-/-*, *n* = 16) and wild type control mice (*+/+*, *n* = 16). Statistical differences were evaluated using Mann-Whitney rank-sum test (* signifies *p* < 0.05).

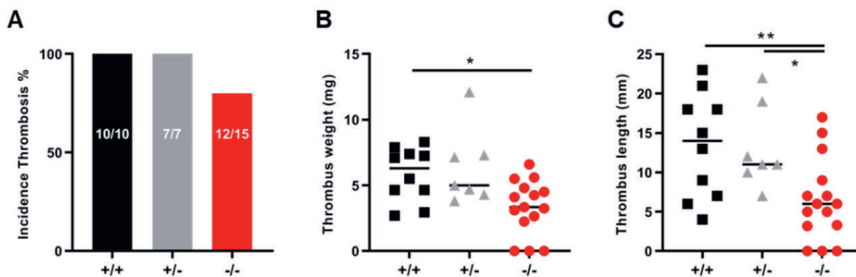


Figure S5. Thrombosis in SLC44A2 deficient mice following 48 hour stenosis of the inferior vena cava. (A) Incidence of thrombosis after 48 hours in SLC44A2 deficient mice (*-/-*, *n* = 10), mice heterozygous for SLC44A2 (*+/-*, *n* = 7) or wild type control (*+/+*, *n* = 15) shown as percentage. (B) Length and (C) weight of thrombi formed after 48 hours. Black lines represent median value. Statistical differences between 3 genotypes were evaluated using ANOVA Kruskal-Wallis test (*p* = 0.0130 for length; *p* = 0.0090 for weight) and Dunn's multiple comparison test. (* signifies *p* < 0.05; ** signifies *p* < 0.01).

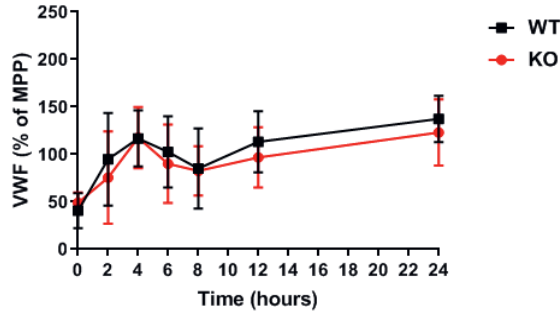


Figure S6. Plasma VWF levels following LPS stimulation. Mice were injected with 2 mg/kg lipopolysaccharides (LPS) and blood samples collected over a time course of 24 hours. Plasma VWF levels were determined by ELISA and compared to a relative standard of mouse pooled plasma (MPP) ($n = 11$ per group).

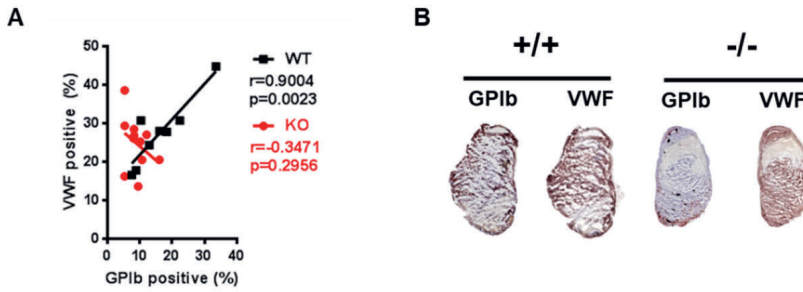


Figure S7. Relationship between VWF and GPIb in thrombi following 48 hour stenosis. (A) Correlation plot between GPIb staining and VWF staining on serial thrombus sections after 48 hour stenosis of SLC44A2 deficient ($Slc44a2^{-/-}$, $n = 11$) and wild type control mice ($Slc44a2^{+/+}$, $n = 8$). (B) Representative images of IHC staining of GPIb and VWF. Coefficient r calculated using Spearman's correlation.

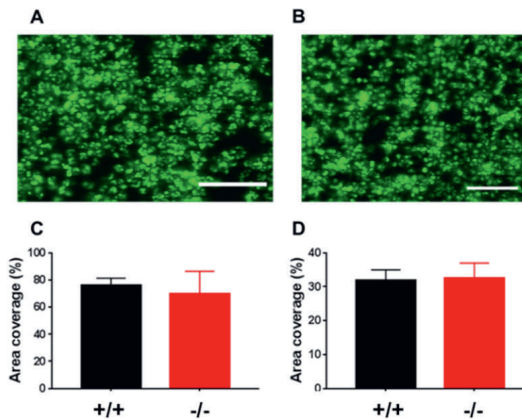


Figure S8. Representative images of platelet adhesion after 3.5 minutes of whole blood perfusion of blood from $Slc44a2^{+/+}$ mice (A) or $Slc44a2^{-/-}$ mice (B) at 1000 s^{-1} over collagen type I. Quantitative analysis of platelet surface area coverage (C) and JON/A surface area coverage (D). Scale is 10 μm . Mean + S.D., $n = 5-7$.

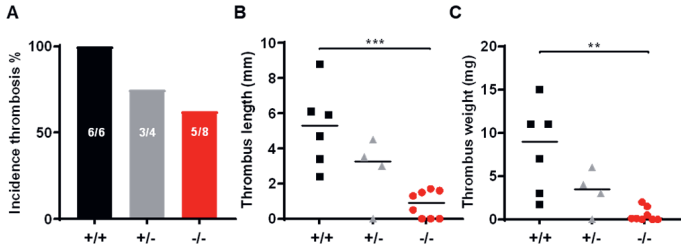


Figure S9. Thrombosis in SLC44A2 deficient mice following 6 hour stenosis of the inferior vena cava. (A) Incidence of thrombosis after 6 hours in mice wild type (*Slc44a2*^{+/+}) (*n* = 6), heterozygous (*Slc44a2*^{+/-}) (*n* = 4) or knockout (*Slc44a2*^{-/-}) (*n* = 8) for SLC44A2, shown as percentage. (B) Length and (C) weight of thrombi formed after 6 hours. Black lines represent median value. Statistical differences between genotypes were evaluated using ANOVA Kruskal-Wallis test (*p*=0.0010 for length; *p*=0.0020 for weight) and Dunn’s multiple comparison test. (** signifies *p*<0.01; *** signifies *p*<0.0001).

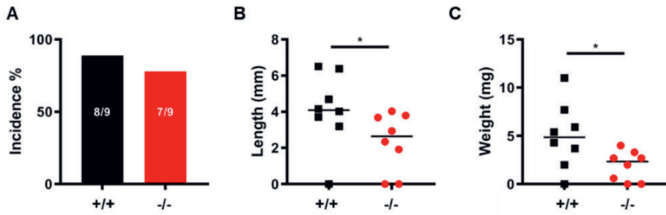


Figure S10. Thrombosis in SLC44A2 deficient mice following 6 hour stenosis of the inferior vena cava. (A) Incidence of thrombosis after 6 hours in mice wild type (*Slc44a2*^{+/+}) or knockout (*Slc44a2*^{-/-}) (*n* = 9) for SLC44A2, shown as percentage. (B) Length and (C) weight of thrombi formed after 6 hours. Black lines represent median value. Statistical differences between genotypes were evaluated using ANOVA Kruskal-Wallis test (*p*=0.0010 for length; *p*=0.0020 for weight) and Dunn’s multiple comparison test. (* signifies *p*<0.05).

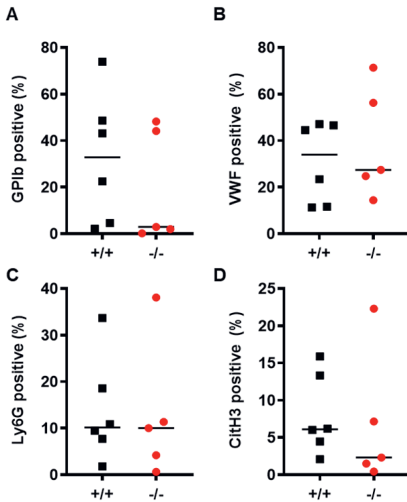


Figure S11. Immunohistochemical characterization of thrombi following 6 hour stenosis. Quantification of immunohistochemical (IHC) staining of (A) glycoprotein Ib (GPIIb), (B) von Willebrand Factor (VWF), (C) neutrophil marker Ly6G and (D) citrullinated histone H3 (CitH3) as a percentage of total thrombus area (%). (*Slc44a2*^{+/+} (+/+) *n* = 6; *Slc44a2*^{-/-} (-/-) *n* = 5). Black lines represent median value. Statistical differences were evaluated using Mann-Whitney rank-sum test.

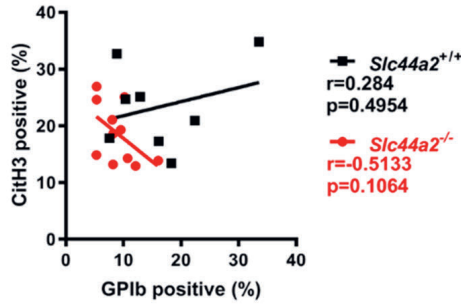


Figure S12. Correlation of platelets and citrullinated histones. Correlation plot of GPIIb and citrullinated histone H3 immunostaining on thrombus sections in SLC44A2 deficient (*Slc44a2*^{-/-}, *n* = 11) and wild type control mice (*Slc44a2*^{+/+}, *n* = 8) following 48 hour stenosis of the inferior vena cava.

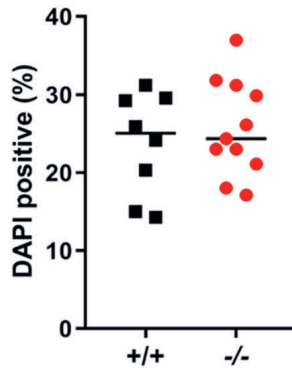


Figure S13. DAPI positive area. Nuclear stain (DAPI) of leukocytes in thrombi from SLC44A2 deficient mice (-/-, *n* = 11) and wildtype control mice (+/+, *n* = 8) as a percentage of total thrombus area following 48 hour stenosis of the inferior vena cava.

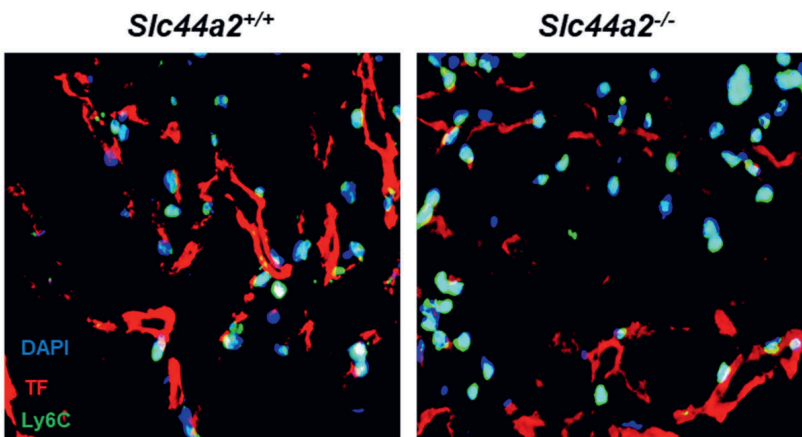


Figure S14 Tissue factor Ly6C staining. Immunofluorescent staining of tissue factor (TF; red), Ly6C (green) and nuclear stain (DAPI; blue) in thrombi from *Slc44a2*^{+/+} and *Slc44a2*^{-/-} mice, light blue signal indicates co-localization of DAPI and Ly6C. 63x magnification.

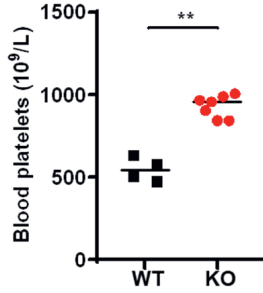


Figure S15. Blood platelet counts at 6 hours post-stenosis of the IVC. Circulating blood platelets counts at sacrifice following 6 hours stenosis procedure. Black lines represent median value. Statistical differences were evaluated using Mann Whitney rank-sum test. (*Slc44a2*^{+/+} *n* = 4; *Slc44a2*^{-/-} *n* = 5) (** signifies *p* < 0.01).

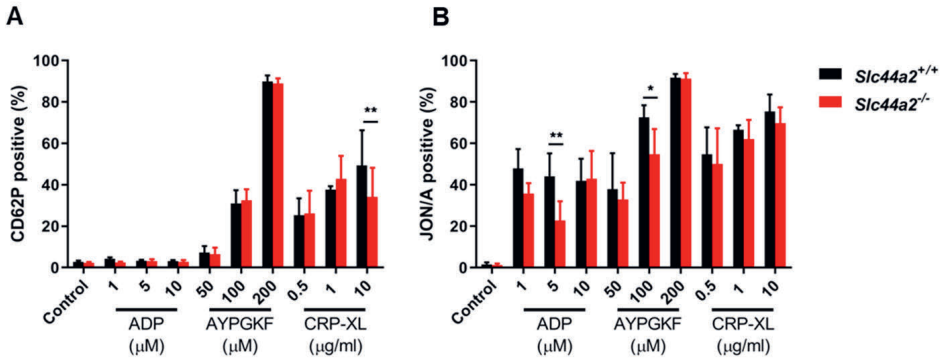


Figure S16. Platelet activation. Percentage of cells positive for (A) exposed P-selectin (CD62P) or (B) activated integrin $\alpha_{IIb}\beta_3$ following activation with adenosine diphosphate (ADP; 1, 5, 10 $\mu\text{mol/L}$), Protease-Activated Receptor 4 (PAR4) agonist AYPGKF (50, 100, 200 $\mu\text{mol/L}$) or collagen related peptide (CRP-XL) (0.5, 1 or 10 $\mu\text{g/mL}$) as determined by flow cytometry and quantified as the percentage of cells staining positive (%) in platelets from SLC44A2 deficient mice (*Slc44a2*^{-/-}, *n* = 5) and wild type control mice (*Slc44a2*^{+/+}, *n* = 5).



Chapter 8

Finding the “switch” in platelet activation – Prediction of key mediators involved in platelet hyperreactivity using a network biology approach

Lemmens TP, Coenen DM, Niessen ICL, Swieringa F, Coort SLM, Koenen RR, Kutmon M, Cosemans JMEM
To be submitted

Abstract

The healthy endothelium controls platelet activity through release of prostaglandin I₂ (PGI₂) and nitric oxide. The loss of this natural brake on platelet activity can cause platelets to become hyperreactive. PGI₂ attenuates platelet activation by adenosine diphosphate (ADP) through stimulating of cyclic adenosine monophosphate (cAMP) production and subsequent phosphorylation changes by protein kinase A (PKA). We hypothesize that proteins or processes involved in platelet hyperactivity downstream of the cAMP-PKA pathway can serve as a “switch” in platelet activation and inhibition.

We designed a network biology approach to explore the entangled platelet signalling pathways downstream of PGI₂ and ADP. The STRING database was used to build a protein-protein interaction network from proteins of interest in which we integrate a quantitative platelet proteome dataset with pathway information, relative RNA expression of hematopoietic cells, the likelihood of the proteins being phosphorylated by PKA, and drug-target information from DrugBank in a biological network.

We distilled 30 proteins from existing phosphoproteomics datasets (PXD000242, PXD001189) that putatively can be “turned on” after ADP-mediated platelet activation and subsequently switched “off” after platelet inhibition with iloprost. A protein-protein interaction network with 20 additional interactors was created to also include related proteins. Gene ontology enrichment analysis revealed biological processes related to vesicle secretion and cytoskeletal reorganization to be overrepresented coinciding with topological clusters in the network. Next to expected proteins like phosphodiesterase 3A, our method highlighted several novel proteins related to vesicle transport, platelet shape change, and small GTPases as potential switch proteins in platelet activation and inhibition. Our novel approach demonstrates the benefit of data integration by combining existing tools and datasets and visualization to obtain a more complete picture of complex molecular mechanisms.

Introduction

Endothelial dysfunction is a common feature of cardiovascular diseases such as atherosclerosis and hypertension.^{1,2} It is characterized by reduced availability of nitric oxide (NO) and the inability to adequately maintain vascular homeostasis.³ Normally, the endothelium limits platelet activity and aggregation through prostaglandin I₂ (PGI₂) and NO. The loss of this natural brake on platelet activity can cause platelets to become hyperreactive, which contributes to the progression of cardiovascular diseases.⁴ For instance, insulin resistance and hypoglycaemia in type 2 diabetes mellitus (T2DM) are known to lead to reduced platelet sensitivity to PGI₂ and NO.^{5,6} Furthermore, platelet hyperreactivity can contribute to antiplatelet drug resistance, which is associated with poor cardiovascular outcome.⁷⁻⁹ PGI₂ attenuates platelet activation through binding to the

IP platelet membrane receptor, inducing activation of adenylyate cyclase (AC), and subsequent production of cyclic adenosine monophosphate (cAMP) and cAMP-dependent activation of protein kinase A (PKA). PKA phosphorylates a range of proteins, consequently leading to inhibition of platelet aggregation, secretion and shape change. Activation of the adenosine diphosphate (ADP) receptor P2Y₁₂ leads to inhibition of AC, thereby releasing the natural brake on platelet activation. A second main signalling route downstream of P2Y₁₂ is activation of phosphoinositide 3-kinase (PI3K), which leads to activation of the platelet integrin $\alpha_{IIb}\beta_3$ receptor and enables platelet aggregation.¹⁰ Taken together, this highlights the cAMP-PKA signalling axis as an interesting starting point to identify novel key players in platelet activation and inhibition.

We hypothesize that downstream of the cAMP-PKA pathway are proteins or processes that can serve as a “switch” in platelet activation and inhibition. Molecular switches are abundant in many different biological functions. A known molecular switch in platelet (in)activation is the Rap1, a small GTPase that is essential in integrin $\alpha_{IIb}\beta_3$ activation after stimulation of G protein-coupled receptors (GPCR).¹¹ Hydrolyzation of Rap1b-GTP by the GTPase Ras GTPase-activating protein 3 (RASA3) to a GDP-bound form causes the protein to be switched off.¹² Binding of ADP to P2Y₁₂ results in inhibition of RASA3 by PI3K, thereby driving $\alpha_{IIb}\beta_3$ activation and platelet aggregation.¹³ Besides this known example of a switch protein, the process of platelet activation/hyperreactivity relies on many more proteins that form a complex system of pathways with numerous interactions. In this article we aim to find proteins that can be utilized as targets to reverse platelet hyperreactivity. We developed a network biology approach to integrate information from different data sources to address our aim and to explore the entangled platelet signalling pathways downstream of PGI₂ and ADP.

Methods

We designed a network biology approach to find putative switches in platelet activation and inhibition. The workflow that we developed is schematically represented in Figure 1 and explained below.

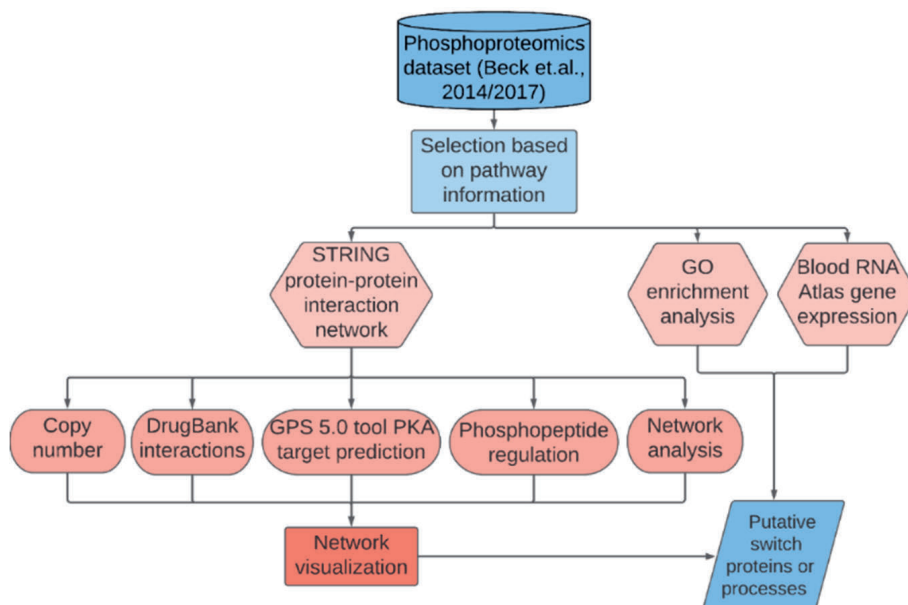


Figure 1. Schematic overview of the methodological workflow to find switches in platelet activation and inhibition downstream of cAMP/PKA signalling using a publicly available phosphoproteomics dataset.^{14,15}

Phosphoproteomics dataset

To create a selection of proteins with putative involvement in the resolution of platelet activation, we made use of publicly available phosphoproteomics datasets. Beck et al. reported on the phosphoproteomics response of iloprost (a stable prostacyclin analogue)-stimulated platelets (dataset containing 2739 phosphopeptides; 360 proteins with regulated (99% confidence) phosphorylation).¹⁵ Additionally, they reported on a dataset combining iloprost and ADP stimulation on platelet protein phosphorylation (containing >4797 phosphopeptides; 608 proteins regulated).¹⁴ These datasets can be accessed through ProteomeXchange under the accession PXD000242 and PXD001189, respectively. In the present study we extracted proteins from these datasets based on known platelet signalling routes, see paragraph 'Data selection and characterization' under Results for detailed description.

Network generation

We utilized the StringApp¹⁶ in Cytoscape 3.7.2¹⁷ to build a protein-protein interaction network with the 30 selected proteins involved in the resolution of platelet activation based on known pathway information downstream IP and P2Y_{12/11} as protein query. A confidence score cut-off of 0.5 was selected to include enough nodes in the network, while maintaining a high selectivity.¹⁶ Subsequently, the network was expanded to incorporate an additional 20 interactors based on their total connectivity relative to their overall connectivity in the STRING database. These proteins may provide mechanistic links between nodes in the network and thereby

might reveal relevant processes. All processes were automated in R (version 3.6.3) using the RCy3 package.¹⁸

Functional enrichment analysis

Gene Ontology (GO) enrichment analysis on all proteins in the resulting network and their corresponding genes was performed using the integrated tool from PANTHER on the GO website (<http://geneontology.org/>).¹⁹⁻²¹ Main settings that were used are: Biological process, Homo sapiens, Fisher's exact test type and false discovery rate as correction ($P < 0.05$). We used a default enrichment significance threshold of 0.05 to find significantly overrepresented pathways or processes corresponding to clusters observed in the network.

Protein Kinase A prediction and druggability

GPS 5.0 is a tool to predict and score phosphorylation sites based on their kinase consensus sequence.²² A higher score indicates an increased probability for protein phosphorylation at the specific site by the specified protein kinase. The threshold was set to the highest probability and the outcome was visualized on nodes using Cytoscape.

Information on FDA-approved drugs and their interactions from the DrugBank database version 5.1.0²³ were incorporated into the network using CyTargetLinker²⁴ and visualized in Cytoscape. CyTargetLinker is a Cytoscape application integrating different "linksets", e.g. drug-target, microRNA-target, and regulatory interactions into a network.

Copy number and relative RNA expression

We incorporated existing²⁵ quantitative data on the platelet proteome dataset in our network to show the estimated copy number in human platelets. To obtain an indication of the relative expression of proteins in our network in hematopoietic cells, we used Blood RNAexpress, which is made freely available by the Blueprint consortium.²⁶

Results

Data selection and characterization

Knowing that the cAMP-PKA pathway is a major platelet inhibitory pathway²⁷ and that phosphorylation events are essential in effectuating signalling events to platelet function, we used a publicly available phosphoproteomics dataset on platelet cAMP/PKA-dependent signalling upon stimulation with ADP, iloprost or both^{14,15} as a starting point. We subtracted a set of proteins from the database of which we presume to be putative switch proteins or part of switch 'processes'. Hereto we made the following assumptions: 1) to specifically investigate the resolution of platelet activation, platelets have to be activated first, 2) proteins involved in platelet deactivation lie downstream of the prostacyclin receptor. We started by selecting

proteins that showed up- and/or downregulation upon platelet treatment with the agonist ADP for 30 seconds followed by treatment with iloprost, a stable prostacyclin analogue. This yielded 349 phosphosites corresponding to 215 unique proteins to be significantly regulated, see Figure 2. This first selection of phosphopeptides still contains a significant number of proteins that are involved in platelet activation through P2Y₁ and not P2Y₁₂ and do not necessarily play a role platelet inhibition by iloprost. We therefore narrowed down our selection by omitting phosphopeptides that were regulated only after ADP stimulation. We then assumed that the group of resting platelets receiving iloprost treatment had phosphorylation that can prevent or “switch off” proteins or processes involved in platelet activation. Thus, we only included peptides that were regulated when treated with iloprost, ultimately obtaining a comprehensive list of proteins with potential switches that can be “turned on” after ADP stimulation and “off” after iloprost mediated platelet inhibition. The final protein selection consisted of 30 proteins (Supplemental Table 1). Twenty of these proteins had significant upregulated phosphosites while 13 proteins had significant downregulated phosphosites. The validity of this approach was supported by the identification of PDE3A, an established effector of cAMP/PKA signalling, among the 30 selected proteins. Interestingly, CNST, FGA and KALRN had both up and downregulated phosphosites. Moreover, most proteins had differential regulation of phosphorylation sites between the different experimental groups often at the same phosphorylation site. In sum, using a publicly available dataset we used knowledge about related pathways to extract 30 proteins downstream cAMP/PKA signalling with potential involvement in activation and subsequent inactivation of platelets.

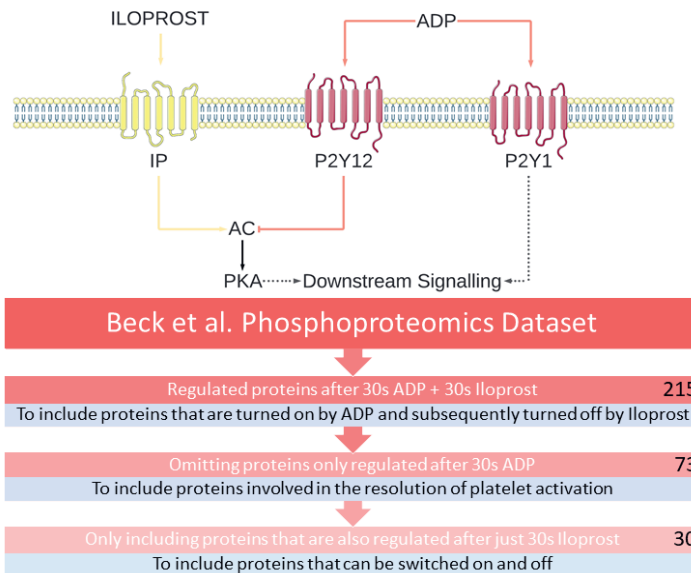


Figure 2. Summary of pathway information and protein selection. After 30 seconds ADP stimulation and subsequent 30 seconds iloprost treatment 349 phosphosites corresponding to 215 unique proteins were significantly regulated. Omitting those regulated only after just 30 seconds ADP stimulation resulted in 73 proteins. Cross-referencing these 73 proteins with those regulated after just 30 seconds iloprost treatments resulted in a final selection of 30 proteins.

Enrichment of vesicle-related biological processes

GO enrichment analysis can reveal over-represented, also termed ‘enriched’, biological processes found in a dataset. If processes are enriched in the dataset, it means that genes annotated to a specific GO process are over-represented compared to the entire background set. On the 30 selected proteins, GO enrichment analysis for biological processes revealed only vesicle-mediated transport to be significantly enriched. When including the additional 20 interactors from the STRING database not only vesicle-related biological processes (46.93 to > 100 fold enrichment) but also positive regulation of cyclin-dependent protein kinase activity (36.34 fold enrichment), processes involving small GTPases (7.53 fold enrichment) and tight junctions (26.57 fold enrichment) were found to be enriched, see Table 1.

Table 1. Table of significantly enriched GO biological processes. Fold enrichment with raw p-value and false discovery rate (FDR) is shown. For statistical analysis, the Fisher Exact test was used.

GO biological processes	Fold enrichment	Raw P-value	FDR
SNARE complex assembly (GO:0035493)	> 100	4.77E-06	6.31E-03
Vesicle fusion (GO:0006906)	46.93	6.63E-13	1.05E-08
Positive regulation of cyclin-dependent protein kinase activity (GO:1904031)	36.34	9.80E-05	5.02E-02
Tight junction organization (GO:0120193)	26.57	1.96E-05	1.73E-02
Vesicle targeting (GO:0006903)	18.11	8.24E-05	4.84E-02
Cytosolic transport (GO:0016482)	16.7	1.89E-06	3.00E-03
Endosomal transport (GO:0016197)	10.56	2.40E-05	1.81E-02
Vesicle-mediated transport (GO:0016192)	4.4	1.70E-09	5.40E-06
Regulation of protein localization (GO:0032880)	4.31	8.95E-05	4.89E-02
Regulation of small GTPase mediated signal transduction (GO:0051056)	7.53	1.50E-04	6.24E-02

Network analysis

Phosphopeptide regulation

The protein-protein interaction network was created with the 30 selected proteins mentioned under ‘Data selection and characterization’. We added 20 additional interactors to include proteins that are likely to play a role in the major biological processes covered by the network. Ultimately, it contained 30 regulated proteins, 20 additional interactors and 79 edges connecting the nodes (Figure 3). Regulated phosphosites – according to Beck et al.^{14,15} - were visualized on the nodes with pie charts and node size was mapped to indicate the total number of phosphosites found in each protein. The network contained 4 major clusters consisting of 4 or more nodes. 13 out of 15 nodes from the largest cluster (Figure 3a) are related to vesicle-mediated transport and 6 out of 9 nodes from the second largest cluster (Figure 3b) are related to cell shape or regulation of small GTPase mediated signal transduction. The smaller clusters are related to cyclin-dependent kinases (Figure 3c) and tight junctions (Figure 3d) and contain less than 6 nodes. Finally, 14 nodes did not have any protein interaction to other nodes in the constructed network (Figure 3e). Some proteins, like CCNY, are additional

interactors but also show regulation, because they did have relevant phosphorylation sites according to the dataset but did not pass our selection (Figure 2). Other proteins, such as CABLES1, did have phosphorylation sites but none of these were significantly changed by ADP/iloprost treatment. The topological clusters in the network correspond with the results from the enrichment analysis, indicating that these are functional clusters related to specific biological processes. In the dataset generated by Beck et. al., STXBP5, SEC22B, STON2 and LRMP, all proteins from the largest cluster, show no phosphopeptide regulation after just ADP stimulation. However after ADP + iloprost and after just iloprost, they show multiple upregulated sites. FGA seemed to be downregulated when treated with ADP but upregulated when treated with only iloprost (Figure 3a).

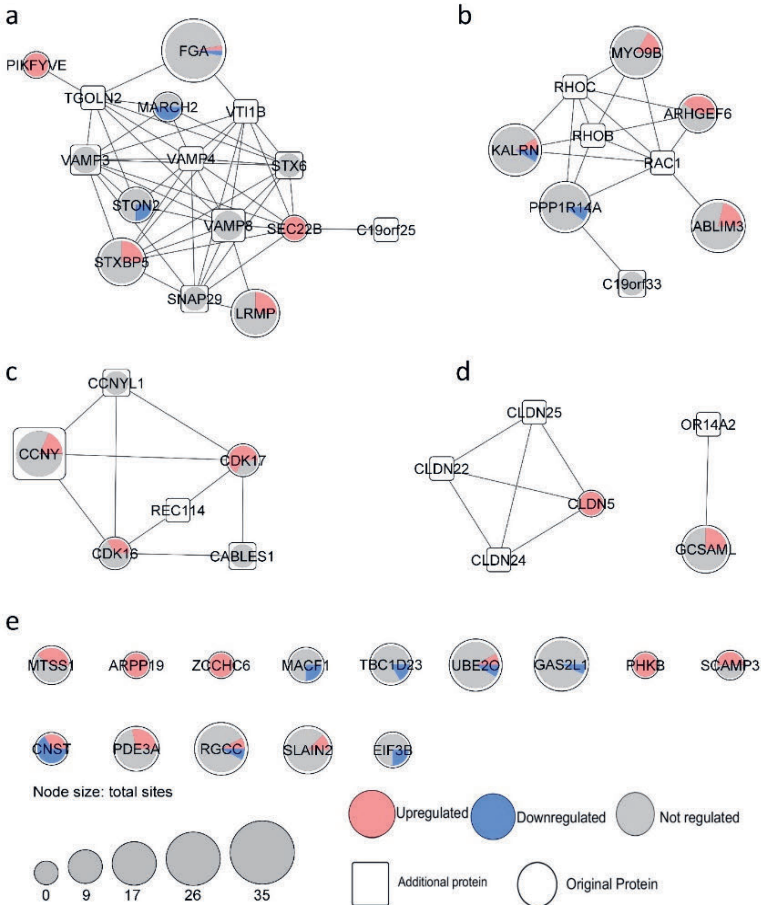
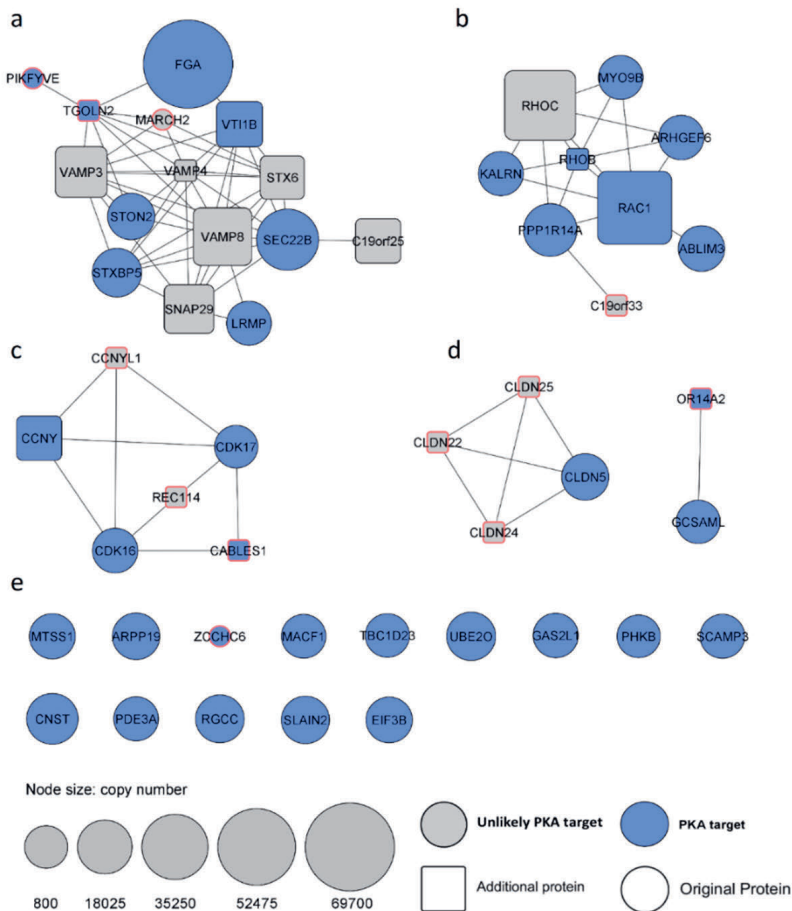


Figure 3. Protein-protein interaction network of potential “switch” candidates in the platelet activation. Total number of phosphorylation sites as reported by Beck et al. (15) are represented by node size and regulation is visualized by either red or blue for upregulated or downregulated sites respectively. Proteins added to the network by StringApp are represented by squares. Corresponding gene names are indicated per node. **(a)** Cluster of proteins related to vesicle-mediated transport. **(b)** Cluster of proteins related to regulation of small GTPase mediated signal transduction and cell shape. **(c)** Cluster related to cyclin-dependent kinases. **(d)** Cluster related to tight junctions. **(e)** Single nodes representing proteins that do not have direct interactions with other proteins in the network.

PKA phosphorylation scores and quantitative platelet proteome

We hypothesized that phosphorylation by PKA plays a role in regulating molecular switches of platelet activity and inhibition. Proteins with a high likelihood of being phosphorylated by PKA were identified with the GPS tool algorithm and visualized as blue nodes in an alternative representation of the network (Figure 4). As expected, almost all of the 30 proteins in our original list had GPS scores above the highest threshold and matched with the found phosphorylation sites of the dataset with the exception of MARCH2. Interestingly, several interactors added using StringApp, such as RAC1, VTI1B and CCNY, also had high GPS scores. The estimated copy number per platelet, based on mass spectrometric (MS) quantitation by Burkhardt et al.,²⁵ was incorporated in the network visualization as node size (Figure 4). The 12 proteins that did not have an estimated copy number were indicated with a red outline (Figure 4), meaning that they are either absent in platelets or present below the MS detection limit. No quantitative data was available for VAMP4 (Figure 4a) and RHOB (Figure 4b) and in the cluster corresponding to tight junctions, no proteins other than CLDN5 were detected in the platelet proteome (Figure 4c).



< **Figure 4. Protein-protein interaction network of potential “switch” candidates in the platelet activation.** Estimated copy numbers are visualized as node size and the fill colour indicates potential PKA substrates. Red outline indicates no known copy number in platelets. Proteins added to the network by StringApp are represented by squares. **(a)** Cluster of proteins related to vesicle-mediated transport. **(b)** Cluster of proteins related to regulation of small GTPase mediated signal transduction and cell shape. **(c)** Cluster related to Cyclin-dependent kinases. **(d)** Cluster related to tight junctions. **(e)** Single nodes representing proteins that do not have direct interactions with other proteins in the network.

To obtain an indication of the relative expression of proteins in our network in hematopoietic cells, we used the publicly available database Blood RNAexpress.²⁶ For reference, the gene GP1BA, coding for part of the GP1b receptor and well known to be abundant in platelets, had an average relative normalized gene expression, log₂ fpkm, of over 9. All genes had a log₂ fpkm higher than 1, with the exception of FGA, OR14A2, CLDN4/22/25 and REC114 (named C15orf60 in dataset). Several genes revealed by our analysis; SLAIN2, MARCH2, VAMP3, ARPP19, STON2, PHKB, ABLIM3, and IMUP (named C19orf33 in dataset) had a log₂ fpkm higher than 9 (Supplemental Table 2 log₂fpkm_heatmap). This indicates that these genes are more abundantly expressed in platelets when compared to other hematopoietic cells.

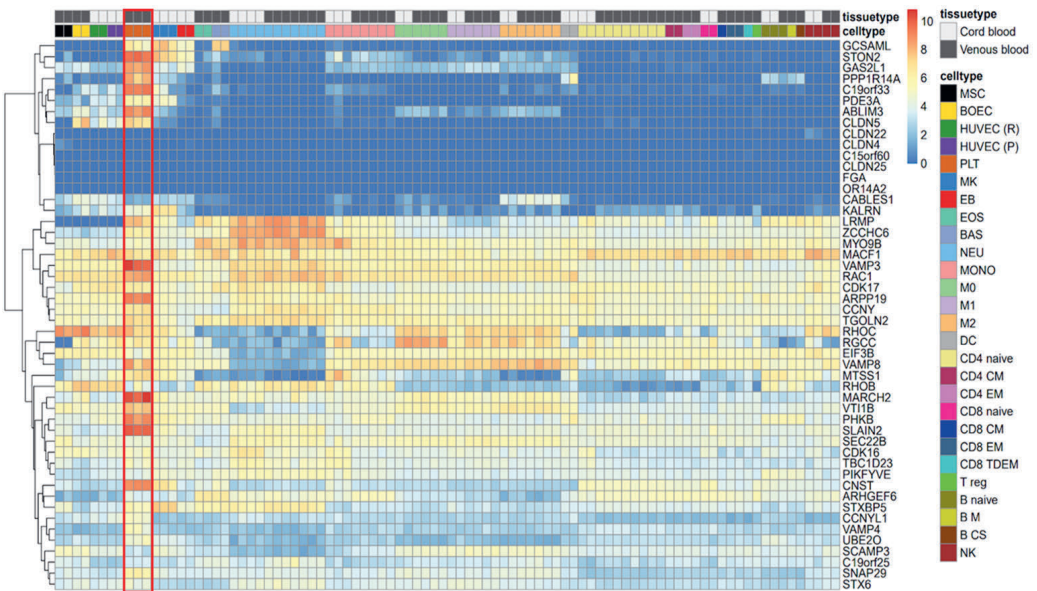


Figure 5. Clustered heatmap of relative hematopoietic cell-specific RNA expression of genes in the network. Orange colour marks platelet cell type RNA expression relative to other hematopoietic cell populations (log₂ fpkm). Red indicates high relative expression and blue indicates low relative expression. Data source and further information on: <https://blueprint.haem.cam.ac.uk/mRNA/>.

Integration of DrugBank database

Drug-target interactions were integrated into the network to give a clear and quick overview of current FDA-approved drugs that have one of the proteins in the network as target. In Figure 6, blue diamonds represent drugs and orange shapes

Discussion

In this study we developed a network biology approach to find putative novel switches in the cAMP-PKA signalling pathway in platelets. The network analyses were automated in R and can be adapted to include different proteins or an entirely different dataset. Our method can be used to repurpose existing datasets and provide a coherent overview of mechanisms involved to predict novel connections, by visually integrating multiple datasets. Here, this method was utilized to distil proteins from an existing phosphoproteomics dataset containing both activation and inhibition of platelets.^{14,15} Proteins not related to phosphorylation were inherently not included in the original phosphoproteomics datasets, as well as proteins excluded by our stringent selection, *e.g.* effectors downstream PKA after only ADP stimulation. However, such candidates might still be included through the addition of interactors using tools like the StringApp. Furthermore, although cAMP-PKA signalling is a major platelet inhibitory pathway, other pathways such as NO-cGMP/PKG signalling inhibit platelet activation. An advantage of our workflow is that it is designed in such a way that it could be readily adapted to process an alternate data selection or a different dataset entirely. Following our rationale, we were able to extract a subset of 30 proteins from this dataset, *i.e.* those proteins displaying both altered phosphorylation status upon sequential treatment of platelets with ADP plus iloprost and altered phosphorylation by iloprost treatment only. We postulate that the activity of these 30 proteins can be modified after ADP-mediated platelet activation and subsequently remodified after platelet inhibition with iloprost.

GO enrichment analysis revealed that multiple biological processes related to vesicle secretion, regulation of small GTPases and regulation of cyclin-dependent protein kinase activity were significantly overrepresented in our obtained list of 30 proteins. These processes are known to be important in platelet physiology. Platelets influence haemostasis by secreting granules and communicate with their environment by producing extracellular vesicles. Small GTPases play a pivotal in the control of vesicle trafficking and platelet aggregation or thrombus formation via $\alpha_{IIb}\beta_3$. Network analysis showed several clusters corresponding to these enriched biological processes to be well defined. We will discuss regulated proteins that are detected/detectable in the platelet proteome (27 out of 30, Figure 4) and have a high GPS score for PKA according to the cut-off of the GPS tool, as our hypothesis is that downstream of the cAMP-PKA pathway are proteins or processes that can serve as a “switch” in platelet activation and inhibition.

The largest cluster in our analysis is related to vesicle mediated transport. Interesting proteins in this cluster included FGA, STXBP5, STON2, SEC22B, LRMP, and VTI1B. The role proteins of these 6 proteins in platelet function has well been described for FGA and less well for the others. Fibrin is a major constituent of thrombi and essential to normal hemostasis. Syntaxin-binding protein 5 (STXBP5) has contradicting in platelets and endothelial cells, it promotes granule secretion in platelets but inhibits exocytosis in endothelial cells.²⁸ A single-nucleotide

polymorphism in the STXBP5 locus has also been associated with a decreased thrombotic phenotype.²⁹ In this study STXBP5 is indicated as a putative PKA substrate, which is in line with other phosphoproteomics studies on resting platelets.³⁰ Stonin-2 (STON2) is involved in the endocytic machinery, synaptic vesicle recycling and clathrin coated vesicle uncoating.³¹ To our knowledge Stonin-2's function has not been described in platelets even though Stonin-2 mRNA expression is relatively high in platelets compared to other haematopoietic cells, making it an interesting target for future research. SEC22B is a membrane-resident trafficking protein that is required for α -granule production in megakaryocytes and can interact with NBEAL2, which is associated with grey platelet syndrome. LRMP better known as inositol 1,4,5-triphosphate receptor associated 2 (IRAG2), interacts with the inositol 1,4,5-triphosphate receptor in mice indicating a potential role in calcium homeostasis.³² Platelet endocytosis/exocytosis is important in *e.g.* loading/release of α -granules. Studies have also implicated that integrin trafficking contributes to platelet activation and thrombosis by controlling their surface expression.³³ As more mechanistic studies show platelet endocytosis to be involved in platelet function,³⁴ it is interesting to see a pronounced representation in our network analysis.

The second largest cluster of proteins was related to regulation of small GTPase mediated signal transduction and cell shape. This cluster included ARHGEF6, PPP1R14A, KALRN, MYO9B, and ABLIM3, all with high PKA score. Not much is known about ABLIM3's function in platelets. However, the other proteins have been studied extensively in relation to platelet function. ARHGEF6 has previously been reported to be substrates for PKA and PKG and acts as a mediator in reducing Rac1-GTP levels leading to less outside-in platelet signalling.³⁵ Protein phosphatase 1 regulatory subunit 14A (PPP1R14A or CPI-17) is a phosphorylation dependent inhibitor protein of myosin phosphatase. Phosphorylation at Thr-38 causes a conformational change that greatly increases its inhibitory potential.³⁶ Although phosphorylation happens mainly through PKC and Rho-associated protein kinase (ROCK), it has a potential PKA target consensus sequence, as indicated by the GPS 5.0 algorithm. Phosphorylation of PPP1R14A has been shown to regulate shape change in platelets through calcium-independent signalling pathways. Platelet shape change is necessary for complete platelet activation. PPP1R14A could therefore be involved in a potential switch in platelet hyperreactivity as it can regulate myosin light chain phosphatase.³⁷ Another protein related to Rac/Rho protein signalling is kalirin (KALRN). In platelets, adenosine 5'-diphosphate-ribosylation factor 6 (ARF6) controls platelet spreading via integrin α IIb β 3 trafficking and can recruit KALRN to the plasma membrane leading to Rac activation.^{33,38} The ATP binding site within KALRN might be used as a starting point in the design of specific inhibitors. Inhibition of Rac1 by small molecules has been studied in the context of platelet secretion as a potential future antiplatelet drug.³⁹ MYO9B has recently been indicated to regulate RhoA activation through phosphorylation by PKA and PKG.⁴⁰ RhoA is a molecular switch controlled by GTPases. Platelet activation by ADP in

RhoA knockout mice results in defective platelet function and unstable thrombi formation.⁴¹ RAC1 and RHOB were central nodes interacting with most of these proteins. Rho GTPases are known key regulators of platelet cytoskeleton and function and serve as molecular switches downstream of platelet surface receptors. It is therefore expected that these proteins emerge as potential candidates from our selection.

The cluster related to Cyclin-dependent kinases contained at least three interesting proteins all with significantly upregulated phosphorylation sites after ADP and iloprost treatment; CDK16/17 and Cyclin-Y (CCNY). Regulation of cyclin-dependent protein kinase activity might seem surprising at first sight as cyclin-dependent proteins belong to a class of proteins involved in cell cycle, transcription and mRNA processing and platelets do not have a nucleus with limited mRNA processing capacity.⁴² However, recent focus on the role of non-coding RNA, nuclear receptors and post-transcriptional modifications in platelets reveal a more intricate transcriptional landscape than previously thought.^{43,44} In HEK293a cells, CDK16 is recruited to the plasma membrane and activated by CCNY. This process is regulated by Ser-153 and can be inhibited by PKA phosphorylation.⁴⁵ In line with these findings, we found Ser-153 to be a putative PKA phosphorylation site. Platelets lacking CCNY show decreased spreading and clot retraction, but increased adhesion to collagen.⁴⁶ Taken together, these new findings suggest that CCNY could play an important role in the outside-in signalling in platelets.

Finally, the smaller clusters and single nodes in our network also contain interesting proteins that are worth mentioning. PDE3A, CLDN5, GCSAML, MTSS1, ARPP19, MACF1, TBC1D23, UBE20, GAS2L1, PHKB, SCAMP3, CNST, RGCC, SLAIN2, and EIF3B. As expected, among the 30 proteins revealed by pathway analysis, we found proteins known to be involved in the cAMP-PKA signalling axis, e.g. PDE3A. While iloprost causes cAMP levels to go up, PDE3A hydrolyses cAMP. In diabetes mellitus, platelet hyperreactivity is believed to at least partly be caused by reduced platelet sensitivity to insulin, which leads to decreased endothelial PG12 expression, increased P2Y₁₂-mediated G_i activity and decreased platelet cAMP levels, thus leading to increased platelet activation.^{47,48} PKA-induced phosphorylation of PDE3A creates a negative feedback loop, indicating PDE3A being a key element in the cAMP/PKA pathway at least in initiation of platelet activation.⁴⁹ Although not directly connected to any other nodes in the PPI network, it is foreseeable that PDE3A is returned from the analysis as an interesting target. In fact, the validity of the method presented in this study can be inferred by its identification of PDE3A.

As more large datasets are generated daily by innovative studies utilizing high-throughput methods, integration of these datasets to put them in a specific context are necessary. Finding novel players in platelet activation/inhibition can help us better understand pathologies where platelet hyperreactivity is prevalent. Further experimental studies using a more causal analysis approach can reveal what effect a phosphorylation event has on a protein's function.⁵⁰ Experimental knockout mice

or using inhibitors in flow experiments for the aforementioned proteins are valid options to further validate the roles of these proteins in platelet hyperreactivity. Finally, this study shows the importance and benefit of data integration and visualization with existing tools and datasets to obtain a complete picture of complex molecular mechanisms involved.

References

1. Konukoglu D, Uzun H. Endothelial dysfunction and hypertension. *Hypertension: from basic research to clinical practice*. Springer International Publishing; 2017;511-40.
2. Davignon J, Ganz P. Role of endothelial dysfunction in atherosclerosis. *Circulation*. 2004;109(23 Suppl 1):III27-32.
3. Tabit CE, Chung WB, Hamburg NM, et al. Endothelial dysfunction in diabetes mellitus: molecular mechanisms and clinical implications. *Rev Endocr Metab Disord*. 2010;11(1):61-74.
4. Coenen DM, Heinzmann ACA, Karel MFA, et al. The multifaceted contribution of platelets in the emergence and aftermath of acute cardiovascular events. *Atherosclerosis*. 2021;319:132-41.
5. Nissen SE, Nicholls SJ, Wolski K, et al. Comparison of pioglitazone vs glimepiride on progression of coronary atherosclerosis in patients with type 2 diabetes: the PERISCOPE randomized controlled trial. *JAMA*. 2008;299(13):1561-73.
6. Kahal H, Aburima A, Spurgeon B, et al. Platelet function following induced hypoglycaemia in type 2 diabetes. *Diabetes Metab*. 2018;44(5):431-6.
7. Matetzky S, Shenkman B, Guetta V, et al. Clopidogrel resistance is associated with increased risk of recurrent atherothrombotic events in patients with acute myocardial infarction. *Circulation*. 2004;109(25):3171-5.
8. Michelson AD, Linden MD, Furman MI, et al. Evidence that pre-existent variability in platelet response to ADP accounts for 'clopidogrel resistance'. *J Thromb Haemost*. 2007;5(1):75-81.
9. Cuisset T, Frere C, Quilici J, et al. High post-treatment platelet reactivity identified low-responders to dual antiplatelet therapy at increased risk of recurrent cardiovascular events after stenting for acute coronary syndrome. *J Thromb Haemost*. 2006;4(3):542-9.
10. Kamea T, Shiraga M, Kahsiwagi H, et al. Critical role of ADP interaction with P2Y₁₂ receptor in the maintenance of $\alpha_{IIb}\beta_3$ activation: association with Rap1B activation. *J Thromb Haemost*. 2006;4(6):1379-87.
11. Chrzanowska-Wodnicka M, Smyth SS, Schoenwaelder SM, et al. 2nd. Rap1b is required for normal platelet function and hemostasis in mice. *J Clin Invest*. 2005;115(3):680-7.
12. Cattaneo M. 14 - The platelet P2 receptors. *Platelets* (Fourth Edition): Academic Press; 2019;259-77.
13. Stefanini L, Paul DS, Robledo RF, et al. RASA3 is a critical inhibitor of RAP1-dependent platelet activation. *J Clin Invest*. 2015;125(4):1419-32.
14. Beck F, Geiger J, Gambaryan S, et al. Temporal quantitative phosphoproteomics of ADP stimulation reveals novel central nodes in platelet activation and inhibition. *Blood*. 2017;129(2):e1-e12.
15. Beck F, Geiger J, Gambaryan S, et al. Time-resolved characterization of cAMP/PKA-dependent signaling reveals that platelet inhibition is a concerted process involving multiple signaling pathways. *Blood*. 2014;123(5):e1-e10.
16. Doncheva NT, Morris JH, Gorodkin J, et al. Cytoscape StringApp: network analysis and visualization of proteomics data. *J Proteome Res*. 2019;18(2):623-32.
17. Smoot ME, Ono K, Ruscheinski J, et al. Cytoscape 2.8: new features for data integration and network visualization. *Bioinformatics*. 2011;27(3):431-2.
18. Gustavsen J, Pai S, Isserlin R, et al. RCy3: Network biology using Cytoscape from within R. *F1000Research*. 2019;8:1774.
19. Ashburner M, Ball CA, Blake JA, et al. Gene ontology: tool for the unification of biology. The Gene Ontology Consortium. *Nat Genet*. 2000;25(1):25-9.
20. The Gene Ontology Consortium. The Gene Ontology Resource: 20 years and still GOing strong. *Nucleic Acids Res*. 2019;47(D1):D330-D8.
21. Mi H, Muruganujan A, Casagrande JT, et al. Large-scale gene function analysis with the PANTHER classification system. *Nat Protoc*. 2013;8(8):1551-66.
22. Xue Y, Liu Z, Cao J, et al. GPS 2.1: enhanced prediction of kinase-specific phosphorylation sites with an algorithm of motif length selection. *Protein Eng Des Sel*. 2011;24(3):255-60.
23. Wishart DS, Feunang YD, Guo AC, et al. DrugBank 5.0: a major update to the DrugBank database for 2018. *Nucleic Acids Res*. 2018;46(D1):D1074-D82.

24. Kutmon M, Kelder T, Mandaviya P, et al. CyTargetLinker: a cytoscape app to integrate regulatory interactions in network analysis. *PLoS One*. 2013;8(12):e82160.
25. Burkhart JM, Vaudel M, Gambaryan S, et al. The first comprehensive and quantitative analysis of human platelet protein composition allows the comparative analysis of structural and functional pathways. *Blood*. 2012;120(15):e73-82.
26. Chen L, Kostadima M, Martens JHA, et al. Transcriptional diversity during lineage commitment of human blood progenitors. *Science*. 2014;345(6204):1251033.
27. Li Z, Smyth SS. 16 - Interactions between platelets, leukocytes, and the endothelium. *Platelets* (Fourth Edition): Academic Press; 2019;295-310.
28. Zhu Q, Yamakuchi M, Ture S, et al. Syntaxin-binding protein STXBP5 inhibits endothelial exocytosis and promotes platelet secretion. *J Clin Invest*. 2014;124(10):4503-16.
29. Zhu QM, Ko KA, Ture S, et al. Novel thrombotic function of a human SNP in STXBP5 revealed by CRISPR/Cas9 gene editing in mice. *Arterioscler Thromb Vasc Biol*. 2017;37(2):264-70.
30. Zahedi RP, Lewandrowski U, Wiesner J, et al. Phosphoproteome of resting human platelets. *J Proteome Res*. 2008;7(2):526-34.
31. Martina JA, Bonangelino CJ, Aguilar RC, et al. Stonin 2: an adaptor-like protein that interacts with components of the endocytic machinery. *J Cell Biol*. 2001;153(5):1111-20.
32. Shindo Y, Kim MR, Miura H, et al. Lrmp/Jaw1 is expressed in sweet, bitter, and umami receptor-expressing cells. *Chem Senses*. 2010;35(2):171-7.
33. Huang Y, Joshi S, Xiang B, et al. Arf6 controls platelet spreading and clot retraction via integrin $\alpha_{IIb}\beta_3$ trafficking. *Blood*. 2016;127(11):1459-67.
34. Banerjee M, Whiteheart SW. The ins and outs of endocytic trafficking in platelet functions. *Curr Opin Hematol*. 2017;24(5):467-74.
35. Nagy Z, Wynne K, von Kriegsheim A, et al. Cyclic nucleotide-dependent protein kinases target ARHGAP17 and ARHGEF6 complexes in platelets. *J Biol Chem*. 2015;290(50):29974-83.
36. Eto M, Kitazawa T, Matsuzawa F, et al. Phosphorylation-induced conformational switching of CPI-17 produces a potent myosin phosphatase inhibitor. *Structure*. 2007;15(12):1591-602.
37. Aslam M, Härtel FV, Arshad M, et al. cAMP/PKA antagonizes thrombin-induced inactivation of endothelial myosin light chain phosphatase: role of CPI-17. *Cardiovasc Res*. 2010;87(2):375-84.
38. Koo TH, Eipper BA, Donaldson JG. Arf6 recruits the Rac GEF Kalirin to the plasma membrane facilitating Rac activation. *BMC Cell Biol*. 2007;8:29.
39. Dwivedi S, Pandey D, Khandoga AL, et al. Rac1-mediated signaling plays a central role in secretion-dependent platelet aggregation in human blood stimulated by atherosclerotic plaque. *J Transl Med*. 2010;8:128.
40. Comer S, Nagy Z, Bolado A, et al. The RhoA regulators Myo9b and GEF-H1 are targets of cyclic nucleotide-dependent kinases in platelets. *J Thromb Haemost*. 2020;18(11):3002-12.
41. Pleines I, Hagedorn I, Gupta S, et al. Megakaryocyte-specific RhoA deficiency causes macrothrombocytopenia and defective platelet activation in hemostasis and thrombosis. *Blood*. 2012;119(4):1054-63.
42. Ventura E, Giordano A. *Cell Cycle. Reference Module in Life Sciences*: Elsevier; 2019.
43. Bray PF, McKenzie SE, Edelstein LC, et al. The complex transcriptional landscape of the anucleate human platelet. *BMC Genomics*. 2013;14(1):1.
44. Schwertz H, Rowley JW, Zimmerman GA, et al. Retinoic acid receptor- α regulates synthetic events in human platelets. *J Thromb Haemost*. 2017;15(12):2408-18.
45. Mikolcevic P, Sigl R, Rauch V, et al. Cyclin-dependent kinase 16/PCTAIRE kinase 1 is activated by cyclin Y and is essential for spermatogenesis. *Mol Cell Biol*. 2012;32(4):868-79.
46. Kyselova A, Siragusa M, Anthes J, et al. Cyclin Y is expressed in platelets and modulates integrin outside-in signaling. *Int J Mol Sci*. 2020;21(21).
47. Morel O, Jesel L, Abbas M, et al. Prothrombotic changes in diabetes mellitus. *Semin Thromb Hemost*. 2013;39(5):477-88.
48. Kaur R, Kaur M, Singh J. Endothelial dysfunction and platelet hyperactivity in type 2 diabetes mellitus: molecular insights and therapeutic strategies. *Cardiovasc Diabetol*. 2018;17(1):121.
49. Smolenski A. Novel roles of cAMP/cGMP-dependent signaling in platelets: cAMP/cGMP-signaling in platelets. *J Thromb Haemost*. 2012;10(2):167-76.
50. Babur Ö, Melrose AR, Cunliffe JM, et al. Phosphoproteomic quantitation and causal analysis reveal pathways in GPVI/ITAM-mediated platelet activation programs. *Blood*. 2020;136(20):2346-58.

Abbreviations

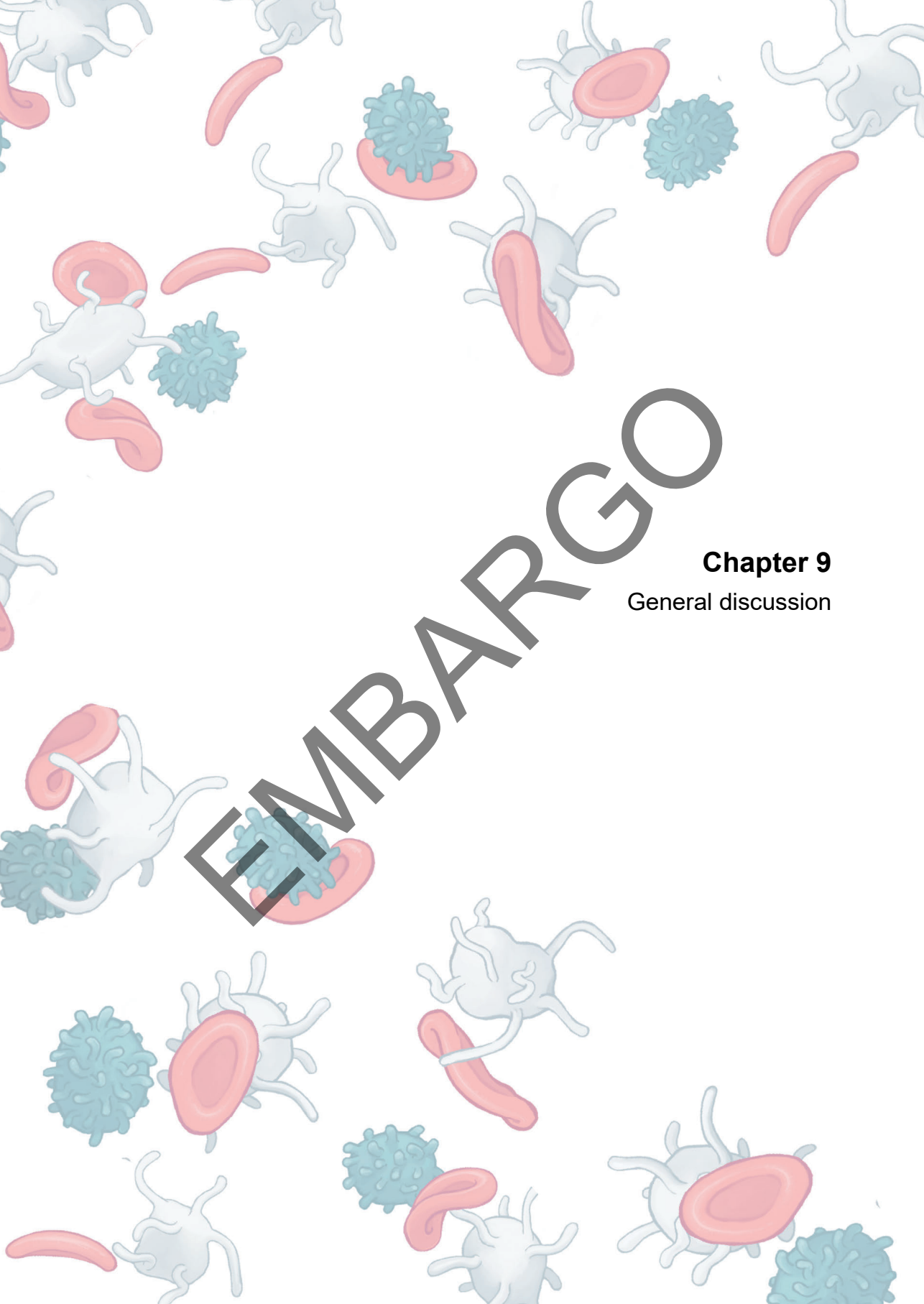
ABLIM	Actin-binding LIM protein
AC	Adenylate cyclase
ADP	Adenosine diphosphate
ARF6	Adenosine 5'-diphosphate-ribosylation factor 6
ARPP19	cAMP-regulated phosphoprotein 19
CABLES1	CDK5 and ABL1 enzyme substrate 1
CaIDAG-GEFI	Calcium- and DAG-regulated guanine exchange factor-1
cAMP	Cyclic adenosine monophosphate
CCNY	Cyclin-Y
CLDN	Claudin
CNST	Consortin
FGA	Fibrinogen alpha chain
GO	Gene Ontology
GPCR	G protein-coupled receptors
IMUP	Immortalization up-regulated protein
KALRN	Kalirin
MARCH2	E3 ubiquitin-protein ligase MARCHF2
NO	Nitric oxide
OR14A2	Olfactory receptor 14A2
PDE3A	Phosphodiesterase 3A
PGI ₂	Prostaglandin I ₂
PHKB	Phosphorylase b kinase regulatory subunit beta
PI3K	Phosphoinositide 3-kinase
PKA	Protein kinase A
PPP1R14A	Protein phosphatase 1 regulatory subunit 14A
RAC1	Ras-related C3 botulinum toxin substrate 1
RASA3	Ras GTPase-activating protein 3
REC114	Meiotic recombination protein REC114
RHOB	Rho-related GTP-binding protein RhoB
ROCK	Rho-associated protein kinase
SLAIN2	SLAIN motif-containing protein 2
STON2	Stonin-2
T2DM	Type 2 diabetes mellitus
VAMP	Vesicle-associated membrane protein
VTI1B homolog 1B	Vesicle transport through interaction with t-SNAREs

Supplemental tables

Supplemental Table 1. Overview of characteristics of the proteins in our network related to network position, platelet expression, and involved biological processes.

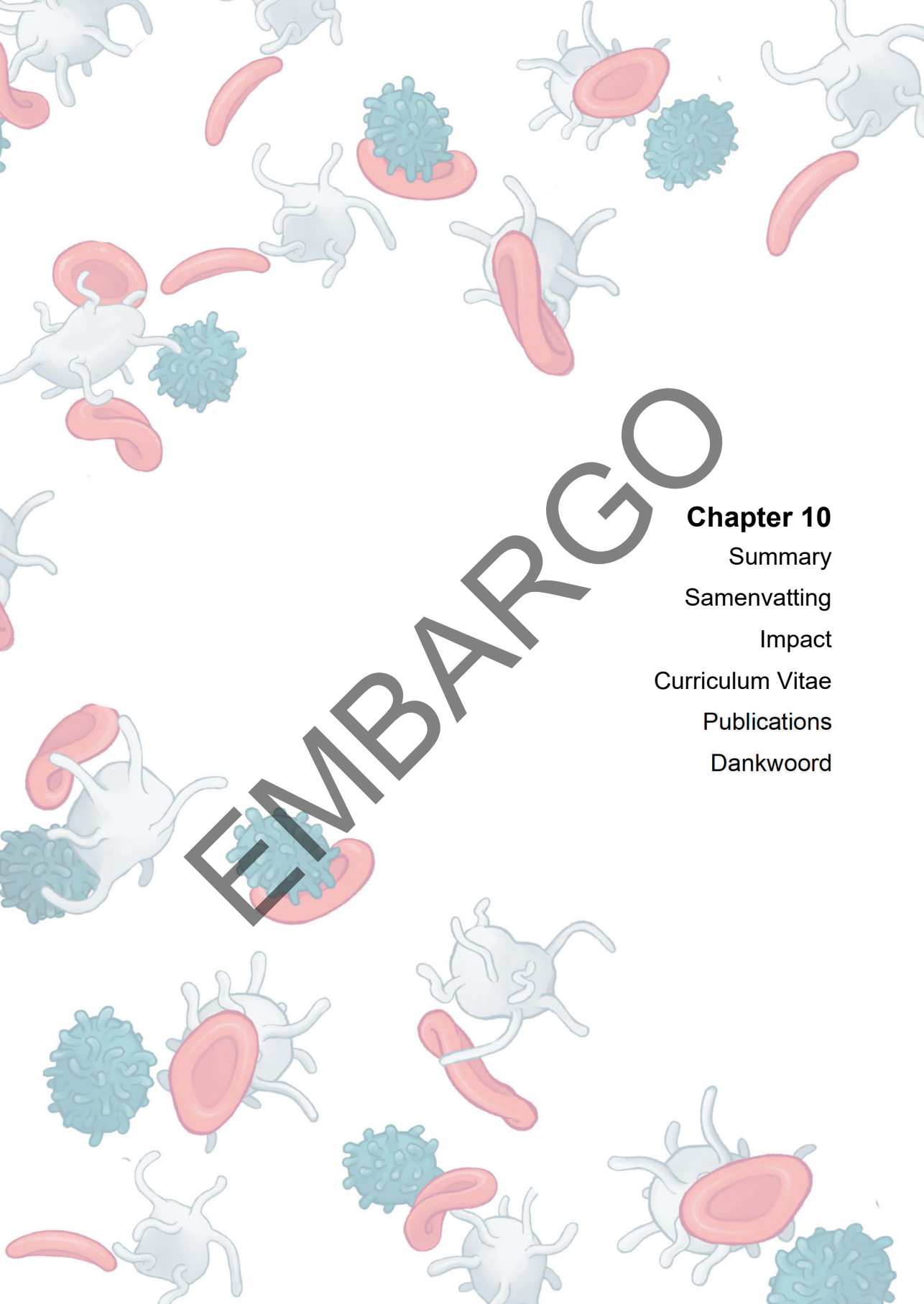
Gene	has at least 1 regulated pHcDegree	NeighborhoodConnectivity	Copy # in PLT	Gem expression in PLT	PLT specific (RT/gem/ves/gem) (MK)	Cluster	has druggable targ baaten Blood model
ABLIM3	1	1	2100	8.85272555	11.3140184	Small GTPases mediated signal transduction and cell shape	0
ARHGGEF	1	3	1600	3.91164426	0.93867201	Small GTPases mediated signal transduction and cell shape	0
ARPP19	1	0	2500	9.14440626	1.707483581	Small GTPases mediated signal transduction and cell shape	0
CBORF25	0	8	1600	9.548049473	1.029151678	Vesicle mediated transport	0
CBORF33	1	1	4	9.264389226	18.13294356	Small GTPases mediated signal transduction and cell shape	0
CAB151	1	2	4	1.855669336	1.548615933	Cyclin-dependent kinases	0
CCNY1	1	3	1500	6.810240328	1.30070756	Cyclin-dependent kinases	0
CCNY2	1	3	1500	5.021403852	1.829231754	Cyclin-dependent kinases	0
CDK17	1	2.5	1700	5.286280657	1.223303895	Cyclin-dependent kinases	0
CDK22	1	2.5	800	6.37653598	1.217877522	Cyclin-dependent kinases	0
CDN22	3	3	3	1.95497436	8.92736365	Tight junctions	0
CDN24	3	3	3	0.76288959	0.76288959	Tight junctions	0
CDN25	3	3	3	0.5654545	0.5654545	Tight junctions	0
CDN3	3	3	3	7.024232486	15.527129246	Tight junctions	0
CDN5	3	3	3	8.961061545	2.446546451	Tight junctions	0
CNST	1	0	2100	4.910615091	0.929632183		0
EF3B	1	0	2100	0.003728883	0.587712684	Vesicle mediated transport	1
FGA	1	2	69700	8.486652417	6.788624778		0
GAS2L1	1	0	1600	8.486652417	14.22727507		0
GC-SAM1	1	1	1100	5.843350067	5.108497443	Small GTPases mediated signal transduction and cell shape	0
KALRN	1	3	1500	4.722705332	1.651157354	Vesicle mediated transport	0
LRRMP	1	9	1400	7.671633083	1.054912871		0
MARCF1	1	0	1300	6.727271674			0
MARCH2	1	9.25	1900	10.31904527	2.357042018	Vesicle mediated transport	0
MTS1	1	0	1900	6.950379256	2.36469723		0
MYO9B	1	3	1400	5.104304769	0.897778488	Small GTPases mediated signal transduction and cell shape	0
OR14A2	0	1	1	7.65178E-06	4.874642994		0
PDE3A	1	0	1400	5.95630619	18.67275581		0
PHKB	1	0	840	8.876459728	1.985403745		0
PHFYVE	1	8	840	4.12854304			0
PPP1R14A	1	4	5000	7.894980019	19.33343163	Vesicle mediated transport	0
RAC1	0	7	3200	8.820303262	1.400175291	Small GTPases mediated signal transduction and cell shape	0
REC114	0	4	3000	0.00124578	0.208888175	Cyclin-dependent kinases	1
REGC	1	0	3000	9.57723552	1.343346637		0
RHOA	0	4	2500	1.9305828	1.45457804	Small GTPases mediated signal transduction and cell shape	1
SCAMP3	0	6	1400	4.33333333	0.838782603		0
SEC22B	1	4	1400	2.31472627			0
SEC22E	1	8	8500	4.632907904	0.932985182	Vesicle mediated transport	0
SLAIN2	1	0	2800	9.925225029	2.20597864		0
SNAP29	1	8	3400	6.1171701	1.757746003	Vesicle mediated transport	0
STON2	1	4	2400	9.575826457	10.48281233	Vesicle mediated transport	1
STX6	1	9.5	1100	4.476885233	1.236010415	Vesicle mediated transport	0
STXBP5	1	8.1111111	1100	5.468145468	1.333007201	Vesicle mediated transport	0
STXBP5	1	9	3300	5.468145468	1.212513167	Vesicle mediated transport	0
TBC1D23	1	0	1200	5.000163608			0
TGOLN2	0	6.25	3000	7.18157045	1.267326443	Vesicle mediated transport	0
UBE2O	1	0	3200	4.946103169	1.88637822		0
VAMP3	1	0	4200	10.13749664	1.850970522	Vesicle mediated transport	1
VAMP4	0	7.6	700	5.086600657	1.893180721	Vesicle mediated transport	0
VAMP8	1	10	700	7.97898197	1.524134193	Vesicle mediated transport	0
VTG1B	1	7.4	1900	7.669913137	1.659549355	Vesicle mediated transport	0
ZCCHC6	1	8	8	6.289397861	1.3003475		0

Supplemental Table 2. Average relative normalized gene expression (log2fpm values) of the proteins in our network in hematopoietic cells derived from Blood RNAexpress. Available upon request.



EMBARGO

Chapter 9
General discussion



EMBARGO

Chapter 10

Summary

Samenvatting

Impact

Curriculum Vitae

Publications

Dankwoord